Univerzita Karlova

2. lékařská fakulta

Studijní program: Imunologie

Mgr. Kamila Hladíková

Význam složení a funkčních vlastností imunitního infiltrátu nádorového mikroprostředí pro klinický průběh nádorů hlavy a krku

Impact of pattern and functional properties of tumor-infiltrating immune cells for clinical outcome of head and neck cancer

Dizertační práce

Vedoucí závěrečné práce: prof. MUDr. Radek Špíšek, Ph.D.

Konzultant: RNDr. Anna Fialová, Ph.D.

Praha, 2020

Prohlášení

Prohlašuji, že jsem závěrečnou práci zpracovala samostatně a že jsem řádně uvedla a citovala všechny použité prameny a literaturu. Současně prohlašuji, že práce nebyla využita k získání jiného nebo stejného titulu

Souhlasím s trvalým uložením elektronické verze mé práce v databázi systému meziuniverzitního projektu Theses.cz za účelem soustavné kontroly podobnosti kvalifikačních prací.

V Praze, 27.2.2020

KAMILA HLADÍKOVÁ

Podpis

Identifikační záznam

HLADÍKOVÁ, Kamila. *Význam složení a funkčních vlastností imunitního infiltrátu nádorového mikroprostředí pro klinický průběh nádorů hlavy a krku. [Impact of pattern and functional properties of tumor-infiltrating immune cells for clinical outcome of head and neck cancer]*. Praha, 2020. 113 stran, 5 příloh. Dizertační práce (Ph.D.). Univerzita Karlova, 2. lékařská fakulta, Ústav imunologie. Vedoucí závěrečné práce: Špíšek, Radek.

Poděkování

Děkuji svému školiteli prof. MUDr. Radku Špíškovi, Ph.D. za odborné vedení během celého doktorského studia a cenné rady a připomínky, které přispěly k vypracování této dizertační práce. Děkuji své konzultantce RNDr. Anně Fialové, Ph.D., která mě provázela celým doktorským studiem, podporovala mě při plánování i realizaci vědeckých projektů a dávala mi cenné rady, jak při samotné experimentální práci, tak při psaní manuskriptů. Děkuji také všem kolegům z výzkumného oddělení biotechnologické společnosti Sotio, kde jsem dostala zcela jedinečnou příležitost svou dizertační práci vypracovávat, za velmi profesionální, ale zároveň přátelské prostředí a za pomoc při řešení projektů, které jsou součástí této práce.

Speciální poděkování patří celé mé rodině a blízkým přátelům za podporu ve studiu, neustálé snaze mě motivovat a podporovat.

ABSTRAKT

Nádory hlavy a krku představují z imunologického hlediska velmi komplexní a heterogenní skupinu onemocnění. Původně byly tyto nádory spojovány především s kouřením a alkoholem. V posledních desetiletích ale výrazně narůstá procento nádorů asociovaných s perzistující infekcí lidským papilomavirem s onkogenním potenciálem v imunologicky privilegované oblasti tonzilárních krypt. Vzhledem k nezastupitelné roli imunitního systému, jak v protivirové, tak v protinádorové imunitní odpovědi je prognóza pacientů významně ovlivněna velikostí, složením a funkční kapacitou imunitního infiltrátu v nádorovém mikroprostředí. Pro nádory hlavy a krku je charakteristické silně imunosupresivní prostředí, zhoršující průběh onemocnění a snižující účinnost imunoterapie. Většina pacientů s touto diagnózou dobře odpovídá na standardní terapii, ta je ale spojená s velmi závažnými časnými a pozdními toxicitami, které mají zásadní vliv na kvalitu života. V roce 2016 byla schválena první imunoterapeutika pro léčbu refrakterních nádorů hlavy a krku – inhibitory kontrolních bodů imunitních reakcí blokující PD-1 – PD-L1 dráhu, nivolumab a pembrolizumab. Tento druh terapie, založený na odblokování imunosuprese, se v protokolech kombinujících více léčebných modalit ukázal být velmi účinný a zároveň výrazně méně toxický oproti standardní chemoradioterapii. Proto byla monoterapie PD-1 inhibitory nebo kombinovaná léčba PD-1 inhibitorů s chemoterapií nedávno schválena jako první možnost léčby pro pacienty s metastatickými nebo refrakterními nádory hlavy a krku. I přes nadějné klinické výsledky ale stále existuje vysoké procento pacientů, kteří na tuto léčbu neodpovídají. Lepší porozumění jednotlivým populacím imunokompetentních buněk, zapojujících se do protinádorové imunitní odpovědi, by pomohlo hlouběji pochopit principy ovlivňující funkční orientaci imunitní odpovědi, a zvýšit tak úspěšnost léčby pacientů díky personalizovaným imunoterapeutickým protokolům. Předkládaná dizertační práce významně prohlubuje znalosti o roli HPV-specifických CD8+ T lymfocytů, B lymfocytů infiltrujících do nádoru a dalších buněčných populací v kontextu komplexního nádorového mikroprostředí HPV-asociovaných a chemicky indukovaných nádorů hlavy a krku. A dále poukazuje na význam kombinované imunoterapie založené na odblokování imunosuprese, která vzniká především díky expresi některých inhibičních molekul v nádorovém mikroprostředí, spolu s chronickou aktivací specifické složky imunitního systému.

Klíčová slova

Nádory hlavy a krku, lidský papilomavirus, imunitní systém, kontrolní body imunitních reakcí, inhibitory kontrolních bodů imunitních reakcí, imunoterapie

ABSTRACT

Head and neck squamous cell carcinoma encompasses a complex and heterogeneous group of malignant diseases. Originally, this tumor type was associated with tobacco and alcohol consumption. However, a significantly expanding subset of tumors associated with oncogenic human papillomavirus infection arising in deep tonsillar crypts was identified within the last decades. Due to the essential role of the immune system in antiviral and anticancer immune response, the prognosis of patients is significantly influenced by the volume, composition and functional capacity of the immune infiltrate. The immunosuppressive landscape of head and neck cancer leads to unfavorable outcome of patients and decreased efficacy of immunotherapy. The response rate to standard treatment is high, however, standard therapy is accompanied by considerable toxicity influencing the quality of life. In 2016, the first immunotherapeutics for the treatment of patients with recurrent squamous cell carcinoma of the head and neck were approved – the anti-PD-1 immune checkpoint inhibitors nivolumab and pembrolizumab. This type of therapy, based on mitigation of immunosuppression, shows strong efficacy and less toxicity in combination with other therapies. Therefore, anti-PD-1 immunotherapy was recently approved in the first-line treatment setting as monotherapy or in combination with chemotherapy for patients with metastatic or unresectable, recurrent head and neck cancer. Despite the therapeutic benefit of immune checkpoint inhibitors, there is still a large proportion of nonresponding patients. Thus, better understanding of the individual immune cell populations playing key role in anticancer immune response could reveal the principles influencing functional orientation of the immune response. Personalized immunotherapeutic protocols created with respect to these principles could enhance the efficacy of current therapeutic strategies. This dissertation thesis broadens the knowledge of the significance of HPV-specific CD8+ T cells, B cells and other immune cell populations infiltrating to the tumor microenvironment of HPV-associated vs. HPV-negative tumors of head and neck. This thesis also highlights the importance of combined immunotherapy based on the elimination of immunosuppression, which arises due to a chronic activation of adaptive immune system and consequent expression of inhibitory molecules.

Key words

Head and neck cancer, human papillomavirus, immune system, immune checkpoints, immune checkpoint inhibitors, immunotherapy

OBSAH

SEZNAM ZKRATEK

αPD-1	anti - programmed cell death 1
Akt	thymomas of *AKR* mice - protein kinase B
APC	antigen-presenting cell
Bcl-xL	B-cell lymphoma-extra large
BTLA	B and T lymphocyte attenuator
Ceacam-1	carcinoembryonic antigen-related cell adhesion molecule 1
CCL	(C-C motif) ligand
CD	cluster of differentiation
CDK	cyclin-dependent kinase
CRT	chemoradiotherapy
CTLA-4	cytotoxic T-lymphocyte-associated antigen 4
CXCL	(C–X–C motif) ligand
DC	dendritic cell
ECOG	Eastern Cooperative Oncology Group
EGFR	epidermal growth factor receptor
EMA	Europen Medicine Agency
E2F	E2 factor
E6AP	ubiquitin-ligase E6-associated protein
FDA	Food and Drug Administration
FFPE	formalin-fixed paraffin-embedded
Gal-9	galectin-9
HGSC	high-grade serous carcinoma
HLA	human leukocyte antigen
HLA-DR	Human leukocyte antigen – DR isotype

HMGB1	high mobility group box 1
HNSCC	head and neck squamous cell carcinoma
HPV	human papillomavirus
hrHPV	high-risk human papillomavirus
IFNγ	interferon gamma
IgV	variable immunoglobulin domain
IL	interleukin
ITIM	immunoreceptor tyrosine-based inhibition motif
ITT	immunoreceptor tail tyrosine
LAG-3	lymphocyte activation gene 3
lrHPV	low-risk human papillomavirus
MAPK	mitogen-activated protein kinases, mitogenem aktivované proteinkinázy
mDC	myeloid dendritic cell
MDSC	myeloid-derived suppressor cell
MHC	major histocompatibility complex
mTOR	mammalian target of rapamycin
NK	natural killer
NSCLC	non-small-cell lung carcinoma
OPC	oropharyngeal cancer
OPSCC	oropharyngeal squamous cell carcinoma
ORR	objective response rate
PARP	poly-ADP-ribose polymerase
PARPi	Poly-ADP-ribose polymerase inhibitor
pDC	plasmacytoid dendritic cell
PD-L1	programmed death-ligand 1

PD-L2	programmed death-ligand 2
PD-1	programmed cell death 1
PGE2	prostaglandin E2
PI3K	phosphatidylinositol 3-kinase
PP2A	protein phosphatase 2A
pRb	retinoblastoma protein
PT	platinum
PtdSer	phosphatidylserine
$p16^{INK4A}$	cyclin-dependent kinase inhibitor 2A
qPCR	quantitative polymerase chain reaction
RECIST	Response Evaluation Criteria In Solid Tumors
TAM	tumor-associated macrophages
TCR	T cell receptor
TGFβ	transforming growth factor beta
TIGIT	T-cell immunoreceptor with Ig and ITIM domains
TIL	tumor infiltrating lymphocytes
TIL-B	tumor infiltrating B lymphocytes
TIM-3	T-cell immunoglobulin and mucin domain 3
TLR9	toll-like receptor 9
TMB	tumor mutation burden
TME	tumor microenvironment
TNFα	tumor necrosis factor alfa
WHO	World Health Organisation
2B4	CD244
5-FU	5-fluorouracil

1 ÚVOD

Imunitní systém hraje klíčovou roli v patogenezi maligní transformace. Na základě mnoha vědeckých a klinických důkazů této premisy se imunoterapie nádorových onemocnění stala součástí klinické onkologie a účinnost zdokonalujících se imunoterapeutických protokolů stále roste. Ačkoli protinádorové imunitní odpovědi se účastní všechny složky nespecifické i specifické imunity, ústřední úlohu plní adaptivní buněčná složka, T a B lymfocyty. Nové přístupy protinádorové imunoterapie se tak zaměřují právě na aktivaci a posílení především efektorových T lymfocytů, jejichž pozitivní prognostická role byla prokázána u mnoha indikací, včetně nádorů hlavy a krku. Vlivem silně imunosupresivního mikroprostředí ale dochází u většiny pacientů k postupné ztrátě funkční kapacity efektorových T lymfocytů, jejímž důsledkem je nekontrolovaná progrese nádorového onemocnění. Porozumění biologické podstatě procesů probíhajících v nádorovém mikroprostředí, jež vedou k úniku nádorových buněk před imunitním dohledem, a navržení vhodných imunoterapeutických postupů by tak mohlo zvýšit úspěšnost léčby a dosáhnout trvalých výsledků.

První část této dizertační práce shrnuje současné poznatky o roli adaptivního imunitního systému v nádorovém mikroprostředí pacientů s nádory hlavy a krku, a význam lidského papilomaviru (human papillomavirus, HPV) pro průběh tohoto onemocnění. Dále je zde popsán význam imunoterapie v léčbě HPV-indukovaných nádorů a nádorů vzniklých na podkladě toxického agens. Pozornost je věnována zejména inhibitorům kontrolních bodů imunitních reakcí, vzhledem k jejich klinické účinnosti v celé řadě nádorových onemocnění. Druhou část tvoří soubor publikovaných prací, které souvisí s tématem této dizertační práce, prošly recenzním řízením a byly publikovány v mezinárodních vědeckých časopisech se známým impakt faktorem.

2 NÁDORY HLAVY A KRKU

Nádory hlavy a krku jsou heterogenní skupinou nádorových onemocnění vznikajících v oblasti dutiny ústní, dutiny nosní, hltanu (pharynx), hrtanu (larynx), ze slinných žláz a místní lymfatické tkáně. S celosvětovou incidencí 550 až 600 tisíc případů ročně se nádory hlavy a krku vyskytují jako šesté nejčastější nádorové onemocnění tvořící 5 % všech malignit. V souvislosti s onemocněním ročně zemře přibližně 300 tisíc pacientů (Jemal et al., 2011). Nádory hlavy a krku často z počátku nevykazují žádné vážné klinické příznaky nebo se podobají běžným zánětlivým onemocněním horních cest dýchacích. Až 70 % pacientů je tak diagnostikováno ve stádiu lokálně pokročilého onemocnění, čímž je výrazně negativně ovlivněna i prognóza. Pětileté přežití se tak pohybuje v rozmezí pouhých 10- 50 %. Navíc, přes 95 % pacientů s rekurentním nebo metastatickým karcinomem umírá již do jednoho roku. V opačném případě, při diagnóze v časných stádiích, dosahuje pětileté přežití až 80 % (Leon et al., 2005), (Argiris et al., 2017). I přes výraznou heterogenitu se histologicky z více než 90 % jedná o squamózní karcinomy (head and neck squamous cell carcinoma, HNSCC), vznikající z dlaždicového epitelu vystýlajícího dutiny v této oblasti (Vigneswaran and Williams, 2014). Squamózní karcinomy hlavy a krku tvoří velmi komplexní skupinu onemocnění, charakterizovanou klinickou, fenotypickou a biologickou heterogenitou, která je způsobena zejména genetickými změnami, lokalizací nádoru a etiologickým agens (Cancer Genome Atlas, 2015).

2.1 Etiologie HNSCC

Hlavními prokázanými rizikovými faktory HNSCC jsou historicky kouření tabákových výrobků, konzumace alkoholu a především synergický efekt těchto dvou faktorů (Andre et al., 1995). Pacienti s nádory vzniklými na podkladě této etiologie se pohybují ve vyšší věkové skupině, většinou přes šedesát let. Se vzrůstající osvětou lidí v oblasti životosprávy v rozvinutých zemích se ale počet kuřáků a alkoholiků ve vyšších sociálních vrstvách postupně snižuje, a klesá tak i incidence nádorů podmíněných těmito mutagenními fyzikálními faktory. Dlouho ale zůstával nevyjasněnou otázkou stále narůstající počet nádorů v oblasti orofaryngu (oropharyngeal squamous cell carcinoma, OPSCC). V souvislosti s rostoucím rizikovým chováním zejména mladých lidí bylo na základě experimentálních a epidemiologických dat popsáno další signifikantní etiologické agens, a to infekce HPV (Brandsma and Abramson, 1989), (Snijders et al., 1992). Lidský

papilomavirus, způsobující až 90 % OPSCC, se tímto zařadil mezi nejvýznamnější rizikové faktory nádorů v oblasti hlavy a krku, a změnil tak i pohled na jejich biologickou podstatu (Gillison et al., 2000). Nádory asociované s HPV a toxicky indukované nádory jsou proto považovány za dvě zcela rozdílné entity, odlišující se nejen na základě molekulární podstaty mechanismu vzniku, ale také prognózou pacientů (Weinberger et al., 2006). Heterogenita těchto nádorů je natolik významná, že v roce 2017 došlo k oddělení jejich klasifikace Americkým výborem proti rakovině (American Joint Committee on Cancer, AJCC). Toto rozdělení poskytlo významně přesnější informace o přežití nově diagnostikovaných pacientů (Lydiatt et al., 2017). Komplexní srovnání HPV-pozitivních a HPV-negativních nádorů je shrnuto v Tab. 1. (Husain and Neyaz, 2017).

Parametr	HPV+	HPV-
Věk (průměr)	mladší (40 - 60)	starší (> 60)
Rasa	europoidní >> ostatní	europoidní > ostatní
Geografické rozložení	sev.Evropa a sev.Amerika	Asie - Pacifik
Pohlaví	muži > ženy (8:1)	muži > ženy (3:1)
Socioekonomický status	vyšší	nižší - střední
Incidence	rostoucí	klesající
Prevalence - odhad	proměnlivá v regionech	stabilní
Rizikové faktory	sexuální chování (HPV-16)	tabák, alkohol
Kofaktory	marihuana	dieta, orální hygiena, stres
Histologické místo vzniku	dlaždicový epitel krypt	squamózní epitel dutiny ústní
Anatomické místo vzniku	orofarynx	celá dutina ústní
E6 a E7 onkoproteiny	exprimovány	nedetekovány
p53	wild-type, degradován	mutovaný
P16INK4a	zvýšená exprese	obvykle nedetekováno
Prognóza	příznivá	nepříznivá
Patologický nález	nekeratinizující,basaloidní, imunitní infiltrát	keratinizující, dysplázie povrchového epitelu
Metastázy do spádových uzlin	často, cystické	méně často nekrotizující, solidní
ECOG performance status	nižší (0 u 33 % pacientů)	vyšší (0 u 66 % pacientů)
Převažující TNM klasifikace	T1-T2 N++	T3-T4 N+
Tříleté přežití	82,4 % (95 % CI, 77,2-87,6)	57,1 % (95 % CI, 48,1-66,1)
Tříleté přežití bez progrese	73,7 % (95 % CI, 67,7-79,8)	43,3 % (95 % CI, 34,4-52,4)
Celková odpověď na léčbu	94 % (95 % CI, 87-100)	58 % (95 % CI, 49-74)

Tab. 1. Srovnání demografických, klinických, histologických, genetických a prognostických parametrů u nádorů asociovaných s HPV vs. nádorů jiné etiologie. ECOG (Eastern Cooperative Oncology Group, Východní kooperativní onkologická skupina v USA). Převzato a upraveno dle (Husain and Neyaz, 2017)

2.2 Prognóza a léčba pacientů s HNSCC

Strategie léčby pacientů s HNSCC je založena na lokalizaci primárního nádoru, histologické klasifikaci a stádiu onemocnění (rozsahu primárního nádoru, případně uzlinových a vzdálených metastáz) a celkovém stavu pacienta. Základními kurativními léčebnými modalitami v léčbě HNSCC jsou chirurgická léčba a radioterapie a v některých případech i chemoterapie nebo radiochemoterapie. Ti pacienti, u nichž došlo k nádorové transformaci díky onkogennímu potenciálu HPV, jsou na rozdíl od těch, jejichž nádor byl vyvolán toxickým agens, většinou diagnostikováni v pokročilém stádiu onemocnění, mnohdy s rozvinutým metastatickým postižením regionálních lymfatických uzlin. I přesto ale odpovídají lépe na standardní léčbu a mají významně lepší prognózu, i pětileté přežití (81 % vs. 49 %) ve srovnání s pacienty s HPV-negativními nádory (Licitra et al., 2006), (Ang et al., 2010). Vzhledem k výše zmíněným faktům je zřejmé, že HPV-pozitivní pacienti vyžadují většinou méně agresivní léčbu (Martin, 2014). HPV-typizace ale doposud není zohledňována při výběru léčebné modality v rámci standardní léčby. Jaká je příčina lepší prognózy pacientů, u nichž byla karcinogeneze vyvolána virovou infekcí, zatím nebylo zcela objasněno. Experimentální i klinická data ale ukazují, že jednou z hlavních příčin může být mimo jiné přítomnost viru, který vyvolává aktivní buněčnou imunitní odpověď namířenou proti infikovaným buňkám, a tudíž i proti nádorovým buňkám samotným (Dahlstrand and Dalianis, 2005).

2.3 Lidský papilomavirus (HPV)

Lidský papilomavirus (HPV), patřící do rodiny papillomaviridae – malých neobalených dvouvláknových (double-strand, ds) DNA virů, zahrnuje více než 150 doposud popsaných genotypů infikujících kožní epitel a slizniční povrch anogenitálního traktu, močové trubice, dýchacích cest a ústní části hltanu – orofaryngu. Z hlediska rizikovosti a onkogenního potenciálu se HPV dělí na nízce rizikové (low-risk, lrHPV) a vysoce rizikové (high-risk, hrHPV) HPV. Nízce rizikové genotypy HPV způsobují zejména benigní bradavice a respirační papilomatózu a v 90 % případů je infekce přirozeně eliminována imunitním systémem. V případě nákazy vysoce rizikovým genotypem HPV ale většinou infekce přetrvává dlouhodobě v asymptomatické podobě a díky onkogennímu potenciálu těchto virů je perzistentní infekce asociována s rozvojem karcinomů v anogenitální oblasti, zejména s karcinomem děložního hrdla - cervixu (Franco et al., 1999). Vysoce rizikové

genotypy HPV jsou zodpovědné také za vznik karcinomu orofaryngu, kde dominuje genotyp HPV 16. Dle odhadů by do roku 2020 měl v USA počet HPV-asociovaných HNSCC dokonce překonat incidenci cervikálního karcinomu (Chaturvedi et al., 2011).

2.3.1 Mechanismus infekce HPV

K přenosu infekce HPV dochází během přímého kontaktu z člověka na člověka, většinou při pohlavním styku, během něhož vznikají mikroskopická poranění v povrchovém stratifikovaném squamózním epitelu. Pro vznik karcinomu orofaryngu dokonce není potřeba mechanické poškození povrchového epitelu, protože místem infekce jsou krypty tonzilární tkáně vystýlané specializovaným retikulovaným epitelem, jež má fyziologicky narušenou strukturu pro migraci imunitních buněk do lymfoidní tkáně (Perry, 1994). Těmito přirozeně se vyskytujícími mikroabrazemi pronikají virové částice až k bazální membráně, na níž se váží přes proteoglykany přítomné na membráně, a infikují zde bazální buňky dlaždicového epitelu, keratinocyty, vazbou na jejich povrch a následnou endocytózou. Po internalizaci je virus transportován do pozdních endozómů, kde je změnou pH aktivován a s využitím hostitelského cytoskeletárního transportu vstupuje do buněčného jádra (Schelhaas et al., 2012). Keratinocyty mají přirozeně silný diferenciační a proliferační potenciál. Během diferenciace dochází nezávisle na infekci k neustálému dělení dceřiných kopií bazální buňky, odpoutání od bazální membrány a vystupování k povrchu. Během tohoto pěti až sedmidenního procesu keratinocyty postupně mění svoji morfologii. Dochází ke kondenzaci jádra a plošnému roztažení cytoplazmy. Buňka se zplošťuje a celý proces je zakončen deskvamací z povrchu. Vzhledem k tomu, že replikace viru je závislá na biochemickém aparátu hostitelské buňky, využívá HPV právě intenzivně proliferující dlaždicobuněčný epitel k dokončení životního cyklu tisíce nových kopií viru, které jsou uvolňovány nelyticky během deskvamace odumírajících keratinocytů. Takto dochází k neviremickému šíření infekce, bez vyvolání imunitní reakce (Faraji et al., 2017). Výše popsaný proces je znázorněn na Obr. 1.

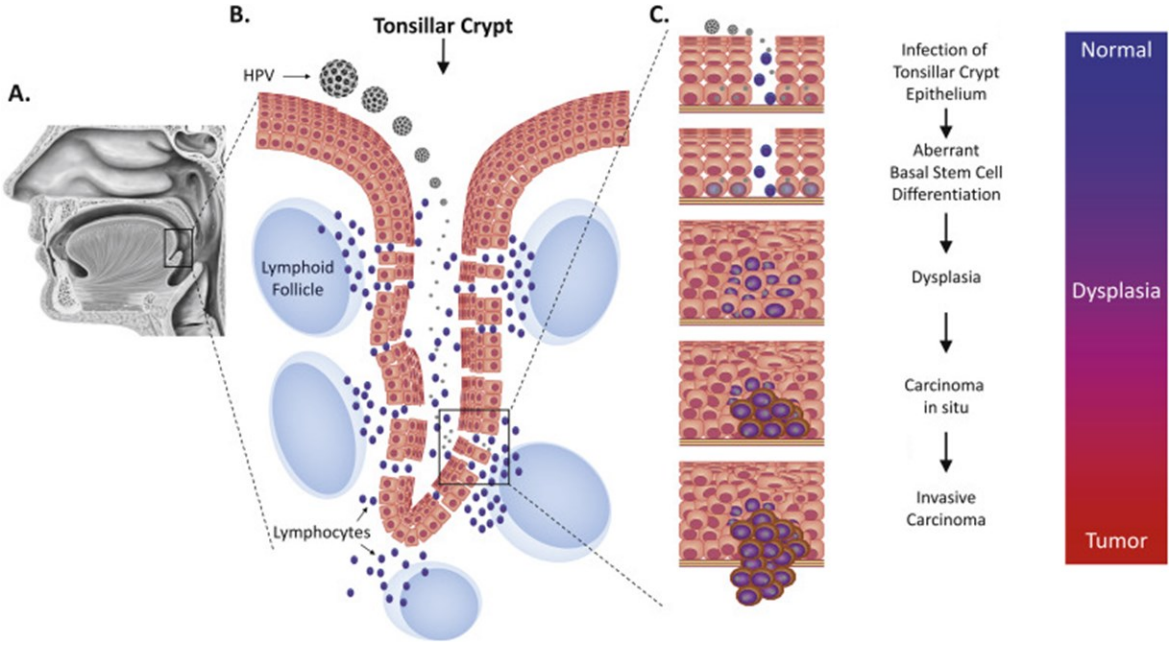

Obr. 1. Mechanismus infekce HPV a progrese onemocnění. (A) Vzhledem k tkáňovému tropismu HPV v rámci HNSCC dochází k infekci sekundárních lymfatických orgánů v oblasti orofaryngu. (B) HPV infikuje progenitory keratinocytů v bazální vrstvě přirozeně fenestrovaného retikulovaného epitelu tonzilárních krypt. (C) Infekce squamózního epitelu tonzil vede postupně k narušení diferenciace bazálních epiteliálních buněk, displázii, vzniku karcinomu in situ, až k propuknutí invazivní karinogeneze. Převzato a upraveno dle (Faraji et al., 2017).

2.3.2 Molekulární mechanismus indukce karcinogeneze u HPV-asociovaných nádorů

Genom HPV, dlouhý 8 000 párů bazí, obsahuje dva kódující regiony a jeden nekódující, regulační region. Součástí kódující oblasti jsou geny proteinů časné fáze (E, early) E1, E2, E4, E5, E6 a E7 a geny kódující kapsidové proteiny, k jejichž expresi dochází v pozdní fázi životního cyklu viru, a jsou proto označované jako pozdní geny (L, late) L1 a L2. Časné geny řídí replikaci virové DNA a regulují kritické kroky buněčného cyklu: E1 spouští replikaci virového genomu, E2 je iniciačním faktorem pro virovou transkripci a řídí segregaci virových genomů, E4 zodpovídá za maturaci nových virových partikulí, E5 udržuje kontinuální proliferaci hostitelské buňky, E6 a E7 jsou označované jako onkoproteiny, jelikož narušují základní kroky regulace buněčného cyklu vedoucí k amplifikaci virového genomu (Rautava, 2012). E6 vyvazuje základní tumor supresorový protein p53 a zprostředkovává jeho ubiquitinylaci vazbou na protein asociovaný s ubikvitin-ligázou E6 (ubiquitin-ligase E6-associated protein, E6AP) a následnou degradaci skrze proteazom. Výsledkem je imortalizovaná hostitelská buňka (Martinez-Zapien et al., 2016). U HPV-asociovaných OPSCC tedy není dysfunkce p53 způsobena jeho mutací, jako u většiny nádorových onemocnění včetně HPV-negativních nádorů, ale řízenou degradací

přirozeně se vyskytující formy proteinu − wild-type p53. Onkoprotein E7 inaktivuje další esenciální tumor-supersor: retinoblastomový protein (retinoblastoma protein, pRb), jehož funkcí je regulace přechodu z G1 do S fáze buněčného cyklu interakcí s transkripčním faktorem E2 (E2 factor, E2F). Dokud je E2F v komplexu s pRb, nemůže dojít k iniciaci replikace (Chellappan et al., 1992). Absence pRb tak vede ke kontinuální aktivaci cílových genů E2F, jimiž jsou mimo jiné cyklin A a cyklin E, které umožňují vstup do S fáze buněčného cyklu a nekontrolovanou replikaci (Zerfass et al., 1995). Funkční inaktivace pRb vede dále k akumulaci $p16^{INK4A}$ (cyclin-dependent kinase inhibitor 2A, CDKN2A), dalšího proteinu podílejícího se na regulaci buněčného cyklu, jež je za fyziologických podmínek inhibitorem cyklin-dependentních kináz (cyclin-dependent kinases, CDKs) fosforylujících pRb. Dokud nedojde k fosforylaci pRb a k následnému uvolnění E2F z komplexu E2F-pRb, buněčný cyklus je pozastaven v G1 fázi a buňka setrvává ve stavu senescence (Giarre et al., 2001). U nádorů vzniklých na podkladě infekce HPV tak na základě negativní zpětné vazby dochází inaktivací pRb k nárůstu cytoplazmatické hladiny $p16^{INK4A}$. Tato hodnota je spolu s detekcí virové DNA/RNA standardně používána jako nepřímý marker pro diagnostiku karcinogeneze asociované s HPV (Hoffmann et al., 2010) a může mít i prognostický význam (Lin et al., 2014). Molekulární mechanismus indukce karcinogeneze u HPV-asociovaných nádorů je znázorněn na Obr. 2.

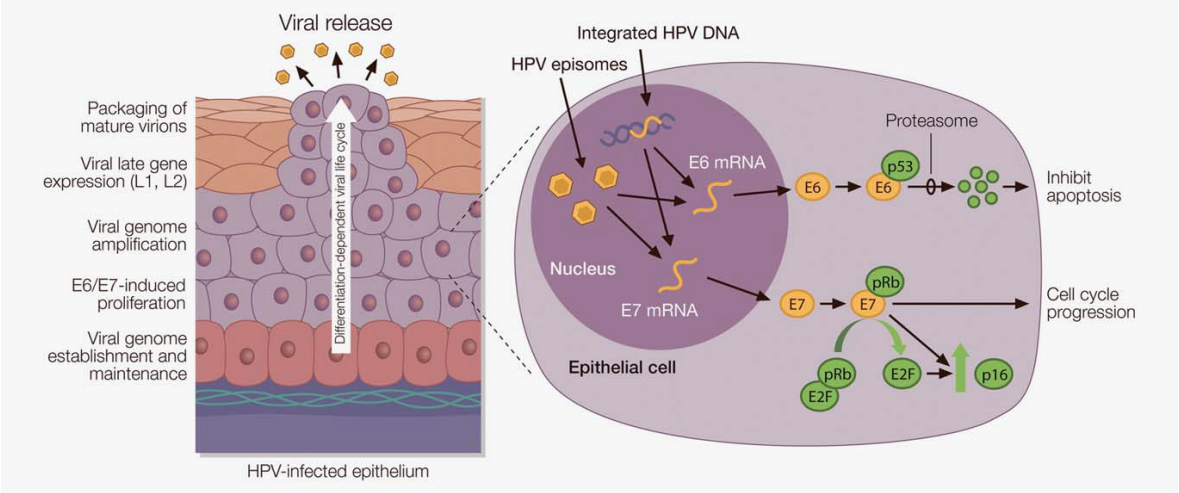

Obr. 2. Molekulární mechanismus indukce karcinogeneze HPV. Po vstupu do buňky se virus přesouvá do jádra, kde je udržován ve formě episomu nebo proběhne integrace do hostitelské DNA a jeho životní cyklus je závislý na diferenciaci hostitelské buňky. Za udržení proliferativního stavu keratinocytů a inhibici apoptózy jsou zodpovědné onkoproteiny E6 a E7, které řídí inaktivaci a degradaci p53 a pRb. V pokročilých fázích diferenciace infikovaných keratinocytů dochází k expresi pozdních genů L1 a L2, kódujících virové kapsidy, a k sestavování nových virových partikulí. Následně se během přirozené deskvamace keratinocytů uvolňují až tisíce nových infekčních virionů. Převzato a upraveno dle (Andersen et al., 2014).

I přesto, že HPV-pozitivní nádory nevznikají na podkladě dlouhodobého vystavování tkání karcinogenům s mutagenním potenciálem, jako je tabák a alkohol, vykazují HPV-asociované nádory překvapivě vysokou genomovou nestabilitu, srovnatelnou s nádory jiné etiologie. Tato mutační zátěž, doprovázená hromaděním somatických mutací, je pravděpodobně způsobená absencí výše zmíněných tumor-supresorů, zajišťujících kontrolu integrity genomu, což značně zvyšuje pravděpodobnost maligní transformace u buněk infikovaných HPV (Seiwert et al., 2015). Pacienti s nádory hlavy a krku se tak celkově řadí mezi indikace s vyšší mutační náloží (tumor mutation burden, TMB) (Alexandrov et al., 2013), jak je znázorněno na Obr. 3., a mají proto potenciál odpovídat lépe na některé imunoterapeutické léčebné postupy. Hlavním důvodem je to, že množství somatických mutací v nádoru zvyšuje pravděpodobnost vzniku neoantigenů, které mohou být rozpoznány a následně cíleny efektorovými buňkami specifické imunity. Obzvláště např. po terapii inhibitory kontrolních bodů imunitních reakcí (Riaz et al., 2016).

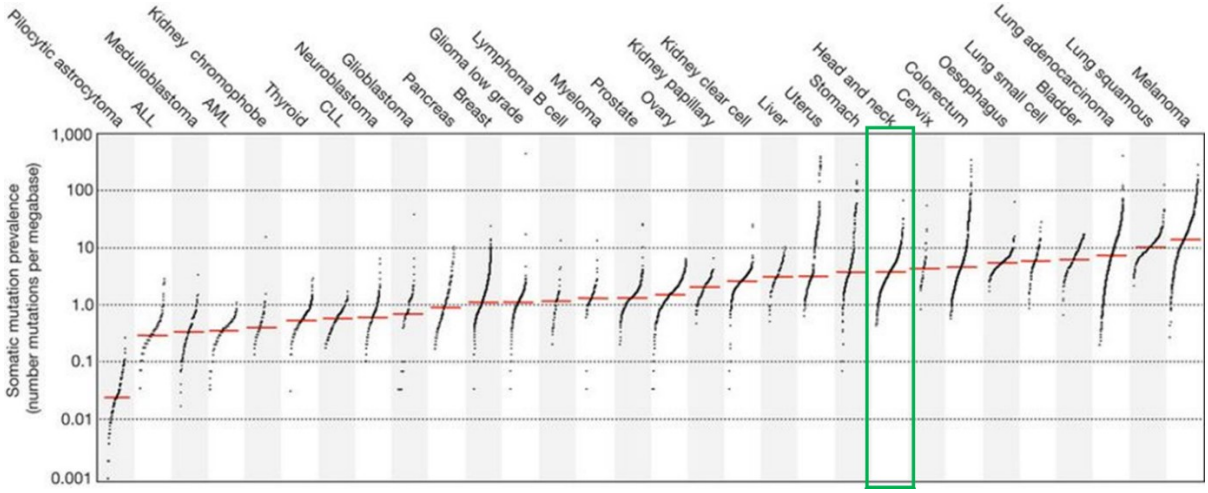

Obr. 3. Porovnání mutační zátěže mezi jednotlivými typy nádorových onemocnění. Data ukazují počet somatických mutací v jednotlivých nádorech. ALL, acute lymphoblastic leukaemia, akutní lymfoblastická leukémiee; AML (acute myeloid leukaemia, akutní myeloidní leukémie); CLL (chronic lymphocytic leukaemia, chronická lymfocytární leukémie). Převzato a upraveno dle (Alexandrov et al., 2013).

2.3.3 Nádorové mikroprostředí HNSCC

Nádorové mikroprostředí (tumor microenvironment, TME) je komplexní, organizovaná a dynamická nika, složená z neoplastických buněk v kontextu nádorového stromatu, tvořeného extracelulární matrix, fibroblasty, epiteliálními buňkami, endoteliemi, tukovými buňkami a produkty těchto buněčných populací a dále v různé míře infiltrujícími imunitními buňkami (Balkwill et al., 2012). Vzhledem k tomu, že nádory hlavy a krku,

na rozdíl od ostatních nádorových indikací, vznikají téměř jednotně ze stejného histopatologického subtypu, jedná se zdánlivě o homogenní skupinu squamózních karcinomů. Ve skutečnosti ale jde o velmi heterogenní onemocnění a každý individuální nádor je unikátní jak složením nádorového mikroprostředí, tak svým chováním (Canning et al., 2019). Nejvýznamnější rozdíly jsou pozorovány mezi skupinou pacientů s HPV-pozitivními a HPV-negativními nádory, a to zejména ve složení imunitního infiltrátu, který má zásadní vliv na prognózu (Partlova et al., 2015).

2.3.4 Složení a význam imunitního infiltrátu u HPV-pozitivních a HPV- negativních pacientů s HNSCC

Imunitní infiltrát je komplexní a dynamickou součástí nádorového mikroprostředí a role jednotlivých imunitních populací se mezi nádorovými typy výrazně liší. U nádorů hlavy a krku navíc složení imunitního infiltrátu i výslednou imunitní reakci ovlivňuje potenciální přítomnost viru. HPV infikuje epiteliální tkáně. Na rozdíl od mukózního epitelu, který HPV infikuje v anogenitální oblasti, v rámci orofaryngu dochází k infekci dlaždicového epitelu, který je v těsném kontaktu s lymfatickou tkání. Lymfatická tkáň zde v podobě tonzil sehrává klíčovou imunologickou roli v obraně proti patogenům. Je tedy pravděpodobné, že virem indukovaná protinádorová imunitní odpověď bude odlišná od imunitní odpovědi nádorů orofaryngu jiné etiologie a zároveň od imunitní odpovědi namířené proti HPV v jiných oblastech organismu.

V posledních letech bylo provedeno několik studií zaměřených na analýzu vztahu mezi imunitní odpovědí, HPV statutem a prognózou pacientů s HNSCC. Vzhledem k náročnosti získání nádorové tkáně byla ve většině těchto studií analyzována pouze periferní krev pacientů. I přesto ale Wansom a kol. detekovali zvýšený počet CD8+ T lymfocytů u pacientů s HPV-pozitivními nádory, který dokonce lépe predikoval odpověď na léčbu než samotný HPV status, jež byl doposud považován za nejsilnější prediktivní znak (Wansom et al., 2010). Turksma a kol. dále v periferní krvi pacientů s HPV-pozitivními nádory detekovali vyšší zastoupení efektorových a efektorových paměťových T lymfocytů oproti HPV-negativním pacientům, což pravděpodobně svědčí o virem indukované imunitní odpovědi (Turksma et al., 2013). Genová analýza potvrdila profil silné specifické imunitní odpovědi u HPV-pozitivních pacientů oproti HPV-negativním pacientům, jejichž profil měl charakter spíše přirozené imunitní odpovědi (Thurlow et al., 2010).

Vzhledem k tomu, že stav periferní krve nemusí vždy odrážet skutečnost, která se odehrává v rámci samotného nádorového mikroprostředí, je analýza nádorové tkáně nezbytnou součástí získání ucelené informace o zastoupení jednotlivých imunitních populací a také o jejich fenotypu a funkčnosti. Komplexní analýza nativních tkání HNSCC provedená v naší laboratoři, zabývající se mimo jiné složením imunitního infiltrátu a fenotypizací jednotlivých populací, ukázala významné rozdíly mezi nádory indukovanými HPV a nádory jiné etiologie. HPV-pozitivní nádory byly dle očekávání infiltrovány signifikantně vyšším množstvím CD8+ T lymfocytů. Tyto cytotoxické lymfocyty infiltrující nádor (tumor infiltrating lymphocytes, TILs) měly navíc schopnost produkovat významně vyšší hladiny prozánětlivých cytokinů interferonu-γ (interferon-γ, IFNγ) a interleukinu-17 (IL-17). Detekováno bylo i výrazně více naivních CD4+ T lymfocytů a myeloidních DC. Dále pak ve srovnání s HPV-negativními nádory v buněčných kulturách HPV-pozitivních vzorků byla zaznamenána signifikantně vyšší produkce prozánětlivých chemokinů CXCL9, CXCL10, CXCL12, CCL17 a CCL21 (Partlova et al., 2015). Zajímavé ovšem bylo, že analýza mRNA potvrdila u HPV-pozitivních nádorů zvýšenou expresi proteinu programované buněčné smrti 1 (programmed cell death 1, PD-1), která je spolu s dalšími inhibičními molekulami považována za marker vyčerpání TILs (Day et al., 2006). Tato studie, provedená v naší laboratoři, je v souladu s výsledky studie Badoualové a kol, kteří pozorovali významně delší přežívání HPV-pozitivních pacientů s karcinomem orofaryngu (oropharynegal cancer, OPC), které byly silně infiltrované PD-1+ T lymfocyty. (Badoual et al., 2013). Molekula PD-1 tak u HNSCC pravděpodobně necharakterizuje vyčerpané TILs neschopné efektorových funkcí. Ward a kol. dále prokázali, že přítomnost TILs u HPV+ OPC pacientů pozitivně koreluje s přežíváním a odpovědí na léčbu na rozdíl od pacientů s nízkým infiltrátem (Ward et al., 2014). Podle nejnovějších výsledků Salomona a kol. hojná infiltrace CD8+ TILs u HPV-asociovaných OPC identifikuje skupinu pacientů s vynikajícími klinickými výsledky a poskytuje tak významnou prognostickou informaci (Solomon et al., 2018).

Na rozdíl od TILs, jejichž pozitivní úloha v nádorovém mikroprostředí byla mnohokrát prokázána, role B lymfocytů infiltrujících do nádoru (tumor-infiltrating B cells, TIL-Bs) zůstává kontroverzní. Navzdory studiím prokazujícím pozitivní prognostickou roli TIL-Bs (Mahmoud et al., 2012) existují i přesvědčivé důkazy naznačující jejich opačný efekt (Lundgren et al., 2016). Za účelem rozšíření znalostí o imunitním infiltrátu u HNSCC a pochopení kontextu mezi jednotlivými imunitními populacemi jsme navázali na předchozí

studii popisující roli CD8+ TILs specifických k HPV16, a zaměřili se na analýzu populace TIL-Bs, jejichž role u HNSCC zatím téměř nebyla popsána. K objasnění této problematiky jsme tak přispěli naší experimentální prací, jejíž výsledky jsou detailně popsány ve výsledkové části této práce.

Celkově větší infiltrát s prozánětlivým charakterem svědčí o silnější specifické imunitní odpovědi u HPV-pozitivních pacientů. I přesto ale imunitní systém většinou nedokáže úspěšně bojovat s nádorovými buňkami a eradikovat je. V rámci nádorové imunologie je tento nežádoucí jev vysvětlován mimo jiné navozením stavu funkčního vyčerpání TILs v rámci imunosupresivního prostředí v nádoru, jež vede k toleranci nádoru a k úniku nádorových buněk imunitnímu dohledu. Z tohoto důvodu je zapotřebí zaměřit se hlouběji na fenotyp vyčerpání nádorově/virově specifických TILs, který je mnohdy reverzibilní.

2.3.5 Imunosupresivní prostředí HNSCC

Nádorové mikroprostředí HNSCC je silně imunosupresivní, což je způsobeno jednak přítomností supresivních buněčných populací, především regulačních T lymfocytů (regulatory T cells, Treg), myeloidních supresorových buněk (myeloid-derived suppressor cells, MDSC), makrofágů asociovaných s nádory (tumor-associated macrophages, TAM) a jednak funkčními defekty efektorových TILs, jež jsou považovány za klíčové komponenty protinádorové imunitní odpovědi (Duray et al., 2010). Funkční defekty efektorových buněk infiltrujících nádor jsou přítomností imunosupresivních buněčných populací amplifikovány. Výsledkem je účinné potlačení aktivní nádorově specifické imunitní odpovědi. Vytváření imunosupresivních podmínek v nádorovém mikroprostředí je jednou z hlavních strategií, jimiž se nádorové buňky efektivně vyhýbají imunitnímu systému, tzv. mechanismů úniku nádorových buněk imunitnímu systému hostitele.

2.3.6 Mechanismy úniku nádorových buněk imunitnímu systému

Z evolučního hlediska je pro přežití nádorových buněk, stejně jako pro parazity, nezbytně nutné vyvinout strategie, jimiž dokáží uniknout dohledu imunitního systému hostitele. Imunitní reakce na nově vznikající nádor má komplexní charakter a jsou do ní zapojeny mechanismy jak nespecifické, tak i specifické imunity. S progresí nádoru jsou však tyto imunitní mechanismy potlačeny a často působí dokonce ve prospěch nádorových buněk. Nádor se tak stává neviditelný před útoky imunitního systému.

Kromě výrazného zastoupení výše zmíněných imunosupresivních buněčných populací v nádorovém mikroprostředí byla u HNSCC prokázána úniková strategie založená na snížení exprese či úplné ztrátě lidského leukocytárního antigenu (human leukocyte antigen, HLA) I. třídy z povrchu nádorových buněk a/nebo narušení mechanismu antigenní prezentace, jejímž cílem je neschopnost rozpoznání nádorových buněk cytotoxickými T lymfocyty, a tak i nemožnost aktivace specifické imunitní odpovědi proti nádorovým buňkám (Ogino et al., 2006), (Lopez-Albaitero et al., 2006).

Z hlediska funkčních vlastností imunitního infiltrátu byly u HNSCC zaznamenány, podobně jako u dalších nádorů, defekty různých imunitních populací. V nádorové tkáni byly detekovány nezralé CD1+ myeloidní dendritické buňky (myeloid dendritic cells, mDC), neschopné zahájit specifickou imunitní odpověď (Li et al., 2009) a makrofágy typu M2, které produkují imunosupresivní cytokiny IL-10 a transformující růstový faktor beta (transforming growth factor beta, TGFβ) a jejich denzita v nádoru koreluje s progresí onemocnění (Mori et al., 2011). Přítomnost nefunkčních NK buněk (Duffey et al., 1999) a plasmatocytoidních dendritických buněk (plasmacytoid dendritic cells, pDC) v nádorové tkáni (Hartmann et al., 2003) je pravděpodobně z velké části způsobena vysokými hladinami TGFβ a prostaglandinu E2 (PGE2), produkovaných nádorovými buňkami (Bekeredjian-Ding et al., 2009).

I přes fakt, že pro efektivní protinádorovou imunitní odpověď je zapotřebí souhra specifické i nespecifické, buněčné i humorální složky imunity, klíčovou roli zde stále hrají T lymfocyty infiltrující nádor. Navození stavu vyčerpání těchto klíčových hráčů imunitního systému je tak jedním z hlavních mechanismů úniku imunitnímu dohledu a vzniku tolerance vůči nádoru.

2.3.7 Kontrolní body imunitních reakcí a vyčerpání T lymfocytů

Stav částečného či úplného vyčerpání specifických CD8+ T lymfocytů nastává při dlouhodobě přetrvávající stimulaci T-receptoru (T cell receptor, TCR) v prostředí chronického zánětu nebo nádorového mikroprostředí. Nejedná se o skokovou, ale naopak o postupnou změnu funkčního fenotypu, projevující se hierarchickým způsobem. V počátečních fázích dochází ke ztrátě schopnosti cytotoxického zabíjení cílových buněk a sekrece IL-2. Následuje ztráta produkce faktoru nekrotizujícího nádory (tumor necrosis factor alfa, TNF-a) a až v pokročilém stavu vyčerpání daná buňka přestává produkovat i IFNγ, případně granzym B (Wherry et al., 2003).

Charakteristickým znakem vyčerpání T lymfocytů je povrchová exprese tzv. kontrolních bodů imunitních reakcí neboli inhibičních molekul, jejichž fyziologickou funkcí je tlumení imunitní odpovědi, a to zejména T lymfocytární, po proběhnutí adekvátní imunitní reakce, jakožto ochrany před poškozením vlastních tkání a rozvojem autoimunit (Wang et al., 2005), Obr. 4. Přítomnost TILs s narušeným funkčním fenotypem v nádorovém mikroprostředí ale není dostačující k zahájení efektivní protinádorové imunitní odpovědi a k eradikaci nádoru.

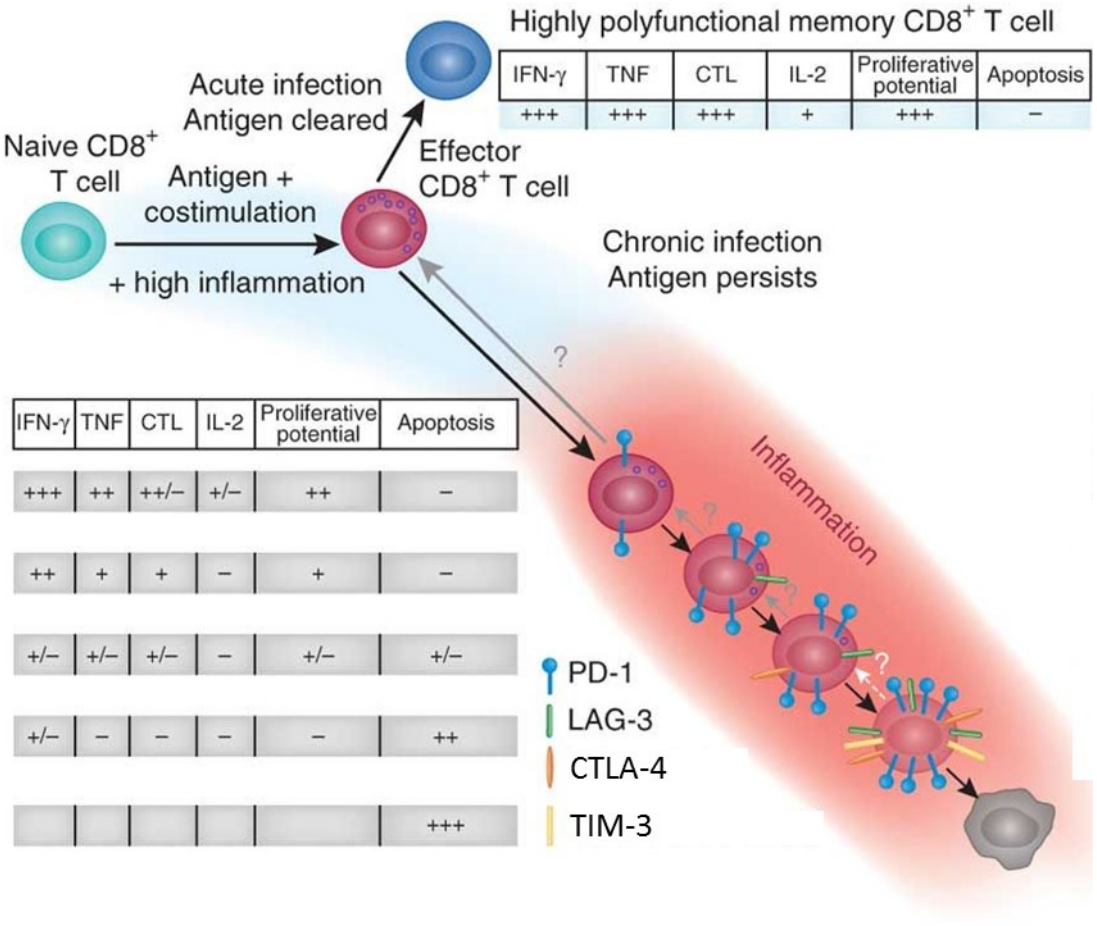

Obr. 4. Hierarchické vyčerpání efektorových T lymfocytů v místě přetrvávajícího zánětu (nádor/chronická infekce). K eliminaci akutního zánětu spolu s antigenem, který zánět vyvolal, dochází pomocí plně funkčních efektorových T lymfocytů, které poté dále zrají do polyfunkčních paměťových T lymfocytů, produkujících prozánětlivé cytokiny, se silnou cytolytickou a proliferativní schopností. V případě chronického zánětu antigen stimulující specifickou imunitní odpověď přetrvává i po efektorové fázi. Dochází k nárůstu exprese inhibičních receptorů na povrchu dlouhodobě aktivovaných T lymfocytů a ke ztrátě jejich efektorových schopností. Převzato a upraveno dle (Wherry, 2011).

Mezi nejvíce prozkoumané inhibiční molekuly patří antigen asociovaný s cytotoxickými T lymfocyty 4 (cytotoxic T-lymphocyte-associated antigen 4, CTLA-4), protein programované buněčné smrti 1 (programmed cell death 1, PD-1) a jeho ligand - ligand programované buněčné smrti 1 a 2 (programmed death-ligand 1 and 2, PD-L1 a PD-L2), molekula TIM3 (T-cell immunoglobulin and mucin domain 3, TIM-3), imunoreceptor T lymfocytů s imunoglubulinem a ITIM doménou (T-cell immunoreceptor with Ig and ITIM domains, TIGIT), tlumič B a T lymfocytů (B and T lymphocyte attenuator, BTLA), aktivační gen lymfocytů 3 (lymphocyte activation gene 3, LAG-3), (Blackburn et al., 2009) (Catakovic et al., 2017).

2.3.7.1 CTLA-4

CTLA-4 je ve vysoké míře exprimován na povrchu regulačních T lymfocytů (regulatory T cells, Treg) a aktivovaných TILs. CTLA-4 je kompetitivním vazebným partnerem kostimulačních ligandů rodiny B7 (CD80 a CD86) na povrchu buněk prezentujících antigen (antigen presenting cells, APC). Tato vazba ale na rozdíl od kostimulačního receptoru CD28 vyvolává silný negativní signál, zprostředkovaný trans-endocytózou a následnou degradací kostimulačních molekul CD80 a CD86 a aktivací signálů blokujících proliferaci T lymfocytů a sekreci IL-2 (Qureshi et al., 2011). Výsledkem je inhibice efektorových funkcí aktivovaných T lymfocytů, která v nádorovém mikroprostředí vede k potlačení specifické protinádorové imunitní odpovědi cytotoxických CD8+ T lymfocytů (Zou and Chen, 2008).

2.3.7.2 PD-1

PD-1 je klíčovým inhibičním receptorem, jehož exprese narůstá po aktivaci především T lymfocytů, ale i dalších imunitních populací. Vazbou na svůj ligand PD-L1 (B7-H1) nebo PD-L2 (B7-H2) a spuštěním příslušných signálních drah, přispívá k regulaci imunitní odpovědi i k následnému navrácení do stavu homeostáze (Zhang et al., 2004). Interakce PD-1 se svým ligandem, stejně jako u CTLA-4, vede k zablokování PI3K-Akt signální dráhy, která spouští mechanismy vedoucí k aktivaci buňky, progresi buněčného cyklu, proliferaci, produkci cytokinů, aerobní glykolýze a dalším procesům zajišťujícím přežití (Schildberg et al., 2016). Mechanismus intracelulární signalizace je ale u obou inhibičních molekul odlišný. PD-1 inhibuje fosfatidylinozitol 3-kinázu (phosphatidylinositol 3-kinase, PI3K), která je nezbytná k aktivaci protein kinázy B (protein kinase B, Akt), a na jejíž aktivitě je závislá také exprese anti-apoptotického proteinu Bcl-xL

(B-cell lymphoma-extra large), tzv. faktoru přežití, zatímco CTLA-4 blokuje Akt přímo pomocí serin/threonin fosfatázy 2A (protein phosphatase 2A, PP2A) a aktivita PI3K, nutná k expresi Bcl-xL, tak zůstává zachována (Parry et al., 2005).

2.3.7.3 PD-L1

PD-L1 je imunomodulační membránový glykoprotein, jehož exprese je indukována stimulací prozánětlivých cytokinů zejména na povrchu nádorových a hematopoetických buněk (Mimura et al., 2018). Díky silnému prediktivnímu potenciálu je exprese PD-L1 v některých případech používána jako biomarker pro selekci pacientů dobře odpovídajících na imunoterapii. Imunohistochemická exprese PD-L1 byla dokonce schválena americkým Úřadem pro kontrolu potravin a léčiv (Food and Drug Administration, FDA) jako doprovodný diagnostický test pro léčbu pembrolizumabem, monoklonální protilátkou proti PD-1, u karcinomu děložního čípku (NCT02628067), gastrického a gastroesofageálního adenokarcinomu (NCT02335411), nemalobuněčného karcinomu plic (non-small-cell lung carcinoma, NSCLC) (NCT01905657; NCT02142738) a uroteliálního karcinomu (NCT02256436).

2.3.7.4 TIM-3

TIM-3 je membránovým receptorem vysoce exprimovaným především populací pomocných T lymfocytů Th1, cytotoxických T lymfocytů Tc1 a také profesionálními fagocyty, jako jsou makrofágy nebo DCs. Zatím byly popsány čtyři ligandy interagující s variabilní částí imunoglobulinové domény (variable immunoglobulin domain, IgV) TIM-3: galektin 9 (galectin-9, Gal-9), protein HMGB1 (high mobility group box 1), molekula Ceacam-1 (carcinoembryonic antigen-related cell adhesion molecule 1) a fosfatidylserin (phosphatidylserine, PtdSer) (Du et al., 2017). Vazba TIM-3 na Gal-9, první popsaný ligand TIM-3, indukuje u cílových buněk periferní toleranci (Sabatos et al., 2003) nebo apoptózu (Zhu et al., 2005), což svědčí o supresivní regulační funkci TIM-3 v Th1 imunitní odpovědi. Interakce s dalším ligandem, PtdSer, jednak indukuje fagocytózu apoptotických tělísek a jednak podporuje zkříženou prezentaci antigenů dendritickými buňkami (Nakayama et al., 2009). TIM-3 na povrchu DCs infiltrujících do nádoru kompetuje o vazbu HMGB1 s nukleovými kyselinami, uvolňovanými z umírajících nádorových buněk. Vazbou TIM-3 – HMGB1 dochází k negativní regulaci stimulace vrozené imunitní odpovědi pomocí nukleových kyselin (Chiba et al., 2012). Poslední doposud popsaný ligand TIM-3, Ceacam-1, může být ko-exprimován společně s TIM-3 na

povrchu aktivovaných T lymfocytů, kde tvoří specifický heterodimer, který slouží jako negativní regulátor imunitní odpovědi (Huang et al., 2015). Golden-Mason a kol. zjistili, že v průběhu chronické infekce dochází ke zvýšení exprese TIM-3 na povrchu CD4+ i CD8+ T lymfocytů. Nárůst TIM-3 negativně koreluje s produkcí cytokinů a schopností proliferace efektorových T lymfocytů v odpovědi na antigen. Zablokováním interakce TIM-3 a jeho ligandu ale dojde k částečné obnově jejich efektorové funkce (Golden-Mason et al., 2009). Ferris a kol. pozorovali, že z hlediska exprese inhibičních molekul PD-1 a TIM-3 u HNSCC vykazují nejvíce vyčerpaný fenotyp dvojitě pozitivní TILs, tedy PD-1+ TIM-3+ TILs, čímž potvrdili výsledky předešlých studií provedených u melanomu (Fourcade et al., 2010) a leukémie (Kong et al., 2015).

2.3.7.5 TIGIT

TIGIT je imunomodulačním receptorem obsahujícím imunoglobulinové (immunoglobulin, Ig) a tyrozinové inhibiční (immunoreceptor tyrosine-based inhibitory motif, ITIM) domény. TIGIT je exprimovaným na povrchu aktivovaných a paměťových T lymfocytů, přirozených zabíječů (natural killers, NK) a NK T-lymfocytů. Vazba na ligand, receptor polioviru (poliovirus receptor, PVR) exprimovaný DC, spouští fosforylaci cytosolické tyrozinové domény imunoreceptoru (immunoreceptor tail tyrosine, ITT), která skrze zablokování PI3K a mitogenem aktivovaných protein kináz (mitogen-activated protein kinases, MAPK) vede ke snížení cytotoxické schopnosti NK a NKT buněk a k produkci supresivních cytokinů, jako je IL-10 (Liu et al., 2013). TIGIT dále tlumí sekreci IFN-γ a inhibicí maturace DC nepřímo brání aktivaci T lymfocytů (Yu et al., 2009).

2.3.7.6 LAG-3

LAG-3 je strukturním homologem koreceptoru CD4, exprimovaným na povrchu aktivovaných T lymfocytů, NK buněk, B lymfocytů a plazmacytoidních DC (pDC) (Goldberg and Drake, 2011). Vzhledem k molekulární struktuře LAG-3 je jejím ligandem, stejně jako ligandem CD4, molekula hlavního histokompatibilního komplexu II (major histocompatibility complex class II, MHC II), ke které se ale váže s vyšší afinitou a tato vazba, na rozdíl od interakce s CD4, vede k negativní regulaci buněčné proliferace a expanze aktivovaných T lymfocytů (Workman et al., 2004). Exprese LAG-3 byla ve zvýšené míře detekována na povrchu TILs u několika myších nádorových modelů. Zablokování LAG-3 spolu s PD-1 vedlo k posílení T-buněčné protinádorové imunitní odpovědi (Woo et al., 2012). Výsledky některých studií ale naopak popisují LAG-3 jako pozitivní prognostický

marker. Triebel a kol. ukázali, že u karcinomu prsu přítomnost solubilního LAG-3 v séru pacientek signifikantně korelovala s lepší prognózou (Triebel et al., 2006).

2.3.8 Inhibitory kontrolních bodů imunitních reakcí v léčbě nádorových onemocnění

Objev inhibitorů kontrolních bodů imunitních reakcí otevřel novou cestu k revitalizaci T-buněčné odpovědi. Tyto léky v posledních 5-7 letech prokazují účinnost v celé řadě nádorových onemocnění a postupně se stávají součástí prvních linií léčby, často i před donedávna standartní chemoterapií (Pacheco et al., 2019). Za objev těchto molekul a jejich cestu do klinické praxe byli v roce 2018 po zásluze oceněni James P. Allison a Tasuku Honjo Nobelovou cenou za fyziologii nebo lékařství. Imunoterapie monoklonálními protilátkami blokujícími jednotlivé inhibiční molekuly je ve srovnání se standardní léčbou doprovázena výrazně nižší toxicitou a zároveň vykazuje u některých typů nádorů silný terapeutický efekt. Na základě slibných výsledků probíhají také klinické studie využívající synergizující efekt jednotlivých inhibitorů kontrolních bodů imunitních reakcí (Long et al., 2018) a nebo kombinující inhibitory s dalšími léčebnými modalitami, jako jsou onkolytické viry (Ribas et al., 2017), inhibitory poly-ADP-ribóza polymerázy, tzv. PARP inhibitory (poly-ADP-ribose polymerase inhibitor, PARPi) (Higuchi et al., 2015) či agonisté toll-like receptorů (toll-like receptor, TLR) (Sato-Kaneko et al., 2017).

Prvním přípravkem ze skupiny inhibitorů kontrolních bodů imunitních reakcí, schváleným pro klinické použití, byla protilátka proti CTLA-4, ipilimumab. Ipilimumab byl v roce 2011 jako první léčebný přípravek tohoto typu schválen americkou FDA pro léčbu metastatického maligního melanomu, a to na základě výsledků randomizované, multicentrické klinické studie fáze III (MDX010-20), zahrnující 676 pacientů. Medián přežití pacientů v léčeném rameni byl 10 měsíců oproti 6,4 měsíce v kontrolním rameni (Hodi et al., 2010). Pozitivní výsledky byly potvrzeny v několika navazujících studiích fáze III (Robert et al., 2011), (Coens et al., 2017). Navíc, přibližně 20 % pacientů léčených ipilimumabem dosáhlo dlouhodobého přežití oproti nulovému dlouhodobému přežití při léčbě do té doby standartními chemoterapeutickými protokoly (Schadendorf et al., 2015). Léčba ipilimumabem je ale často doprovázena nežádoucími účinky, které vznikají v důsledku odblokování supresivního prostředí v nádoru, a se svým charakterem se tak podobají autoimunitním onemocněním. Jedná se o tzv. imunitně podmíněné vedlejší účinky (immune related adverse events – ir-AEs), projevující se různě závažnými orgánovými toxicitami (Fecher et al., 2013).

Největšího klinického úspěchu zatím dosáhla plně humanizovaná monoklonální protilátka proti molekule PD-1, která se tak prosadila v imunoterapeutických léčebných protokolech celé řady onkologických onemocnění. Nivolumab a pembrolizumab byly na základě dlouhotrvající protinádorové odpovědi a méně závažným vedlejším účinkům schváleny FDA v roce 2014 pro léčbu metastatického melanomu (Robert et al., 2014), (Weber et al., 2015). Blokace PD-1 dráhy měla revoluční dopad i na léčbu Hodgkinova lymfomu (Ansell et al., 2015), nemalobuněčného karcinomu plic (Garon et al., 2015), renálního karcinomu (Motzer et al., 2015) a dalších indikací. Na základě pozitivních výsledků klinické studie EMPOWER-CSCC-1, testující další monoklonální protilátku proti PD-1, cemiplimab, vstoupila v roce 2018 imunoterapie i do léčby spinocelulárního karcinomu (Migden et al., 2018). Schématické znázornění inhibičních molekul, které jsou cíleny monoklonálními protilátkami v klinické praxi, je zobrazeno na Obr. 5.

I přes velmi slibné výsledky imunoterapie založené na blokaci inhibičních molekul u výše zmíněných indikací je ale u některých typů solidních nádorů odpověď na léčbu nízká.

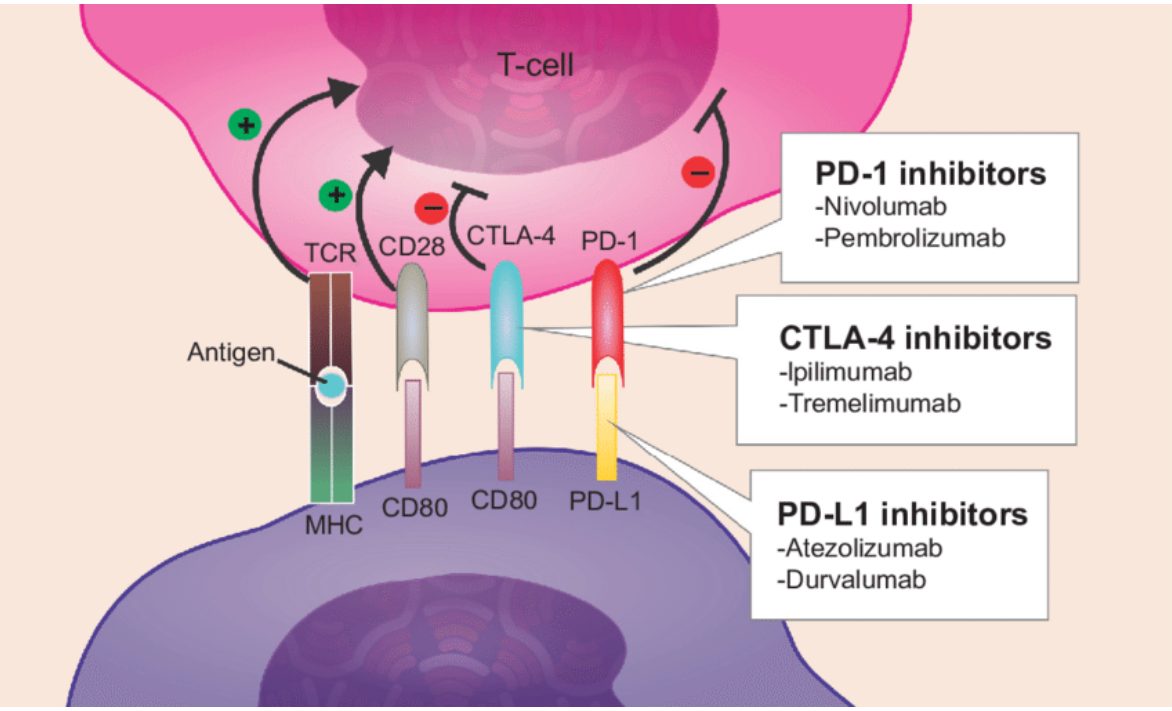

Obr. 5. Schématické znázornění cílových molekul inhibitorů kontrolních bodů imunitních reakcí, doposud schválených FDA. Převzato a upraveno dle (de Mello et al., 2017).

2.3.9 Inhibitory kontrolních bodů imunitních reakcí v léčbě HNSCC

V roce 2016 schválila na základě výsledků dvou pilotních studií KEYNOTE 012 a CHECKMATE 141 americká FDA pembrolizumab a nivolumab pro léčbu pacientů s rekurentním nebo metastatickým HNSCC, u kterých došlo k progresi onemocnění již během léčby platinovými deriváty nebo touto cytostatickou léčbou nebyl nádor vůbec ovlivněn (Ferris et al., 2016), (Larkins et al., 2017). O rok později následovalo schválení obou monoklonálních protilátek pro léčbu stejné populace pacientů i Evropskou lékovou agenturou (European Medicines Agency, EMA). V roce 2019 byl na základě výsledků studie KEYNOTE 048 pembrolizumab zařazen i do první linie léčby pacientů s metastatickým nebo rekurentním HNSCC (Burtness et al., 2019). Míra objektivní odpovědi (objective response rate, ORR), hodnotící odpovídavost pacientů se solidními nádory na léčbu αPD-1 (Response Evaluation Criteria In Solid Tumors, RECIST), se ale pohybuje mezi 15-20 % a většina pacientů s HNSCC tak na léčbu neodpovídá (Seiwert et al., 2016), (Ferris et al., 2016). Pro zvýšení efektivity léčby na bázi zablokování imunosupresivních drah v nádorovém mikroprostředí je proto potřeba zaměřit se jednak na identifikaci tzv. prediktivních biomarkerů, určujících pravděpodobnost odpovědi na léčbu u jednotlivých pacientů a jejich následnou stratifikaci, a jednak najít další cílové molekuly, jejichž blokování by vedlo ke zvýšení účinnosti imunoterapie u HNSCC. Monoklonální protilátka proti PD-1 je ale spolu s cetuximabem, tedy inhibitorem receptoru epidermálního růstového faktoru (epidermal growth factor receptor, EGFR), doposud jedinou cílenou terapií u HNSCC, schválenou FDA. Přičemž klinické studie založené na monoterapii cetuximabem ukazují ještě nižší klinický účinek než αPD-1 terapie, a to 8-11 % (Fury et al., 2012). Další inhibitory molekul kontrolních bodů imunitních reakcí a komplexní protokoly zahrnující kombinace několika terapeutických přístupů u HNSCC jsou zatím v různých fázích klinického testování. Studie, které se již dostaly do pokročilejších fází testování (fáze II a výš), jsou shrnuty v Tab. 2. (Zolkind and Uppaluri, 2017).

Fáze	Cílová molekula	mAb/léčba	Klinická studie
Monoterapie			
II	PD-L1	durvalumab	NCT02207530
II	PD-1	nivolumab	NCT03226756
II	PD-1	pembrolizumab	NCT02255097
II	PD-1	pembrolizumab	NCT02644369
II	PD-1	pembrolizumab	NCT02769520
II	PD-1	pembrolizumab	NCT02296684
II	PD-1	pembrolizumab	NCT02841748
II	PD-1	pembrolizumab	NCT02641093
II	PD-1	pembrolizumab	NCT02710396
III	PD-L1	avelumab	NCT02952586
III	PD-1	pembrolizumab	NCT03040999
III	PD-1	pembrolizumab	NCT02252042
Kombinovaná terapie			
II	PD-1	pembrolizumab/EphB4-HAS fúzní protein	NCT03049618
II	PD-1, CTLA-4	nivolubam/ipilimumab	NCT02823574
II	PD-1, CTLA-4	nivolubam/ipilimumab	NCT02834013
II	PD-1, TLR9	pembrolizumab/SD-101	NCT02521870
II	PD-1	pembrolizumab/RT,cetuximab/RT	NCT02707588
II	PD-1	pembrolizumab/cetuximab	NCT02318901
II	PD-1	pembrolizumab/RT	NCT02609503
II	PD-1	pembrolizumab/CRT	NCT02777385
II	PD-1	nivolumab/SBRT	NCT02684253
II	PD-1	pembrolizumab/reirradiation	NCT02289209
II	PD-1	pembrolizumab/acalabrutinib	NCT02454179
II	PD-1, CTLA-4	nivolumab/ipilimumab	NCT02919683
II	PD-L1	durvalumab/cetuximab/RT	NCT03051906
II	PD-L1, CTLA-4	durvalumab/tremelimumab	NCT02319044
II	PD-1	nivolumab/HPV-vakcína ISA101	NCT02426892
III	PD-1	pembrolizumab, pembrolizumab/ PT/5-FU, cetuximab/PT/5-FU	NCT02358031
III	PD-1, CTLA-4	nivolumab/ipilimumab	NCT02741570
III	PD-L1, CTLA4	durvalumab/tremelimumab	NCT02551159
III	PD-L1, CTLA-4	durvalumab/tremelimumab	NCT02369874
III	PD-L1	avelumab/cetuximab/RT	NCT02999087

Tab. 2. Přehled probíhajících klinických studií fáze II a III, využívajících inhibitory kontrolních bodů imunitních reakcí u HNSCC. RT (radioterapie), CRT (chemoradioterapie), PT (platina), 5-FU (fluorouracil), TLR9 (toll-like receptor 9). Převzato a upraveno dle (Zolkind and Uppaluri 2017).

2.3.10 Vznik adaptivní rezistence k αPD-1 terapii

I přes velký klinický úspěch s monoklonální protilátkou proti PD-1 v rámci nádorové imunoterapie existuje stále velká část pacientů se solidními nádory, která na tuto léčebnou modalitu neodpovídá. A navíc, i část responderů, tedy pacientů odpovídajících na léčbu, v průběhu času zrelabuje. Důvodem je, mimo jiné, zatím ne zcela objasněný mechanismus úniku před protinádorovou aktivitou imunomodulačních protilátek potlačujících imunosupresivní prostředí v nádoru, tzv. adaptivní rezistence.

Adaptivní rezistence popisuje mechanismus indukce únikových supresorových signálních drah, vznikajících jako odpověď na zablokování interakce PD-1/PD-L1 pomocí inhibitorů molekul imunitních kontrolních bodů. Jedná se o dynamický proces probíhající v nádorovém mikroprostředí, během něhož dochází k postupné adaptaci TILs na přerušení PD-1 supresivní signální dráhy nárůstem exprese alternativních inhibičních molekul a aktivity jejich signálních drah (Koyama et al., 2016). Shayan a kol. zjistili, že zablokováním PD-1 signální dráhy u HNSCC pomocí blokující protilátky dojde k signifikantnímu nárůstu exprese TIM-3. Sekvenčním podáním αPD-1 a αTIM-3 se ale podařilo zabránit vzniku adaptivní rezistence k αPD-1 terapii, a bylo tak dosaženo signifikantní protinádorové aktivity TILs a zastavení růstu nádoru. Shayan a kol. dále popsali molekulární podstatu vzniku adaptivní rezistence k αPD-1 terapii u HNSCC, která je založena na aktivaci PI3K/Akt/mTOR signální dráhy (Shayan et al., 2017). Genová deplece PD-1 vede k nárůstu exprese dalších alternativních inhibičních molekul, jako je LAG-3, TIGIT, 2B4 (CD244) a CD160 (Odorizzi et al., 2015). Mechanismus adaptivní rezistence je tedy možné alespoň z části překonat duální blokací PD-1 spolu s dalšími inhibitory molekul kontrolních bodů imunitních reakcí, a zesílit tak účinnost αPD-1 terapie (Lichtenegger et al., 2018).

2.3.11 Prognostická role inhibičních molekul

Ačkoli blokace funkce inhibičních molekul vede k obnovení specifické protinádorové imunitní odpovědi, a dosáhla tak významného klinického úspěchu u různých typů nádorových onemocnění, dle nejnovějších výzkumů je exprese některých inhibičních molekul, jako je PD-1 nebo PD-L1, úzce spjata nejen s funkčními defekty a hladinou vyčerpaní, ale u některých nádorů naopak také s efektorovými schopnostmi těchto buněk (Badoual et al., 2013), (Hladikova et al., 2018) a s aktivací protinádorové imunitní odpovědi (Fucikova et al., 2019). V roce 2007 Hamanishi a kol. popsali roli PD-L1 jako negativního

prognostického markeru u ovariálního karcinomu na základě korelace mezi expresí PD-L1 a nízkým infiltrátem TILs v nádorovém mikroprostředí (Hamanishi et al., 2007). V následujících letech byla ale u různých nádorových typů, včetně HNSCC, pozorována opačná korelace (Kogashiwa et al., 2017), (Webb et al., 2016), (Wu et al., 2017). Stejná diskrepance se objevuje také u molekuly PD-1, jejíž exprese byla asociována s pozitivní prognózou u pacientů s kolorektálním karcinomem (Li et al., 2016), ovariálním karcinomem (Webb et al., 2015) i u pacientů s HNSCC (Badoual et al., 2013). Skutečná role molekuly PD-1 v nádorové imunologii tak zůstává rozporuplná. Vzhledem k nízkému terapeutickému účinku αPD-1 terapie u HNSCC je zásadním krokem objasnit roli PD-1 molekuly u tohoto nádorového onemocnění a popsat mechanismus navozující stav vyčerpání TILs, jehož důsledkem je silné imunosupresivní prostředí a neschopnost eliminace nádoru. V naší laboratoři jsme se proto zabývali funkční charakterizací HPV-specifických TILs u pacientů s HNSCC, v souvislosti s expresí inhibičních molekul PD-1 a TIM-3. Výsledky této práce objasňují roli jednotlivých inhibičních molekul a jsou v souladu se studiemi popisujícími PD-1 jako marker aktivace a diferenciace, jež nemusí vždy svědčit o míře vyčerpání a nefunkčnosti (Legat et al., 2013). Pozitivní roli PD-1 u HNSCC navíc podporují data Badoualové a kol., kteří detekovali expresi celé škály aktivačních markerů, jako je HLA-DR, CD38 nebo CD137, na povrchu PD-1+ TILs (Badoual et al., 2013). Molekula PD-1 tak pravděpodobně charakterizuje spíše fenotyp efektorových paměťových TILs než jejich vyčerpání.

Zablokování PD-1 signální dráhy pomocí monoklonální protilátky nivolumabu tak podle očekávání nevedlo v naší studii k nárůstu produkce IFNγ, jak lze pozorovat u indikací s vysokým terapeutickým účinkem αPD-1 terapie. Částečného odblokování supresivního prostředí a revitalizace T-buněčné odpovědi bylo docíleno až duální blokací PD-1 dráhy i TIM-3 dráhy současně, čímž došlo k signifikantnímu nárůstu produkce IFNγ a k zesílení protinádorové imunitní odpovědi (Hladikova et al., 2018). V nádorovém mikroprostředí HNSCC tak během αPD-1 terapie pravděpodobně dochází ke vzniku adaptivní rezistence, jež byla popsána výše. Paralelní blokace více inhibičních molekul tak vyvolává synergický efekt těchto inhibitorů a předchází vzniku adaptivní rezistence (Hladikova et al., 2018), (Shayan et al., 2017). Fučíková a kol. pozorovali významnou diskrepanci v prognóze, vzhledem k expresi jednotlivých inhibičních molekul, také u karcinomu ovaria. Zejména míra exprese molekuly PD-L1 v nádorovém mikroprostředí je asociována s aktivací protinádorové imunitní odpovědi a s lepší prognózou pacientek, zatímco exprese molekuly

TIM-3 významně koreluje s inhibicí protinádorové imunitní odpovědi, a negativně tak ovlivňuje prognózu pacientek s HGSC (Fucikova et al., 2019).

2.3.12 Další možnosti imunoterapie u HNSCC

Vzhledem k významným odlišnostem v biologické podstatě, chování i prognóze HPV-asociovaných nádorů hlavy a krku vs. nádorů vyvolaných toxickými látkami, je nezbytně nutné přistupovat odlišně i k léčbě těchto dvou entit. Současná léčba je založena na TNM klasifikaci nádoru, tedy postoperační patologické klasifikaci zahrnující určení velikosti nádoru (T), zasažení regionálních lymfatických uzlin (N) a založení vzdálených metastáz (M). Následná postoperativní léčba zahrnující radioterapii nebo konkomitantní chemoradioterapii, nejčastěji v kombinaci s cisplatinou, ale zatím nezohledňuje HPV status pacientů. Pro pacienty s HPV-asociovanými nádory by řešením mohla být právě vhodně zvolená imunoterapie využívající potenciál specifické buněčné imunity k eradikaci nádoru.

V současné době jsou v klinické praxi již běžně zavedeny profylaktické vakcíny, založené na principu prevence vzniku virové infekce indukcí humorální imunitní odpovědi v podobě neutralizačních protilátek proti konformačním epitopům kapsidového proteinu L1. U již probíhajícího onemocnění ale dochází k významnému snížení exprese HPV L1 infikovanými buňkami, a profylaktické vakcíny tak nemohou mít žádný terapeutický účinek (Ault and Future, 2007). Pro léčbu pacientů s HPV-asociovanými nádory je tak zapotřebí aktivace buněčné imunity v podobě terapeutických vakcín. Vzhledem ke komplexnosti vývoje těchto vakcín jsou ale různé imunoterapeutické postupy u HNSCC stále ve fázi preklinického a klinického testování. Největší léčebný potenciál zatím mají terapeutické vakcíny využívající přítomnosti virových onkoproteinů, které jsou exprimovány všemi infikovanými buňkami, a tudíž i nádorovými buňkami, v nichž byl maligní potenciál vyvolán právě infekcí HPV. Tyto onkoproteiny tak slouží jako silně imunogenní nádorově specifické antigeny, které indukují odpověď specifických cytotoxických T lymfocytů. Exprese těchto onkoproteinů je navíc úzce spjata s maligním fenotypem nádorových buněk, a zůstává tak neměnná i přes vysoký selekční tlak za účelem evaze nádorových buněk imunitnímu systému (Best et al., 2012). Výsledky klinické studie fáze II, založené na podávání vakcíny obsahující syntetické peptidy onkoproteinu E6 a E7 HPV-pozitivním pacientkám s vulvární intraepiteliální neoplázií, ukázaly velmi silný léčebný potenciál. Po uplynutí jednoho roku od vakcinace vykazovalo 15 z 19 pacientek objektivní klinickou odpověď, mezi nimiž bylo dokonce devět kompletních odpovědí. Zásadní pro tuto studii

bylo, že se u všech pacientek jednalo o specifickou T buněčnou odpověď indukovanou právě podáním výše uvedené vakcíny (Kenter et al., 2009). V roce 2017 byly zveřejněny výsledky klinické studie fáze II u pacientů s neléčitelnými HPV 16-asociovanými nádory, včetně karcinomu orofaryngu. Tato studie také testovala přístup založený na podávání HPV16 E6 a E7 peptidů, ale v kombinaci s nivolumabem. Míra objektivní odpovědi u pacientů dosáhla 33 %, včetně dvou kompletních odpovědí (NCT02426892). Kombinace těchto dvou odlišných léčebných přístupů tak vykazuje synergický efekt. V klinickém testování fáze I/II pro HNSCC je také personalizovaná autologní vakcína obsahující nádorový lyzát pacientů (jako zdroj nádorových antigenů) v kombinaci s polyklonálně aktivovanými alogenními Th1 paměťovými buňkami. Vakcína tvořená těmito dvěma komponentami by také měla vyvolat imunitní odpověď namířenou specificky přímo proti nádorovým buňkám (NCT01998542).

3 CÍLE PRÁCE

Hlavním cílem této práce bylo charakterizovat složení a funkční vlastnosti imunitního infiltrátu nádorové tkáně u pacientů s nádory hlavy a krku, se zaměřením na adaptivní složku vytvářející specifickou protinádorovou imunitní odpověď. Dalším záměrem bylo definovat význam těchto parametrů pro klinický průběh onemocnění a pro navržení efektivních imunoterapeutických protokolů. Jednotlivé cíle jsou rozděleny do následujících částí:

1. Analýza vlivu etiologického agens (infekce HPV vs. kouření/alkohol) na složení a četnost imunitního infiltrátu u nádorů hlavy a krku.
   - Hypotéza: Lepší prognóza pacientů s HPV-indukovanými nádory je dána vyšší infiltrací nádorového mikroprostředí imunokompetentními buňkami.

2. Testování funkční kapacity HPV-specifických TILs u nádorů hlavy a krku.
   - Hypotéza: Exprese inhibičních molekul a proces adaptivní rezistence brání efektivní protinádorové imunitní odpovědi zprostředkované HPV-specifickými TILs s vyčerpaným fenotypem.

3. Analýza významu B lymfocytů pro podporu specifické CD8+ T-buněčné imunitní odpovědi u pacientů s nádory hlavy a krku.
   - Hypotéza: B lymfocyty infiltrující do nádoru podporují specifické CD8+ T lymfocyty v protinádorové imunitní odpovědi u pacientů s HPV-asociovanými nádory hlavy a krku.

4. Sledování vlivu exprese inhibičních molekul na funkční zaměření imunitního infiltrátu u ovariálního karcinomu.
   - Hypotéza: Prognóza pacientek s HGSCC je významně ovlivněna mírou exprese inhibičních molekul v nádorovém mikroprostředí.

5. Stanovení expresního profilu nádorových antigenů u primárního nádoru ovariálního karcinomu a ovariálních nádorových linií.
   - Hypotéza: Vhodně zvolená kombinace nádorových linií, použitá jako zdroj nádorových antigenů pro vakcíny na bázi DC, dokáže pokrýt široké spektrum antigenů detekovaných u primárních nádorů ovária.

4 SEZNAM PUBLIKACÍ

Publikace, které jsou podkladem dizertační práce:

Partlová S, Bouček J, **Kloudová K**, Lukešová E, Zábrodský M, Grega M, Fučíková J, Truxová I, Tachezy R, Špíšek R, Fialová A. Distinct patterns of intratumoral immune cell infiltrates in patients with HPV-associated compared to non-virally induced head and neck squamous cell carcinoma. Oncoimmunology. 2015 Jan 30;4(1):e965570.
IF: 5,33

Hladíková K*, Partlová S*, Koucký V, Bouček J, Fonteneau JF, Zábrodský M, Tachezy R, Grega M, Špíšek R, Fialová A. Dysfunction of HPV16-specific CD8+ T cells derived from oropharyngeal tumors is related to the expression of Tim-3 but not PD-1. Oral Oncol. 2018 Jul;82:75-82.
*oba autoři přispěli stejnou měrou
IF: 3,73

Hladíková K, Koucký V, Bouček J, Laco J, Grega M, Hodek M, Zábrodský M, Vošmik M, Rozkošová K, Vošmiková H, Čelakovský P, Chrobok V, Ryška A, Špíšek R, Fialová A. Tumor-infiltrating B cells affect the progression of oropharyngeal squamous cell carcinoma via cell-to-cell interactions with CD8+ T cells. J Immunother Cancer. 2019 Oct 17;7(1):261.
IF: 8,73

Fucikova J, Rakova J, Hensler M, Kasikova L, Belicova L, **Hladikova K**, Truxova I, Skapa P, Laco J, Pecen L, Praznovec I, Halaska MJ, Brtnicky T, Kodet R, Fialova A, Pineau J, Gey A, Tartour E, Ryska A, Galluzzi L, Spisek R. TIM-3 Dictates Functional Orientation of the Immune Infiltrate in Ovarian Cancer. Clin Cancer Res. 2019 Aug 1;25(15):4820-4831.
IF: 8,91

Kloudová K, Hromádková H, Partlová S, Brtnický T, Rob L, Bartůňková J, Hensler M, Halaška MJ, Špíšek R, Fialová A. Expression of tumor antigens on primary ovarian cancer cells compared to established ovarian cancer cell lines. Oncotarget. 2016 Jul 19;7(29):46120-46126.
IF: 5,17

Publikace, které nejsou zahrnuty v dizertační práci:

Truxova I, Pokorna K, **Kloudova K**, Partlova S, Spisek R, Fucikova J. Day 3 Poly (I:C)-activated dendritic cells generated in CellGro for use in cancer immunotherapy trials are fully comparable to standard Day 5 DCs. Immunol Lett. 2014 Jul;160(1):39-49.
IF: 2,55

Partlová S, Bouček J, **Kloudová K**, Zábrodský M, Špíšek R, Fialová A. Immune System in Patients with Head and Neck Carcinoma. Klin Onkol. 2015;28 Suppl 4:4S86-94. Review

5 VÝSLEDKY

5.1 Nádory hlavy a krku, indukované infekcí lidským papilomavirem, mají signifikantně vyšší imunitní infiltrát ve srovnání s nádory jiné etiologie.

Lidský papilomavirus (HPV) je v současné době jedním z hlavních etiologických agens invazivní karcinogeneze u nádorů hlavy a krku. I přes častou diagnózu v pozdních stádiích onemocnění s metastatickým rozšířením do lymfatických uzlin mají pacienti s nádory vzniklými na základě této etiologie lepší klinický průběh onemocnění i lepší prognózu, než pacienti s HPV-negativními nádory indukovanými převážně kouřením. I přesto, že příčina tohoto jevu doposud nebyla zcela objasněna, dle dosavadních poznatků lze usuzovat, že jedním z hlavních důvodů je právě přítomnost viru v nádorové tkáni, od které se odvíjí i charakter imunitní odpovědi. Vzhledem k faktu, že u některých indikací má složení a denzita imunitního infiltrátu v nádorové tkáni prognostický a prediktivní význam, zaměřili jsme se v této studii na analýzu imunitního infiltrátu u pacientů se squamózním karcinomem hlavy a krku (head and neck squamous cell carcinoma, HNSCC), ve vztahu k HPV statutu těchto pacientů. V rámci detailní cytometrické analýzy jsme charakterizovali zastoupení a distribuci jednotlivých populací imunitního infiltrátu, které se účastní protinádorové imunitní odpovědi, jako jsou buňky prezentující antigen (antigen presenting cells, APCs), efektorové T lymfocyty a naivní T lymfocyty, nebo naopak populace imunosupresivních buněk, podporujících růst nádoru, jako jsou regulační T lymfocyty (regulatory T cells, Treg). Analyzovali jsme také produkci cytokinů a chemokinů, jež významně přispívají k chemotaxi imunokompetentních buněk do nádorového mikroprostředí. V rámci této studie jsme pozorovali významný rozdíl mezi složením a mírou imunitního infiltrátu nádorů asociovaných s HPV a nádorů jiné etiologie. HPV-pozitivní nádory vykazovaly signifikantně vyšší zastoupení IFNγ+ CD8+ T lymfocytů, IL-17+ T-lymfocytů, mDC a vyšší produkci prozánětlivých chemokinů. Na úrovni mRNA jsme dále zjistili, že HPV-pozitivní nádory měly ve srovnání s HPV-negativními nádory významně nižší expresi cyklooxygenázy 2 (cyclooxygenase 2, Cox-2) a vyšší expresi PD-1. Z naší studie vyplývá, že přítomnost výrazného imunitního infiltrátu může hrát zásadní roli v odpovědi pacientů s HPV-asociovanými nádory na standardní terapii. Charakterizace imunitního infiltrátu u HNSCC se zdá být vhodným

doplněním TNM klasifikace a může tak vedle HPV statutu zpřesnit prognózu pacientů. Navíc může být užitečným nástrojem v rámci vývoje nových imunoterapeutických přístupů.

K této práci jsem přispěla následovně: 20 %; zpracování nádorové tkáně a periferní krve pacientů, izolace RNA a stanovení exprese vybraných genů pomocí qPCR, analýza dat a účast na přípravě manuskriptu.

ORIGINAL RESEARCH

OncoImmunology 4:1, e965570; January 2015; Published with license by Taylor & Francis Group, LLC

Distinct patterns of intratumoral immune cell infiltrates in patients with HPV-associated compared to non-virally induced head and neck squamous cell carcinoma

Simona Partlová[1,2], Jan Bouček[3,4], Kamila Kloudová[1,2], Eva Lukešová[5,6], Michal Zábrodský[3], Marek Grega[7], Jitka Fučíková[1,2], Iva Truxová[1], Ruth Tachezy[5,6], Radek Špíšek[1,2], and Anna Fialová[1,2,*]

[1]Sotio, Prague, Czech Republic; [2]Department of Immunology; 2nd Faculty of Medicine; Charles University; Motol University Hospital; Prague, Czech Republic; [3]Department of Otorhinolaryngology and Head and Neck Surgery; 1st Faculty of Medicine; Charles University and Motol University Hospital; Prague, Czech Republic; [4]Institute of Microbiology ASCR; Prague, Czech Republic; [5]Department of Experimental Virology; Institute of Hematology and Blood Transfusion; Prague, Czech Republic; [6]Department of Genetics and Microbiology; Faculty of Science; Charles University; Prague, Czech Republic; [7]Department of Pathology and Molecular Medicine; 2nd Faculty of Medicine; Charles University and Motol University Hospital; Prague, Czech Republic

Keywords: $CD8^+$ T lymphocytes, HNSCC, HPV, PD-1, Tim-3

Abbreviations: Cox-2, cyclooxygenase 2; HNSCC, head and neck squamous cell carcinoma; HPV, human papillomavirus; mDC, myeloid dendritic cell; PD-1, programmed cell death 1; pDC, plasmacytoic dendritic cell; PD-L1, programmed cell death-ligand 1; Tim-3, T cell immunoglobulin and mucin protein 3; Treg, regulatory T cell

Human papillomavirus (HPV) infection is one of the most important etiologic causes of oropharyngeal head and neck squamous cell carcinoma (HNSCC). Patients with HPV-positive HNSCC were reported to have a better clinical outcome than patients with HPV-negative cancers. However, little is known about the possible causes of different clinical outcomes. In this study, we analyzed a detailed immune profile of tumor samples from HNSCC patients with respect to their HPV status. We analyzed the characteristics of immune cell infiltrates, including the frequency and distribution of antigen-presenting cells and naïve, regulatory and effector T cells and the cytokine and chemokine levels in tumor tissue. There was a profound difference in the extent and characteristics of intratumoral immune cell infiltrates in HNSCC patients based on their HPV status. In contrast to HPV-negative tumor tissues, HPV-positive tumor samples showed significantly higher numbers of infiltrating $IFN\gamma^+$ $CD8^+$ T lymphocytes, $IL\text{-}17^+$ $CD8^+$ T lymphocytes, myeloid dendritic cells and proinflammatory chemokines. Furthermore, HPV-positive tumors had significantly lower expression of *Cox-2* mRNA and higher expression of PD1 mRNA compared to HPV-negative tumors. The presence of a high level of intratumoral immune cell infiltrates might play a crucial role in the significantly better response of HPV-positive patients to standard therapy and their favorable clinical outcome. Furthermore, characterization of the HNSCC immune profile might be a valuable prognostic tool in addition to HPV status and might help identify novel targets for therapeutic strategies, including cancer immunotherapy.

Introduction

HNSCC is a heterogeneous group of tumors located in the oral cavity, oropharynx, hypopharynx and larynx. Originally, tobacco and/or alcohol exposure were the main risk factors for HNSCC, but in an expanding subset of patients with oropharyngeal carcinoma, HPV infection has been described in the last two decades as a crucial etiologic agent.[1,2] Although patients with HPV-associated tumors are more often diagnosed at advanced stages of the disease with large metastatic lymph nodes, their prognosis is reported to be significantly better than that of patients with non-HPV induced cancers.[3,4]

Despite the improved response of HPV-positive HNSCC to conventional treatment involving a combination of surgery, radiation therapy and chemotherapy, HPV-positive cell lines were shown to be more resistant to radiation and cisplatin *in vitro* when compared to HPV-negative cells. However, *in vivo*, HPV-positive tumors were more sensitive to

*Correspondence to: Anna Fialová; Email: Askallova@centrum.cz

Submitted: 07/04/2014; Revised: 09/05/2014; Accepted: 09/10/2014

http://dx.doi.org/10.4161/21624011.2014.965570

radio- and chemotherapy in immunocompetent mice. Importantly, neither radiotherapy nor cisplatin therapy cured immunocompromised mice, indicating an important role for the immune system in HPV-positive HNSCC outcome.[5] Although contradictory results recently published by Kimple et al.[6] showed enhanced radiation sensitivity in HPV-positive cancer cell lines, this finding does not explain why HPV-positive patients treated with surgery alone also have a better prognosis.[3] Moreover, in addition to the high proportion of relapses, especially in HPV-negative patients, conventional therapy remains associated with significant toxicity. Therefore, there is great interest in developing less toxic and more targeted therapies, including immunotherapy. Consequently, a better understanding of the interplay between the tumor microenvironment, HPV and the infiltrating immune cells is essential.

Indeed, characterization of the adaptive immune response has been shown to be an important prognostic tool in a wide range of carcinomas, potentially even more relevant than the current cancer staging system.[7-11] In HNSCC, recently published studies indicate that the assessment of the level of circulating $CD8^+$ T lymphocytes,[12] the extent of tumor infiltration by $CD8^+$ T lymphocytes and the ratio of infiltrating $CD8^+$/$FoxP3^+$ T lymphocytes[13,14] might have a prognostic significance. However, a complex profile of the particular tumor-infiltrating immune cell subsets, including antigen-presenting cells, has not been evaluated to date.

In this study, we analyzed the distribution and phenotype of $CD8^+$ and $CD4^+$ T cell subsets, dendritic cell subsets (DCs) and monocytes/macrophages as well as the chemokine and cytokine profile in fresh HNSCC samples with regard to HPV status. Our findings confirm that HPV-positive tumor samples show a distinct immunologic profile compared to HPV-negative samples, with high levels of infiltrating $IFN\gamma^+$ CD8+ T lymphocytes, $IL\text{-}17^+$ $CD8^+$ T lymphocytes (Tc17 lymphocytes), myeloid DCs and spontaneously produced proinflammatory chemokines and cytokines. Additionally, HPV-positive samples expressed significantly lower levels of *Cox-2* mRNA and higher levels of *PD-1* mRNA than HPV-negative samples.

Results

HPV-positive tumors are mostly localized in the oropharynx

As expected, only the HPV 16 type was detected in all of the samples that were positive for HPV DNA. The expression of HPV 16 E6 mRNA was detected in 45.5% ($n = 20$) of patients; 55.0% ($n = 11$) of the HPV-positive tumors were localized in the tonsils, 40.0% ($n = 8$) at the base of the tongue and 5.0% ($n = 1$) at the base of the oral cavity (**Table 1**). Lymph node metastases were histologically confirmed (pN^+) in 90.5% of HPV-positive and 66.7% of HPV-negative patients, but this difference did not reach a statistical significance. The tumor grade and the stage were equivalent in patients with HPV-positive and HPV-negative HNSCC.

Table 1. Frequency of HPV-positive and HPV-negative tumors

	HPV negative -		HPV positive +	
	N	%	N	%
Total	24	54.5	20	45.5
Tongue	9	37.5	8	40.0
Tonsil	2	8.3	11	55.0
Larynx	8	33.3	0	0
Others	5	20.8	1	5.0

Patients with HPV-positive HNSCC have significantly higher levels of tumor-infiltrating $CD8^+$ T cells with the capacity to produce IFNγ and IL-17 after *in vitro* stimulation.

The presence of tumor-infiltrating leukocytes, particularly $CD8^+$ T cells, was shown to be a strong prognostic marker in various types of cancer; therefore, we analyzed the numbers and proportions of tumor-infiltrating immune cells in HPV-positive and HPV-negative HNSCC patients. The levels of tumor-infiltrating $CD45^+$ leucocytes were significantly higher in HPV-positive tumor samples (**Fig. 1A**). As expected, there were significantly higher numbers of $CD8^+$ T cells in HPV-positive tumor tissue samples compared to HPV-negative samples (**Fig. 1B**). Additionally, significantly higher proportions of $CD8^+$ cells from HPV-positive samples produced IFNγ (**Fig. 1C and D**) or IL-17 (**Fig. 1E and F**) upon PMA and ionomycin stimulation *in vitro*.

Patients with HPV-positive HNSCC have higher numbers of $CD4^+$ T cells in tumor tissue

We observed a trend to an increase in the numbers of total $CD4^+$ T cells as well as IFNγ-producing $CD4^+$ cells (Th1 cells) in the HPV-positive tumor samples ($p < 0.1$) (**Fig. 2A–C**). The proportion of Th17 cells did not show any differences between HPV-positive and -negative tumors (**Fig. 2D and E**); however, single cell suspensions isolated from HPV-positive tumors produced significantly higher levels of IL-17 upon PMA and ionomycin stimulation *in vitro* ($p = 0.030$) (**Fig. 4C**). Additionally, we observed a slightly lower proportion of Tregs in HPV-positive tumors (**Fig. 2G**). None of the subsets of $CD4^+$ T cells listed above showed any statistically significant differences between patients with HPV-positive and -negative tumors, but significantly higher numbers of naïve T cells were detected in HPV-positive tumor tissues compared to HPV-negative tumor samples ($p = 0.018$) (**Fig. 2H and I**).

HPV-positive HNSCC samples have increased numbers of tumor-infiltrating antigen presenting cells

Additionally, we also analyzed subsets of antigen presenting cells, namely mDCs, pDCs and monocytes/macrophages in the tumor tissue. We observed an increased frequency of all of these cell populations in patients with HPV-positive tumors. The total numbers of mDCs in HPV-positive tumor samples showed a statistically significant increase compared to HPV-negative samples; however, the frequency of pDCs and monocytes/macrophages were not statistically

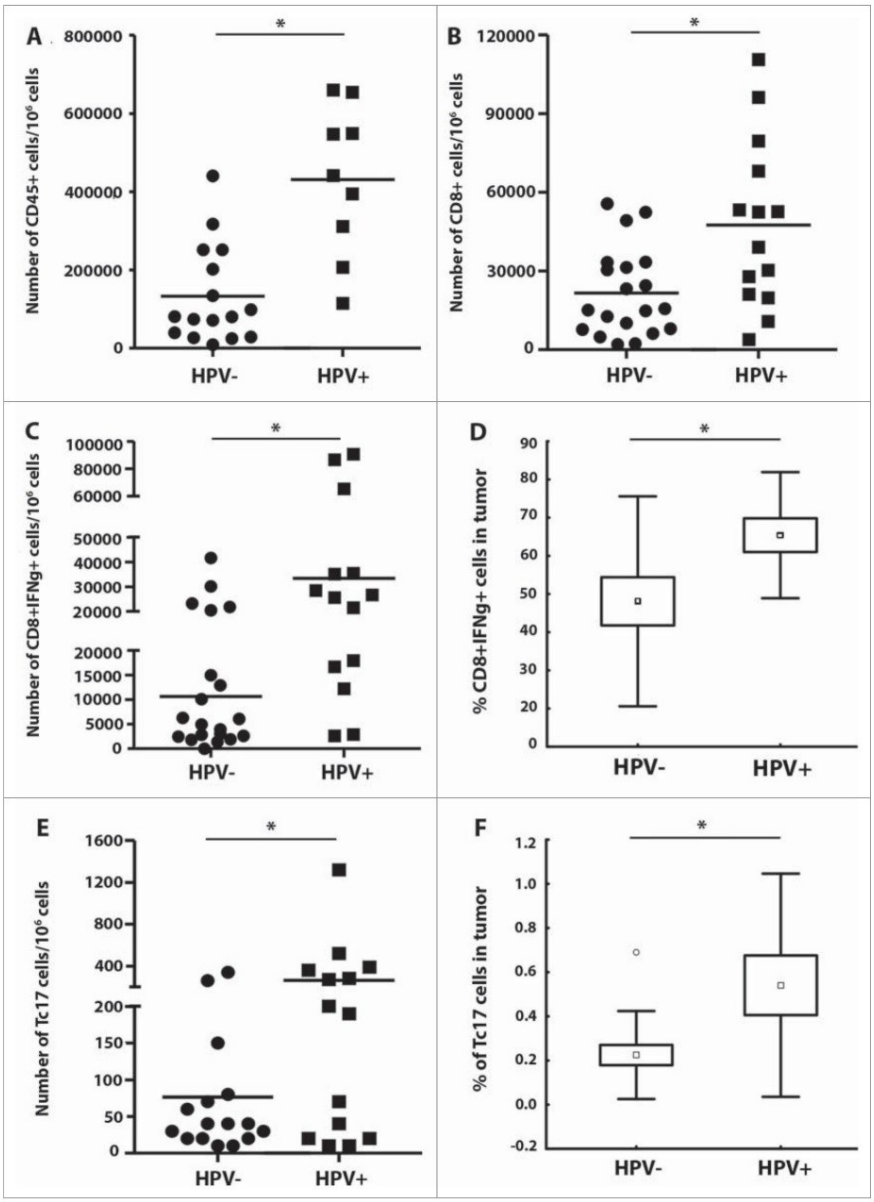

Figure 1. Proportions of leukocytes within tumor tissues of head and neck squamous cell carcinoma (HNSCC) patients ($n = 44$) according to human papillomavirus (HPV)-status. To evaluate the pattern of the immune cell infiltrates, tumor-derived single cell suspensions were stimulated with PMA and ionomycin in the presence of Brefeldin A and analyzed by flow cytometry. (**A–C, and E**) The data are expressed as the numbers of $CD45^+$ cells, $CD8^+$ cells, $CD8^+IFN\gamma^+$ cells and Tc17 in 1×10^6 isolated tumor-derived cells; the line represents the mean value. (**D and F**) Box plots represent the proportions of $CD8^+IFN\gamma^+$ cells and $CD8^+IL\text{-}17^+$ (Tc17 cells) among the tumor-infiltrating $CD8^+$ T cells. The boundaries of the box indicate the standard error of the mean (SEM), and the lines in the box represent the median. Whiskers indicate the standard deviation (SD). * $p < 0.05$ (General Linear Models; age was added as a covariate).

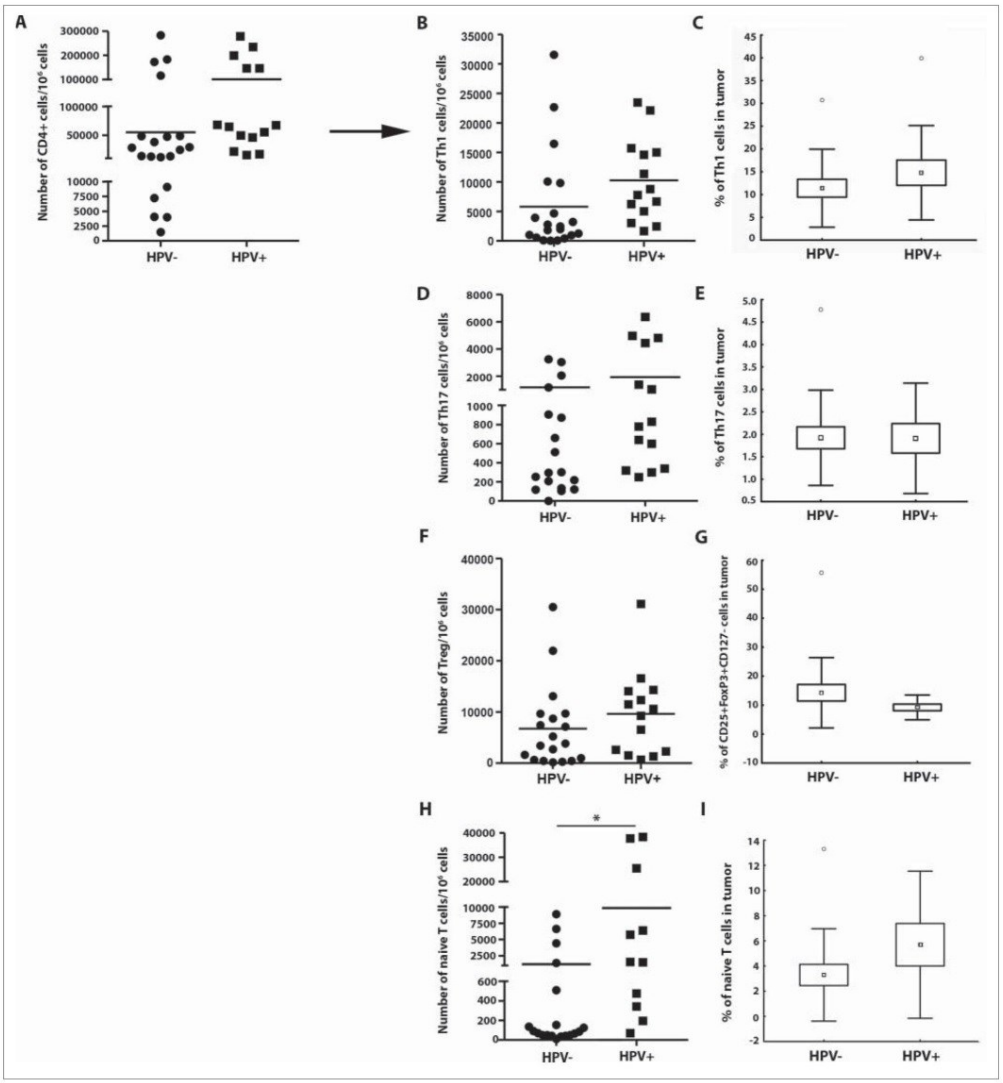

Figure 2. The frequency of $CD4^+$ T cell subsets in the tumor tissues ($n = 44$) with regard to human papillomavirus (HPV)-status. To evaluate the subtypes of tumor-infiltrating $CD4^+$ T cells, tumor-derived single cell suspensions were stimulated with PMA and ionomycin in the presence of Brefeldin A and analyzed by flow cytometry. (**A, B, D, F, and H**) The plots represent the numbers of Th1 cells, Th17 cells, Tregs or naïve T cells within 10^6 isolated tumor-derived cells; the lines in the box represent the median. (**C, E, G, and I**) The data are expressed as the proportion of Th1 cells, Th17 cells, Tregs and naïve T cells, respectively, among the tumor-infiltrating $CD4^+$ cells. The boundaries of the box indicate the SEM, and the lines in the box represent the mean. Whiskers indicate the SD * $p < 0.05$ (General Linear Models; age was added as a covariate).

significantly different (**Fig. 3**). As expected, we detected high proportions of $CD16^+$ HNSCC-infiltrating mDCs, but these proportions did not differ between HPV-negative and HPV-positive tumor tissues (70.9 ± 4.5% and 65.5 ± 2.3%, respectively).

HPV-positive tumor tissue-derived single cell suspensions produced higher levels of chemokines, but the cytokine profile was not significantly different

To evaluate whether the increased frequency of leukocytes in HPV-positive tumor samples could be caused by the recruitment

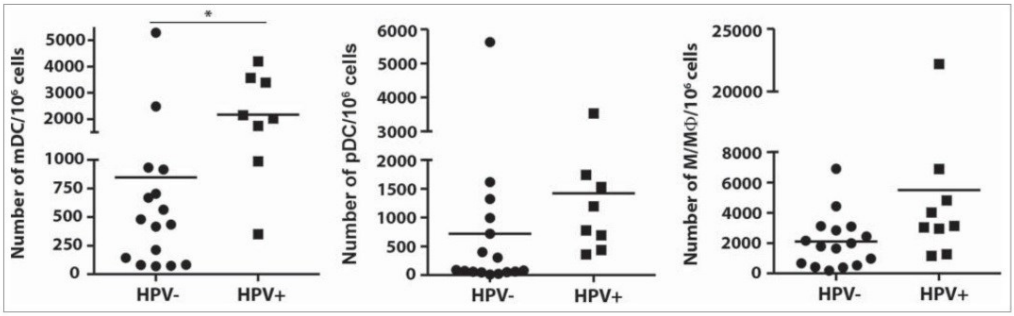

Figure 3. Numbers of dendritic cells (DCs) and monocytes/macrophages within the tumor tissue of head and neck squamous cell carcinoma (HNSCC) patients ($n = 26$) in relation to human papillomavirus (HPV)-status. To assess the pattern of tumor-infiltrating antigen presenting cells, fresh tumor-derived single cell suspensions were analyzed by flow cytometry. (**A**) The data are expressed as the numbers of myeloid dendritic cells (mDCs, characterized as CD45+LIN-HLA-DR+CD14-CD11c+), plasmacytoid dendritic cells (pDCs, characterized as CD45+LIN-HLA-DR+CD14-CD123+) and monocytes/macrophages (Mo/M^{Φ}, characterized as CD45+LIN-HLA-DR+CD14+) in 10^6 isolated tumor-derived cells. The lines represent the mean value. * $p < 0.05$ (General Linear Models; age was added as a covariate).

of leukocytes to tumor sites rather than their polarization *in situ*, as shown in our previous study,[15] we analyzed the chemokine and cytokine profiles of the tumor-derived cell culture supernatants.

In the supernatants from unstimulated cell cultures, high levels of CXCL9, CXCL10, CXCL12, CCL20, CCL21 and CCL22 were detected. Of the other chemokines measured, only CCL5, CCL17 and CCL19 were at low levels (**Fig. 4A**). Markedly higher production of CXCL9, CXCL10, CXCL12, CCL17 and CCL21 was detected in the supernatants of HPV-positive patient samples compared to HPV-negative patient samples; however, only the levels of CCL17 and CCL21 showed statistically significant differences ($p = 0.023$ and $p = 0.040$, respectively). As expected, the levels of CXCL12 positively correlated with the lymph node status (average values: N0 = 0 pg/mL and N1–3 = 8331.3 ± 2357.1 pg/mL).

Surprisingly, even in unstimulated cell cultures, we were able to detect most of the cytokines analyzed with the exception of IL-4 and IL-12 (**Fig. 4B**). HPV-positive cell cultures tended to produce higher levels of IL-2, IL-17, IL-23 and IFNγ and lower levels of IL-1 β, but these differences were not statistically significant. In supernatants of HPV-positive tumors upon PMA and ionomycin stimulation we detected higher levels of IL-10, IL-17, IL-21, TNFα and IFNγ compared to supernatants of HPV-negative tumor samples; however, only the levels of IL-17 showed statistically significant differences ($p = 0.030$) (**Fig. 4C**).

HPV-positive tumor samples expressed lower levels of *Cox-2* and Tim-3 mRNA and higher levels of PD-1 mRNA

In addition to the flow cytometry data described above, we analyzed the mRNA expression levels of four regulatory genes, *Cox-2*, *PD-1*, *PD-L1* and *Tim-3*, in the tumor tissue samples and in metastatic and control lymph nodes of patients with HPV-positive and HPV-negative tumors.

We observed markedly higher expression of all of the analyzed genes except *PD-1* in tumor tissues and metastatic lymph nodes compared to control lymph nodes, regardless of HPV status (**Fig. 5A**). In comparison to the HPV-positive tumor tissues, we detected a significant increase in the expression of the negative prognostic marker *Cox-2* in the HPV-negative samples ($p = 0.016$). On the contrary, we observed a significantly higher expression of PD-1 in HPV-positive tumor tissues compared to HPV-negative samples ($p = 0.018$). The mRNA expression level of Tim-3 was similar in both groups of patients (**Fig. 5E**). However, because we observed markedly higher numbers of $CD45^+$ cells in the HPV-positive tumor tissues (**Fig. 1A**), we decided to normalize the expression levels of PD-1 and Tim-3 mRNA to the expression level of $CD45^+$ mRNA. When the results were normalized to $CD45^+$ mRNA expression, we observed higher levels of PD-1 and lower levels of Tim-3 in HPV-positive tissue samples compared to HPV-negative tumors, but these differences were not statistically significant (**Fig. 5F**).

In addition to mRNA expression, we analyzed the expression of *PD-1* and *Tim-3* on freshly isolated tumor-derived cells using flow cytometry. Both *PD-1* and *Tim-3* were mainly expressed on $CD3^+$ T lymphocytes (**Fig. 5C**). Whereas *PD-1* was frequently expressed on $CD8^+$ and $CD4^+$ T cells in all of the tissues analyzed, particularly in the peripheral blood, control lymph nodes, metastatic lymph nodes and tumor tissue, *Tim-3* was mainly expressed on tumor-infiltrating T-lymphocytes (**Fig. 5D**). As expected, we observed substantially decreased production of IFNγ by Tim-3+PD-1+ $CD8^+$ T cells compared to both Tim-3-PD-1-$CD8^+$ T cells and Tim-3-PD-1+ $CD8^+$ T cells (**Fig. 5B**), whereas there was no difference in IFNγ production in $CD4^+$ T cells with regard to the expression of PD-1 and Tim-3.

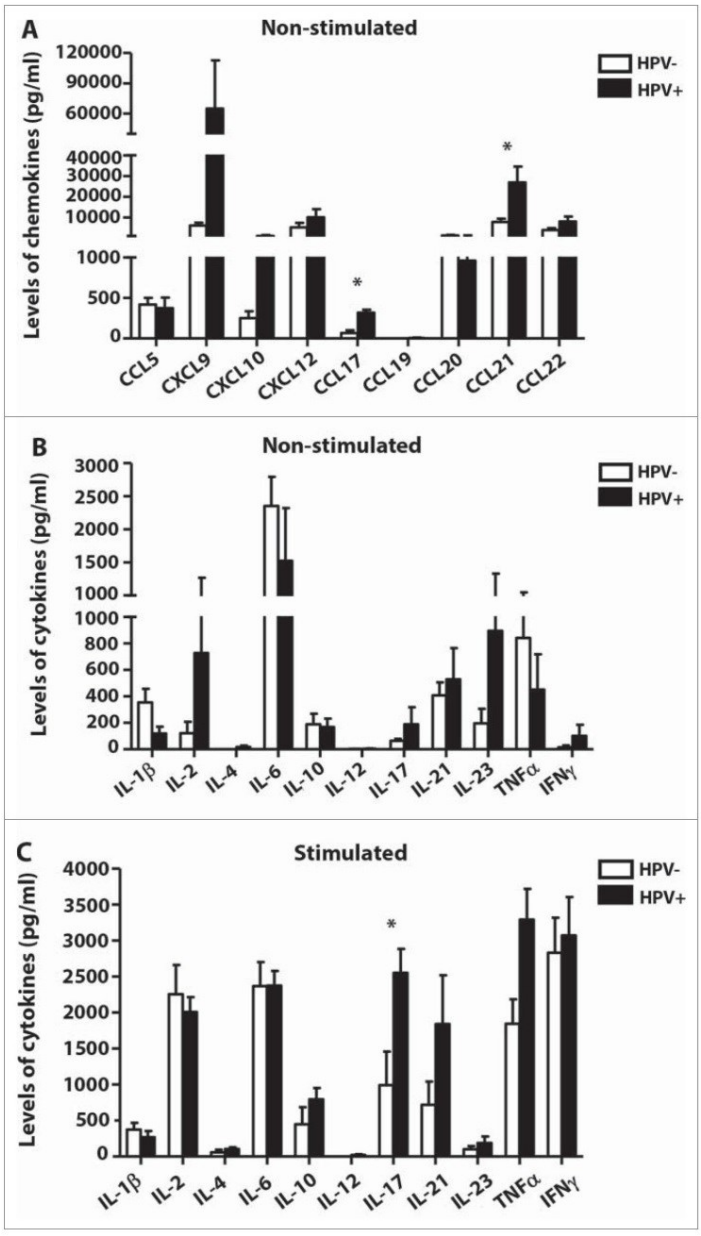

Figure 4. Chemokine and cytokine profiles of tumor-derived single cell suspensions (HPV-negative samples: $n = 7$; HPV-positive samples: $n = 7$). Supernatants of tumor-derived single cell suspension cultures were analyzed using a Quantibody Array Kit (Raybiotech, Norcross, GA). (**A**) The white columns represent the mean spontaneous chemokine production after 24 h for culture supernatants from HPV-negative patients; the black columns represent the mean production from human papillomavirus (HPV)-positive patients. (**B**) The white columns represent the mean spontaneous cytokine production after 24 h for culture supernatants from HPV-negative patients; the black columns represent the mean production from HPV-positive patients. (**C**) The white columns represent the mean cytokine production upon PMA and ionomycin stimulation after 24 h for culture supernatants from HPV-negative patients; the black columns represent the mean production from HPV-positive patients. All of the error bars indicate the SEM * $p <$ 0.05 (General Linear Models; age was added as a covariate).

Discussion

There are two major causative agents of HNSCC, namely tobacco and/or alcohol consumption and a high-risk HPV infection. HPV-associated tumors are known to show a different molecular profile than tobacco/alcohol-induced cancers, similar to HPV-positive cervical tumors. Although HPV-positive HNSCC patients are often diagnosed at a late stage of the disease with developed nodal metastases, their prognosis is significantly better compared to HPV-negative cancers.[2] It has been suggested that the improved response of HPV-positive HNSCC patients to the conventional treatment was related to the immune system[5]; however, a detailed analysis of the pattern of tumor-infiltrating immune cells in HPV-positive compared to HPV-negative HNSCC tissues has not been performed to date.

In this prospective study, we analyzed the immune profile of 54 fresh HNSCC samples with regard to their HPV status. We report that HPV-positive tumors have a markedly different immunologic profile compared to HPV-negative tumors, with high levels of infiltrating $CD8^+$ $IFN\gamma^+$ T lymphocytes, Tc17 lymphocytes, naïve $CD4^+$ T lymphocytes and myeloid DCs. HPV-positive tumor tissue-derived cell cultures produced markedly higher levels of chemokines, namely CXCL9, CXCL10, CXCL12, CCL17 and CCL21, and slightly higher levels of the cytokines IL-2, IL-17, IL-23 and IFNγ. Additionally, HPV-positive samples expressed significantly lower levels of *Cox-2* mRNA and higher levels of PD-1 mRNA.

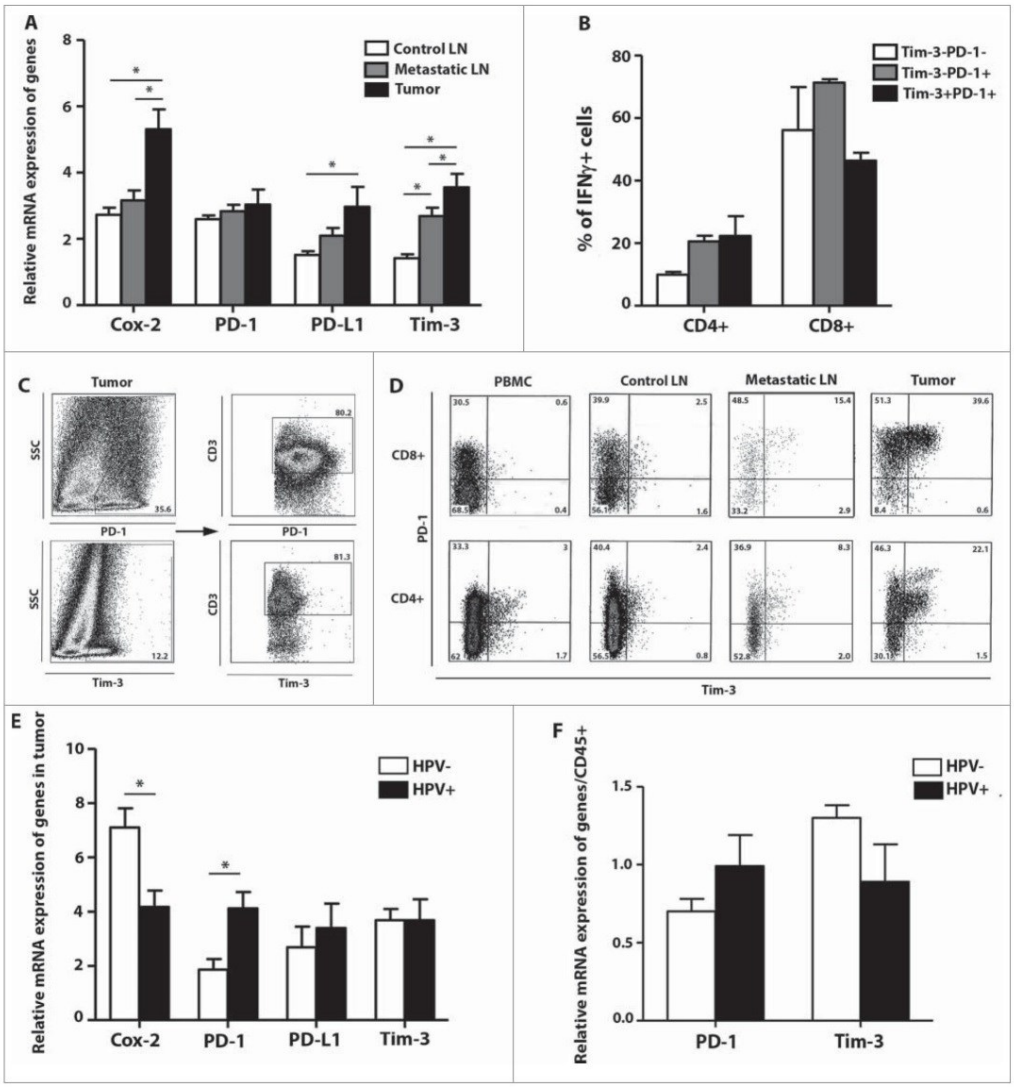

Figure 5. The levels of cyclooxygenase 2 (*Cox-2*), programmed cell death 1 (PD-1), programmed cell death-ligand 1 (PD-L1) and T cell immunoglobulin and mucin domain containing protein-3 (Tim-3) in control and metastatic lymph nodes and tumor tissue from head and neck squamous cell carcinoma (HNSCC) patients. (**A**) The white columns represent the relative mRNA expression of *Cox-2*, *PD-1*, *PD-L1* and *Tim-3* in control lymph nodes (LN; $n = 14$); the gray columns represent the relative mRNA expression of genes in metastatic lymph nodes ($n = 14$); the black columns represent the relative mRNA expression of these genes in tumor tissues ($n = 14$). To assess the expression levels of mRNA, cDNA was synthesized from total tumor and lymph node RNA and amplified by quantitative real time PCR. As an internal reference, β-actin housekeeping gene was used. (**B**) The columns represent the mean proportion of $IFN\gamma^+$ cells among Tim-3-PD-1- (white column), Tim-3-PD-1+ (gray column) and Tim-3+PD-1+ (black column) cells in the tumor tissue ($n = 6$). To analyze the IFNγ production, tumor-derived single cell suspensions were stimulated with PMA and ionomycin in the presence of Brefeldin A and analyzed by flow cytometry. (**C**) Dot plots show the expression of $CD3^+$ on $PD\text{-}1^+$ or $Tim\text{-}3^+$ tumor-infiltrating cells from a representative patient. (**D**) Dot plots are gated on $CD3^+CD8^+$ cells (upper line) and $CD3^+CD4^-$ cells (lower line) and show the expression of *Tim-3* and *PD-1* in the peripheral blood, control LN, metastatic LN and tumor tissue from a representative patient. The columns represent the mean relative mRNA expression of *Cox-2*, *PD-1*, *PD-L1* and *Tim-3* or *PD-1* and *Tim-3*, respectively, in HPV- (white columns) and HPV+ (black columns) tumor samples ($n = 14$) with (**F**) or without (**E**) normalization to the expression level of $CD45^+$ mRNA. All of the error bars indicate the SEM * $p < 0.05$ (**A**, paired t-test; **B**, Friedman ANOVA; **E and F**, General Linear Models; age was added as a covariate).

It has been convincingly shown that a high density of tumor-infiltrating $CD8^+$ T lymphocytes is predictive of a favorable clinical outcome in different types of cancers, including HNSCC.[7,9,10,14,16] Because most of the studies focusing on the quantification of tumor-infiltrating immune cells in HNSCC were retrospective and based on immunohistochemical data, the detailed phenotype of $CD8^+$ T cells had not yet been evaluated. Importantly, recent HNSCC studies[17,18] suggest that other characteristics of the intratumoral $CD8^+$ T lymphocytes, such as their location within the tumor, PD-1 expression, as well as the expression of HLA-class I, SCINDERIN and EPHRIN-A1 in the tumor cells might have a strong impact on the prognostic value of the $CD8^+$ T cells. Therefore, not only a quantitative, but also a qualitative analysis of the immune cell infiltrates seems to be crucial for the identification of clinically relevant prognostic markers. Our data show that tumor-infiltrating $CD8^+$ T cells in HPV-positive tumor samples not only were more frequent but also had a higher capacity to produce IFNγ and IL-17 upon PMA and ionomycin stimulation compared to HPV-negative tumors, indicating a stronger immune response.

The role of $CD4^+$ T cells in anticancer immunity is more controversial. Most of the studies examining tumor-infiltrating $CD4^+$ T cells as possible prognostic markers focused on regulatory T cells. The role of Tregs seems to differ according to the type and etiology of the cancer. On one hand, Tregs are known to be the key mediators of tumor immune suppression, and high numbers of tumor-infiltrating Tregs have been related to poor outcome in many types of cancer.[19-22] On the other hand, Tregs have been described as a positive prognostic factor in colorectal cancer and lymphomas.[23,24] In HNSCC, Badoual et al.[25] showed that high numbers of tumor-infiltrating Tregs positively correlated with locoregional control. Similarly, other groups studying these cells confirmed the positive correlation between the numbers of intratumoral Tregs and the overall survival.[26,27]On the contrary, Nasman et al.[13] demonstrated that a high $CD8^+$/FoxP3$^+$ T cell ratio correlated with longer disease-free survival. With regard to the significance of peripheral blood Tregs, Boucek et al.[28] showed that high levels of Tregs in the peripheral blood of HNSCC patients at the time of primary diagnosis might predict an early recurrence of the disease. In our study, we found higher numbers of $CD4^+$ T cells in HPV-positive tumor samples, with slightly higher proportions of Th1 cells and a significantly higher number and frequency of naïve T cells. No statistically significant differences were observed in the numbers and proportions of Tregs and Th17 cells. For understanding the possible relationship between the increased immune infiltration of HPV-positive tumors and HPV-specific immune response, it will be important to analyze the specificity of infiltrating T cells. It is conceivable that, at least some, infiltrating T cells in HPV-positive head and neck tumors will be HPV specific as already suggested by recent studies.[29] These results are comparable to what is found in anogenital HPV16 induced lesions.[30,31] However, the detailed analysis of tumor specificity and viral specificity of T cells present in the head and neck tumors needs to be performed in future studies.

In addition to the increased lymphocytic infiltration, we observed higher numbers of mDCs and slightly higher numbers of pDCs and monocytes/macrophages in HPV-positive tumors. High numbers of $CD68^+$ macrophages infiltrating HNSCC were shown to correlate with lymph node metastasis, extracapsular spread and an advanced stage of disease.[32] In accordance with these results, we found that the numbers of monocytes/macrophages significantly positively correlated with the lymph node status ($p = 0.048$, data not shown). The prognostic impact of DC subtypes on the tumor microenvironment is less clear. Most likely, the phenotype, not only the number, of DCs might be crucial.[10] It was shown that in HNSCC, monocytes and DCs express the low-affinity FcγRIII (CD16).[33] As HNSCC patients are known to have high levels of antigen-antibody immune complexes[34] that activate monocytes and DCs via CD16,[35] CD16 crosslinking might promote pro-tumor and angiogenic activities.[36] Indeed, in our study, we also found a markedly higher number of tumor-infiltrating CD16+ mDCs (70.9± 4.5% for HPV-negative tumors and 65.5 ± 2.3% for HPV-positive tumors) than CD16-mDCs. However, the prognostic value of these mDC subtypes remains to be elucidated.

In addition to differences in immune cell infiltrates, we also observed a markedly different chemokine profile in HPV-positive and HPV-negative tumor tissue-derived cell cultures. HPV-positive tumor tissue-derived cell cultures produced much higher levels of chemokines, namely CXCL9, CXCL10, CXCL12, CCL17 and CCL21. The chemokine CXCL12 (SDF-1) and its receptor CXCR4 were shown to play a key role in regulating the trafficking of cancer cells to sites of metastases.[37,38] Indeed, in our study, only cell cultures derived from patients with lymph node metastases produced CXCL12 (N0 = 0 pg/mL compared to N1–3 = 8331.3± 2357.1 pg/mL). As nodal metastases were detected in 90.5% of the patients with HPV-positive and 66.7% of the patients with HPV-negative tumor samples, the differences in CXCL12 levels most likely reflect this fact. The levels of CCL17 (TARC), a ligand for CCR4, positively correlated with the numbers of tumor-infiltrating Th17, Th1 and $CD8^+$ T lymphocytes. In mice, CCL17 was shown to be mainly produced by mature DCs of myeloid origin.[39] We did not observe any correlation between CCL17 production and the numbers of mDCs in the tumor tissue; however, we observed a significant positive correlation between the CCL17 levels and the numbers of tumor-infiltrating pDCs ($r = 0.91$; $p < 0.001$). Surprisingly, the levels of CCL21, a ligand for CCR7, positively correlated only with the frequency of Th17 cells but not with the number or frequency of DCs and naïve T cells. Although tumor-derived cells of HPV-positive tumors also expressed higher levels of proinflammatory cytokines, namely IL-2, IL-17, IL-23 and IFNγ, these differences did not reach statistical significance due to high variability in the samples.

Analysis of the mRNA expression levels of four regulatory genes, *Cox-2*, *PD-1*, *PD-L1* and *Tim-3*, also showed differences associated with HPV status. The expression of *Cox-2*, which specifically catalyzes the production of prostaglandins, is undetectable in most healthy tissues but is usually overexpressed in inflammation, premalignant lesions and tumors. Functionally,

Cox-2-derived prostaglandins were shown to promote angiogenesis and induce tumor invasion.[40,41] Consequently, high *Cox-2* expression was associated with an unfavorable outcome in breast cancer patients.[42] We detected basal expression of *Cox-2* in control lymph nodes and significant overexpression of *Cox-2* in tumor tissues from our cohort of HNSCC patients (**Fig. 5A**). The levels of *Cox-2* mRNA negatively correlated with the numbers of tumor-infiltrating Th1 and Th17 lymphocytes ($p = 0.002$ and $p = 0.003$, respectively, data not shown) and positively correlated with the mRNA expression of *Tim-3* ($p = 0.008$, data not shown). Interestingly, the HPV-positive tumor samples expressed significantly lower levels of *Cox-2* mRNA compared to the HPV-negative samples, which is in accordance with a previous report stating an improved outcome in HPV-positive HNSCC patients.[2]

The surface receptors *PD-1* and *Tim-3* belong to a group of immune checkpoint proteins that decrease T-cell reactivity and were identified, together with CTLA-4 and Lag-3, as benchmarks for exhausted T cells.[43] Dysfunctional, exhausted T cells develop after long-term exposure to a high antigen load[44] and are incapable of exhibiting robust effector responses to further antigen re-challenge.[45,46] Interestingly, in cancer, dysfunctional T cells expressing *Tim-3* and *PD-1* were only found in tumor tissue but not in the peripheral blood.[47] Importantly, tumor-infiltrating $CD8^+$ Tim-3+ PD-1+ cells exhibited a surface phenotype that is consistent with effector/memory T cells, indicating that exhausted T cells emerge from effector T cells.[48] Indeed, it was recently shown that exhausted T cells are successfully re-functionalized by blocking checkpoint receptors. Consequently, cancer immunotherapy using T-cell checkpoint inhibitors has become one of the most promising new therapeutic approaches.

In agreement with published data, we only found high proportions of Tim-3+ PD-1+ T cells in tumor tissue but not in the peripheral blood and control lymph nodes of HNSCC patients. On the contrary, Tim-3-PD-1+ T cells were observed in all of the tissues analyzed. Consistent with the flow cytometry data, we detected significantly higher levels of Tim-3 but not *PD-1* mRNA in tumor tissue compared to control lymph nodes. To examine the capacity of Tim-3-PD-1-, Tim-3-PD-1+ and Tim-3+PD-1+ tumor-infiltrating T cells to produce IFNγ, we analyzed the phenotype of these cells after *in vitro* stimulation with PMA and ionomycin using flow cytometry. Although we detected IFNγ-producing cells in all of the subtypes of T cells tested, the proportions of $IFN\gamma^+$ T cells were markedly lower in $CD8^+$PD-1+Tim-3+ T cells compared to $CD8^+$PD-1+Tim-3- and $CD8^+$PD-1-Tim-3- T cells, as expected. These data indicate that Tim-3 together with PD-1 might be considered a better exhaustion marker in HNSCC-infiltrating $CD8^+$ T cells than PD-1 alone.

Badoual et al.[18] showed that high levels of tumor-infiltrating PD-1+ T cells correlated with better survival in HNSCC patients. In agreement with these results, we observed higher *PD-1* expression in HPV-positive tumor samples compared to HPV-negative tumors. In a preclinical model, Badoual et al.[18] showed that partial grafting of the HPV E7-expressing TC-1 epithelial cell line, which constitutively expresses PD-L1, is dependent on the presence of HPV-specific PD-1+ $CD8^+$ T cells. An anti-PD-L1 monoclonal antibody vaccine further enhanced this immune response. Here, we confirmed that *PD-L1* was markedly more expressed in tumor tissue than in the control lymph nodes. As *Tim-3* expression was also tumor tissue specific, these two molecules, instead of *PD-1* alone, might be a very promising target for immunotherapy in HNSCC.

Taken together, our data show that HPV-positive tumor tissues have a distinct immune profile compared to HPV- negative tumors. Substantial infiltrates of immune cells are usually associated with a good prognosis and indicate a strong past antitumor immune response in HPV-positive tumors, which might be reactivated/reprogrammed by not only a targeted immunotherapy approach, but even during the standard therapy. Better understanding of targets of the immune response in HPV-positive vs. HPV-negative tumors and of mechanisms directing the recruitment of immune cells to the tumor will hopefully lead to the design of successful immunotherapeutic strategies.

Materials and Methods

Patients and samples

Blood samples, primary HNSCC specimens metastatic and control lymph nodes were obtained from 54 patients immediately after radical surgery at the Department of Otorhinolaryngology and Head and Neck Surgery, 1st Faculty of Medicine, Charles University and Motol University Hospital in Prague between April 2011 and November 2013. The patients enrolled in this study had not received any neoadjuvant chemo- or radiotherapy. All of the patients signed an informed consent approved by the Institutional Review Board of the University Motol. The clinical-pathological characteristics of the patients are summarized in **Table 2**.

The tumor tissues, metastatic and control lymph nodes were minced into small pieces with scissors and digested in RPMI 1640 containing 1 mg/mL of Collagenase D and 0.05 mg/mL of DNase I (both from Roche, 11088866001, 11284932001) for 30 min at 37°C under permanent gentle rocking motion. Afterwards, the specimens were passed through a 100-μm nylon cell strainer (BD Biosciences, 352360) and washed with PBS. The PBMCs were isolated from the peripheral blood by centrifugation on a Ficoll-Paque density gradient (GE Healthcare, 17-1440-03).

Flow cytometry

Single cell suspensions from peripheral blood, tumor tissue and control lymph nodes were used for cell surface labeling using monoclonal antibodies (mAbs) against CD3, $CD8^+$, CD11 c, CD14, CD16, CD19, CD20, CD45, CD45RA, CD45RO, CD56, CD62 L (Exbio), $CD4^+$, CD123 (eBioscience, 12-1239-41), HLA-DR (BD Biosciences, 335830) and CCR7 (BioLegend, 353220) for detection of myeloid DCs (mDCs characterized as CD45+LIN-HLA-DR+CD14-CD11c+), plasmacytoid DCs (pDCs; CD45+LIN-HLA-

Table 2. Clinical-pathological characteristics of the patients

Variable	No.	%
Total no. of patients	54	
Age		
Mean	62	
Range	38–78	
Sex		
Male	44	81.5
Female	10	18.5
Tumor grade		
1	8	14.8
2	30	55.6
3	16	29.6
4	0	0
Nodal status		
N0	13	24.1
N1	11	20.4
N2	28	51.9
N3	2	3.7
Stage		
I	3	5.6
II	5	9.3
III	9	16.7
IV	37	68.5
Tumor site		
Tongue	20	37
Tonsil	17	31.5
Larynx	10	18.5
Verbal base	3	5.6
Hypopharynx	2	3.7
Gl. submandibularis	1	1.9
Floor of mouth	1	1.9
HPV status		
HPV−	24	44.4
HPV+	20	37
Non-defined	10	18.5

DR+CD14-CD123+), monocytes/macrophages (M/Mϕ; CD45+LIN-HLA-DR+CD14+) and naïve T lymphocytes (defined as CD3+CD4+CD45RA+CD45RO-CCR7+ CD62L+). The following anti-human mAbs were used for staining regulatory T cells (Tregs): anti-CD3 (Exbio, A7-202-T100), anti-$CD4^+$ (eBioscience, 25-0049-42), anti-$CD8^+$ (Exbio, 1 T-207-T100), anti-CD25 and anti-CD127 (BioLegend, 302626, 351318) for surface labeling, which was followed by fixation and permeabilization using the FoxP3 staining buffer set (eBioscience) and intracellular staining with anti-FoxP3 (eBioscience, 53-4776-42) and anti-Helios (BioLegend, 137216) antibodies. For analysis of Th17 and Th1 lymphocytes, cell suspensions were stimulated for 4 h with 50 ng/mL of PMA and 1 μg/mL of ionomycin (Sigma-Aldrich, P8139-1MG, I0634-1MG) in the presence of Brefeldin A (BioLegend, 420601) before intracellular staining. Next, the cells were stained with anti-CD3 (Exbio), anti-$CD4^+$ (eBioscience), anti-$CD8^+$ (Exbio), anti-PD-1 (BioLegend, 329908) and anti-Tim-3 (BioLegend, 345006) antibodies, fixed, permeabilized and labeled with mAbs against IL-17 (BioLegend, 512310) and IFNγ (BD Biosciences, 554551). The cells were analyzed on a BD FACSCanto II (BD Biosciences) and evaluated with FlowJo software (TreeStar).

Chemokine and cytokine analysis

For the analysis of IL-1β, IL-2, IL-4, IL-6, IL-10, IL-12, IL-17, IL-21, IL-23, TNFα, IFNγ, CCL5, CCL17, CCL19, CCL20, CCL21, CCL22, CXCL9, CXCL10, and CXCL12 in culture supernatants harvested from tumor tissue-derived cell suspensions, a Quantibody Array Kit (Raybiotech) was used. Cell suspensions at the concentration of 1×10^6/mL in the presence or absence of PMA and ionomycin were cultured for 24 h in RPMI 1640 supplemented with 10% FCS, Glutamax and penicillin-streptomycin (Invitrogen, A12860-01, 15140-130). The supernatants were then collected and stored at -80°C until use.

RNA extraction and quantitative real time PCR

Total RNA was extracted from 2×10^6 tumor-tissue derived cells using an RNA Easy Mini Kit (Qiagen). RNA concentrations were determined with a NanoDrop© 2000 c UV-Vis spectrophotometer (Thermo Scientific), and the RNA integrity was assessed using an Experion automated system (BioRad). cDNA was synthesized from total RNA using the M-MLV reverse transcriptase (Invitrogen) and amplified by quantitative real time PCR in the presence of primers and TaqMan© probes specific for *Cox-2*, *PD-1*, *PD-L1* and *Tim-3*, as well as the β-actin housekeeping gene, which was used as an internal reference. All primers and probes were commercially synthesized (TIB MOLBIOL). The identity of the qPCR products in each assay was verified by sequencing. The relative expression of the target genes was normalized to the expression of β-actin.

HPV Detection

Tumor samples

The pathologist obtained two side-by-side sections of the tumor from the primary site. One of the paired sections from each anatomical location was labeled, snaps frozen in liquid nitrogen, and stored for future analysis. The other section from each pair was fixed in 10% neutral formalin and paraffin embedded. From each paraffin block, the first and last sections were histologically analyzed to confirm that the sections in between that were designated for the detection of viral nucleic acids and immuno-histochemical (IHC) analysis contained at least 10% of the tumor cells from the entire volume of the sample. Both DNA and RNA, were extracted from the tumor tissue using the Ambion Recover All TM Total Nucleic Acid Isolation Kit for FFPE Tissues (Applied Bioscience) as previously reported.[49] Care was taken to avoid sample cross-contamination.

PCR

All procedures have been described in detail previously.[49,50] HPV DNA detection was performed by PCR with primers specific for the L1 region ($GP5^+/GP6^+$) as described previously.[51] As an internal control, a 110-bp fragment of the human β-globin gene was amplified.[52] HPV typing was performed by reverse line

blot hybridization (RLB) with probes specific for 37 types as specified in detail by van den Brule et al.[53] From the total RNA, cDNA was prepared by reverse transcription. The absence of contaminating DNA was confirmed by amplification of the internal GAPDH internal control gene.[54] As a control for the integrity of the mRNA, the β-globin gene was amplified. Amplification of the HPV 16E6*I mRNA oncoprotein was performed with primers that amplify the 86-bp fragment.[55]

Immunohistochemical analysis

IHC examination was performed as described previously.[49] Briefly, the antibody *p*16INK4 a (purified mouse anti-human p16, Clone G175-405, BD PharMingen TM, dilution 1:100) was used. The intensity of staining (graded + to +++) and the proportion of cells stained (scored in percentages) were evaluated. For *p*16 immunostaining, the location of the signal (cytoplasmic and/or nuclear) was also specified. A semi-quantitative evaluation was performed. The samples considered positive for *p*16 expression exhibited more than 50% positive cells and nuclear and/or cytoplasmic staining.

Statistical analysis

Statistical analyses were performed using Statistica® 10.0 software (StatSoft).

The parametric assumptions of the data were verified using the Kolmogorov–Smirnov test for normality. The homogeneity of the variances was tested by the Levene test. The differences between HPV-positive and HPV-negative tumor samples were analyzed using a general linear model (GLM), and age was added as a covariate. The differences between control lymph nodes and tumor tissue were analyzed using a paired t-test. The results were considered statistically significant when $p < 0.05$.

Disclosure of Potential Conflicts of Interest

No potential conflicts of interest were disclosed.

Acknowledgments

The authors thank Dr. Ludek Sojka for the analysis and interpretation of mRNA data.

Funding

This project was supported by research grant NT 11542 from the Grant Agency of the Ministry of Health of the Czech Republic, GAUK 5734/2012 from Charles University, grant 00064203 from University Hospital Motol, Prague, Czech Republic, grants SVV 266513; UNCE 204013 and PRVOUK 27-1, Biocev, the joint project of Academy of Science and Charles University (CZ.1.05/1.1.00/02.0109) and from the European Regional Development Fund.

References

1. Nasman A, Attner P, Hammarstedt L, Du J, Eriksson M, Giraud G, Ahrlund-Richter S, Marklund L, Romanitan M, Lindquist D et al. Incidence of human papillomavirus (HPV) positive tonsillar carcinoma in Stockholm, Sweden: an epidemic of viral-induced carcinoma? Int J Cancer 2009; 125:362-6; PMID:19330833; http://dx.doi.org/10.1002/ijc.24339
2. Lajer CB, von Buchwald C. The role of human papillomavirus in head and neck cancer. APMIS 2010; 118:510-9; PMID:20553531; http://dx.doi.org/10.1111/j.1600-0463.2010.02624.x
3. Licitra L, Perrone F, Bossi P, Suardi S, Mariani L, Artusi R, Oggionni M, Rossini C, Cantu G, Squadrelli M et al. High-risk human papillomavirus affects prognosis in patients with surgically treated oropharyngeal squamous cell carcinoma. J Clin Oncol 2006; 24:5630-6; PMID:17179101; http://dx.doi.org/10.1200/JCO.2005.04.6136
4. Lassen P, Eriksen JG, Hamilton-Dutoit S, Tramm T, Alsner J, Overgaard J. Effect of HPV-associated p16INK4 A expression on response to radiotherapy and survival in squamous cell carcinoma of the head and neck. J Clin Oncol 2009; 27:1992-8; PMID:19289615; http://dx.doi.org/10.1200/JCO.2008.20.2853
5. Spanos WC, Nowicki P, Lee DW, Hoover A, Hostager B, Gupta A, Anderson ME, Lee JH. Immune response during therapy with cisplatin or radiation for human papillomavirus-related head and neck cancer. Arch Otolaryngol Head Neck Surg 2009; 135:1137-46; PMID:19917928; http://dx.doi.org/10.1001/archoto.2009.159
6. Kimple RJ, Harari PM, Torres AD, Yang RZ, Soriano BJ, Yu M, Armstrong EA, Blitzer GC, Smith MA, Lorenz LD et al. Development and characterization of HPV-positive and HPV-negative head and neck squamous cell carcinoma tumorgrafts. Clin Cancer Res 2013; 19:855-64; PMID:23251001; http://dx.doi.org/10.1158/1078-0432.CCR-12-2746
7. Galon J, Costes A, Sanchez-Cabo F, Kirilovsky A, Mlecnik B, Lagorce-Pages C, Tosolini M, Camus M, Berger A, Wind P et al. Type, density, and location of immune cells within human colorectal tumors predict clinical outcome. Science 2006; 313:1960-4; PMID:17008531; http://dx.doi.org/10.1126/science.1129139
8. Clemente CG, Mihm MC Jr, Bufalino R, Zurrida S, Collini P, Cascinelli N. Prognostic value of tumor infiltrating lymphocytes in the vertical growth phase of primary cutaneous melanoma. Cancer 1996; 77:1303-10; PMID:8608507; http://dx.doi.org/10.1002/(SICI)1097-0142(19960401)77:7%3c1303::AID-CNCR12%3e3.0.CO;2-5
9. Sato E, Olson SH, Ahn J, Bundy B, Nishikawa H, Qian F, Jungbluth AA, Frosina D, Gnjatic S, Ambrosone C et al. Intraepithelial $CD8^+$ tumor-infiltrating lymphocytes and a high $CD8^+$/regulatory T cell ratio are associated with favorable prognosis in ovarian cancer. Proc Natl Acad Sci USA 2005; 102:18538-43; PMID:16344461; http://dx.doi.org/10.1073/pnas.0509182102
10. Kocian P, Sedivcova M, Drgac J, Cerna K, Hoch J, Kodet R, Bartunkova J, Spisek R, Fialova A. Tumor-infiltrating lymphocytes and dendritic cells in human colorectal cancer: their relationship to KRAS mutational status and disease recurrence. Hum Immunol 2011; 72:1022-8; PMID:21884745; http://dx.doi.org/10.1016/j.humimm.2011.07.312
11. Kawai O, Ishii G, Kubota K, Murata Y, Naito Y, Mizuno T, Aokage K, Saijo N, Nishiwaki Y, Gemma A et al. Predominant infiltration of macrophages and CD8(+) T Cells in cancer nests is a significant predictor of survival in stage IV nonsmall cell lung cancer. Cancer 2008; 113:1387-95; PMID:18671239; http://dx.doi.org/10.1002/cncr.23712
12. Wansom D, Light E, Worden F, Prince M, Urba S, Chepeha DB, Cordell K, Eisbruch A, Taylor J, D'Silva N et al. Correlation of cellular immunity with human papillomavirus 16 status and outcome in patients with advanced oropharyngeal cancer. Arch Otolaryngol Head Neck Surg 2010; 136:1267-73; PMID:21173378; http://dx.doi.org/10.1001/archoto.2010.211
13. Nasman A, Romanitan M, Nordfors C, Grun N, Johansson H, Hammarstedt L, Marklund L, Munck-Wikland E, Dalianis T, Ramqvist T. Tumor infiltrating $CD8^+$ and Foxp3 +lymphocytes correlate to clinical outcome and human papillomavirus (HPV) status in tonsillar cancer. PLoS One 2012; 7:e38711; PMID:22701698; http://dx.doi.org/10.1371/journal.pone.0038711
14. Nordfors C, Grun N, Tertipis N, Ahrlund-Richter A, Haeggblom L, Sivars L, Du J, Nyberg T, Marklund L, Munck-Wikland E et al. CD8(+) and CD4(+) tumour infiltrating lymphocytes in relation to human papillomavirus status and clinical outcome in tonsillar and base of tongue squamous cell carcinoma. Eur J Cancer 2013; 49:2522-30; PMID:23571147; http://dx.doi.org/10.1016/j.ejca.2013.03.019
15. Fialova A, Partlova S, Sojka L, Hromadkova H, Brtnicky T, Fucikova J, Kocian P, Rob L, Bartunkova J, Spisek R. Dynamics of T-cell infiltration during the course of ovarian cancer: the gradual shift from a Th17 effector cell response to a predominant infiltration by regulatory T-cells. Int J Cancer 2013; 132:1070-9; PMID:22865582; http://dx.doi.org/10.1002/ijc.27759
16. Naito Y, Saito K, Shiiba K, Ohuchi A, Saigenji K, Nagura H, Ohtani H. $CD8^+$ T cells infiltrated within cancer cell nests as a prognostic factor in human colorectal cancer. Cancer Res 1998; 58:3491-4; PMID:9721846
17. Hasmim M, Badoual C, Vielh P, Drusch F, Marty V, Laplanche A, de Oliveira Diniz M, Roussel H, De Guillebon E, Oudard S et al. Expression of EPHRIN-A1, SCINDERIN and MHC class I molecules in head and neck cancers and relationship with the prognostic value of intratumoral $CD8^+$ T cells. BMC Cancer

2013; 13:592; PMID:24330498; http://dx.doi.org/10.1186/1471-2407-13-592
18. Badoual C, Hans S, Merillon N, Van Ryswick C, Ravel P, Benhamouda N, Levionnois E, Nizard M, Si-Mohamed A, Besnier N et al. PD-1-expressing tumor-infiltrating T cells are a favorable prognostic biomarker in HPV-associated head and neck cancer. Cancer Res 2013; 73:128-38; PMID:23135914; http://dx.doi.org/10.1158/0008-5472.CAN-12-2606
19. Curiel TJ, Coukos G, Zou L, Alvarez X, Cheng P, Mottram P, Evdemon-Hogan M, Conejo-Garcia JR, Zhang L, Burow M et al. Specific recruitment of regulatory T cells in ovarian carcinoma fosters immune privilege and predicts reduced survival. Nat Med 2004; 10:942-9; PMID:15322536; http://dx.doi.org/10.1038/nm1093
20. Miracco C, Mourmouras V, Biagioli M, Rubegni P, Mannucci S, Monciatti I, Cosci E, Tosi P, Luzi P. Utility of tumour-infiltrating CD25+FOXP3+ regulatory T cell evaluation in predicting local recurrence in vertical growth phase cutaneous melanoma. Oncol Rep 2007; 18:1115-22; PMID:17914561; http://dx.doi.org/10.3892/or.18.5.1115
21. Bohling SD, Allison KH. Immunosuppressive regulatory T cells are associated with aggressive breast cancer phenotypes: a potential therapeutic target. Mod Pathol 2008; 21:1527-32; PMID:18820666; http://dx.doi.org/10.1038/modpathol.2008.160
22. Hiraoka N, Onozato K, Kosuge T, Hirohashi S. Prevalence of FOXP3+ regulatory T cells increases during the progression of pancreatic ductal adenocarcinoma and its premalignant lesions. Clin Cancer Res 2006; 12:5423-34; PMID:17000676; http://dx.doi.org/10.1158/1078-0432.CCR-06-0369
23. Salama P, Phillips M, Grieu F, Morris M, Zeps N, Joseph D, Platell C, Iacopetta B. Tumor-infiltrating FOXP3+ T regulatory cells show strong prognostic significance in colorectal cancer. J Clin Oncol 2009; 27:186-92; PMID:19064967; http://dx.doi.org/10.1200/JCO.2008.18.7229
24. Alvaro T, Lejeune M, Salvado MT, Bosch R, Garcia JF, Jaen J, Banham AH, Roncador G, Montalban C, Piris MA. Outcome in Hodgkin's lymphoma can be predicted from the presence of accompanying cytotoxic and regulatory T cells. Clin Cancer Res 2005; 11:1467-73; PMID:15746048; http://dx.doi.org/10.1158/1078-0432.CCR-04-1869
25. Badoual C, Hans S, Rodriguez J, Peyrard S, Klein C, Agueznay Nel H, Mosseri V, Laccourreye O, Bruneval P, Fridman WH et al. Prognostic value of tumor-infiltrating $CD4^+$ T-cell subpopulations in head and neck cancers. Clin Cancer Res 2006; 12:465-72; PMID:16428488; http://dx.doi.org/10.1158/1078-0432.CCR-05-1886
26. Bron L, Jandus C, Andrejevic-Blant S, Speiser DE, Monnier P, Romero P, Rivals JP. Prognostic value of arginase-II expression and regulatory T-cell infiltration in head and neck squamous cell carcinoma. Int J Cancer 2013; 132:E85-93; PMID:22815199; http://dx.doi.org/10.1002/ijc.27728
27. Loose D, Signore A, Bonanno E, Vermeersch H, Dierckx R, Deron P, Van de Wiele C. Prognostic value of CD25 expression on lymphocytes and tumor cells in squamous-cell carcinoma of the head and neck. Cancer Biother Radiopharm 2008; 23:25-33; PMID:18298326; http://dx.doi.org/10.1089/cbr.2007.0373
28. Boucek J, Mrkvan T, Chovanec M, Kuchar M, Betka J, Boucek V, Hladikova M, Betka J, Eckschlager T, Rihova B. Regulatory T cells and their prognostic value for patients with squamous cell carcinoma of the head and neck. J Cell Mol Med 2010; 14:426-33; PMID:19183242; http://dx.doi.org/10.1111/j.1582-4934.2008.00650.x
29. Heusinkveld M, Goedemans R, Briet RJ, Gelderblom H, Nortier JW, Gorter A, Smit VT, Langeveld AP, Jansen JC, van der Burg SH. Systemic and local human papillomavirus 16-specific T-cell immunity in patients with head and neck cancer. Int J Cancer 2012; 131:E74-85; PMID:22020783; http://dx.doi.org/10.1002/ijc.26497
30. Piersma SJ, Welters MJ, van der Hulst JM, Kloth JN, Kwappenberg KM, Trimbos BJ, Melief CJ, Hellebrekers BW, Fleuren GJ, Kenter GG et al. Human papilloma virus specific T cells infiltrating cervical cancer and draining lymph nodes show remarkably frequent use of HLA-DQ and -DP as a restriction element. Int J Cancer 2008; 122:486-94; PMID:17955486; http://dx.doi.org/10.1002/ijc.23162
31. Welters MJ, Kenter GG, Piersma SJ, Vloon AP, Lowik MJ, Berends-van der Meer DM, Drijfhout JW, Valentijn AR, Wafelman AR, Oostendorp J et al. Induction of tumor-specific $CD4^+$ and $CD8^+$ T-cell immunity in cervical cancer patients by a human papillomavirus type 16 E6 and E7 long peptides vaccine. Clin Cancer Res 2008; 14:178-87; PMID:18172269; http://dx.doi.org/10.1158/1078-0432.CCR-07-1880
32. Marcus B, Arenberg D, Lee J, Kleer C, Chepeha DB, Schmalbach CE, Islam M, Paul S, Pan Q, Hanash S et al. Prognostic factors in oral cavity and oropharyngeal squamous cell carcinoma. Cancer 2004; 101:2779-87; PMID:15546137; http://dx.doi.org/10.1002/cncr.20701
33. Lam-ubol A, Hopkin D, Letuchy EM, Kurago ZB. Squamous carcinoma cells influence monocyte phenotype and suppress lipopolysaccharide-induced TNF-alpha in monocytes. Inflammation 2010; 33:207-23; PMID:20084448; http://dx.doi.org/10.1007/s10753-009-9175-6
34. Tan TT, Coussens LM. Humoral immunity, inflammation and cancer. Curr Opin Immunol 2007; 19:209-16; PMID:17276050; http://dx.doi.org/10.1016/j.coi.2007.01.001
35. Ziegler-Heitbrock L. The $CD14^+$ CD16+ blood monocytes: their role in infection and inflammation. J Leukoc Biol 2007; 81:584-92; PMID:17135573; http://dx.doi.org/10.1189/jlb.0806510
36. Ramanathapuram LV, Hopkin D, Kurago ZB. Dendritic Cells (DC) facilitate detachment of squamous carcinoma cells (SCC), while SCC promote an immature CD16(+) DC phenotype and control DC migration. Cancer Microenviron 2013; 6:41-55; PMID:21809059; http://dx.doi.org/10.1007/s12307-011-0077-4
37. Muller A, Homey B, Soto H, Ge N, Catron D, Buchanan ME, McClanahan T, Murphy E, Yuan W, Wagner SN et al. Involvement of chemokine receptors in breast cancer metastasis. Nature 2001; 410:50-6; PMID:11242036; http://dx.doi.org/10.1038/35065016
38. Cojoc M, Peitzsch C, Trautmann F, Polishchuk L, Telegeev GD, Dubrovska A. Emerging targets in cancer management: role of the CXCL12CXCR4 axis. Onco Targets Ther 2013; 6:1347-61; PMID:24124379; http://dx.doi.org/10.2147/OTT.S36109
39. Alferink J, Lieberam I, Reindl W, Behrens A, Weiss S, Huser N, Gerauer K, Ross R, Reske-Kunz AB, Ahmad-Nejad P et al. Compartmentalized production of CCL17 *in vivo:* strong inducibility in peripheral dendritic cells contrasts selective absence from the spleen. J Exp Med 2003; 197:585-99; PMID:12615900; http://dx.doi.org/10.1084/jem.20021859
40. Gupta RA, Dubois RN. Colorectal cancer prevention and treatment by inhibition of cyclooxygenase-2. Nat Rev Cancer 2001; 1:11-21; PMID:11900248; http://dx.doi.org/10.1038/35094017
41. Howe LR, Subbaramaiah K, Brown AM, Dannenberg AJ. Cyclooxygenase-2: a target for the prevention and treatment of breast cancer. Endocr Relat Cancer 2001; 8:97-114; PMID:11397667; http://dx.doi.org/10.1677/erc.0.0080097
42. Ristimaki A, Sivula A, Lundin J, Lundin M, Salminen T, Haglund C, Joensuu H, Isola J. Prognostic significance of elevated cyclooxygenase-2 expression in breast cancer. Cancer Res 2002; 62:632-5; PMID:11830510
43. Melero I, Hervas-Stubbs S, Glennie M, Pardoll DM, Chen L. Immunostimulatory monoclonal antibodies for cancer therapy. Nat Rev Cancer 2007; 7:95-106; PMID:17251916; http://dx.doi.org/10.1038/nrc2051
44. Mueller SN, Ahmed R. High antigen levels are the cause of T cell exhaustion during chronic viral infection. Proc Natl Acad Sci USA 2009; 106:8623-8; PMID:19433785; http://dx.doi.org/10.1073/pnas.0809818106
45. Yi JS, Cox MA, Zajac AJ. T-cell exhaustion: characteristics, causes and conversion. Immunology 2010; 129:474-81; PMID:20201977; http://dx.doi.org/10.1111/j.1365-2567.2010.03255.x
46. Wherry EJ. T cell exhaustion. Nat Immunol 2011; 12:492-9; PMID:21739672; http://dx.doi.org/10.1038/ni.2035
47. Gao X, Zhu Y, Li G, Huang H, Zhang G, Wang F, Sun J, Yang Q, Zhang X, Lu B. TIM-3 expression characterizes regulatory T cells in tumor tissues and is associated with lung cancer progression. PLoS One 2012; 7:e30676; PMID:22363469; http://dx.doi.org/10.1371/journal.pone.0030676
48. Yang ZZ, Grote DM, Ziesmer SC, Niki T, Hirashima M, Novak AJ, Witzig TE, Ansell SM. IL-12 upregulates TIM-3 expression and induces T cell exhaustion in patients with follicular B cell non-Hodgkin lymphoma. J Clin Invest 2012; 122:1271-82; PMID:22426209; http://dx.doi.org/10.1172/JCI59806
49. Koslabova E, Hamsikova E, Salakova M, Klozar J, Foltynova E, Salkova E, Rotnaglova E, Ludvikova V, Tachezy R. Markers of HPV infection and survival in patients with head and neck tumors. Int J Cancer 2013; 133:1832-9; PMID:23564321; http://dx.doi.org/10.1002/ijc.28194
50. Rotnaglova E, Tachezy R, Salakova M, Prochazka B, Kosl'abova E, Vesela E, Ludvikova V, Hamsikova E, Klozar J. HPV involvement in tonsillar cancer: prognostic significance and clinically relevant markers. Int J Cancer 2011; 129:101-10; PMID:21190188; http://dx.doi.org/10.1002/ijc.25889
51. Klozar J, Kratochvil V, Salakova M, Smahelova J, Vesela E, Hamsikova E, Betka J, Tachezy R. HPV status and regional metastasis in the prognosis of oral and oropharyngeal cancer. Eur Arch Otorhinolaryngol 2008; 265 Suppl 1:S75-82; PMID:18094985; http://dx.doi.org/10.1007/s00405-007-0557-9
52. Tachezy R, Klozar J, Salakova M, Smith E, Turek L, Betka J, Kodet R, Hamsikova E. HPV and other risk factors of oral cavityoropharyngeal cancer in the Czech Republic. Oral Dis 2005; 11:181-5; PMID:15888110; http://dx.doi.org/10.1111/j.1601-0825.2005.01112.x
53. van den Brule AJ, Pol R, Fransen-Daalmeijer N, Schouls LM, Meijer CJ, Snijders PJ. GP5+6 +PCR followed by reverse line blot analysis enables rapid and high-throughput identification of human papillomavirus genotypes. J Clin Microbiol 2002; 40:779-87; PMID:11880393; http://dx.doi.org/10.1128/JCM.40.3.779-787.2002
54. Gravitt PE, Peyton C, Wheeler C, Apple R, Higuchi R, Shah KV. Reproducibility of HPV 16 and HPV 18 viral load quantitation using TaqMan real-time PCR assays. J Virol Methods 2003; 112:23-33; PMID:12951209; http://dx.doi.org/10.1016/S0166-0934(03)00186-1
55. Smeets SJ, Hesselink AT, Speel EJ, Haesevoets A, Snijders PJ, Pawlita M, Meijer CJ, Braakhuis BJ, Leemans CR, Brakenhoff RH. A novel algorithm for reliable detection of human papillomavirus in paraffin embedded head and neck cancer specimen. Int J Cancer 2007; 121:2465-72; PMID:17680565; http://dx.doi.org/10.1002/ijc.22980

5.2 Funkční kapacita HPV-specifických TILs je u pacientů s nádory hlavy a krku ovlivněna expresí inhibičních molekul

Nádory vzniklé na podkladě infekce lidským papilomavirem (HPV) disponují přítomností onkoproteinů E6 a E7, jež jsou konstitutivně exprimovány nádorovými buňkami a jako cizí, vysoce imunogenní specifické nádorové antigeny, by měly vyvolávat silnou protinádorovou imunitní odpověď, zprostředkovanou především HPV-specifickými TILs. Nízká úspěšnost cílené terapie pomocí imunomodulačních protilátek u pacientů s rekurentním HNSCC ale nasvědčuje komplexním změnám ve funkční kapacitě specifické složky imunitního systému. Cílem této studie byla komplexní analýza frekvence, fenotypu a funkční kapacity HPV 16 E6/E7- specifických TILs u pacientů s orofaryngeálním karcinomem a posouzení efektu zablokování PD-1 dráhy pomocí monoklonální protilátky proti PD-1, nivolumabu, a TIM-3 dráhy pomocí solubilního TIM-3 na efektorové schopnosti HPV 16-specifických TILs. Přítomnost HPV 16-specifických TILs jsme detekovali u 73,1 % HPV-asociovaných nádorů orofaryngu. Tyto HPV 16-specifické CD8+ TILs, schopné produkce IFNγ po specifické stimulaci autologními CD14+ monocyty pulzovanými peptidy onkoproteinů E6 a E7, byly charakteristické expresí PD-1, ale nepřítomností TIM-3. Přítomnost PD-1 a nepřítomnost TIM-3 u populace funkčních CD8+ T-lymfocytů poukazuje na Tim-3, spíše než na PD-1, jako na znak vyčerpání těchto buněk. Specifická produkce IFNγ byla navíc zýšena pouze u TILs ošetřených kombinací nivolumabu spolu se sTIM-3, zatímco použití nivolumabu samotného produkci IFNγ neovlivnilo. Na rozdíl od nespecifické stimulace nivolumab překvapivě nezvyšoval expresi Tim-3 u specificky stimulovaných TILs, absence vlivu nivolumabu na funkční kapacitu buněk tedy nebyla způsobená mechanismem adaptivní rezistence popsaným ve studii Shayanové (Shayan et al., 2017). Z výsledků naší studie vyplývá, že kombinovaná léčba zahrnující zablokování PD-1 dráhy pomocí nivolumabu v kombinaci s blokováním dalších inhibičních molekul, jako je TIM-3, může vést k zesílení účinku HPV-16 terapeutických vakcín u pacientů s orofaryngeálním karcinomem.

K této práci jsem přispěla následovně: 50 %; zpracování nádorové tkáně a periferní krve pacientů, homeostatická expanze TILs, detekce HPV 16-specifických TILs pomocí průtokové cytometrie, funkční a fenotypová analýza těchto buněk, detekce cytokinů a dalších solubilních molekul v supernatantech pacientů, izolace RNA a stanovení exprese inhibičních molekul pomocí qPCR, analýza dat a účast na přípravě manuskriptu.

Oral Oncology 82 (2018) 75–82

Contents lists available at ScienceDirect

Oral Oncology

journal homepage: www.elsevier.com/locate/oraloncology

Dysfunction of HPV16-specific CD8+ T cells derived from oropharyngeal tumors is related to the expression of Tim-3 but not PD-1

Kamila Hladíková[a,b,1], Simona Partlová[a,1], Vladimír Koucký[a,c], Jan Bouček[c,d], Jean-Francois Fonteneau[e], Michal Zábrodský[c], Ruth Tachezy[f], Marek Grega[g], Radek Špíšek[a,b], Anna Fialová[a,*]

[a] Sotio, Jankovcova 1518/2, 170 00 Prague, Czech Republic
[b] Department of Immunology, 2nd Faculty of Medicine, Charles University, Motol University Hospital, V Úvalu 84, 150 06 Prague, Czech Republic
[c] Department of Otorhinolaryngology and Head and Neck Surgery, 1st Faculty of Medicine, Charles University and University Hospital Motol, V Úvalu 84, 150 06 Prague, Czech Republic
[d] Institute of Microbiology ASCR, v.v.i., Vídeňská 1083, 142 20 Prague, Czech Republic
[e] CRCINA, INSERM U1232, Université de Nantes, 8 Quai Moncousu, 44007 Nantes, France
[f] Department of Genetics and Microbiology, Faculty of Science, Charles University in Prague, Viničná 5, 128 44 Prague, Czech Republic
[g] Department of Pathology and Molecular Medicine, 2nd Faculty of Medicine, Charles University and Motol University Hospital, V Úvalu 84, 150 06 Prague, Czech Republic

ARTICLE INFO

Keywords:
Oropharyngeal cancer
Human papillomavirus
PD-1
Tim-3
Tumor-infiltrating lymphocytes

ABSTRACT

Background: Human papillomavirus (HPV) type 16 infection is one of the most important etiological agents of oropharyngeal squamous cell carcinoma. Patients with HPV-associated carcinomas of the head and neck were reported to have a better clinical outcome than patients with HPV-negative tumors. Because HPV16 E6 and E7 oncoproteins are highly immunogenic and constitutively expressed, HPV-specific T cell immunity may play the key role in improving the prognosis of these patients.
Methods: Tumor-derived T cells were expanded in high levels of IL-2 and stimulated with HPV16 E6/E7 peptides in the presence or absence of anti-PD-1 monoclonal antibody nivolumab and soluble Tim-3.
Results: HPV16-specific tumor-infiltrating T cells were present in 73.1% of HPV-associated oropharyngeal tumors. HPV16 specific CD8+ TILs were able to produce IFNγ upon specific stimulation and predominantly expressed PD-1 but not Tim-3. Specific IFNγ production was further enhanced after a blockade of both PD-1 and Tim-3 pathways but not after a PD-1 blockade alone. Additionally, the specific stimulation of anti-HPV16 CD8+ T cells suppressed Tim-3 upregulation after the PD-1 blockade.
Conclusion: Our data provide the rationale for combination cancer immunotherapy approaches, including the dual blockade of PD-1 and Tim-3 and, potentially, the use of HPV16-directed therapeutic vaccines.

Introduction

Over the past two decades, an increase in incidence of oropharyngeal squamous cell carcinoma (OPC) has been reported in patients with no history of alcohol and tobacco use. Human papillomavirus type 16 has been identified as the most important etiological agent of this malignancy [1]. Following the standard treatment regimes, patients with HPV-associated tumors have a better clinical outcome than patients with tobacco-related carcinomas; however, standard chemo- and radiotherapy is still associated with considerable morbidity and toxicity in these patients. Therefore, more effective and less toxic therapeutic strategies are needed. However, no new targeted therapies have been approved since cetuximab in 2006, which, as a monotherapy, shows a therapeutic benefit in only 10–15% of head and neck squamous cell carcinoma (HNSCC) patients [2]. Similarly, clinical trials with PD-1:PD-L1 targeting agents, which are promising in other tumor histologies, only report modest response rates (13–18%) in HNSCC, including HPV-associated OPC [3–5]. Recently, preclinical studies have shown that targeting PD-1 pathway simultaneously with an alternative checkpoint molecule, T cell immunoglobulin and mucin domain 3 (Tim-3), emerges as a promising approach for improvement of current immunotherapy [6,7].

* Corresponding author at: Sotio a.s., Jankovcova 1518/2, CZ-17000 Prague 7, Czech Republic.
E-mail address: fialova@sotio.com (A. Fialová).
[1] These authors contributed equally to this work.

https://doi.org/10.1016/j.oraloncology.2018.05.010
Received 26 February 2018; Received in revised form 9 May 2018; Accepted 15 May 2018

In the development of efficient immunotherapeutic strategies, the identification of tumor-specific antigens remains essential. In HPV-associated cancers, the HPV E6 and E7 oncoproteins represent optimal specific antigens. They are constitutively expressed and presented by cancer cells and they are highly immunogenic [8]. Indeed, preclinical studies have reported that anti-HPV E7 vaccines elicited E7-specific CD8+ T cells in tumor-bearing mouse models. The presence of HPV-specific T cells was associated with partial regression of E7-expressing TC-1 tumors in immunized mice [9–11]. Moreover, therapeutic vaccines targeted against HPV16 E6 and E7 oncoproteins have been reported to induce a complete response in 47% of patients with HPV-associated vulvar intraepithelial neoplasia in a phase II clinical trial [12]. With HPV16 being a leading etiological agent in oropharyngeal cancer (OPC), the induction of a robust HPV-specific immune response may represent a promising therapeutic strategy. However, there are only a few reports concerning the existence of HPV16-specific T cell immunity in HNSCC patients, and most are focused on the detection of virus-specific T cells in the peripheral blood [13–16].

The aim of this study was to analyze the frequency, phenotype and function of HPV16 E6/E7-specific tumor-infiltrating T cells (TILs) in oropharyngeal tumors and to test the effect of anti-PD1 mAb (nivolumab), soluble Tim-3 (sTim-3) and homeostatic *in vitro* expansion on these characteristics.

Materials and methods

Patients and samples

Blood samples and primary oropharyngeal squamous cell carcinoma specimens were obtained from 51 patients immediately after radical surgery at the Department of Otorhinolaryngology and Head and Neck Surgery, Motol University Hospital in Prague between April 2015 and August 2017. Patients enrolled in this study had not received any neoadjuvant chemo- or radiotherapy. All of the patients signed an informed consent approved by the Institutional Review Board of the University Motol. The clinical-pathological characteristics of the patients are summarized in Table 1.

The tumor tissues were processed as described previously [17]. Peripheral blood mononuclear cells (PBMCs) were isolated from the peripheral blood by centrifugation on a Ficoll-Paque density gradient (GE Healthcare, Waukesha, WI).

Table 1
Clinical-pathological characteristics of the patients.

Variable	No.	%
Total no. of patients	51	
Age		
Mean	59	
Range	36–75	
Sex		
Male	36	70.6
Female	15	29.4
Nodal status		
N0	9	17.6
N1-N3	42	82.4
Stage		
I	1	1.9
II	8	15.7
III	13	25.5
IV	29	56.9
Tumor site		
Base of tongue	10	19.6
Tonsil	32	62.7
Oropharynx	9	17.7
HPV status		
HPV-	10	19.6
HPV+	41	80.4

TIL expansion

All T cell cultures were performed in RPMI 1640 supplemented with 10% human AB serum, penicillin-streptomycin, L-glutamine (all from Invitrogen, Carlsbad, USA) and 450 U IL-2 (Proleukin, Prometheus Laboratories Inc., San Diego, USA). Freshly isolated TILs at a concentration of 3×10^5 cells/ml were expanded for two weeks with the addition of fresh medium and IL-2 every 3 days. After 2 weeks of homeostatic expansion, the cells were harvested, and their phenotype was analyzed using flow cytometry and qPCR. Proportional frequency of TILs within fresh tumor single cell suspension and expanded TILs is shown in Fig. S1.

For quantification of cytokines, free fatty acids, adenosine and sPD-1 production, expanded tumor-derived TILs and PBMCs (1×10^6 cells/ml) were cultured in culture medium in the presence or absence of HPV16 E6/E7 peptide-loaded autologous monocytes. After 24 h of incubation, the culture supernatants were harvested and stored at −80 °C until use.

Flow cytometry

Single cell suspensions derived from tumor tissues were labeled using monoclonal antibodies (mAbs) against CD3 (Exbio, Vestec, Czech Republic), CD4 (eBioscience, San Diego, USA), CD8 (Exbio), PD-1 and Tim-3 (both from BioLegend, San Diego, USA). For the intracellular detection of cytokines, the cells were fixed and permeabilized with a FoxP3 Staining Buffer Set (eBioscience) and intracellularly labeled with mAbs against IFNγ (BD Biosciences) and TNFα (BioLegend). The cells were then analyzed on a BD FACSCanto II (BD Biosciences) and evaluated with FlowJo software (TreeStar, Ashland, OR).

Detection of HPV16-specific T cells

Monocytes from autologous PBMCs were isolated using a Human CD14 Positive Selection Kit (Stemcell Technologies, Vancouver, Canada). The obtained monocytes were loaded with HPV16 E6 and E7 peptide pools (5 μg/ml) (JPT, Berlin, Germany) and added to expanded TILs at a ratio of 1:10. The cells were incubated for 6 h in the presence of Brefeldin A (BioLegend). After the 6-h incubation, the cells were stained with antibodies for the intracellular detection of cytokines as described above. Cut off was calculated as the mean proportion of IFNγ-/TNFα-positive CD8+ T cells detected upon specific stimulation in HPV-negative patients + 3SD.

For *in vitro* blocking studies, anti-PD-1 mAb (10 μg/ml) (nivolumab, Bristol-Myers-Squibb, New York, USA) and soluble Tim-3 (5 μg/ml) (Recombinant Human Tim-3 protein, Abcam, Cambridge, UK) were added to the TIL cultures 42 h prior to specific stimulation with HPV16 E6 and E7 peptide-loaded autologous monocytes.

Detection of cytokines, soluble PD-1, free fatty acids and free adenosine in culture supernatants

To detect the concentrations of cytokines released into culture supernatant, the MILLIPLEX™ Human Cytokine Kit (Millipore, Billerica, MA) was used. Levels of soluble PD-1, free fatty acids and adenosine were analyzed using a PD-1 Human ELISA Kit (Thermo Fisher Scientific), Free Fatty Acid Quantification Kit (Abcam) and Adenosine Assay Kit (BioVision, Milpitas, USA), respectively. All assays were performed according to the manufacturer's instructions.

RNA extraction and quantitative real-time PCR

Total RNA was extracted from 1×10^6 tumor-tissue derived cells

using an RNA Easy Mini Kit (Qiagen, Hilden, Germany). RNA concentrations were determined with a NanoDrop© 2000c UV–Vis spectrophotometer (Thermo Scientific), and the RNA integrity was assessed using an Experion automated system (BioRad, Hercules, USA). Complementary DNA was synthesized from total RNA using the M-MLV reverse transcriptase (Invitrogen) and amplified by quantitative real-time PCR in the presence of primers and TaqMan© probes specific for PD-1, PD-L1, CTLA-4, Tim-3, LAG-3, TIGIT and BTLA, and the β-actin housekeeping gene, which was used as an internal reference. All primers and probes were commercially synthesized (TIB MOLBIOL, Berlin, Germany). The identity of the qPCR products in each assay was verified by sequencing. The relative expression of the target genes was normalized to the expression of β-actin.

HPV detection

PCR

HPV DNA detection was performed by PCR with primers specific for the L1 region (GP5+/GP6+). As an internal control, a 110-bp fragment of the human beta-globin gene was amplified. HPV typing was performed by reverse line blot hybridization (RLB) with probes specific for 37 types as specified in detail by van den Brule et al. [18]. From the total RNA, cDNA was prepared by reverse transcription. The absence of contaminating DNA was confirmed by amplification of the internal GAPDH internal control gene. As a mRNA integrity control, the beta-globin gene was amplified. Amplification of the HPV 16E6∗I mRNA oncoprotein was performed with primers that amplify the 86-bp fragment. The samples positive for viral mRNA expression were considered HPV-positive for future analyses.

Immunohistochemical analysis

The antibody p16INK4a (Purified Mouse Anti-Human p16, Clone G175-405, BD Pharmingen TM) was used. The intensity of staining and the proportion of positive cells were evaluated. The sample considered as positive for p16 expression had to show more than 70% of positive cells and reveal nuclear and/or cytoplasmic staining.

Statistical analysis

Statistical analyses were performed using Statistica® 10.0 software (StatSoft, Tulsa, OK). Differences between T cells responding vs non-responding to specific stimulation, proportions of CD3+, CD4+ and CD8+ T cells in fresh vs expanded samples and supernatants harvested from HPV peptide pools-stimulated vs unstimulated cell cultures were analyzed using paired t-tests. Differences between control PBMCs and TILs were analyzed using the Mann-Whitney *U* test. Correlations between levels of check-point molecules were evaluated using the Pearson r coefficient. The results were considered to be statistically significant when $p < 0.05$.

Results

HPV-specific TILs are detected in HPV-associated but not HPV-negative tumor samples

The expression of HPV 16 E6 mRNA was detected in 80.4% (n = 41) of the OPC samples enrolled in this study. We were able to expand TILs from 33 tumor tissues (64.7%). After a 2-week homeostatic expansion, 31 samples of TILs were tested for reactivity against autologous monocytes pulsed with HPV16 E6 and E7 peptide pools. We have detected HPV-specific IFNγ-producing CD8+ T cells in 73.1% of HPV-associated OPC samples, but not in TILs derived from HPV-negative tumor tissues (Fig. 1A). Similarly, TNFα-producing CD8+ T cells were detected in 40% of HPV-associated and none of the HPV-negative tumor tissue samples (Fig. 1D).

IFNγ and TNFα are produced by PD-1+Tim-3- and PD-1-Tim-3- CD8+ T cells upon HPV16 E6/E7 pepmix stimulation

Specific HPV16 E6/E7 pepmix stimulation induced IFNγ production preferentially in PD-1-Tim-3- and PD-1+Tim-3-CD8+ T cells (29.7 ± 13.6% and 55.1 ± 11.0% from all IFNγ producing cells, respectively). Conversely, the frequency of PD-1+Tim-3- cells was significantly lower among the CD8+ T cells that did not produce cytokines upon HPV pepmix stimulation (Fig. 1B and C). Consistently, when gated on PD-1 and Tim-3, the main producers of IFNγ were detected in the PD-1+Tim-3- gate (9.3 ± 14.4% of the PD-1+Tim-3-CD8+ T cells were IFNγ-positive) (Fig. 1G). Similarly, TNFα production was also induced in Tim-3-CD8+ cells (51.6 ± 11.5% of PD-1+ and 41.3 ± 18.3% of PD-1- cells) (Fig. 1E and F), and the highest production was observed in the PD-1+Tim-3- gate (29.2 ± 17.4% of PD-1+Tim-3-CD8+ T cells were TNFα-positive) (Fig. 1H). Contrary to PD-1, the expression of Tim-3 correlated with defects in functionality. Indeed, CD8+ T cells that did not respond to HPV pepmix stimulation had a significantly higher expression of Tim-3 than IFNγ and TNFα-producing cells (Fig. 1B and E). As a high intensity of PD-1 expression might be associated with exhaustion rather than the presence/absence only, we compared the levels of PD-1 MFIs in IFNγ+ and IFNγ- CD8+ T cells. Surprisingly, slightly higher MFI of PD-1 was observed in IFNγ-producing PD-1+CD8+ T cells (2564 ± 929) than in IFNγ-negative PD-1+CD8+ T cells (2187 ± 610).

TIL expansion impacts the response to anti-PD-1 mAb nivolumab treatment

To confirm the effect of the PD-1/PD-L1 pathway blockade on IFNγ production and Tim-3 expression in CD8+ T cells, we analyzed the phenotype of expanded TILs after 48 h incubation with nivolumab with/without the addition of recombinant sTim-3. Surprisingly, we only observed a slight effect of nivolumab alone on IFNγ production in HPV16 E6/E7 pepmix stimulated CD8+ T cells; however, IFNγ production significantly increased in the presence of nivolumab in combination with sTim-3. Surprisingly, IFNγ production was slightly downregulated in the presence of sTim-3 alone (Fig. 2A). We did not observe any effect of PD-1 blockade on Tim-3 upregulation on expanded TILs (Fig. 2B).

To assess whether the absent effect of nivolumab on Tim-3 expression might be associated with the expansion, we analyzed freshly isolated tumor-derived cell suspensions under the same conditions. In the fresh samples, we observed a significant increase in Tim-3 expression on CD8+ T cells in nivolumab-treated cell cultures without any added stimuli, but there was only a minor increase in specifically stimulated cell cultures (Fig. 2B).

Homeostatic expansion in the presence of IL-2 shifts the phenotype of OPC-derived TILs

To describe the alterations in TILs associated with the expansion, we analyzed the phenotype of freshly isolated TILs and TILs expanded for 2 weeks in the presence of high doses of IL-2. As expected, we observed a significant shift towards higher proportions of bulk CD4+ T cells and CD8+ T cells within expanded TIL cultures, but there were no significant alterations in the frequency of CD4+CD25^{hi}FoxP3+Tregs. Interestingly, the frequency of CD8+ T cells increased preferentially in TIL cultures derived from HPV+ tumor samples, whereas proportions of CD4+ T cells increased preferentially in TIL cultures derived from HPV- tissues (Fig. S2). Importantly, "homeostatic" expansion significantly affects the levels of check-point molecules PD-1 and Tim-3 on CD8+ and CD4+ T cells (Fig. 3A and B). Indeed, we observed a shift from the prevailing PD-1+Tim-3-CD8+ population to the functionally impaired Tim-3+CD8+ population. The increase in proportions of the Tim-3+CD8+ T cell population was statistically significant in HPV-negative tumor samples and PBMC cultures ($p < 0.01$ and $p = 0.02$,

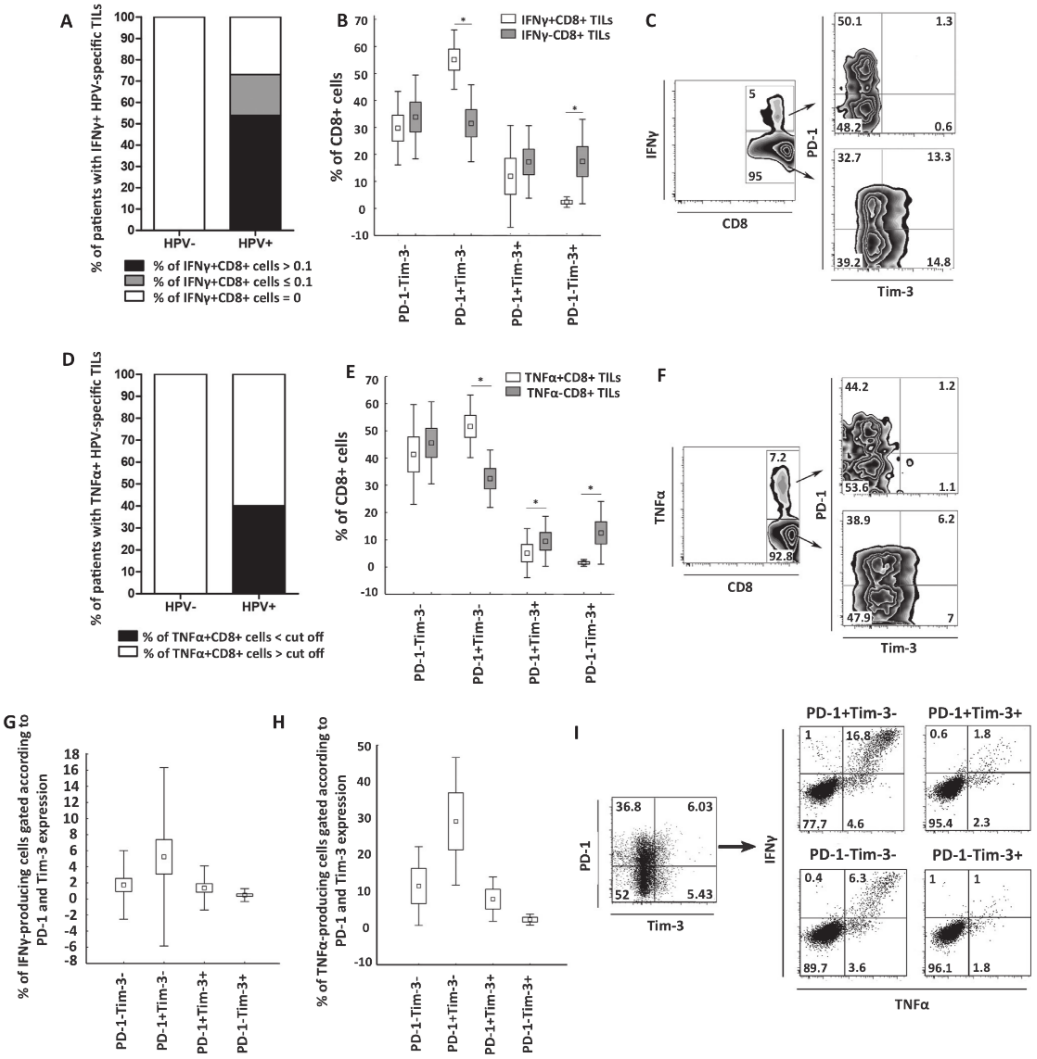

Fig. 1. Proportions of HPV16 E6/E7-specific tumor infiltrating lymphocytes (TILs) derived from tumor tissues of oropharyngeal carcinoma (OPC) patients (n = 31). After two weeks of homeostatic expansion, tumor-derived CD8+ TILs were tested for reactivity against autologous monocytes pulsed with HPV16 E6/E7 peptide pools. (A, D) Columns show the proportions of tumor samples positive for HPV-specific IFNγ+ (A) and TNFα+ (D) CD8+ T cells. (B, E) Boxes show the differences between IFNγ+ and IFNγ- CD8+ T cells in PD-1 and Tim-3 expression after stimulation with HPV16 E6/E7. The boundaries of the boxes indicate the SEM, and the squares in the boxes represent the mean. Whiskers indicate the SD. (C, F) Dot plots are gated on CD3+ CD8+ cells and show PD-1 and Tim-3 expression on CD8+ T cells according to the production of IFNγ (C) and TNFα (F) in a representative patient. (G, H) Box plots show the proportions of IFNγ-producing (G) and TNFα-producing (H) CD8+ T cells in populations gated according to PD-1 and Tim-3 expression. The boundaries of the boxes indicate the SEM, and the squares in the boxes represent the mean. Whiskers indicate the SD. (I) Dot plots are gated on CD3+ CD8+ cells and show the proportions of IFNγ and TNFα-producing cells according to PD-1 and Tim-3 expression in a representative patient. $^{*}p < 0.05$.

respectively). In HPV-positive samples, we also observed a decrease in proportions of PD-1 expressing cells and an increase in proportions of Tim-3 expressing cells; however, the prevailing population in expanded TILs was PD-1-Tim-3-. The trend was similar in CD4+ T cells (Fig. 3B). In control PBMCs obtained from healthy donors, we observed an increase in both PD-1+ and Tim-3+ cell populations. This effect was more pronounced in CD4+ T cells (Fig. 3A and B).

Culture supernatants of expanded TILs contain high levels of pro-inflammatory cytokines

To further characterize the phenotype and function of expanded TILs, we assessed the levels of free adenosine, free fatty acids, sPD-1 and cytokines IL-4, IL-6, IL-10, IL-17A, IFNγ and TNFα in culture supernatants. Free adenosine and fatty acids are proposed to affect the

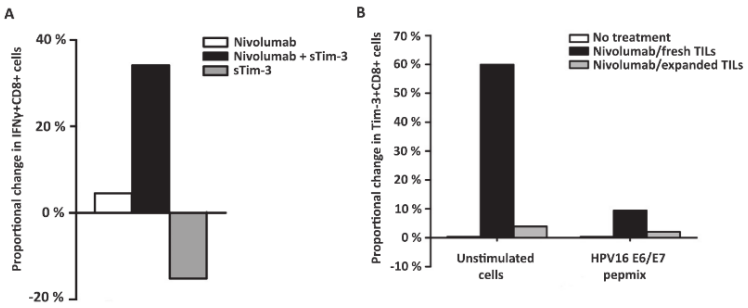

Fig. 2. Effect of PD-1 and/or Tim-3 blockade on IFNγ-production and Tim-3 expression in HPV16-specific CD8+ T cells. (A) Columns represent the percentage increase/decrease in proportions of IFNγ-producing cells induced by anti-PD-1 mAb nivolumab and soluble Tim-3 (n = 4). The change was counted from the baseline represented by HPV16 E6/E7 stimulated TILs. (B) Columns represent the percentage increase in proportions of Tim-3-producing cells induced by anti-PD-1 mAb nivolumab in freshly isolated (n = 4) or two weeks expanded (n = 4) cells. The change was counted from the baseline represented by unstimulated TILs without any treatment.

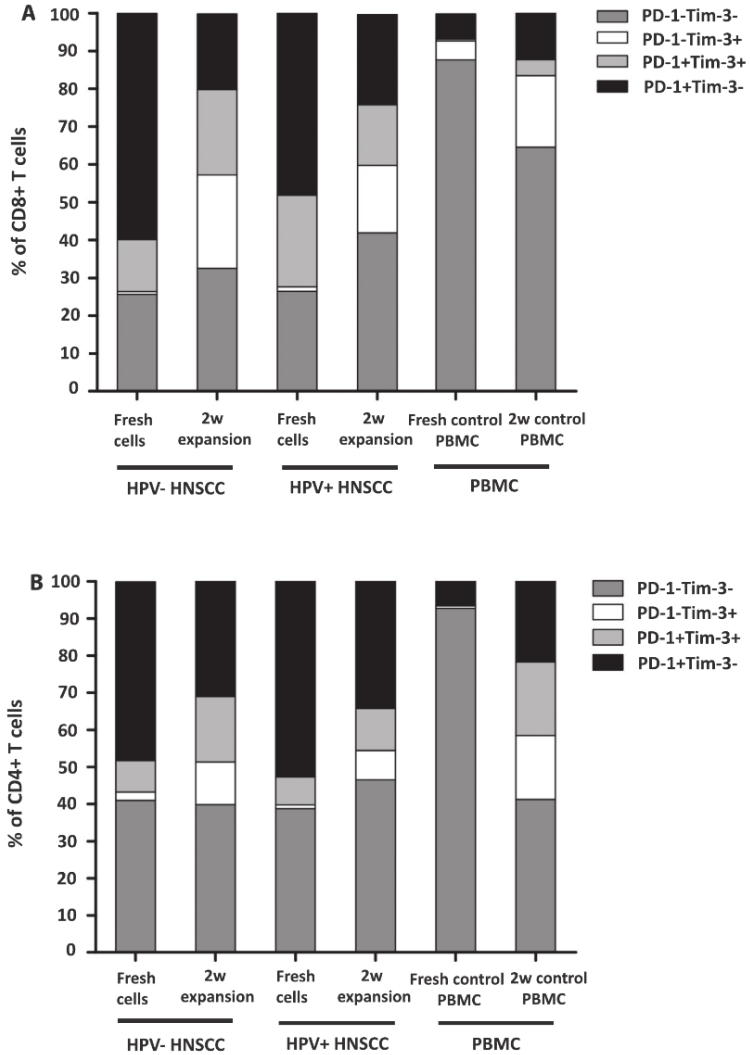

Fig. 3. Columns show the percentages of individual populations according to PD-1 and Tim-3 expression within (A) CD8+ and (B) CD4+ T cells.

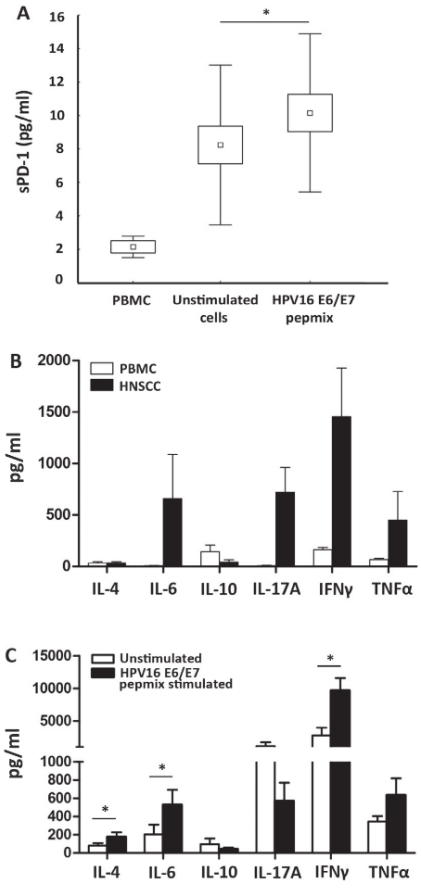

Fig. 4. Cytokine profile and soluble PD-1 (sPD-1) concentration in culture supernatants of tumor-derived two week-expanded TILs. (A) Boxes show the spontaneous release of sPD-1 or the release of sPD-1 upon HPV16 E6/E7 stimulation. The boundaries of the boxes indicate the SEM, and the squares in the boxes represent the mean. Whiskers indicate the SD. (B) Columns show the mean spontaneous cytokine production. (C) White columns represent the mean spontaneous production; black columns represent the mean cytokine production upon HPV16 E6/E7 stimulation. All error bars indicate SEM. $^{*}p < 0.05$.

expression of PD-1; however, we did not find any substantial levels of these factors. The concentration of sPD-1 was significantly higher in TIL cultures than in expanded PBMCs and was further enhanced upon HPV16 E6/E7 pepmix stimulation; nevertheless, the levels were < 20 pg/ml in all of the tested samples (Fig. 4A). Expanded TILs produced high levels of pro-inflammatory cytokines, namely, IL-6, IL-17A, IFNγ and TNFα (Fig. 4B). The levels of IL-4, IL-6, IFNγ and TNFα were further enhanced upon HPV16 E6/E7 pepmix stimulation (Fig. 4C).

Expression of Tim-3 in expanded TILs is positively correlated with the expression of LAG-3 and TGFβ, but not PD-1

In addition to flow cytometry phenotyping, we analyzed the expression levels of checkpoint inhibitors Tim-3, PD-1, PD-L1, CTLA-4, LAG-3, TIGIT, BTLA and immunosuppressive cytokines TGFβ and IL-10 in expanded TILs using qPCR. The mRNA levels of Tim-3 were significantly positively correlated with the expression of regulatory T cell (Treg) markers CTLA-4, LAG-3 and TGFβ ($r = 0.46$, $r = 0.72$ and $r = 0.53$, respectively; $p < 0.05$), but not with PD-1 (Fig. 5).

Discussion

Despite being more often diagnosed at advanced stages of the disease, patients with HNSCC associated with HPV infection have a significantly better prognosis than patients with HPV-negative tumors [19]. It has been suggested that the improved response of HPV-positive HNSCC patients to the conventional treatment was related to the immune response [20]. Indeed, HPV-associated tumors were shown to have a markedly different immune profile compared to HPV-negative tumors, with substantial infiltrates of CD8+ T cells and mDCs [17]. In a preclinical murine model, Badoual et al. [9] showed that the activation of an anti-HPV immune response by the anti-E7 vaccine elicited PD-1 expression by CD8+ T cells and was associated with partial regression of E7-expressing TC-1 tumors. Moreover, therapeutic vaccination against HPV16 oncoproteins has been reported to be successful in the treatment of HPV-associated vulvar intraepithelial neoplasias [12,21]. Therefore, in HPV-associated cancers, HPV-specific T cells seem to play an essential role in the anti-tumor immune response. However, whether the HPV-specific tumor infiltrating T cells express a functional phenotype has not been fully elucidated so far.

In this study, we characterized a phenotype and functionality of HPV-specific tumor-infiltrating T lymphocytes (TILs) derived from oropharyngeal tumors and considered the effect of homeostatic expansion on these characteristics.

In accordance with data published by Hausinkveld et al. [14], we found that HPV16-specific CD8+ T cells react against HPV16 E6/E7 peptides by IFNγ production in 73.1% of OPC patients with HPV-associated tumors. TNFα production was observed in 40% of TIL samples, which may indicate a proceeding loss of functionality [22]. Neither IFNγ+ nor TNFα+ CD8+ T cells were detected in TILs derived from HPV-negative tumors. Upon specific stimulation, IFNγ was mainly produced by PD-1+Tim-3- and PD-1-Tim-3- CD8+ T cells, thus affirming Tim-3 rather than PD-1 as a marker of advanced dysfunction. Indeed, we observed the highest proportion of IFNγ-producing cells exactly in the PD-1+Tim-3-CD8+ T cell subset. Whether this phenotype is in OPC associated preferentially with HPV-specific CD8+ T cells, or is also relevant in tumor-associated antigen (TAA)-specific CD8+ TILs, remains to be addressed. However, in TILs expanded from melanoma samples, reactivity and specificity to autologous or HLA-matched tumor cells was highly enriched in the PD-1+CD8+ fraction [23]. Interestingly, in several reports, PD-1 expression positively correlated with activation markers such as HLA-DR, CD38 or 4-1BB [9,24]. Moreover, in HPV-associated HNSCC, high levels of PD-1+T cells were positively correlated to a favorable clinical outcome [9]. In accordance with these results, Granier et al. [25] have recently described intratumoral Tim-3+PD-1+CD8+ but not Tim-3-PD-1+CD8+ T cells as critical mediators of an aggressive phenotype in renal cell carcinoma.

Consistently with the abovementioned data, we only observed a minor effect of anti-PD-1 mAb nivolumab alone on the IFNγ production by TILs; however, proportions of IFNγ-producing CD8+ T cells substantially increased in the cultures treated with nivolumab in combination with sTim-3. Our data are in accordance with the previously reported synergistic effect of Tim-3 and PD-1 blockade in CT26 tumor-bearing mice [26] and in a mouse model of orthotopic HPV16-positive HNSCC [27]. Surprisingly, following a PD-1 blockade in TILs isolated from HNSCC samples, we did not observe an increase of Tim-3 expression reported by Shayan et al. [27]. To assess whether this might be an effect of TIL expansion, we analyzed the effect of nivolumab treatment on Tim-3 expression in freshly isolated TILs. Indeed, Tim-3 expression was substantially increased in fresh CD8+ TILs following the PD-1 blockade; however, this effect was markedly lower in cells stimulated with HPV16 E6/E7 peptides than in unstimulated cells. These

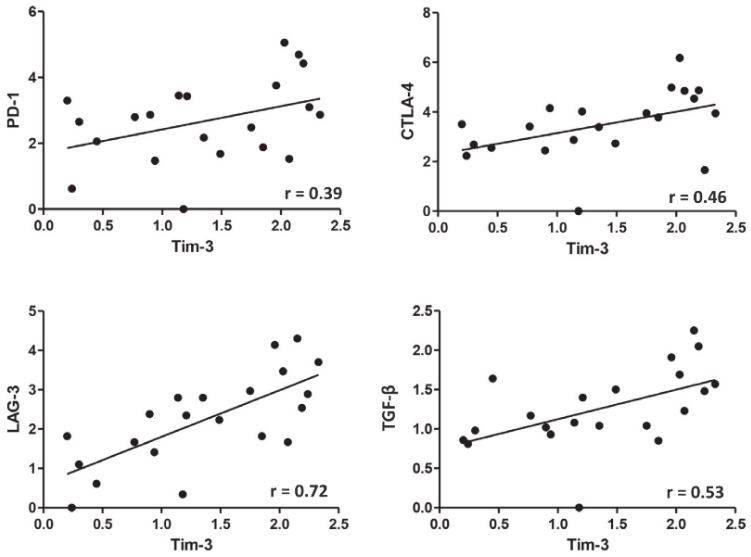

Fig. 5. Correlation between mRNA levels of Tim-3 (x-axis) and PD-1, CTLA-4, LAG-3, and TGFβ (y-axis) in expanded TILs. Linear trend lines and regression coefficients are shown.

data suggest that the specific stimulation of anti-HPV16 CD8+ T cells might suppress the upregulation of Tim-3 expression in response to the PD-1 blockade and thus likely has the capacity to overcome the Tim-3 mediated escape from anti-PD1-1 therapy described by Koyama et al. [7] and Shayan et al. [27].

The phenotype analysis of fresh vs. expanded TILs showed a clear shift from a dominant PD-1+Tim-3- population to PD-1+Tim-3+ and PD-1-Tim-3+ populations. This alteration was more pronounced in cultures derived from HPV- than from HPV+ OPC samples. The shift was similar in both CD8+ and CD4+ T cells. In control PBMCs obtained from healthy donors, we observed an increase in both PD-1+ and Tim-3+ cell populations, which likely reflects significant differences in PD-1 and Tim-3 levels in fresh PBMCs and TILs. Similar to our observations, in melanoma-derived TIL cultures, Inozume et al. [23] reported the down-regulation of PD-1 during *in vitro* expansion in IL-2; however, this study does not consider the expression alterations in other check-point molecules such as Tim-3. Thus, the general effect of "homeostatic" expansion upon high levels of IL-2 on TILs derived from various tumor samples must be further tested. In our study, high basal expression of Tim-3 in expanded TILs could abrogate the effect of the PD-1 blockade on both IFNγ production and further increase in Tim-3 expression.

The expression levels and functionality of check-point molecules were reported to be influenced by free fatty acids, free adenosine [28], soluble PD-1 [29] and cytokines [29–31]; therefore, we analyzed the presence of these factors in TIL culture supernatants. Although we only observed insignificant levels of free fatty acids and adenosine, the spontaneous production of pro-inflammatory cytokines IL-6, IL-17A, IFNγ and TNFα was surprisingly high in TIL cultures. It was shown that TNFα and IL-6 consistently abrogate PD-1-mediated suppression in CD4+ T cell cultures through the induction of sPD-1 [29]. In our study, we found significantly higher levels of sPD-1 in TIL culture supernatants compared to control PBMC cultures, which were further enhanced upon HPV16 E6/E7 pepmix stimulation. However, the levels of sPD-1 were most likely too low to explain the impaired effect of nivolumab in expanded TILs.

Taken together, in this study, we have shown that 73.1% of OPC patients with HPV-associated tumors had HPV16-specific TILs able to produce IFNγ upon specific stimulation. Additionally, these HPV-specific TILs were mainly PD-1+Tim-3-CD8+ T cells, designating Tim-3 rather than PD-1 as a marker of dysfunction. Indeed, upon specific stimulation with HPV16 E6/E7 pepmix, IFNγ production was enhanced by anti-PD-1 mAb nivolumab in combination with sTim-3, but not with nivolumab alone. Our data suggest that complementary treatments combining anti-PD-1 blockade with therapeutic HPV vaccination and/or the additional blockade of inhibitory pathways, such as Tim-3, might substantially increase the HPV-specific immune response in HPV-associated OPC. Subsequently, such a complex therapeutic approach could increase the objective response rate in OPC patients with HPV-associated tumors compared to anti-PD-1 monotherapy.

Conflict of interest

None.

Acknowledgements

This work was supported by research grants #17-28055A, 16-28594A and 16-28600A from the Ministry of Health of the Czech Republic, by grant No. LQ1604 from the Ministry of Education, Youth and Sports of the Czech Republic and by the "BIOCEV" project grant (CZ.1.05/1.1.00/02.0109).

Appendix A. Supplementary material

Supplementary data associated with this article can be found, in the online version, at http://dx.doi.org/10.1016/j.oraloncology.2018.05.010.

References

[1] Torre LA, Bray F, Siegel RL, Ferlay J, Lortet-Tieulent J, Jemal A. Global cancer statistics, 2012. CA Cancer J Clin 2015;65:87–108.
[2] Vermorken JB, Trigo J, Hitt R, Koralewski P, Diaz-Rubio E, Rolland F, et al. Open-label, uncontrolled, multicenter phase II study to evaluate the efficacy and toxicity

of cetuximab as a single agent in patients with recurrent and/or metastatic squamous cell carcinoma of the head and neck who failed to respond to platinum-based therapy. J Clin Oncol 2007;25:2171–7.
[3] Seiwert TY, Burtness B, Mehra R, Weiss J, Berger R, Eder JP, et al. Safety and clinical activity of pembrolizumab for treatment of recurrent or metastatic squamous cell carcinoma of the head and neck (KEYNOTE-012): an open-label, multicentre, phase 1b trial. Lancet Oncol 2016;17:956–65.
[4] Bauml J, Seiwert TY, Pfister DG, Worden F, Liu SV, Gilbert J, et al. Pembrolizumab for platinum- and cetuximab-refractory head and neck cancer: results from a single-arm, Phase II study. J Clin Oncol 2017;35:1542–9.
[5] Ferris RL, Blumenschein Jr. G, Fayette J, Guigay J, Colevas AD, Licitra L, et al. Nivolumab for recurrent squamous-cell carcinoma of the head and neck. N Engl J Med 2016;375:1856–67.
[6] Fourcade J, Sun Z, Benallaoua M, Guillaume P, Luescher IF, Sander C, et al. Upregulation of Tim-3 and PD-1 expression is associated with tumor antigen-specific CD8+ T cell dysfunction in melanoma patients. J Exp Med 2010;207:2175–86.
[7] Koyama S, Akbay EA, Li YY, Herter-Sprie GS, Buczkowski KA, Richards WG, et al. Adaptive resistance to therapeutic PD-1 blockade is associated with upregulation of alternative immune checkpoints. Nat Commun 2016;7:10501.
[8] Best SR, Niparko KJ, Pai SI. Biology of human papillomavirus infection and immune therapy for HPV-related head and neck cancers. Otolaryngol Clin North Am 2012;45:807–22.
[9] Badoual C, Hans S, Merillon N, Van Ryswick C, Ravel P, Benhamouda N, et al. PD-1-expressing tumor-infiltrating T cells are a favorable prognostic biomarker in HPV-associated head and neck cancer. Cancer Res 2013;73:128–38.
[10] Best SR, Peng S, Juang CM, Hung CF, Hannaman D, Saunders JR, et al. Administration of HPV DNA vaccine via electroporation elicits the strongest CD8+ T cell immune responses compared to intramuscular injection and intradermal gene gun delivery. Vaccine 2009;27:5450–9.
[11] Macedo R, Rochefort J, Guillot-Delost M, Tanaka K, Le Moignic A, Noizat C, et al. Intra-cheek immunization as a novel vaccination route for therapeutic vaccines of head and neck squamous cell carcinomas using plasmo virus-like particles. Oncoimmunology 2016;5:e1164363.
[12] Kenter GG, Welters MJ, Valentijn AR, Lowik MJ, Berends-van der Meer DM, Vloon AP, et al. Vaccination against HPV-16 oncoproteins for vulvar intraepithelial neoplasia. N Engl J Med 2009;361:1838–47.
[13] Albers A, Abe K, Hunt J, Wang J, Lopez-Albaitero A, Schaefer C, et al. Antitumor activity of human papillomavirus type 16 E7-specific T cells against virally infected squamous cell carcinoma of the head and neck. Cancer Res 2005;65:11146–55.
[14] Heusinkveld M, Goedemans R, Briet RJ, Gelderblom H, Nortier JW, Gorter A, et al. Systemic and local human papillomavirus 16-specific T-cell immunity in patients with head and neck cancer. Int J Cancer 2012;131:E74–85.
[15] Heusinkveld M, Welters MJ, van Poelgeest MI, van der Hulst JM, Melief CJ, Fleuren GJ, et al. The detection of circulating human papillomavirus-specific T cells is associated with improved survival of patients with deeply infiltrating tumors. Int J Cancer 2011;128:379–89.
[16] Hoffmann TK, Arsov C, Schirlau K, Bas M, Friebe-Hoffmann U, Klussmann JP, et al. T cells specific for HPV16 E7 epitopes in patients with squamous cell carcinoma of the oropharynx. Int J Cancer 2006;118:1984–91.
[17] Partlova S, Boucek J, Kloudova K, Lukesova E, Zabrodsky M, Grega M, et al. Distinct patterns of intratumoral immune cell infiltrates in patients with HPV-associated compared to non-virally induced head and neck squamous cell carcinoma. Oncoimmunology 2015;4:e965570.
[18] van den Brule AJ, Pol R, Fransen-Daalmeijer N, Schouls LM, Meijer CJ, Snijders PJ. GP5+/6+ PCR followed by reverse line blot analysis enables rapid and high-throughput identification of human papillomavirus genotypes. J Clin Microbiol 2002;40:779–87.
[19] Lajer CB, von Buchwald C. The role of human papillomavirus in head and neck cancer. APMIS 2010;118:510–9.
[20] Spanos WC, Nowicki P, Lee DW, Hoover A, Hostager B, Gupta A, et al. Immune response during therapy with cisplatin or radiation for human papillomavirus-related head and neck cancer. Arch Otolaryngol Head Neck Surg 2009;135:1137–46.
[21] Daayana S, Elkord E, Winters U, Pawlita M, Roden R, Stern PL, et al. Phase II trial of imiquimod and HPV therapeutic vaccination in patients with vulval intraepithelial neoplasia. Br J Cancer 2010;102:1129–36.
[22] Wherry EJ. T cell exhaustion. Nat Immunol 2011;12:492–9.
[23] Inozume T, Hanada K, Wang QJ, Ahmadzadeh M, Wunderlich JR, Rosenberg SA, et al. Selection of CD8+PD-1+ lymphocytes in fresh human melanomas enriches for tumor-reactive T cells. J Immunother 2010;33:956–64.
[24] Verbrugge I, Hagekyriakou J, Sharp LL, Galli M, West A, McLaughlin NM, et al. Radiotherapy increases the permissiveness of established mammary tumors to rejection by immunomodulatory antibodies. Cancer Res 2012;72:3163–74.
[25] Granier C, Dariane C, Combe P, Verkarre V, Urien S, Badoual C, et al. Tim-3 expression on tumor-infiltrating PD-1(+)CD8(+) T cells correlates with poor clinical outcome in renal cell carcinoma. Cancer Res 2017;77:1075–82.
[26] Sakuishi K, Apetoh L, Sullivan JM, Blazar BR, Kuchroo VK, Anderson AC. Targeting Tim-3 and PD-1 pathways to reverse T cell exhaustion and restore anti-tumor immunity. J Exp Med 2010;207:2187–94.
[27] Shayan G, Srivastava R, Li J, Schmitt N, Kane LP, Ferris RL. Adaptive resistance to anti-PD1 therapy by Tim-3 upregulation is mediated by the PI3K-Akt pathway in head and neck cancer. Oncoimmunology 2017;6:e1261779.
[28] Buck MD, Sowell RT, Kaech SM, Pearce EL. Metabolic instruction of immunity. Cell 2017;169:570–86.
[29] Bommarito D, Hall C, Taams LS, Corrigall VM. Inflammatory cytokines compromise programmed cell death-1 (PD-1)-mediated T cell suppression in inflammatory arthritis through up-regulation of soluble PD-1. Clin Exp Immunol 2017;188:455–66.
[30] Kinter AL, Godbout EJ, McNally JP, Sereti I, Roby GA, O'Shea MA, et al. The common gamma-chain cytokines IL-2, IL-7, IL-15, and IL-21 induce the expression of programmed death-1 and its ligands. J Immunol 2008;181:6738–46.
[31] Matsuzaki J, Gnjatic S, Mhawech-Fauceglia P, Beck A, Miller A, Tsuji T, et al. Tumor-infiltrating NY-ESO-1-specific CD8+ T cells are negatively regulated by LAG-3 and PD-1 in human ovarian cancer. Proc Natl Acad Sci USA 2010;107:7875–80.

5.3 Význam B lymfocytů pro podporu specifické CD8+ T-buněčné imunitní odpovědi u pacientů s nádory hlavy a krku

Imunoterapie se díky nevídaným úspěchům v onkologii zařadila mezi základní pilíře léčby některých nádorových onemocnění, a posunula tak hranice onkologické léčby. Většina imunoterapeutických přístupů je dnes založena na aktivaci specifické T-buněčné protinádorové imunitní odpovědi, která je většinou působením imunosupresivního nádorového mikroprostředí silně utlumena. Ani nejaktuálnější imunoterapeutické přístupy založené na imunomodulačních protilátkách ale nedokáží tento mechanismus úniku nádoru před imunitním dohledem zcela překonat, a i přes silný terapeutický účinek tak na léčbu odpovídá pouze část pacientů, u kterých se většinou nepodaří dosáhnout trvalé remise, neboť aktivace T-buněčné protinádorové imunitní odpovědi je často pouze přechodná. Specifická imunitní reakce je založena na komplexní spolupráci jednotlivých složek adaptivní imunity, zejména T a B lymfocytů. Tato kooperace vede k silné a dlouhotrvající imunitní odpovědi. Pro dosažení efektivní protinádorové imunitní odpovědi je proto potřeba zaměřit se nejen na aktivaci T-buněčné složky, ale i B-buněčné, která je zatím v klinickém testování spíše opomíjena. Z tohoto důvodu jsme se v rámci komplexní studie nádorového infiltrátu pacientů s OPSCC zaměřili na funkční a fenotypovou analýzu CD20+ TIL-Bs, jejich kvantitativní zastoupení a schopnost interakce s CD8+ TILs. Pozorovali jsme signifikantní prognostický význam denzity CD20+ TIL-Bs pro celkové přežití pacientů s OPSCC. Vysoká denzita těchto CD20+ TIL-Bs byla navíc asociována s jejich aktivovaným fenotypem, produkcí chemokinového ligandu 9 (C-X-C motif chemokine ligand 9, CXCL9) a infiltrací CD8+ TILs, které jsou pravděpodobně atrahovány do nádoru právě díky chemotaktickému gradientu CXCL9, z velké části produkovanému B lymfocyty. V nádorovém mikroprostředí potom může docházet k funkčním interakcím mezi CD20+ TIL-Bs a CD8+ TILs. U OPSCC míra těchto interakcí signifikantně korelovala s lepším přežíváním pacientů. Způsob, jakým TIL-Bs a CD8+ TILs v nádorové tkáni interagují ani dráhy ovlivněné touto interakcí nejsou zatím známé. Naše studie navrhuje, že přímo v nádorové tkáni hrají aktivované TIL-Bs zásadní roli při sekundární kostimulaci CD8+ TILs, zprostředkovanou skrze zapojení jedné z popsaných kostimulačních signálních drah. Z výsledků naší studie vyplývá, že prognóza pacientů s OPSCC je významně ovlivněna infiltrací TIL-Bs do nádorové tkáně, jejichž vysoce funkční fenotyp a schopnost interakce s CD8+ TILs umožňuje dlouhodobé přežívání CD8+ TILs v nádorovém mikroprostředí, a pravděpodobně tak vede k dlouhodobé protinádorové imunitní odpovědi. Zahrnutí

B-buněčné složky do současných imunoterapeutických postupů by tak mohlo zvýšit účinnost nejmodernějších přístupů zaměřených doposud převážně na aktivaci T lymfocytů.

K této práci jsem přispěla následovně: 60 %; příprava vzorků pro analýzu exprese genů spojených s imunitní odpovědí, optimalizace protokolů pro imunohistochemické značení jednotlivých populací imunitního infiltrátu na řezech z parafínových bločků formalinem fixované tkáně (formalin-fixed paraffin-embedded, FFPE), následné barvení a kvantitativní analýza, izolace RNA a stanovení exprese vybraných genů pomocí qPCR, analýza dat a účast na přípravě manuskriptu.

Hladíková et al. Journal for ImmunoTherapy of Cancer (2019) 7:261
https://doi.org/10.1186/s40425-019-0726-6

Journal for ImmunoTherapy of Cancer

RESEARCH ARTICLE Open Access

Tumor-infiltrating B cells affect the progression of oropharyngeal squamous cell carcinoma via cell-to-cell interactions with CD8$^+$ T cells

Kamila Hladíková[1,2], Vladimír Koucký[1,3], Jan Bouček[3], Jan Laco[4], Marek Grega[5], Miroslav Hodek[6], Michal Zábrodský[3], Milan Vošmik[6], Kateřina Rozkošová[4], Hana Vošmiková[4], Petr Čelakovský[7], Viktor Chrobok[7], Aleš Ryška[4], Radek Špíšek[1] and Anna Fialová[1*]

Abstract

Background: Standard treatment of oropharyngeal squamous cell carcinoma (OPSCC) is associated with high morbidity, whereas immunotherapeutic approaches using PD-1:PD-L1 checkpoint blockade only show moderate response rates in OPSCC patients. Therefore, a better stratification of patients and the development of novel therapeutic protocols are crucially needed. The importance of tumor-infiltrating B cells (TIL-Bs) in shaping antitumor immunity remains unclear; therefore, we analyzed frequency, phenotype, prognostic value and possible roles of TIL-Bs in OPSCC.

Methods: We utilized transcriptomic analysis of immune response-related genes in 18 OPSCC samples with respect to human papillomavirus (HPV) status. The density and localization of CD20$^+$, CD8$^+$ and DC-LAMP$^+$ cells were subsequently analyzed in 72 tissue sections of primary OPSCC samples in relation to patients' prognosis. The immunohistochemical approach was supplemented by flow cytometry-based analysis of phenotype and functionality of TIL-Bs in freshly resected primary OPSCC tissues.

Results: We observed significantly higher expression of B cell-related genes and higher densities of CD20$^+$ B cells in HPV-associated OPSCC samples. Interestingly, CD20$^+$ TIL-Bs and CD8$^+$ T cells formed non-organized aggregates with interacting cells within the tumor tissue. The densities of both intraepithelial CD20$^+$ B cells and B cell/CD8$^+$ T cell interactions showed prognostic significance, which surpassed HPV positivity and CD8$^+$ TIL density in stratification of OPSCC patients. High density of TIL-Bs was associated with an activated B cell phenotype, high CXCL9 production and high levels of tumor-infiltrating CD8$^+$ T cells. Importantly, the abundance of direct B cell/CD8$^+$ T cell interactions positively correlated with the frequency of HPV16-specific CD8$^+$ T cells, whereas the absence of B cells in tumor-derived cell cultures markedly reduced CD8$^+$ T cell survival.

Conclusions: Our results indicate that high abundance of TIL-Bs and high density of direct B cell/CD8$^+$ T cell interactions can predict patients with excellent prognosis, who would benefit from less invasive treatment. We propose that in extensively infiltrated tumors, TIL-Bs might recruit CD8$^+$ T cells via CXCL9 and due to a highly activated phenotype contribute by secondary costimulation to the maintenance of CD8$^+$ T cells in the tumor microenvironment.

Keywords: HNSCC, Tumor-infiltrating B lymphocytes, HPV

* Correspondence: fialova@sotio.com
[1]SOTIO a.s, Jankovcova 1518/2, CZ-17000 Prague 7, Prague, Czech Republic
Full list of author information is available at the end of the article

Background

Oropharyngeal squamous cell carcinoma (OPSCC) forms a specific subset of head and neck squamous cell carcinoma (HNSCC), associated in up to 90% of patients with human papillomavirus (HPV) infection [1, 2]. A positive HPV-status has been reported to correlate with better locoregional control, a longer overall survival [3, 4] and a higher immunogenicity of the tumor [5, 6]. The immune response has been suggested as a key factor in the better outcome of patients with HPV-associated tumors [7].

Indeed, in a wide range of malignancies, characterization of the adaptive immune response has been shown to be a valid prognostic tool for improving the stratification of the patients compared to the current staging system [8–12]. During the past two decades, extensive immuno-oncology research has been mainly focused on T cells and several studies have reported the association between a high density of tumor infiltrating T lymphocytes (TILs) and increased patient survival [8, 11–13]. Consequently, most of the recent immunotherapeutic approaches target T cell-mediated immunity. In 2016, the immune checkpoint inhibitors pembrolizumab and nivolumab were approved by the American Food and Drug Administration (FDA) for HNSCC patients whose disease has progressed during or after platinum-based chemotherapy. However, clinical trials with the above mentioned PD-1:PD-L1 targeting agents only reported modest response rates (13–23%) in HNSCC patients [14–17]. Therefore, novel immunotherapy targets and consequent effective therapeutic strategies are still needed for this type of carcinoma.

In contrast to T cells, the role of B cells in the tumor microenvironment remains controversial. Both positive and negative impacts of B cells on tumor immunity and disease progression have been reported [18, 19]. Most of the studies concerning mouse models assign B cells a tumor-promoting character, whereas studies of human solid tumors mainly associated a high density of tumor-infiltrating B cells (TIL-Bs) with a favorable clinical outcome [20–24]. It has been proposed that TIL-Bs generate antitumor antibodies [20, 25, 26], produce antitumor cytokines, exert direct cytotoxicity towards tumor cells and are capable to present tumor-associated antigens (TAA) [19, 27–30].

It has been hypothesized that TAA-specific T cells are primed in tumor-draining lymph nodes and subsequently migrate to the tumor tissue [31, 32]. However, in addition to the primary DC-T cell interactions in the lymph nodes, secondary interactions with activated APCs at the target tissue site are needed for the generation of an effective immune response. Indeed, especially in cases of viral infections, T cell interactions with antigen-experienced activated DCs and/or B cells at the site of infection have been shown to be essential for the secondary recall and long-term survival of T cells [33–35]. Therefore, TIL-Bs might act as local APCs essential for the secondary stimulation of tumor-specific T cells.

In this study, we assessed the frequency, distribution and phenotype of TIL-Bs in OPSCC samples. For the first time, we showed significant differences between patients with low versus high infiltrates of $CD20^+$ B cells not only in the clinical outcome but also in the activation status of TIL-Bs and the density of tumor-infiltrating HPV 16 E6/E7-specific $CD8^+$ T cells. Our results indicate that in immunologically "hot" OPSCCs, highly activated TIL-Bs may provide crucial secondary costimulatory stimuli to the tumor-infiltrating $CD8^+$ T cells, resulting in the maintenance of $CD8^+$ T cell-mediated antitumor immunity and prolonged patient survival.

Materials and methods

Patients and samples

Cohort 1

Formalin-fixed paraffin-embedded (FFPE) primary OPSCC specimens were obtained from 72 patients who underwent radical surgery at the University Hospital Hradec Kralove in Czech Republic between 2001 and 2014. All of the patients underwent surgical resection of the primary tumor using external approach with therapeutic neck dissection, followed by postoperative radiotherapy. Concomitant chemotherapy was applied in 30.5% ($n = 22$) of patients.

Cohort 2

Primary fresh OPSCC tissues and matching FFPE tumor sections were obtained from 21 patients after therapeutic surgery at the University Hospital Motol in Prague, Czech Republic, between August 2015 and May 2016.

Cohort 3

Fresh primary OPSCC specimens and blood samples were obtained from 21 patients immediately after therapeutic surgery at the University Hospital Motol in Prague, Czech Republic, between March 2018 and June 2019. Control tonsils were obtained from 6 healthy donors.

None of the patients enrolled in this study had received any neoadjuvant chemo- or radiotherapy. The pathological staging of OPSCC was reviewed and classified by an experienced pathologist according to the 8th edition of the American Join Committee on Cancer. The clinical-pathological characteristics of the patients are summarized in Table 1.

TaqMan low-density array

Total RNA was isolated from 1×10^6 tumor-tissue derived cells using the RNA Easy Mini Kit (Qiagen) according to the manufacturer's instructions. The concentration and purity of the samples were determined by spectrophotometry with a NanoDrop© 2000c (Thermo Scientific), and the RNA integrity

Table 1 Clinico-pathological characteristics of the patients

Variable	Cohort No. 1		Cohort No. 2		Cohort No. 3	
	No.	%	No.	%	No.	%
Total No. of Patients	72		21		21	
Age						
Median	57		63		63	
Range	41–76		40–73		41–75	
Sex						
Male	55	76.4	16	76.2	13	61.9
Female	17	23.6	5	23.8	8	38.1
Tumor site						
Palatine tonsil	62	86.1	18	85.7	14	66.7
Base of tongue	10	13.9	2	9.5	4	19.0
Oropharynx NS	0	0	1	4.8	3	14.3
T status						
T1	17	23.6	6	28.6	6	28.6
T2	36	50.0	11	52.4	12	57.1
T3	13	18.1	4	19	3	14.3
T4	6	8.3	0	0	0	0
N status						
N0	1	1.4	4	19	1	4.8
N1	15	20.8	17	81	16	76.2
N2	53	73.6	0	0	4	19.0
N3	3	4.2	0	0	0	0
Stage 8th edition of AJCC						
I	46	63.9	17	81	15	71.4
II	13	10.1	4	19	6	28.6
III	5	6.9	0	0	0	0
IV	8	19.1	0	0	0	0
Stage 7th edition of AJCC						
I	0	0	1	4.8	1	4.8
II	0	0	3	14.3	2	9.6
III	18	25	4	19.0	1	4.8
IV	54	75	13	61.9	17	80.8
HPV status						
HPV+	63	87.5	21	100	21	100
HPV-	9	12.5	0	0	0	0
Smoking history						
Smoker	22	30.6	7	34.4	9	42.9
Ex-smoker	25	34.7	5	23.8	2	9.5
Non-smoker	25	34.7	9	42.8	10	47.6

was assessed using a 2100 Bioanalyzer (Agilent). Complementary DNA was synthesized from 100 ng of total RNA using the High Capacity RNA-to-cDNA Kit (Applied Biosystems). The gene expression of immune response-associated genes was determined using TaqMan low-density array (TLDA) cards according to the manufacturer's instructions (Applied Biosystems). The TLDA cards (TaqMan® Array Human Immune Panel) were run on a Viia7 instrument (Applied Biosystems) using TaqMan® Universal Master Mix II, no UNG (Applied

Biosystems). Ct values were analyzed using GenEx software (MultiD Analyses). Relative gene expression levels were calculated using the ΔΔCt method and were normalized to the expression levels of reference genes GUSB and TFRC, selected by GeNorm from 6 reference genes assessed in total.

Immunohistochemistry

Staining was carried out on FFPE sections following deparaffinization and antigen retrieval. Endogenous peroxidase was blocked with 3% hydrogen peroxide. The sections were incubated with protein block (DAKO) and stained with primary antibodies against CD8 (SP16, Spring Bioscience), CD20 (L26, Dako) and DC-LAMP (1010E1.01, Dendritics), followed by the manifestation of enzymatic activity and hematoxylin counterstaining. The images were acquired using a Leica Aperio AT2 scanner (Leica).

Quantification of tumor-infiltrating immune cells

Each section was scanned and evaluated for immune cell infiltration in the tumor nest and tumor stroma in 10 representative visual fields at 10× magnification using a Ventana Image Viewer. The cell numbers were related to tumor nest/tumor stroma area assessed by Calopix software (Tribvn). Additionally, a semiquantitative analysis of $CD20^+/CD8^+$ cell-cell interactions was performed (–, negative sections; +, sections positive for B cell/$CD8^+$ T cell interactions in 1–5 visual fields; ++, sections positive for interactions in > 5 visual fields). The cell-cell interaction was defined as a direct cell-cell contact of $CD20^+$ B cell and $CD8^+$ T cell (Fig. 1d) within an aggregate of 20–100 cells (Fig. 1c) or in a distance up to 100 μm from a margin of the aggregate. The quantification was performed by two independent observers and reviewed by an experienced pathologist.

Processing of fresh tumor tissues and blood samples

Fresh tumor tissues were mechanically and enzymatically digested as described previously [6]. Subsequently, the specimens were passed through a 100-μm nylon cell strainer (BD Biosciences) and washed with PBS. Peripheral blood mononuclear cells (PBMCs) were isolated from the peripheral blood samples by centrifugation on a Ficoll-Paque density gradient (GE Healthcare).

Flow cytometry

Single cell suspensions derived from tumor tissues were labeled using a panel of monoclonal antibodies as listed in Additional file 1: Table S1. For the intracellular detection of cytokines and Ki-67, the cells were fixed and permeabilized with the Fixation/Permeabilization Buffer Set (eBioscience) and intracellularly labeled with primary antibodies. The cells were analyzed on a BD LSR Fortessa (BD Biosciences) and evaluated with FlowJo software (TreeStar).

Detection of HPV-specific T cells

The detection of HPV16 E6/E7-specific T cells was performed as described previously [36]. Briefly, freshly prepared tumor-derived single cell suspensions were seeded at a concentration of 3×10^5 cells/ml into 24 well plate and TILs were expanded for two weeks in the presence of IL-2. Monocytes from autologous PBMCs were isolated using the Human CD14 Positive Selection Kit (Stemcell Technologies), loaded with HPV16 E6 and E7 peptide pools (5 μg/ml) (JPT) and added to expanded TILs at a ratio of 1:10. After 6 h of incubation with Brefeldin A (BioLegend), the cells were stained with antibodies for the intracellular detection of IFNγ.

Analysis of T cell viability and functional capacity

Tumor-derived single cell suspensions were split into halves. One half was depleted of B cells using CD19 MicroBeads (Miltenyi Biotech) according to the manufacturer's instructions. The second half was subjected to the same procedures without addition of CD19 MicroBeads. After magnetic separation, cell suspensions (6×10^5 cells/ml) were cultured in RPMI 1640 supplemented with 10% heat-inactivated FCS, L-glutamine and penicillin-streptomycin (Invitrogen) in 48 well plates for 6 days without any additional stimuli. The viability of $CD4^+$ and $CD8^+$ T cells and their capacity to produce cytokines was assessed at day 1 and 6 using LIVE/DEAD™ Fixable Blue Dead Cell Stain Kit (Invitrogen) and intracellular cytokine staining as described above.

Detection of cytokines and chemokines in cell culture supernatants

Tumor-derived single cell suspensions (1×10^6 cells/ml) were cultured in RPMI 1640 supplemented with 10% heat-inactivated FCS, L-glutamine and penicillin-streptomycin (Invitrogen). For some of the patient samples ($n = 3$), the B cells were depleted from the cell suspensions using CD19 MicroBeads (Miltenyi Biotech) according to the manufacturer's instructions. To detect the concentrations of lymphotoxin, IFNγ, TNFα, IL-6, IL-10, IL-12, CXCL9 and CXCL13 released into the culture supernatant, the MILLIPLEX™ Human Cytokine Kit (Merck) was used according to the manufacturer's instructions.

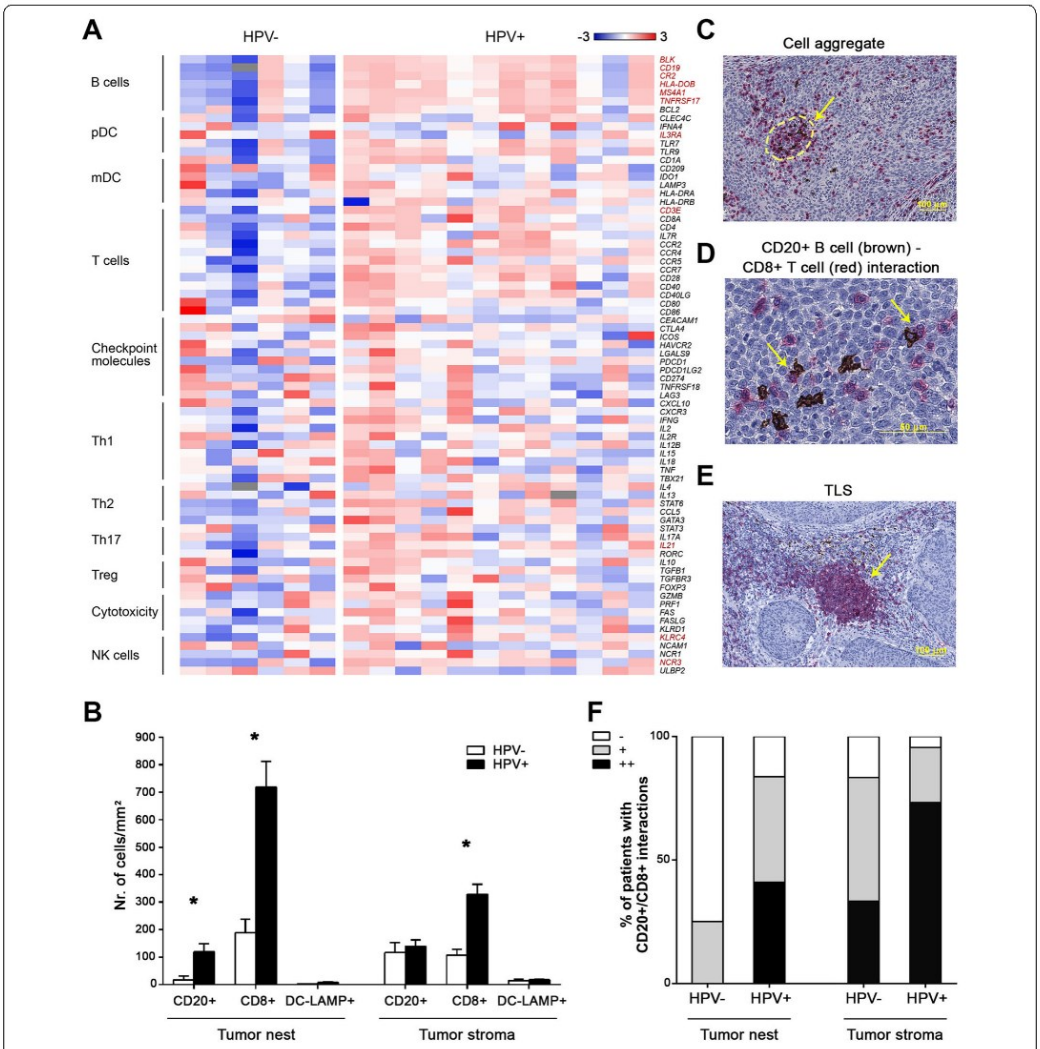

Fig. 1 Differences in frequencies of tumor-infiltrating leucocytes in patients with oropharyngeal squamous cell carcinoma (OPSCC) with respect to the HPV status. **a** The heat-map expresses z-scores of relative mRNA expression of indicated genes within HPV- ($n = 6$) and HPV+ ($n = 12$) tumor samples. Genes with significantly different expression in HPV- and HPV+ tumors are marked in red. **b** Columns represent the mean (+ standard error of mean, SEM) densities of $CD20^+$ B cells, $CD8^+$ T cells and DC-$LAMP^+$ dendritic cells in tumor nests and tumor stroma of immunohistochemically stained FFPE sections of OPC patients from Cohort 1 ($n = 72$). **c** Non-organized $CD20^+$ B cell (brown)/$CD8^+$ T cell (red) aggregate. **d** $CD20^+$ B cell (brown) – CD8+ T cell interactions. **e** TLS with germinal center. **f** Columns show proportions of patients with detected B cell/$CD8^+$ T cell interactions in the tumor nest and the tumor stroma of OPC tissue sections (–, interactions not detected; +, interactions detected in 1–5 visual fields; ++, interactions in > 5 visual fields). * $p < 0.05$ (Mann-Whitney U test)

HPV detection

Immunohistochemical analysis The antibody against p16INK4a (Purified Mouse Anti-Human p16, Clone G175–405, BD Pharmingen TM, dilution 1:100) or the CINtec Histology Kit (Roche) was used. The intensity of staining and the proportion of stained cells were evaluated. Samples positive for p16 expression showed more than 70% of positive cells and revealed nuclear and/or cytoplasmic staining.

PCR HPV DNA from the paraffin-embedded tissue was extracted with the MagCore Genomic DNA FFPE One-Step Kit (RBC Bioscience) according to the manufacturer's protocol.

HPV DNA detection and genotyping were performed by qualitative real-time PCR with the AmoyDx Human Papillomavirus Genotyping Detection Kit (Amoy Diagnostics). The test is designed for the specific amplification of the L1 gene in HPV DNA to detect and genotype 19 high-risk HPVs and 2 low-risk HPVs (HPV 6 and 11). The sensitivity of the test is 100 copies of HPV DNA per reaction. An internal control is provided in the assay to test for sample quality and the presence of inhibiting factors.

HPV $DNA^+/p16^+$ samples were considered HPV-positive.

RNA extraction from isolated $CD8^+$ T cells and quantitative real time PCR

$CD8^+$ T cells were isolated from tumor tissue-derived single cell suspensions and PBMC using the EasySep™ Human CD8 Positive Selection Kit II (StemCell Technologies). Total RNA was isolated from 1×10^6 $CD8^+$ T cells using the RNA Easy Mini Kit (Qiagen) according to the manufacturer's instructions. The concentration and purity of the samples were determined by spectrophotometry with a NanoDrop© 2000c (Thermo Scientific), and the RNA integrity was assessed using a 2100 Bioanalyzer (Agilent). Complementary DNA was synthesized from 100 ng of total RNA using the iScript cDNA Synthesis Kit (BIO-RAD). The gene expression levels of BCL2L1, IL-2, IL-2R, CD27, CD40L, and the β-actin housekeeping gene were evaluated using the CFX 96™ Real-Time System (BIO-RAD). The specificity of the amplified PCR product was assessed using an Agilent DNA 1000 Kit (Agilent). The relative expression of the target genes was normalized to the expression of β-actin.

Statistical analysis

Statistical analyses were performed using Statistica® 10.0 software (StatSoft). The differences between HPV-positive and HPV-negative tumor samples were analyzed using the Mann-Whitney U test. The prognostic value of tumor-infiltrating immune cells was analyzed using the log-rank test. Additionally, the Cox proportional hazard model was used to perform univariate and multivariate analyses of possible prognostic factors. Only variables with significant differences observed in the univariate analysis were included in the multivariate analysis. The correlation between the presence of B cell/CD8+ T cell interactions and HPV positivity/presence of HPV16 E6/E7-specific $CD8^+$ T cells was evaluated using Pearson's chi-square test. Variability in proportions of $Ki\text{-}67^+$ cells was detected using Kruskal-Wallis ANOVA. Differences in the B cell phenotype were analyzed using one-way ANOVA, followed by Tukey's post hoc test. The results were considered statistically significant when $p < 0.05$.

Results

HPV-associated tumors show significantly higher densities of $CD20^+$ B cells and $CD8^+$ T cells in comparison to HPV-negative samples

To evaluate the transcriptional signature of immune response-related genes in HPV-associated and HPV-negative tumors, we assessed the expression of selected genes using TaqMan analysis. Tumor samples with a positive HPV status expressed significantly higher levels of all of the B cell-related genes analyzed, namely, *BLK, CD19, CR2, HLA-DOB, MS4A1* and *TNFRSF17* (Fig. 1a).

To supplement the results of gene expression, we immunohistochemically analyzed the density of $CD20^+$, $CD8^+$ and DC-$LAMP^+$ cells in 72 OPSCC tumor tissue sections (Cohort 1). Compared to HPV-negative tumors, HPV-associated tumors showed significantly higher infiltrates of $CD20^+$ B cells in the tumor nest and significantly higher levels of $CD8^+$ T cells in both the tumor nest and the tumor stroma. No differences were observed in DC-LAMP expression (Fig. 1b). Additionally, we observed that tumor-infiltrating $CD20^+$ B cells and $CD8^+$ T cells create non-organized aggregates in both the tumor nests and the tumor stroma (Fig. 1c) with $CD20^+$ B cells and $CD8^+$ T cells in a direct cell-cell interaction (Fig. 1d). The proportion of these cell-cell interactions was markedly higher in HPV-associated tumors than in HPV-negative tumors (Fig. 1f). In contrast to direct $CD20^+$ B cell/$CD8^+$ T cell interactions, no differences between HPV-associated and HPV-negative samples were observed in the density of tertiary lymphoid structures (TLS) with germinal centers (Fig. 1e). Well-defined TLS with germinal centers were detected in 29.8% of HPV-associated samples and in 25.0% of HPV-negative samples.

High densities of $CD20^+$ B cells, $CD8^+$ T cells and $CD20^+$ B cell/$CD8^+$ T cell interactions in the tumor nest are positive prognostic factors in OPSCC patients

To evaluate the prognostic impact of tumor-infiltrating $CD20^+$ B cells, $CD8^+$ T cells, DC-$LAMP^+$ DCs and B cell/$CD8^+$ T cell interactions in both intratumoral and stromal compartments of OPSCC samples, we investigated overall survival (OS) upon stratifying the patient cohort based on the median of positive cells per 1 mm^2 of the tumor nest and the tumor stroma area. The presence of abundant intratumoral $CD20^+$ B cells and $CD8^+$ T cells was associated with significantly improved OS ($p < 0.001$ and $p = 0.013$, respectively; Fig. 2a, b). Furthermore, the presence of abundant intratumoral and stromal $CD20^+$ B cell/$CD8^+$ T cell interactions was also positively correlated with OS. This correlation was highly statistically significant ($p = 0.001$ and $p = 0.009$, respectively; Fig. 2c). Surprisingly, the

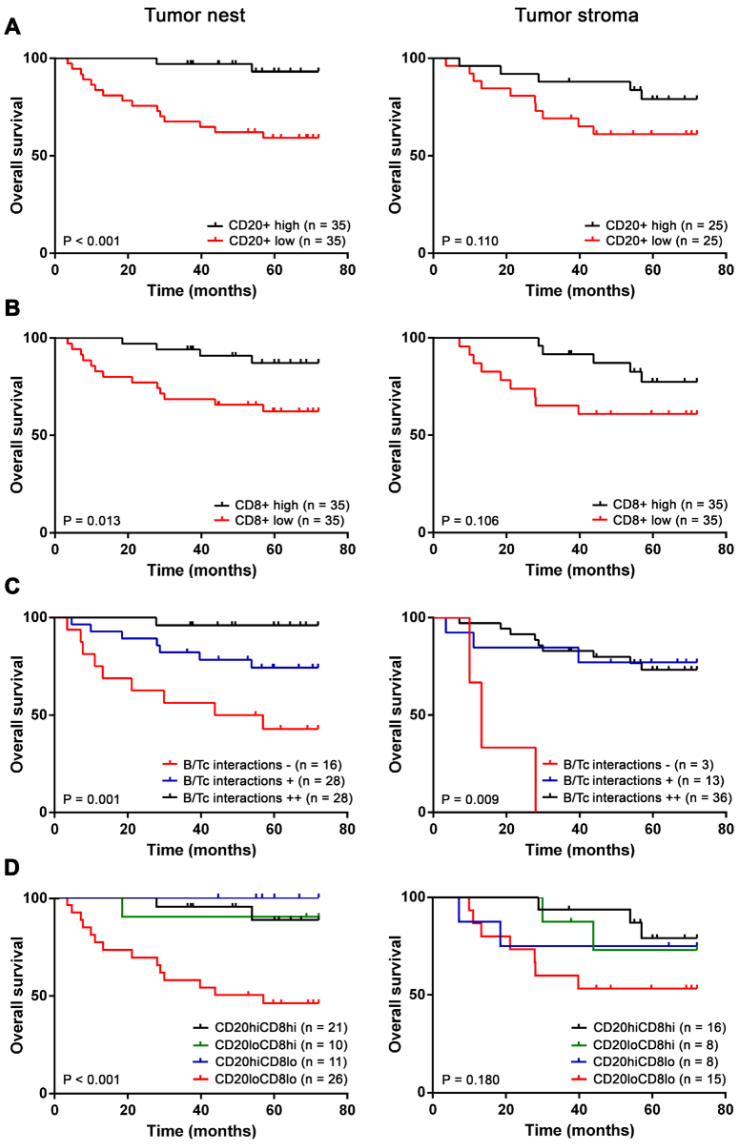

Fig. 2 Prognostic value of tumor-infiltrating $CD20^+$ B cells (**a**), $CD8^+$ T cells (**b**), $CD20^+$B cell/$CD8^+$ T cell (B/Tc) interactions (**c**) and combination of $CD20^+$ B cells and $CD8^+$ T cells (**d**) in patients with OPSCC ($n = 70$). Kaplan-Meier curves show overall survival of patients according to densities of the indicated cells in the tumor nests (left) and in the tumor stroma (right). *P* values were determined using the log-rank test

density of direct $CD20^+$ B cell/$CD8^+$ T cell interactions stratified the patients better than the concurrent presence of both $CD20^+$ B cells and $CD8^+$ T cells (Fig. 2d).

Univariate Cox regression confirmed these results, together with well-described risk factors for HNSCC patients, namely, stage IV ($p = 0.004$), extranodal extension ($p < 0.001$), keratinizing histological subtype ($p = 0.006$), advanced tumor size ($p = 0.042$) and HPV negativity ($p = 0.006$). The results are summarized in Table 2. The multivariate Cox proportional hazard model indicated

Table 2 Prognostic overall survival parameters in univariate analysis

Variable	Class	Hazard Ratio	95% Confidence Interval	*P* value
Sex	Female	1		
	Male	1.14	0.37–3.50	0.816
Stage	I	1		
	II	2.78	0.78–9.87	0.113
	III	3.51	0.71–17.4	0.124
	IV	7.78	1.92–31.5	**0.004**
LN ratio		2.72	0.44–16.89	0.283
Extranodal extension	No	1		
	Yes	6.55	2.46–17.41	**< 0.001**
Perineural spread	No	1		
	Yes	2.10	0.68–6.47	0.194
Resection margin	R0	1		
	R1	1.56	0.57–4.29	0.389
Concomitant chemotherapy	No	1		
	Yes	1.63	0.62–4.28	0.323
Typing SCC	NK	1		
	NK-M	2.31	0.78–6.90	0.131
	K	5.64	1.64–19.41	**0.006**
Tumor size		1.02	1.00–1.06	**0.042**
HPV status	Negative	1		
	Positive	0.23	0.08–0.66	**0.006**
Smoking history	Non-smoker	1		
	Ex-smoker	0.42	0.13–1.42	0.165
	Smoker	0.63	0.20–1.91	0.412
TLS	No	1		
	Yes	1.15	0.40–3.27	0.789
CD20+ B cell density tumor nest		0.96	0.93–0.99	**0.015**
CD20+ B cell density tumor stroma		1.00	0.99–1.00	0.784
CD8+ T cell density tumor nest		0.99	0.99–1.00	**0.013**
CD8+ T cell density tumor stroma		0.99	0.99–1.00	0.231
DC density tumor nest		0.95	0.88–1.03	0.207
DC density tumor stroma		0.98	0.95–1.02	0.328
B cell/T cell clusters tumor nest	-	1		
	+	0.35	0.13–0.95	**0.040**
	++	0.05	0.01–0.41	**0.005**
B cell/T cell clusters tumor stroma	-	1		
	+	0.07	0.01–0.41	**0.003**
	++	0.08	0.02–0.33	**< 0.001**

Statistically significant *P* values are printed in boldface. Abbreviations: *LN* lymph node, *SCC* squamous cell carcinoma, *NK* non-keratinizing, *K* keratinizing, NK-M non-keratinizing with maturation, *TLS* tertiary lymphoid structures

extranodal extension ($p = 0.004$, HR = 5.25, 95% CI = 1.68–16.38), high abundance of $CD20^+$ B cells in tumor nests ($p = 0.044$, HR = 0.97, 95% CI = 0.93–0.99) and high abundance of stromal B cell/CD8+ T cell interactions ($p = 0.019$, HR = 0.10, 95% CI = 0.02–0.69) as independent prognostic factors (Additional file 2: Table S2). HPV negativity and high abundance of B cell/$CD8^+$ T cell interactions in the tumor nests did not reach statistical significance, but there was a strong trend ($p = 0.063$, HR = 0.29, 95% CI = 0.08–1.06 and $p = 0.068$, HR = 0.11, 95%

CI = 0.01–1.17; respectively). The 5-year overall survival (OS) of the patients was 75.7% for the entire Cohort 1 and the median OS was 5.44 years (0.29–14.40).

In HPV-associated tumors, the presence of CD20$^+$ B cell/CD8$^+$ T cell interactions positively correlates with the presence and abundance of HPV16 E6/E7-specific CD8$^+$ TILs

In addition to the differences detected between HPV-positive and HPV-negative tumors, we observed substantial variability in the density of tumor-infiltrating lymphocytes and CD20$^+$ B cell/CD8$^+$ T cell interactions within the group of patients with HPV-associated tumors, splitting HPV-positive samples into "hot" and "cold" subgroups. Therefore, to assess whether the interactions between CD20$^+$ B cells and CD8$^+$ T cells might be important for the HPV-specific T cell response in HPV-driven tumors, we correlated the presence and density of B cell/CD8$^+$ T cell interactions in the FFPE tumor sections with the proportions of HPV16 E6/E7-specific CD8$^+$ T cells detected in TILs expanded from matched native HPV-positive OPSCC samples (Cohort 2). Indeed, 81.8% of patients with detected HPV16 E6/E7-specific CD8$^+$ T cells had a high density of B cell/CD8$^+$ T cell interactions in the tumor stroma and 61.5% of these patients also had high density of these interactions in the tumor nests. In contrast, it was only 42.8 and 14.3%, respectively, in patients without detected HPV16 E6/E7-specific CD8$^+$ T cell responses (Fig. 3a). Moreover, the proportion of HPV16 E6/E7-specific CD8$^+$ T cells was significantly positively correlated with the density of B cell/CD8$^+$ T cell interactions in the tumor nests (Fig. 3b), indicating that patients with low levels of direct B cell – CD8$^+$ T cell interactions also had low levels of HPV16 E6/E7-specific CD8$^+$ T cells. On the contrary, the presence of HPV16-specific CD8$^+$ T cells was neither correlated to the density of CD8$^+$ T cells in general nor to the density of CD20$^+$ B cells (Fig. 3c).

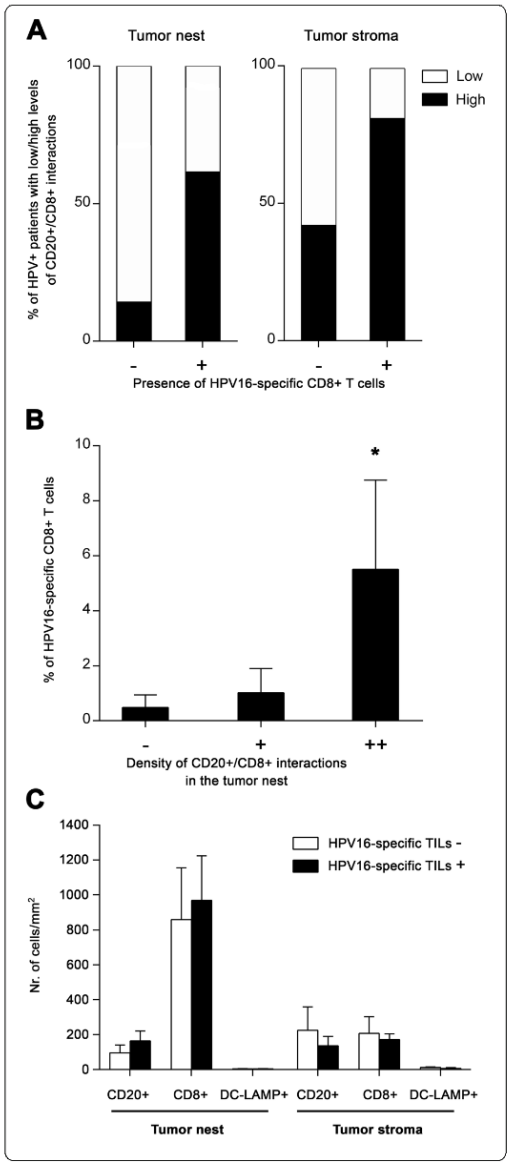

Intratumoral B cells are represented mainly by a memory subtype with an activated, antigen-experienced phenotype

To characterize the phenotype and function of TIL-Bs in HPV-associated tumors with a "hot" versus "cold" phenotype, we analyzed intratumoral and blood-derived B cell subsets by flow cytometry (Cohort 3). Tumor suspensions were divided according to the proportions of TIL-Bs into "cold" B^{lo} samples (B cell proportions < 0.5% of total cells; mean = 0.11 ± 0.05%) and "hot" B^{hi} samples (mean = 4.22 ± 5.96%). In all samples, CD19$^+$ B cells were divided into five subtypes based on the expression level of IgD and CD38, namely, IgD$^-$CD38^{++} plasma cells, IgD$^-$CD38$^+$ germinal center B cells, IgD$^-$CD38$^-$ memory B cells, IgD$^+$CD38$^-$ naive B cells and IgD$^+$CD38$^+$ pre-germinal center B cells (Fig. 4a). Memory B cells represented the major B cell subtype in the tumor tissue (Fig. 4b). There

(See figure on previous page.)
Fig. 3 Positive correlation of direct CD20$^+$ B cell/CD8$^+$ T cell interactions with HPV16 E6/E7-specific CD8$^+$ T cells. **a** Columns show the proportions of patients with low (interactions detectable in 0–5 visual fields) and high (interactions detectable in > 5 visual fields) densities of B cell/CD8$^+$ T cell interactions with respect to the presence or absence of tumor-infiltrating HPV16 E6/E7-specific CD8$^+$ T cells. **b** Columns represent the mean (+ SEM) proportions of tumor-infiltrating HPV16 E6/E7-specific CD8$^+$ T cells with respect to the densities of B cell/CD8$^+$ T cell interactions within the tumor nests. **c** Columns represent the mean (+ SEM) densities of CD20$^+$ B cells, CD8$^+$ T cells and DC-LAMP$^+$ dendritic cells in tumor nests and tumor stroma of patients without/with detected HPV16-specific T cells. *, $p < 0.05$ (Pearson's chi-square test and Mann-Whitney U test)

was no difference in the B cell subtype composition between B^{lo} and B^{hi} samples.

Tumor-infiltrating memory B cells were characterized in both B^{lo} and B^{hi} samples by the high expression of CD27, absent expression of IgD and low expression of IgM, indicating a classical memory, predominantly class-switched phenotype. The positivity for the proliferation marker Ki67 in TIL-Bs derived from B^{hi} samples was comparable to that in CD19$^+$ B cells derived from healthy tonsils and significantly higher than that in peripheral blood B cells. The proportion of Ki67$^+$ TIL-Bs derived from B^{lo} samples was markedly lower in comparison to B^{hi} samples (Additional file 3: Figure S1).

To elucidate whether TIL-Bs might serve as APCs with costimulatory potential, we assessed the expression levels of HLA molecules and costimulatory molecules CD86, CD70 and CD40 on the cell surface. The expression levels of HLA-ABC, HLA-DR, CD86 and CD40 were significantly higher in TIL-Bs derived from B^{hi} OPSCC samples than in TIL-Bs from B^{lo} samples. Additionally, compared to matched peripheral blood B cells, in TIL-Bs derived from B^{hi} samples but not from B^{lo} samples, we observed significantly higher levels of HLA-DR, CD86 and CD40 (Fig. 4c, d, e).

The presence of B cells in the tumor-derived cell suspension enhances the survival of both CD4$^+$ and CD8$^+$ TILs

To assess the impact of TIL-Bs on survival and functional capacity of T cells, we cultivated B^{hi} tumor-derived cell suspensions and analyzed the viability and cytokine production of CD4$^+$ and CD8$^+$ T cells after B cell depletion ($n = 4$). In B cell-depleted suspensions, the viability of both CD4$^+$ T cells and CD8$^+$ T cells did not differ at day 1, but was markedly lower compared to bulk suspensions after 6 days of cultivation without any additional stimuli (15.1 ± 7.8% vs. 11.0 ± 4.5% for CD4$^+$ T cells; $p = 0.068$) and 22.4 ± 10.6% vs. 14.4 ± 8.4% for CD8$^+$ T cells; $p = 0.068$) (Fig. 5a, b, c). Despite the impaired viability, we did not observe any substantial differences in the proportions of IL-2 and IFN-γ producing CD4$^+$ and CD8$^+$ T cells with respect to the presence or absence of B cells in the cell cultures.

Data extracted from TCGA databases confirmed higher expression of costimulatory molecules and IL-2 in B^{hi} HNSCC tumor samples

To estimate the expression levels of a wide spectrum of costimulatory molecules, we analyzed the data extracted from TCGA databases using Statistica® 10.0 software (StatSoft). HNSCC patients with defined p16 status were divided into B^{hi} and B^{lo} subgroups according to the median expression of CD19. With the exception of *BCL2L1*, *TNFSF9* and *CD86*, the B^{hi} samples expressed significantly higher levels of all costimulatory molecules and molecules associated with activation of the TNFR family signaling pathways tested (Fig. 5d).

CD8$^+$ TILs isolated from B^{hi} tumor samples express high levels of IL-2 and IL-2R

In mouse models of viral infections, CD27 was assessed as the key factor in directing the autocrine production of IL-2 that is required for the long-term survival of CD8$^+$ T cells in nonlymphoid tissues [35]. Therefore, we analyzed the levels of expression of *IL-2*, *IL-2RA* and *CD27* together with *CD40LG* and the anti-apoptotic regulator *BCL2L1* on CD8$^+$ TILs isolated from peripheral blood and tumor tissues of B^{hi} OPSCC patients ($n = 4$; Cohort 3). Indeed, significantly higher levels of *IL-2* and *IL-2R* were expressed in tumor-derived CD8$^+$ T cells than in matched peripheral blood CD8$^+$ T cells (Fig. 5e).

IL-10-producing Bregs do not accumulate in B^{hi} OPSCC tumor tissue

Regulatory B cells (Bregs) are characterized by the production of IL-10. To assess the proportion of Bregs in the OPSCC tumor microenvironment, we analyzed the level of IL-10 secreting TIL-Bs after 5 and 24 h of stimulation with CpG ODN 2006 and CD40L in the presence of PMA, ionomycin and brefeldin A using flow cytometry (Cohort 3).

After 5 h of stimulation, the proportion of Bregs, which were found to be predominantly CD5$^+$CD24^{hi}, was slightly higher in the tumor tissue (0.98 ± 0.78%) compared to matched peripheral blood B cells (0.46 ± 0.12%) and control tonsils (0.41 ± 0.09). Surprisingly, the proportion of IL-10-secreting Bregs after 24 h of in vitro maturation with CpG ODN 2006 and CD40L was significantly lower in the tumor samples than in matched peripheral blood B cells (2.74 ± 0.53% vs. 8.01 ± 1.75%, respectively; $p = 0.039$), but similar to the levels of Bregs

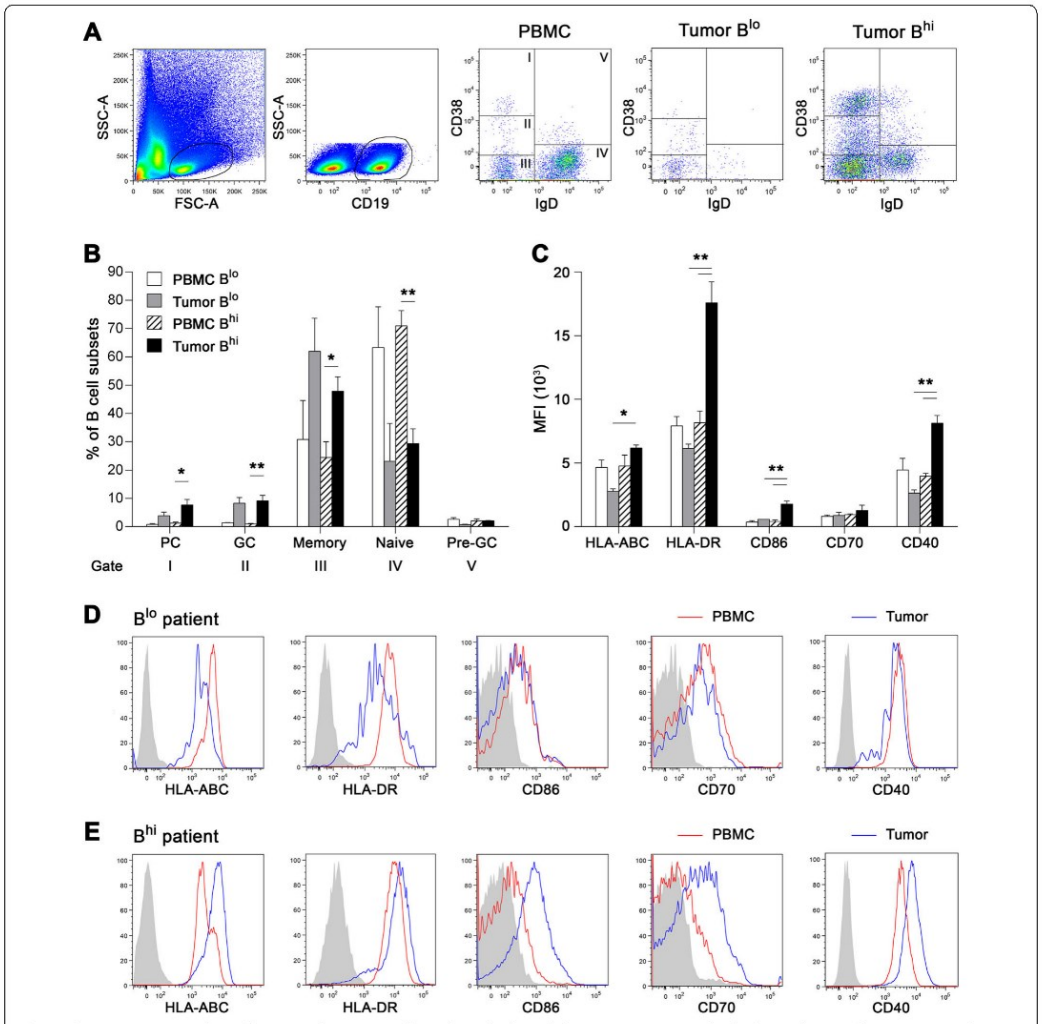

Fig. 4 Flow cytometric analysis of tumor-infiltrating B cells and B cells derived from patients' PBMC divided according to the proportion of TIL-Bs into B^{lo} (% of TIL-Bs < 0.5 of total cells) and B^{hi} samples. Data are expressed as (**a**) representative dot plots and (**b**) mean + SEM of the proportions of B cell subsets within total $CD19^+$ B cells. IgD^-CD38^{++}, plasma cells; IgD^-CD38^+, germinal center B cells; IgD^-CD38^-, memory B cells; IgD^+CD38^-, naive B cells; IgD^+CD38^+, pre-germinal center B cells. **c** Columns represent mean + SEM of the MFI of B cell surface markers assessed on total $CD19^+$ B cells. **d**, **e** Histograms show a representative expression of indicated B cell surface markers in B^{lo} (upper line) and B^{hi} (lower line) patient. Gray-filled areas represent isotype-matched controls, red line represents peripheral blood B cells and blue line represents tumor-infiltrating B cells of the same patient. *, $p < 0.05$; **, $p < 0.01$ (ANOVA followed by Tukey's post-hoc test)

in control tonsils (2.16 ± 1.51%). During the longterm stimulation by TLR ligands and CD40L, Breg progenitors mature into IL-10 producing Bregs [37]; therefore, both Bregs and Breg progenitors were detected after 24 h of cultivation in vitro. Interestingly, the proportion of Bregs was negatively correlated to the frequency of $CD19^+$ B cells in general ($r = -0.69$; $p = 0.085$). Due to a limited number of cells, IL-10 production was assessed in B^{hi} samples only.

B cells are an important source of CXCL9 in the tumor microenvironment

To estimate the impact of TIL-Bs on cytokine production in the tumor microenvironment, we analyzed the

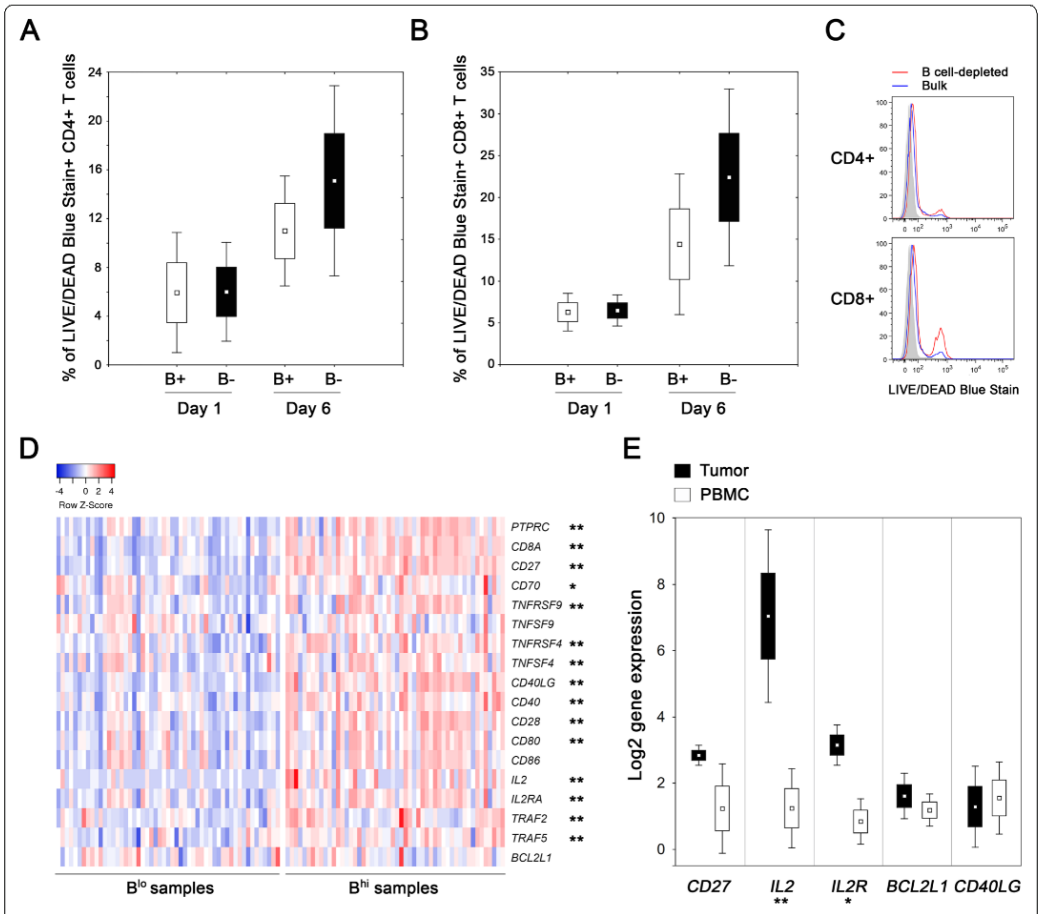

Fig. 5 Proportions of dead cells in cultures of bulk and B cell-depleted tumor-derived single cell suspensions. **a**, **b** Box plots show the mean proportion of dead $CD4^+$ and $CD8^+$ T cells in bulk (B+) and B cell-depleted (B-) tumor-derived cell suspension after 1 and 6 days of cultivation. **c** Histograms show differences in the LIVE/DEAD Blue Stain positivity on day 6 in a representative patient. **d** The heat-map expresses z-scores of relative mRNA expression of indicated genes within B^{lo} ($n = 53$) and B^{hi} ($n = 52$) samples extracted from TCGA databases. **e** Box plots show the mean expression of indicated genes in tumor tissues and matched PBMCs of B^{hi} OPSCC patients ($n = 4$). The boundaries of the box indicate the standard error of the mean and the squares in the box represent the mean. Whiskers indicate the standard deviation. *, $p < 0.05$; **, $p < 0.01$ (t test and Mann-Whitney U test)

spontaneous production of cytokines and chemokines in B^{lo} and B^{hi} tumor-derived cell suspensions and in B^{hi} suspensions depleted of $CD19^+$ B cells (Cohort 3). B^{hi} cell suspensions produced markedly higher levels of CXCL9 than B^{lo} cell suspensions (Additional file 4: Figure S2A). In accordance with these results, we observed significantly lower levels of CXCL9 in B cell-depleted samples than in whole cell suspensions (579.6 ± 262.9 vs. 1238.8 ± 290.6 pg/ml, respectively; $p = 0.025$; Additional file 4: Figure S2B), indicating that TIL-Bs are an important source of this chemokine.

Discussion

We previously described a markedly different immune profile in HPV-associated tumors compared to OPSCCs of other etiologies, characterized by high infiltrates of $CD8^+$ T cells [6], with a substantial proportion of HPV16 E6/E7 specific TILs [36]. Indeed, the role of T cell-mediated antitumor immune responses has been extensively studied in the past decade, and consequently, most of the recent immunotherapeutic approaches have been focused on T cells. However, in HNSCC patients, there is still a large proportion of non-

responders to recently approved immunotherapy based on PD-1:PD-L1 blockade. Additionally, conventional curative treatment of locally-advanced disease, although effective in patients with HPV-associated tumors, is accompanied by significant morbidity. Therefore, novel immunotherapy targets and consequent effective therapeutic strategies are still crucially needed for this type of carcinoma.

In contrast to T cells, considerably less is known about tumor-infiltrating B cells. Studies concerning TIL-Bs are inconsistent, and both tumor-promoting as well as tumor-inhibitory functions of B cells were reported in various malignancies, whereas the role of B cells in HNSCC has not been satisfactorily evaluated so far. In this study, we assessed the density, distribution and phenotype of TIL-Bs in FFPE and fresh samples from 3 independent cohorts of OPSCC patients.

In accordance with previously published results [26, 38], we observed a significant difference in the B cell-related gene signature between HPV-associated and HPV-negative tumor samples and confirmed these data by showing significantly higher densities of intraepithelial $CD20^+$ B cells in FFPE sections of HPV-associated tumors. Moreover, we observed that $CD20^+$ TIL-Bs formed with $CD8^+$ T cells non-organized small aggregates with clear cell-cell interactions between TIL-Bs and CD8+ TILs, and both the densities of intraepithelial $CD20^+$ B cells and B/$CD8^+$ T cell interactions were shown to have prognostic significance for the overall survival of the patients, regardless of the HPV status. In HPV-positive tumors, the formation of B/Tc interactions was also strongly associated with the presence and abundance of HPV16 E6/E7-specific $CD8^+$ T cells. Additionally, we observed a significantly higher expression of activation molecules, namely, HLA-ABC, HLA-DR, CD86 and CD40, in TIL-Bs derived from tumor samples with high levels of B cells in comparison to TIL-Bs derived from B^{lo} (< 5% of total cells) samples. Importantly, depletion of B cells led to markedly lower viability of $CD4^+$ and $CD8^+$ T cells in tumor-derived cell cultures. These data indicate not only quantitative but also qualitative differences in B cell-mediated immune responses between OPSCC patients with high vs. low densities of TIL-Bs.

A positive association between the high density of B cells and prolonged patient overall survival has been previously reported in ovarian cancer [39], hepatocellular carcinoma [24, 40], NSCLC [20] and breast cancer [22, 41]. Whereas in NSCLC, the major importance was assigned to TLS formation and the presence of follicular B cells [20], Nielsen [39] and Garnelo [40] emphasized the cell-to-cell contact of B and T cells within the tumor microenvironment and a positive correlation between B cell and T cell densities. In accordance with the latter studies, we observed the formation of aggregates of B cells and $CD8^+$ T cells with clear cell-to-cell contacts in some OPSCC patients with high densities of $CD20^+$ B cells. Together with intraepithelial $CD8^+$ T cells, a high density of $CD20^+$ B cells within the tumor nest and high densities of B/$CD8^+$ T cell interactions in both the tumor nest and stroma were confirmed as positive prognostic markers. The Cox proportional hazard model determined the intraepithelial density of $CD20^+$ B cells and stromal density of B/$CD8^+$ T cell interactions as independent prognostic markers stronger than HPV and $CD8^+$ T cell density alone. However, as the proportion of HPV-negative samples was markedly lower compared to HPV-positive samples (12.5% vs. 87.5%, respectively) in our cohort of patients, the impact of HPV status might be underestimated. Most importantly, in an independent cohort of patients with HPV-related tumors, the density of B/$CD8^+$ T cell interactions was significantly associated with the proportions of HPV16 E6/E7-specific $CD8^+$ T cells, indicating the importance of in situ B cell-$CD8^+$ T cell interactions in the antigen-specific antitumor immune response. In contrast, DC-$LAMP^+$ DCs occurred at markedly lower densities than TIL-Bs and were neither correlated with patient prognosis nor the abundance of HPV16 E6/E7-specific $CD8^+$ T cells.

In addition to differences in $CD20^+$ B cell and $CD8^+$ T cell densities in HPV-positive and HPV-negative OPSCC samples, we observed substantial variability in the levels of tumor-infiltrating immune cells in patients with HPV-associated tumors, with a clear subgroup of immunologically "cold" HPV-positive tumors. Therefore, we analyzed the phenotype of TIL-Bs in fresh HPV-positive tumor samples with high vs. low infiltrates of B cells. In contrast to ovarian and hepatocellular carcinomas [24, 39], but in accordance with the study published by Lechner et al. [26], OPSCC-derived TIL-Bs showed a classical memory phenotype with high expression of CD27 and low/no expression of CD38, IgD and IgM. Importantly, we observed substantial differences in TIL-Bs derived from highly infiltrated samples and samples with markedly low (< 0.5% of total cells) B cell densities. In B^{hi} samples, TIL-Bs showed an activated phenotype with high levels of HLA-ABC, HLA-DR, CD86 and CD40, whereas the expression of activation markers in TIL-Bs from B^{lo} samples was significantly lower. Additionally, the proportion of proliferating Ki-67^+ TIL-Bs was markedly higher in B^{hi} compared to B^{lo} samples, further indicating a low level of B cell activation in B^{lo} tumors. These data show that the substantial difference between B^{hi} patients with anticipated good outcome and B^{lo} patients with poor outcome may not entirely be due to the B cell quantity but may reflect the distinction in phenotype and consequent functional capacity of TIL-Bs.

In accordance with the study focused on tongue squamous cell carcinoma [42], we have observed higher frequency of $CD19^+$IL-10^+ Bregs in the tumor tissue

compared to peripheral blood and control tonsils; however, the difference did not reach statistical significance, probably due to a high variability within the tumor group. Interestingly, the abundance of Bregs markedly negatively correlated with the frequency of bulk $CD19^+$ B cells, suggesting that a high level of Bregs might be associated with tumor samples with low level of B cell infiltration in general, which mostly show immunologically "cold" phenotype with low densities of $CD8^+$ T cells. This could also explain the discrepancy between our study and the study by Lechner et al. [26], who observed very high proportions of Bregs in mainly HPV-negative, i.e. most probably immunologicaly "cold" HNSCC samples. These data nevertheless need further examination employing a larger cohort of patients, including tumor samples with both high and very low frequencies of B cells (< 0.5% of total cells).

The colocalization of $CD20^+$ B cells with $CD8^+$ T cells, the association of these cell-cell interactions with the presence and frequency of HPV16 E6/E7 $CD8^+$ T cells and the highly activated phenotype of TIL-Bs derived from B^{hi} samples leads to two possible mechanisms for how $CD20^+$ TILs may promote T cell-mediated immune responses. First, B cells are capable of producing chemokines, such as CXCL9, and cytokines, such as lymphotoxin, which recruit T cells to the tumor tissue and promote the formation of local lymphoid structures [20, 39]. Indeed, our data suggest that TIL-Bs may be an important source of CXCL9, a potent T cell chemoattractant [43]. In contrast, we did not detect lymphotoxin production in OPSCC tumor tissue-derived cell suspensions, which is in accordance with low levels of classical TLS observed in OPSCC FFPE sections.

Second, TIL-Bs may serve as local APCs, permitting the long-term persistence of antigen-specific $CD8^+$ T cells in the tumor microenvironment [29]. Indeed, we observed a substantial decrease in both $CD4^+$ T cell and $CD8^+$ B cell viability after depletion of TIL-Bs from tumor-derived cell suspensions. Additionally, we found exceptionally high levels of CD40 on TIL-Bs originating from B^{hi} tumor samples. CD40L principally expressed on activated T cells interacts with CD40, leading to a "licensed" state of APCs [44]. Licensed APCs upregulate the expression of costimulatory molecules, which further interact with mediators of T cell activation from the TNF receptor family, including CD27, 4-1BB and OX40 [45]. Importantly, CD40 stimulation promotes cross-priming of exogenous antigens in APCs, resulting in efficient $CD8^+$ T cell stimulation [46, 47]. In models of viral infections, the accumulation and survival of virus-specific $CD8^+$ T cells at the tissue site relied strongly on CD27/CD70 and to a lesser extent on 4-1BB and OX40 signaling [33, 35]. Interestingly, Peperzak et al. [35] demonstrated that the survival of effector $CD8^+$ T cells in nonlymphoid tissue of influenza-infected mice is directed mainly by CD27/CD70-mediated autocrine production of IL-2.

In accordance with these studies, using data from TCGA databases we observed significantly higher levels of *CD40*, *CD40LG*, *CD27*, *CD70*, *TNFRSF4* (OX40), *TNFSF4* (OX40L), *TRAF2*, *TRAF5*, *IL-2* and *IL-2RA* expression in B^{hi} samples compared to B^{lo} HNSCC tumors. Importantly, we showed that in comparison to matched peripheral blood $CD8^+$ T cells, $CD8^+$ TILs express significantly higher levels of *IL-2* and *IL-2RA*. Therefore, we suggest that in B^{hi} tumors, TIL-Bs might recruit $CD8^+$ T cells via CXCL9 and crucially contribute to the survival of the $CD8^+$ T cells in the tumor microenvironment due to the in situ secondary costimulation employing CD40L/CD40 and TNFR/TNF superfamily signaling pathways.

Conclusions

This study provides an extensive analysis of B cells in the OPSCC microenvironment, highlighting intraepithelial TIL-Bs as a valid prognostic marker, which surpasses the confirmed biomarkers such as HPV positivity and $CD8^+$ TIL density in stratification of OPSCC patients. Thus, the density of B cells and/or the density of direct B cell/$CD8^+$ T cell interactions may help to preselect patients with excellent prognosis who would profit from less invasive treatment and consequently decreased toxicity of the therapy. Additionally, our study suggests that in OPSCC, TIL-Bs might provide costimulatory signals important for $CD8^+$ T cell maintenance in the tumor tissue. Consequently, including B cells as an additional target into novel immunotherapeutic protocols may help to establish sustained antitumor T cell responses in situ and thus improve current approaches mainly focused on T cell (re)stimulation alone. However, as all of the patients in our cohorts received surgery as the main therapeutic option, the application of reported results to patients receiving primary curative chemoradiotherapy needs to be further analyzed.

Additional files

Additional file 1: Table S1. List of monoclonal antibodies used for flow cytometry. (DOCX 16 kb)

Additional file 2: Table S2. Prognostic overall survival parameters in multivariate analysis. (DOCX 13 kb)

Additional file 3: Figure S1. Activation markers in TIL-Bs. (A) Representative figures show expression of CD27 and IgM in $CD38^-IgD^-$ memory B cells (red line) and $CD38^-IgD^+$ naive B cells (blue line). (B) Columns show the mean proportion of $Ki67^+CD19^+$ B cells in peripheral blood and tumor tissue of B^{hi} (proportion of TIL-B cells > 0.5% of total cells) and B^{lo} OPSCC patients and control healthy tonsils. Whiskers represent the standard error of mean (SEM). *$p < 0.05$ (Kruskal-Wallis ANOVA). (PDF 1084 kb)

Additional file 4: Figure S2. Cytokine and chemokine profiles of tumor-derived single cell suspensions. (A) White columns represent the mean

spontaneous cytokine production in B^{lo} samples ($n = 3$); black columns represent cytokine production in B^{hi} samples ($n = 7$). (B) Black columns represent the mean spontaneous cytokine/chemokine production by whole B^{hi} tumor-derived single cell suspensions; white columns represent B cell depleted cell suspensions. All error bars represent SEM. * $p < 0.05$ (paired t-test). (PDF 409 kb)

Acknowledgments
We thank Michal Hensler for help with TLDA array and TCGA databases and Lorenzo Galluzzi for critical reading of the manuscript.

Authors' contributions
Conception and design: AF, RŠ, KH; acquisition of data: KH, VK, KR, HV; analysis and interpretation of data: AF, KH; writing of the manuscript: AF, KH; pathological examination: JL, MG, AR; patient management, construction of patient databases: JB, MH, MZ, MV, PČ, VCh, AR; study supervision: AF, RŠ. All authors read and approved the final manuscript.

Funding
The major sponsor of this study was Sotio a.s. The study was partly financially supported by the Grant Agency of Charles University, project numbers 344216 and 668217, from the European Regional Development Fund-Project BBMRI-CZ.: the Biobank network – a versatile platform for the research of the etiopathogenesis of diseases, No: EF16 013/0001674 and by research grants 16-28594A and 16-28600A from the Czech Health Research Council of the Ministry of Health of the Czech Republic, by Progres Q28 and Progres Q40/11 and by the project BBMRI-CZ LM2015089.

Availability of data and materials
The datasets used and/or analyzed during the current study are available from the corresponding author on reasonable request.

Ethics approval and consent to participate
All patient studies were approved by the Ethics Committee of the University Hospital Hradec Králové and the Ethics Committee of the University Hospital Motol. All of the patients signed an informed consent prior to inclusion to the study.

Consent for publication
Not applicable.

Competing interests
The authors declare that they have no competing interests.

Author details
[1]SOTIO a.s, Jankovcova 1518/2, CZ-17000 Prague 7, Prague, Czech Republic. [2]Department of Immunology, 2nd Faculty of Medicine, Charles University and University Hospital Motol, Prague, Czech Republic. [3]Department of Otorhinolaryngology and Head and Neck Surgery, 1st Faculty of Medicine, Charles University and University Hospital Motol, Prague, Czech Republic. [4]The Fingerland Department of Pathology, Charles University Faculty of Medicine in Hradec Králové and University Hospital Hradec Králové, Hradec Králové, Czech Republic. [5]Department of Pathology and Molecular Medicine, 2nd Faculty of Medicine, Charles University and University Hospital Motol, Prague, Czech Republic. [6]Department of Oncology and Radiotherapy, Charles University Faculty of Medicine in Hradec Králové and University Hospital Hradec Králové, Hradec Králové, Czech Republic. [7]Department of Otorhinolaryngology and Head and Neck Surgery, Charles University Faculty of Medicine in Hradec Králové and University Hospital Hradec Králové, Hradec Králové, Czech Republic.

Received: 15 May 2019 Accepted: 30 August 2019
Published online: 17 October 2019

References

1. Lajer CB, von Buchwald C. The role of human papillomavirus in head and neck cancer. APMIS. 2010;118(6–7):510–9.
2. D'Souza G, Dempsey A. The role of HPV in head and neck cancer and review of the HPV vaccine. Prev Med. 2011;53(Suppl 1):S5–S11.
3. Fakhry C, Westra WH, Li S, Cmelak A, Ridge JA, Pinto H, et al. Improved survival of patients with human papillomavirus-positive head and neck squamous cell carcinoma in a prospective clinical trial. J Natl Cancer Inst. 2008;100(4):261–9.
4. Ang KK, Harris J, Wheeler R, Weber R, Rosenthal DI, Nguyen-Tan PF, et al. Human papillomavirus and survival of patients with oropharyngeal cancer. N Engl J Med. 2010;363(1):24–35.
5. Kaneda MM, Messer KS, Ralainirina N, Li H, Leem CJ, Gorjestani S, et al. PI3Kgamma is a molecular switch that controls immune suppression. Nature. 2016;539(7629):437–42.
6. Partlova S, Boucek J, Kloudova K, Lukesova E, Zabrodsky M, Grega M, et al. Distinct patterns of intratumoral immune cell infiltrates in patients with HPV-associated compared to non-virally induced head and neck squamous cell carcinoma. Oncoimmunology. 2015;4(1):e965570.
7. Spanos WC, Nowicki P, Lee DW, Hoover A, Hostager B, Gupta A, et al. Immune response during therapy with cisplatin or radiation for human papillomavirus-related head and neck cancer. Arch Otolaryngol Head Neck Surg. 2009;135(11):1137–46.
8. Galon J, Costes A, Sanchez-Cabo F, Kirilovsky A, Mlecnik B, Lagorce-Pages C, et al. Type, density, and location of immune cells within human colorectal tumors predict clinical outcome. Science. 2006;313(5795):1960–4.
9. Galon J, Mlecnik B, Bindea G, Angell HK, Berger A, Lagorce C, et al. Towards the introduction of the 'Immunoscore' in the classification of malignant tumours. J Pathol. 2014;232(2):199–209.
10. Kawai O, Ishii G, Kubota K, Murata Y, Naito Y, Mizuno T, et al. Predominant infiltration of macrophages and CD8(+) T cells in cancer nests is a significant predictor of survival in stage IV nonsmall cell lung cancer. Cancer. 2008;113(6):1387–95.
11. Sato E, Olson SH, Ahn J, Bundy B, Nishikawa H, Qian F, et al. Intraepithelial CD8+ tumor-infiltrating lymphocytes and a high CD8+/regulatory T cell ratio are associated with favorable prognosis in ovarian cancer. Proc Natl Acad Sci U S A. 2005;102(51):18538–43.
12. Solomon B, Young RJ, Bressel M, Urban D, Hendry S, Thai A, et al. Prognostic significance of PD-L1(+) and CD8(+) immune cells in HPV(+) oropharyngeal squamous cell carcinoma. Cancer Immunol Res. 2018.
13. Nasman A, Romanitan M, Nordfors C, Grun N, Johansson H, Hammarstedt L, et al. Tumor infiltrating CD8+ and Foxp3+ lymphocytes correlate to clinical outcome and human papillomavirus (HPV) status in tonsillar cancer. PLoS One. 2012;7(6):e38711.
14. Bauml J, Seiwert TY, Pfister DG, Worden F, Liu SV, Gilbert J, et al. Pembrolizumab for platinum- and Cetuximab-refractory head and neck Cancer: results from a single-arm. Phase II Study J Clin Oncol. 2017;35(14):1542–9.
15. Ferris RL, Blumenschein G Jr, Fayette J, Guigay J, Colevas AD, Licitra L, et al. Nivolumab for recurrent squamous-cell carcinoma of the head and neck. N Engl J Med. 2016;375(19):1856–67.
16. Seiwert TY, Burtness B, Mehra R, Weiss J, Berger R, Eder JP, et al. Safety and clinical activity of pembrolizumab for treatment of recurrent or metastatic squamous cell carcinoma of the head and neck (KEYNOTE-012): an open-label, multicentre, phase 1b trial. Lancet Oncol. 2016;17(7):956–65.
17. Burtness B, Harrington KJ, Greil R, Soulières D, Tahara M, De Castro G, Jr, et al. LBA8_PRKEYNOTE-048: Phase III study of first-line pembrolizumab (P) for recurrent/metastatic head and neck squamous cell carcinoma (R/M HNSCC). Annals of Oncology. 2018;29(suppl_8).
18. Sarvaria A, Madrigal JA, Saudemont A. B cell regulation in cancer and anti-tumor immunity. Cell Mol Immunol. 2017;14(8):662–74.
19. Yuen GJ, Demissie E, Pillai S. B lymphocytes and cancer: a love-hate relationship. Trends Cancer. 2016;2(12):747–57.
20. Germain C, Gnjatic S, Tamzalit F, Knockaert S, Remark R, Goc J, et al. Presence of B cells in tertiary lymphoid structures is associated with a protective immunity in patients with lung cancer. Am J Respir Crit Care Med. 2014;189(7):832–44.
21. Kroeger DR, Milne K, Nelson BH. Tumor-infiltrating plasma cells are associated with tertiary lymphoid structures, Cytolytic T-cell responses, and superior prognosis in ovarian Cancer. Clin Cancer Res. 2016;22(12):3005–15.
22. Mahmoud SM, Lee AH, Paish EC, Macmillan RD, Ellis IO, Green AR. The prognostic significance of B lymphocytes in invasive carcinoma of the breast. Breast Cancer Res Treat. 2012;132(2):545–53.
23. Milne K, Kobel M, Kalloger SE, Barnes RO, Gao D, Gilks CB, et al. Systematic analysis of immune infiltrates in high-grade serous ovarian cancer reveals

CD20, FoxP3 and TIA-1 as positive prognostic factors. PLoS One. 2009;4(7): e6412.
24. Shi JY, Gao Q, Wang ZC, Zhou J, Wang XY, Min ZH, et al. Margin-infiltrating CD20(+) B cells display an atypical memory phenotype and correlate with favorable prognosis in hepatocellular carcinoma. Clin Cancer Res. 2013; 19(21):5994–6005.
25. Mizukami M, Hanagiri T, Shigematsu Y, Baba T, Fukuyama T, Nagata Y, et al. Effect of IgG produced by tumor-infiltrating B lymphocytes on lung tumor growth. Anticancer Res. 2006;26(3A):1827–31.
26. Lechner A, Schlosser HA, Thelen M, Wennhold K, Rothschild SI, Gilles R, et al. Tumor-associated B cells and humoral immune response in head and neck squamous cell carcinoma. Oncoimmunology. 2019;8(3):1535293.
27. Candolfi M, Curtin JF, Yagiz K, Assi H, Wibowo MK, Alzadeh GE, et al. B cells are critical to T-cell-mediated antitumor immunity induced by a combined immune-stimulatory/conditionally cytotoxic therapy for glioblastoma. Neoplasia. 2011;13(10):947–60.
28. DiLillo DJ, Yanaba K, Tedder TF. B cells are required for optimal CD4+ and CD8+ T cell tumor immunity: therapeutic B cell depletion enhances B16 melanoma growth in mice. J Immunol. 2010;184(7):4006–16.
29. Nelson BH. CD20+ B cells: the other tumor-infiltrating lymphocytes. J Immunol. 2010;185(9):4977–82.
30. Bruno TC, Ebner PJ, Moore BL, Squalls OG, Waugh KA, Eruslanov EB, et al. Antigen-presenting Intratumoral B cells affect CD4(+) TIL phenotypes in non-small cell lung Cancer patients. Cancer Immunol Res. 2017;5(10):898–907.
31. Wells AD, Gudmundsdottir H, Turka LA. Following the fate of individual T cells throughout activation and clonal expansion. Signals from T cell receptor and CD28 differentially regulate the induction and duration of a proliferative response. J Clin Invest. 1997;100(12):3173–83.
32. Roberts EW, Broz ML, Binnewies M, Headley MB, Nelson AE, Wolf DM, et al. Critical role for CD103(+)/CD141(+) dendritic cells bearing CCR7 for tumor antigen trafficking and priming of T cell immunity in melanoma. Cancer Cell. 2016;30(2):324–36.
33. Grant EJ, Nussing S, Sant S, Clemens EB, Kedzierska K. The role of CD27 in anti-viral T-cell immunity. Curr Opin Virol. 2017;22:77–88.
34. McGill J, Van Rooijen N, Legge KL. Protective influenza-specific CD8 T cell responses require interactions with dendritic cells in the lungs. J Exp Med. 2008;205(7):1635–46.
35. Peperzak V, Xiao Y, Veraar EA, Borst J. CD27 sustains survival of CTLs in virus-infected nonlymphoid tissue in mice by inducing autocrine IL-2 production. J Clin Invest. 2010;120(1):168–78.
36. Hladikova K, Partlova S, Koucky V, Boucek J, Fonteneau JF, Zabrodsky M, et al. Dysfunction of HPV16-specific CD8+ T cells derived from oropharyngeal tumors is related to the expression of Tim-3 but not PD-1. Oral Oncol. 2018;82:75–82.
37. Iwata Y, Matsushita T, Horikawa M, Dilillo DJ, Yanaba K, Venturi GM, et al. Characterization of a rare IL-10-competent B-cell subset in humans that parallels mouse regulatory B10 cells. Blood. 2011;117(2):530–41.
38. Wood O, Woo J, Seumois G, Savelyeva N, McCann KJ, Singh D, et al. Gene expression analysis of TIL rich HPV-driven head and neck tumors reveals a distinct B-cell signature when compared to HPV independent tumors. Oncotarget. 2016;7(35):56781–97.
39. Nielsen JS, Sahota RA, Milne K, Kost SE, Nesslinger NJ, Watson PH, et al. CD20+ tumor-infiltrating lymphocytes have an atypical CD27- memory phenotype and together with CD8+ T cells promote favorable prognosis in ovarian cancer. Clin Cancer Res. 2012;18(12):3281–92.
40. Garnelo M, Tan A, Her Z, Yeong J, Lim CJ, Chen J, et al. Interaction between tumour-infiltrating B cells and T cells controls the progression of hepatocellular carcinoma. Gut. 2017;66(2):342–51.
41. Yeong J, Lim JCT, Lee B, Li H, Chia N, Ong CCH, et al. High densities of tumor-associated plasma cells predict improved prognosis in triple negative breast Cancer. Front Immunol. 2018;9:1209.
42. Zhou X, Su YX, Lao XM, Liang YJ, Liao GQ. CD19(+)IL-10(+) regulatory B cells affect survival of tongue squamous cell carcinoma patients and induce resting CD4(+) T cells to CD4(+)Foxp3(+) regulatory T cells. Oral Oncol. 2016;53:27–35.
43. Tensen CP, Flier J, Van Der Raaij-Helmer EM, Sampat-Sardjoepersad S, Van Der Schors RC, Leurs R, et al. Human IP-9: a keratinocyte-derived high affinity CXC-chemokine ligand for the IP-10/Mig receptor (CXCR3). J Invest Dermatol. 1999;112(5):716–22.
44. Lanzavecchia A. Immunology. Licence to kill Nature. 1998;393(6684):413–4.
45. Watts TH. TNF/TNFR family members in costimulation of T cell responses. Annu Rev Immunol. 2005;23:23–68.
46. Hernandez MG, Shen L, Rock KL. CD40-CD40 ligand interaction between dendritic cells and CD8+ T cells is needed to stimulate maximal T cell responses in the absence of CD4+ T cell help. J Immunol. 2007;178(5):2844–52.
47. Ritchie DS, Yang J, Hermans IF, Ronchese F. B-lymphocytes activated by CD40 ligand induce an antigen-specific anti-tumour immune response by direct and indirect activation of CD8(+) T-cells. Scand J Immunol. 2004;60(6): 543–51.

Publisher's Note

5.4 Přítomnost molekuly TIM-3 ovlivňuje funkční orientaci imunitního infiltrátu v nádorovém mikroprostředí ovariálního karcinomu

Přítomnost inhibičních receptorů a jejich ligandů hraje zásadní roli v navození imunosuprese v nádorovém mikroprostředí u většiny maligních onemocnění, jak vyplývá z výsledků preklinického a klinického testování. Přítomnost těchto molekul tedy nejen zásadním způsobem ovlivňuje prognózu pacientů, ale zároveň představuje i prediktivní informaci pro imunoterapeutickou léčbu nádorových malignit. Nicméně vliv těchto molekul na složení a aktivitu imunitního infiltrátu a následné přežívání pacientek s high-grade serózním karcinomem ovaria (high-grade serous carcinoma, HGSC) nebyl dosud plně objasněn. V rámci retrospektivní studie jsme analyzovali míru exprese PD-L1 a zastoupení PD-1+, CTLA4+, LAG-3+ a TIM-3+ buněk, ve vztahu k funkční orientaci imunitního infiltrátu nádorového prostředí a následné prognóze pacientek s HGSC. Získaná imunohistochemická data byla korelována s transkriptomickou charakterizací nádorové tkáně pomocí analýzy RNA-Seq dat a s funkčními testy provedenými na nezávislé prospektivní kohortě pacientek s HGSC. Z výsledků vyplývá, že vysoká hladina exprese PD-L1 a vyšší zastoupení PD-1+ buněk v nádorovém mikroprostředí pacientek s HGSC jsou silně asociovány s T_H1 orientovanou a cytotoxickou imunitní odpovědí. Naopak přítomnost molekuly TIM-3 negativně ovlivňuje funkční kapacitu efektorových lymfocytů infiltrujících do nádoru a koreluje s horší prognózou onemocnění. Výsledky této studie dokumentují prognostický význam PD-L1 a TIM-3 jako relevantních biomarkerů aktivované vs. suprimované protinádorové imunitní odpovědi, což zásadním způsobem ovlivňuje prognózu pacientek s HGSC. Naše výsledky naznačují, že sledování zastoupení inhibičních molekul v nádorovém mikroprostředí, zejména receptoru TIM-3, může být v budoucnu využito pro stratifikaci pacientek vhodných pro imunoterapeutickou léčbu HGSC.

K této práci jsem přispěla následovně: 10 %; analýza exprese inhibičních molekul v nádorovém mikroprostředí fluorescenčně značených FFPE tkání.

Published OnlineFirst May 10, 2019; DOI: 10.1158/1078-0432.CCR-18-4175

Clinical Cancer Research

TIM-3 Dictates Functional Orientation of the Immune Infiltrate in Ovarian Cancer

Jitka Fucikova[1,2], Jana Rakova[2], Michal Hensler[2], Lenka Kasikova[1,2], Lucie Belicova[2], Kamila Hladikova[1,2], Iva Truxova[1,2], Petr Skapa[3], Jan Laco[4], Ladislav Pecen[2], Ivan Praznovec[5], Michael J. Halaska[6], Tomas Brtnicky[7], Roman Kodet[3], Anna Fialova[2], Josephine Pineau[8,9], Alain Gey[8,9], Eric Tartour[8,9], Ales Ryska[4], Lorenzo Galluzzi[10,11,12,13], and Radek Spisek[1,2]

Abstract

Purpose: In multiple oncological settings, expression of the coinhibitory ligand PD-L1 by malignant cells and tumor infiltration by immune cells expressing coinhibitory receptors such as PD-1, CTLA4, LAG-3, or TIM-3 conveys prognostic or predictive information. Conversely, the impact of these features of the tumor microenvironment on disease outcome among high-grade serous carcinoma (HGSC) patients remains controversial.

Experimental Design: We harnessed a retrospective cohort of 80 chemotherapy-naïve HGSC patients to investigate PD-L1 expression and tumor infiltration by $CD8^+$ T cells, $CD20^+$ B cells, DC-$LAMP^+$ dendritic cells as well as by PD-1^+, CTLA4^+, LAG-3^+, and TIM-3^+ cells in relation with prognosis and function orientation of the tumor microenvironment. IHC data were complemented with transcriptomic and functional studies on a second prospective cohort of freshly resected HGSC samples. *In silico* analysis of publicly available RNA expression data from 308 HGSC samples was used as a confirmatory approach.

Results: High levels of PD-L1 and high densities of PD-1^+ cells in the microenvironment of HGSCs were strongly associated with an immune contexture characterized by a robust T_H1 polarization and cytotoxic orientation that enabled superior clinical benefits. Moreover, PD-1^+TIM-3^+CD8^+ T cells presented all features of functional exhaustion and correlated with poor disease outcome. However, although PD-L1 levels and tumor infiltration by TIM-3^+ cells improved patient stratification based on the intratumoral abundance of $CD8^+$ T cells, the amount of PD-1^+ cells failed to do so.

Conclusions: Our data indicate that PD-L1 and TIM-3 constitute prognostically relevant biomarkers of active and suppressed immune responses against HGSC, respectively.

Introduction

The composition, localization, and functional orientation of the immunologic tumor microenvironment (TME) exhibit considerable degrees of variation, not only across patients, cancer types, and disease stages, but also across distinct metastatic lesions of the same primary tumor (1). Although little is known on how the immunologic profile of metastatic lesions affects disease outcome, in a large number of oncological indications, the immunologic configuration of the primary tumor bears robust prognostic or predictive information (2). For instance, high levels of the coinhibitory molecule CD274 (best known as PD-L1) predict (at least to some extent) the sensitivity of non–small cell lung cancer (NSCLC) patients to immune-checkpoint blockers targeting PD-L1 or its cognate receptor, i.e., programmed cell death 1 (PDCD1, best known as PD-1; refs. 3, 4). Moreover, abundant infiltration by $CD8^+$ cytotoxic T lymphocytes (CTL) as well as signs of a T_H1-polarized immune response is associated with improved disease outcome in a variety of tumors (2, 5–7). However, little is known about the impact of PD-L1 levels and tumor infiltration by immune cells expressing PD-1 and other coinhibitory receptors such as cytotoxic T lymphocyte-associated protein 4 (CTLA4), lymphocyte activating 3 (LAG-3), or hepatitis A virus cellular receptor 2 (HAVCR2, best known as TIM-3) on disease outcome in high-grade serous carcinoma (HGSC) patients.

On the one hand, Hamanishi and colleagues reported that PD-L1 expressed by cancer cells negatively correlates with limited

[1]Department of Immunology, Charles University, 2nd Faculty of Medicine and University Hospital Motol, Prague, Czech Republic. [2]Sotio, Prague, Czech Republic. [3]Department of Pathology and Molecular Medicine, Charles University, 2nd Faculty of Medicine and University Hospital Motol, Prague, Czech Republic. [4]The Fingerland Department of Pathology, Charles University, Faculty of Medicine and University Hospital Hradec Kralove, Czech Republic. [5]Department of Gynecology and Obstetrics, Charles University, Faculty of Medicine and University Hospital Hradec Kralove, Czech Republic. [6]Department of Gynecology and Obstetrics, Charles University, 3rd Faculty of Medicine and University Hospital Kralovske Vinohrady, Prague, Czech Republic. [7]Department of Gynecology and Obstetrics, Charles University, 2nd Faculty of Medicine and University Hospital Motol, Prague, Czech Republic. [8]INSERM U970, Université Paris Descartes, Sorbonne Paris-Cité, Paris, France. [9]Service d'Immunologie Biologique, AP-HP, Hopital Européen Georges Pompidou, Paris, France. [10]Department of Radiation Oncology, Weill Cornell Medical College, New York, New York. [11]Sandra and Edward Meyer Cancer Center, New York, New York. [12]Department of Dermatology, Yale School of Medicine, New Haven, Connecticut. [13]Université Paris Descartes/Paris V, Paris, France.

Note: Supplementary data for this article are available at Clinical Cancer Research Online (http://clincancerres.aacrjournals.org/).

L. Galluzzi and R. Spisek share senior authorship of this article.

Corresponding Author: Jitka Fucikova, Charles University and Sotio, V Uvalu 84, Prague, 150 00, Czech Republic. Phone: 42-022-417-5114; Fax: 42-022-417-5114; E-mail: fucikova@sotio.com

Clin Cancer Res 2019;XX:XX–XX

doi: 10.1158/1078-0432.CCR-18-4175

Published OnlineFirst May 10, 2019; DOI: 10.1158/1078-0432.CCR-18-4175

Translational Relevance

The precise impact of PD-L1 expression levels and infiltration by PD-1$^+$, CTLA4$^+$, LAG-3$^+$, and TIM-3$^+$ T cells on the immunologic configuration of the tumor microenvironment in high-grade serous carcinoma (HGSC) has not yet been determined. Similarly, how these immunologic parameters influence survival in chemotherapy-naïve patients with HGSC undergoing curative surgery remains an open conundrum. Here, we demonstrate that elevated levels of PD-L1 in malignant cells as well as robust infiltration by PD-1$^+$, CTLA4$^+$, or LAG-3$^+$ T cells are not indicative of T-cell exhaustion in patients with HGSC, but rather point to an ongoing IFNγ-dependent immune response with beneficial effects. Conversely, abundant infiltration by TIM-3$^+$ is associated with poor disease outcome, indicating that TIM-3 has a prominent role in limiting immune responses against HGSCs. Our data suggest that TIM-3 inhibitors should be tested as neoadjuvant or adjuvant agents for the management of chemotherapy-naïve patients with HGSC.

infiltration by immune effector cells and hence poor disease outcome, reflecting the largely immunosuppressive activity of this molecule (8). On the other hand, various reports demonstrate that PD-L1 expression as a consequence of interferon gamma (IFNG, best known as IFNγ) signaling is associated with strong infiltration by CD8$^+$ CTLs, representing a mechanism of compensation against a therapeutically beneficial tumor-targeting immune response (9–13). Similarly, although some reports attribute to robust infiltration by PD-1$^+$ cells a negative prognostic value, potentially linked to the highly exhausted status of these cells (14–16), other studies point to a rather beneficial effect (17, 18), perhaps linked to the fact that CD103$^+$PD-1$^+$CD8$^+$ T cells appear to retain functional competence in the ovarian TME (19). We have recently demonstrated that CD20$^+$ B cells and DC-LAMP$^+$ dendritic cells (DC) infiltrating HGSC lesions have a positive prognostic value as they orchestrate a T_H1-polarized immune response coupled to abundant CD8$^+$ CTL infiltration (5). However, the specific effect of PD-L1 levels and infiltration by immune cells expressing coinhibitory receptors on the composition and functional orientation of the TME in ovarian cancer patients, and how this influences disease outcome, remains to be clarified.

Here, we demonstrate that both elevated PD-L1 levels and high densities of PD-1$^+$ cells in the HGSC TME are strongly associated with robust T_H1 polarization and cytotoxic orientation that enable superior clinical benefits, but only the former can be used to improve patient stratification based on the intratumoral abundance of CD8$^+$ T cells. Conversely, not only CD8$^+$ CTLs coexpressing PD-1 and TIM-3 present all the features of functional exhaustion, but their abundance has a negative independent prognostic value. Our data demonstrate that immunosuppression in the TME of therapy-naïve HGSC patients is dictated mainly by TIM-3.

Materials and Methods

Patients

Study group 1. A retrospective series of 80 formalin-fixed paraffin-embedded (PPFE) samples were obtained from patients with HGSC who underwent primary surgery in the absence of neoadjuvant chemotherapy between 2008 and 2014 at University Hospital Hradec Kralove (Czech Republic). Baseline characteristics of these patients are summarized in Table 1. Pathology staging was performed according to the 8th TNM classification (2017), and histologic types were determined according to the current WHO classification (20, 21). Data on long-term clinical outcome were obtained retrospectively by interrogation of municipality registers or families. The protocol was approved by the local ethics committee (reference number 201607 S14P).

Table 1. Main clinical and biological characteristic of study group 1

Variable	Overall cohort (n = 80)
Age	
Mean age (y) ± SEM	61 ± 10
Range	41–79
pTNM stage	
Stage I	20 (25%)
Stage II	7 (8.7%)
Stages III and IV	53 (66.3%)
Debulking	
R0	39 (48.5%)
R1	4 (5%)
R2	37 (46.3%)
Vital status of patients	
Alive	35 (43.7%)
Death	45 (56.3%)

Study group 2. An additional series of 20 samples from HGSC patients was prospectively collected at University Hospital Motol (Prague, Czech Republic). This study was conducted in accordance with the Declaration of Helsinki and the protocol was approved by the local ethics committee (Progress UK, Q40/11). Written informed consent was obtained from patients before inclusion in the study. Baseline characteristics of these patients are summarized in Supplementary Table S1. The experimental design of the study is summarized in Supplementary Fig. S1.

IHC

As previously described, tumor specimens from study group 1 were fixed in neutral buffered 10% formalin solution and embedded in paraffin as per standard procedures (5). Immunostaining with antibodies specific for programmed cell death 1 (PDCD1, best known as PD1), CD274 (best known as PD-L1), lymphocyte activating gene 3 (LAG-3), cytotoxic T lymphocyte-associated protein 4 (CTLA4), lysosomal associated membrane protein 3 (LAMP3; best known as DC-LAMP), CD8, and CD20 was performed according to conventional protocols (Supplementary Table S2). Briefly, tissue sections were deparaffinized, followed by antigen retrieval with Target Retrieval Solution (Leica) at pH 6.0 (for PD-L1), in TRIS EDTA pH 9.0 (for CTLA4, LAG-3, and PD-1) or pH 8.0 (for CD8, CD20, and DC-LAMP) in preheated water bath (98°C, 30 minutes). Sections were allowed to cool down to room temperature for 30 minutes, and endogenous peroxidase and alkaline phosphatase was blocked with 3% H_2O_2, levamisole, and blocking solution Bloxall (Vector), respectively, for 15 minutes. Thereafter, sections were treated with protein block (DAKO) for 15 minutes and incubated with primary antibodies, followed by the revelation of enzymatic activity. Sections were counterstained with hematoxylin (DAKO)

Published OnlineFirst May 10, 2019; DOI: 10.1158/1078-0432.CCR-18-4175

for 30 seconds. Images were acquired using a Leica Aperio AT2 scanner (Leica).

Cell quantification

PD-1$^+$, CTLA4$^+$, and LAG-3$^+$ cells were differentially quantified in the stroma and tumor nests of whole tumor sections with Calopix software (Tribvn). As previously described, the density of CD8$^+$ T cells, DC-LAMP$^+$ DCs, and CD20$^+$ B cells was quantified in the entire TME (5). Data are reported as the absolute number of positive cells/mm^2 (for PD-1$^+$, CTLA4$^+$, LAG-3$^+$, DC-LAMP$^+$, CD8$^+$ cells) or cell surface/tumor section surface (for CD20$^+$ cells). PD-L1 expression was scored in the intratumoral and stromal compartments as a percentage of tumor area and categorized as 1 (0%), 2 (1%–4%), 3 (5%–9%), and 4 (>10%), as previously described (22). Quantitative assessments were performed by three independent investigators (J. Fucikova, J. Rakova, L. Belicova) and reviewed by an expert pathologist (J. Laco and P. Skapa).

Flow cytometry

As previously described, total live mononuclear cells were isolated from fresh tumor specimens (5). Mononuclear cells were stained with multiple panels of fluorescent primary antibodies (Supplementary Table S3) or appropriate isotype controls for 20 minutes at 4°C in the dark, followed by washing and acquisition on a Fortessa flow cytometer (BD Biosciences). Flow cytometry data were analyzed with the FlowJo software (TreeStar).

Degranulation and IFNγ production after anti–PD-1 and anti–TIM-3 cultivation and *in vitro* stimulation

Mononuclear cells isolated from fresh tumor specimens (study group 2) were incubated with 10 μg/mL anti–PD-1, 10 μg/mL anti–TIM-3, and combination of both antibodies for 24 hours in 37°C and 5% CO_2. After cultivation, mononuclear cells were stimulated with 50 ng/mL phorbol 12-myristate 13-acetate (PMA) + 1 μg/mL ionomycin in the presence of anti-CD107a FITC monoclonal antibody (BioLegend) for 1 hour followed by 3-hour incubation with brefeldin A (BioLegend). Unstimulated cells were used as control. Cells were then washed in PBS, stained with anti-CD45 PerCP (EXBIO), anti-CD3 Alexa Fluor 700 (EXBIO), anti-CD4 ECD (Beckman Coulter), and anti-CD8 HV500 (BD Biosciences) monoclonal antibodies, fixed in fixation/permeabilization buffer (eBioscience), permeabilized with permeabilization buffer (eBioscience), and intracellularly stained with anti-IFNγ PE-Cy7 (eBioscience) monoclonal antibody. Flow cytometry was performed on the LSRFortessa analyzer, and data were analyzed with the FlowJo software package (Supplementary Fig. S6B; Tree Star, Inc.).

Next-generation sequencing data analysis

As previously described, hierarchical clustering analysis was conducted for differentially expressed genes (DEG) using the PHEATMAP package in R, based on the Euclidean distance and complete clustering method (5). The MCP-counter R package was used to estimate the abundance of tissue-infiltrating immune cell populations (Supplementary Table S4; ref. 23).

The Cancer Genome Atlas (TCGA) data analysis

Patients with HGSC ($n = 308$) were identified in TCGA public database (https://cancergenome.nih.gov/). DEGs between the *PD-L1*^{Hi} and *PD-L1*^{Lo} groups were determined using the LIMMA-R package (24). Hierarchical clustering analysis was conducted using the ComplexHeatmap package, based on the Euclidean distance and complete clustering method (25). Immune analyses were performed using ClueGo (26). The MCP-counter R package was used to estimate the abundance of tissue-infiltrating immune cell populations (23).

In situ immunofluorescence of tumor-infiltrating lymphocytes

Tumor specimens from study group 1 were fixed in neutral buffered 10% formalin solution and embedded in paraffin as per standard procedures. Sections were therefore subjected to indirect immunofluorescence based on nonlabeled primary antibodies specific for PD-1, TIM-3, and CD8 coupled to appropriate HRP-polymer secondary antibodies, followed by Tyramide Signal Amplification reagents with fluorescent dyes (Supplementary Table S5). Isotype-matched antibodies were used as negative controls and DAPI-containing mounting medium (DAKO) was used for nuclear counterstaining.

Image analysis and automated cell count

Stained sections were imaged with an automated Vectra microscope (PerkinElmer), followed by analysis by inForm software (PerkinElmer) as described previously in detail (27). Data are reported as means of positive cells from 5 imaging fields acquired using a 20× objective. An independent operator and an expert pathologist confirmed phenotyping by visual inspection. In particular, each phenotyping image was double checked to minimize the risk of false determinations owing to potential overlaps in fluorescence and interoperator variance.

Statistical analysis

As previously described, survival analysis was performed using the Survival R package, using both log-rank tests and Cox proportional hazard regressions (5). For log-rank tests, the prognostic value of continuous variables was assessed using median cutoffs. For Cox proportional hazard regressions, cell densities were log-transformed. In multivariate Cox regressions, variables that were not significantly associated with prognosis in univariate analysis were not included, as well as variables intrinsically correlated. Cox proportional hazard regression analysis, log-rank analysis, Fisher exact tests, Student *t* tests, and the Wilcoxon and Mann–Whitney tests were used to assess statistical significance, *P* values are reported (considered not significant when >0.05).

Results

Tumor infiltration by CD8$^+$ T lymphocytes, CD20$^+$ B cells, and DC-LAMP$^+$ DCs correlate with prolonged survival in patients with HGSC

Tumor samples from a retrospective series of 80 patients with HGSC who did not receive neoadjuvant chemotherapy (study group 1; Table 1) were analyzed for the densities of CD8$^+$ T cells, CD20$^+$ B cells, and DC-LAMP$^+$ DCs by IHC (Supplementary Fig. S2A). As published previously by our group, HGSC patients with high density of CD8$^+$ T cells (CD8^{Hi}), CD20$^+$ B cells (CD20^{Hi}), and DC-LAMP$^+$ DCs (DC-LAMP^{Hi}) exhibited significantly longer relapse-free survival (RFS) and overall survival (OS) as compared with their low counterparts (CD8$^+$ T cells RFS: $P = 0.03$, OS $P = 0.01$; CD20$^+$ B cells RFS: $P = 0.02$, OS $P = 0.02$; DC-LAMP$^+$ DCs RFS: $P = 0.0001$, OS $P < 0.0001$; Supplementary Fig. S2B and S2C). To assess whether infiltration by either CD20$^+$ B cells or

Published OnlineFirst May 10, 2019; DOI: 10.1158/1078-0432.CCR-18-4175

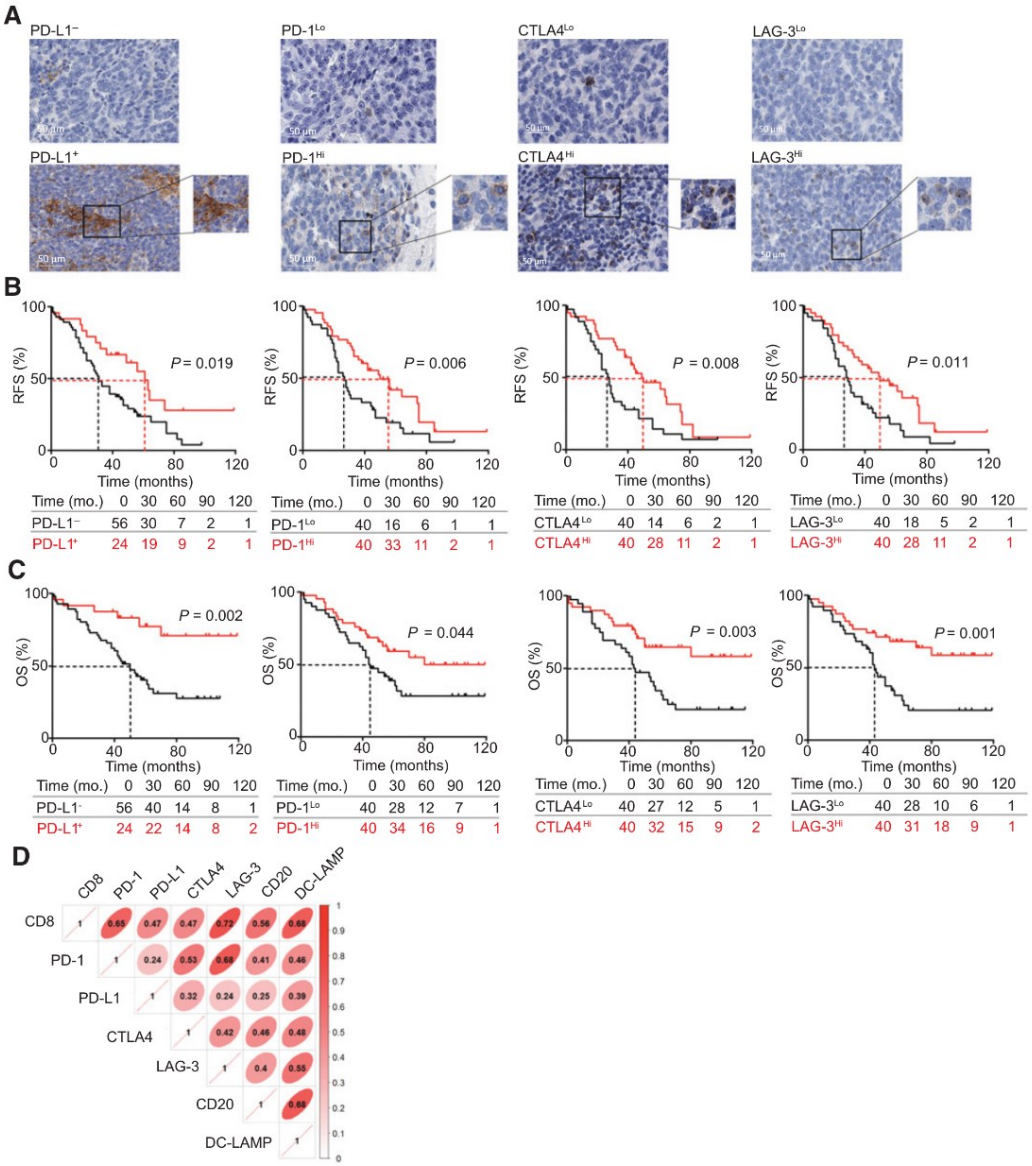

Figure 1.

Prognostic impact of PD-L1$^+$, PD-1$^+$, CTLA4$^+$, and LAG-3$^+$ cells in the TME of chemotherapy-naïve HGSC patients. **A,** Representative images of PD-L1, PD-1, CTLA4, and LAG-3 immunostaining. Scale bar, 50 μm. RFS (**B**) and OS (**C**) of 80 patients with HGSC (study group 1) who did not receive neoadjuvant chemotherapy, upon stratifying patients based on a cutoff of 5% malignant cells with PD-L1 expression and median density of PD-1$^+$, CTLA4$^+$, and LAG-3$^+$ cells in the tumor nests. Survival curves were estimated by the Kaplan–Meier method, and differences between groups were evaluated using the log-rank test. The number of patients at risk is reported. **D,** The correlation matrix for CD8$^+$, PD-1$^+$, PD-L1$^+$, CTLA4$^+$, LAG-3$^+$, CD20$^+$, and DC-LAMP$^+$ cells in the tumor nest of HGSC patients (study group 1).

Published OnlineFirst May 10, 2019; DOI: 10.1158/1078-0432.CCR-18-4175

DC-LAMP$^+$ DCs would improve the prognostic value of intratumoral CD8$^+$ T cells only, we evaluated RFS and OS upon stratifying patients from study group 1 into four subsets for each marker (CD8^{Hi}/CD20^{Hi}, CD8^{Hi}/CD20^{Lo}, CD8^{Lo}/CD20^{Hi}, and CD8^{Lo}/CD20^{Lo} and CD8^{Hi}/DC-LAMP^{Hi}, CD8^{Hi}/DC-LAMP^{Lo}, CD8^{Lo}/DC-LAMP^{Hi}, and CD8^{Lo}/DC-LAMP^{Lo}). Indeed both CD8^{Hi}/CD20^{Hi} and CD8^{Hi}/DC-LAMP^{Hi} patients exhibited improved OS as compared with their CD8^{Hi}/CD20^{Lo} and CD8^{Hi}/DC-LAMP^{Lo} counterparts ($P = 0.006$ and $P = 0.005$, respectively; Supplementary Fig. S2D and S2E). These data confirm previous findings from our group indicating that a high density of tumor-infiltrating CD8$^+$ T cells, CD20$^+$ B cells, and DC-LAMP$^+$ DCs correlates with improved disease outcome in chemotherapy-naïve HGSC patients, and that the density of CD20$^+$ B cells and DC-LAMP$^+$ DCs can be harnessed to identify CD8^{Hi} patients with relatively poor OS (5).

Table 2. Univariate Cox proportional hazard analysis

	OS	
Variable	HR (95% CI)	*P*
Stage 2	0.5 (0.058–4.25)	0.523
Stage 3	3.87 (1.51–9.9)	**0.004**
Stage 4	5.34 (1.27–22.4)	**0.022**
Age	1 (1–1.1)	**0.04**
Debulking R1	1.24 (0.29–5.43)	**0.02**
Debulking R2	2.14 (1.13–4.03)	**0.02**
CA125	1.00 (1.00–1.00)	0.14
PD-1	0.98 (0.96–1.00)	0.10
PD-L1	0.28 (0.12–0.67)	**0.004**
CTLA4	0.89 (0.8–0.98)	**0.017**
LAG-3	0.98 (0.95–1.00)	0.084
TIM-3	1.03 (1.00–1.06)	**0.04**
CD8	1 (1.00–1.00)	**0.017**
DC-LAMP	0.86 (0.76–0.97)	**0.014**
CD20	0.23 (0.05–1.00)	**0.05**

Activation of immune checkpoints correlates with improved disease outcome in HGSC patients

To elucidate the prognostic impact of immune-checkpoint status among chemotherapy-naïve HGSC patients, tumor samples from study group 1 (Table 1) were analyzed for the expression of PD-L1 in the tumor nest, as well as for the density of PD-1$^+$, CTLA4$^+$, and LAG-3$^+$ cells by IHC (Fig. 1A; Supplementary Figs. S3 and S4). PD-L1 levels as well as infiltration by PD-1$^+$, CTLA4$^+$, and LAG-3$^+$ cells were heterogeneous across samples but did not differ based on the site of assessment (tumor stroma vs. tumor nests; Supplementary Fig. S5A) and pathologic disease stage (Supplementary Fig. S5B).

To assess the prognostic impact of PD-L1 expression in the TME, we evaluated RFS and OS upon stratifying patients (study group 1) based on a cutoff of 5% malignant cells with membranous PD-L1 expression, which is currently used in the clinic to identify patients eligible for PD-1/PD-L1 targeting immune-checkpoint blockers (28). Patients with PD-L1$^+$ tumor nests (24 out of 80 patients) had prolonged RFS and OS as compared with their PD-L1$^-$ counterparts (RFS: $P = 0.019$; OS: $P = 0.002$; Fig. 1B and C). Univariate Cox regression analysis confirmed a strong prognostic impact for PD-L1 expression in tumor nests [hazard ratio (HR) = 0.28; 95% confidence interval = 0.12–0.67; $P = 0.004$; Table 2], and the significance of this association was confirmed by multivariate analysis (HR = 0.3; 95% confidence interval = 0.12–0.61; $P = 0.007$; Table 3). These data suggest that high PD-L1 levels in the TME may be indicative of an ongoing immune response that favorably affects disease outcome among HGSC patients, regardless of the stage of the disease.

Next, we investigated RFS and OS upon stratifying study group 1 based on the median density of PD-1$^+$, CTLA4$^+$, or LAG-3$^+$ cells infiltrating tumor nests (Fig. 1A; Supplementary Figs. S3 and S4). Patients with high density of PD-1$^+$ cells (PD-1^{Hi}) in their TME exhibited significantly longer RFS and OS as compared with their PD-1^{Lo} counterparts (RFS: $P = 0.006$; OS: $P = 0.044$; Fig. 1B and C). Similar results were obtained when patients were stratified according to the median density of CTLA4$^+$ and LAG-3$^+$ cells (CTLA4 RFS: $P = 0.008$; OS: $P = 0.003$; LAG-3 RFS: $P = 0.011$; OS: $P = 0.001$; Fig. 1B and C). Univariate Cox regression analysis identified a positive prognostic impact only for tumor infiltration by CTLA4$^+$ cells (HR = 0.89; 95% confidence interval = 0.8–0.98; $P = 0.017$; Table 2), which could not be confirmed on multivariate analysis (Table 3). Most likely, these findings reflect the strong correlation between the density of tumor-infiltrating CD8$^+$ T cells and the intratumoral abundance of PD-1$^+$, CTLA4$^+$, and LAG-3$^+$ cells (Fig. 1D), suggesting that PD-1, CTLA4, and LAG-3 largely behave as T-cell markers in this setting.

PD-L1 levels positively correlate with antitumor immunity and improved disease outcome in HGSC

To further characterize the impact of PD-L1 expression on the immunologic profile of HGSCs, we used RNA-seq to compare gene-expression profiles in PD-L1$^-$ vs. PD-L1$^+$ patients. We identified a set of 1,114 genes that were significantly overrepresented in samples from PD-L1$^+$ patients as compared with their PD-L1$^-$ counterparts (Fig. 2A). Functional studies revealed a strong association between such DEGs with immune system activation and inflammation. Alongside, we used the MCP-counter R package to estimate the relative expression levels of different cell populations in the TME of PD-L1$^+$ and PD-L1$^-$ patients. Compared with their PD-L1$^-$ counterparts, PD-L1$^+$ tumors were enriched in gene sets specific for T cells ($P < 0.0001$) and CD8$^+$ T cells ($P < 0.0001$; Fig. 2B). To validate these findings with another technique, we next analyzed the relationship between PD-L1 expression and the intratumoral abundance of CD8$^+$ CTLs by IHC (study group 1). We observed significantly higher densities of CD8$^+$ CTLs infiltrating tumor nests ($P < 0.0001$) in samples from PD-L1$^+$ versus PD-L1$^-$ patients (Fig. 2C). Similar results were obtained for CD20$^+$ B cells and DC-LAMP$^+$ DCs (Fig. 2C), confirming previous results from our group (5). Moreover, to address the functional properties of HGSC-infiltrating CD8$^+$ CTLs from PD-L1$^+$ versus PD-L1$^-$ patients, we performed a flow cytometry analysis on 20 freshly resected HGSCs (study group 2; Supplementary Table S1) on which PD-L1 status had been previously assessed by IHC. We observed significantly higher percentages of CD8$^+$ CTLs expressing IFNγ$^+$ ($P = 0.015$), as well as of CD8$^+$ CTLs coexpressing IFNγ and granzyme B (GZMB, a key CTL effector; $P = 0.044$) or CD107a (a marker of CTL activation; $P = 0.039$), in PD-L1$^+$ versus PD-L1$^-$ patients (Fig. 2D). Moreover, we observed a correlation between *CD274* mRNA levels and *IFNG* mRNA levels ($R = 0.61$;

Table 3. Multivariate Cox proportional hazard analysis

	OS	
Variable	HR (95% CI)	*P*
Stage 4	119.78 (2.18–4518.48)	**0.01**
PD-L1	0.3 (0.12–0.61)	**0.007**
TIM-3	1.41 (1.1–1.9)	**0.03**

Published OnlineFirst May 10, 2019; DOI: 10.1158/1078-0432.CCR-18-4175

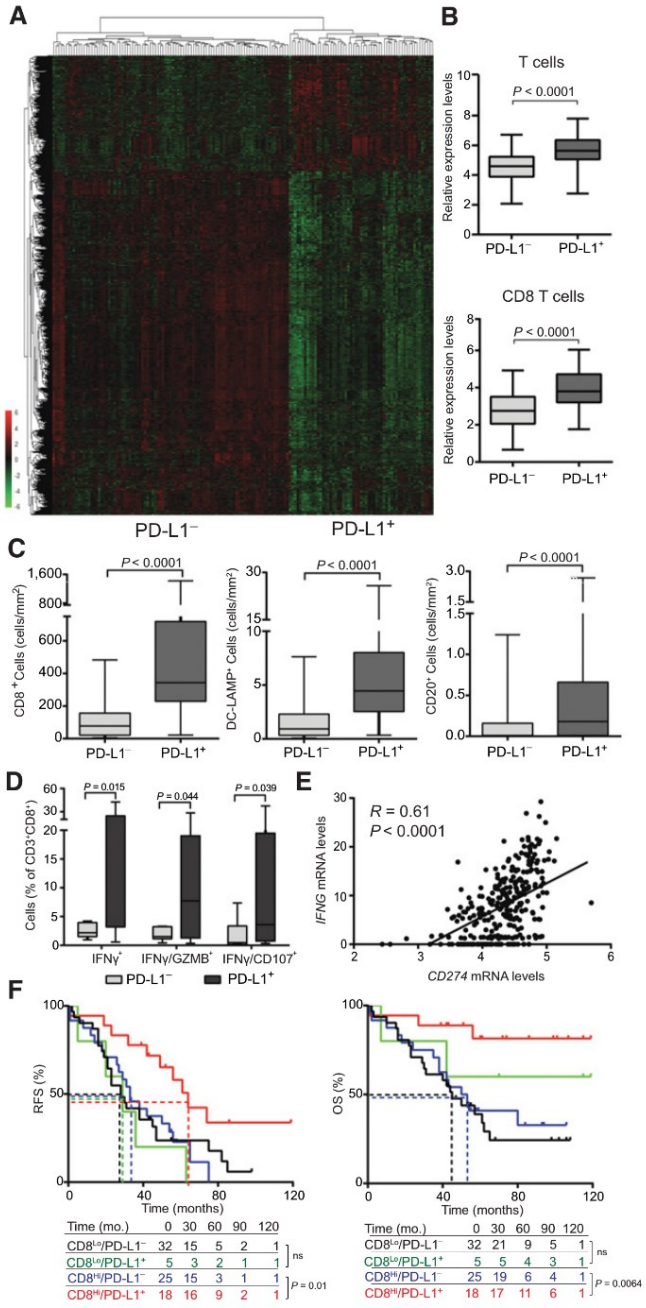

Figure 2.

PD-L1 levels positively correlate with antitumor immunity in HGSC. **A,** Hierarchical clustering of 1,114 genes that were significantly changed in 154 PD-L1$^+$ patients as compared with their 154 PD-L1$^-$ counterparts from the TCGA public database. **B,** Relative expression levels of gene sets associated with T cells and CD8$^+$ T cells across PD-L1$^+$ and PD-L1$^-$ HGSCs, as determined by MCP-counter on RNA-seq data from the TCGA public database. Box plots: lower quartile, median, upper quartile; whiskers, minimum, maximum. **C,** Density of CD8$^+$ T cells, DC-LAMP$^+$ DCs, and CD20$^+$ B cells in the tumor nests in PD-L1$^-$ and PD-L1$^+$ HGSCs ($n = 80$; study group 1). Box plots: lower quartile, median, upper quartile; whiskers, minimum, maximum. **D,** Percentage of IFNγ$^+$, IFNγ$^+$/GZMB$^+$, and IFNγ$^+$/CD107$^+$ cells among CD3$^+$CD8$^+$ cells from the HGSCs of PD-L1$^-$ and PD-L1$^+$ patients after nonspecific stimulation (study group 2). Box plots: lower quartile, median, upper quartile; whiskers, minimum, maximum. **E,** Correlation between the *IFNG* mRNA expression levels and *CD274* mRNA expression in 308 HGSC patients from the TCGA public database. R, Pearson correlation coefficient. **F,** RFS and OS of HGSC patients who did not receive neoadjuvant chemotherapy, upon stratification based on median density of CD8$^+$ T cells and PD-L1 levels (study group 1). Survival curves were estimated by the Kaplan–Meier method, and differences between groups were evaluated using log-rank test. The number of patients at risk is reported.

Published OnlineFirst May 10, 2019; DOI: 10.1158/1078-0432.CCR-18-4175

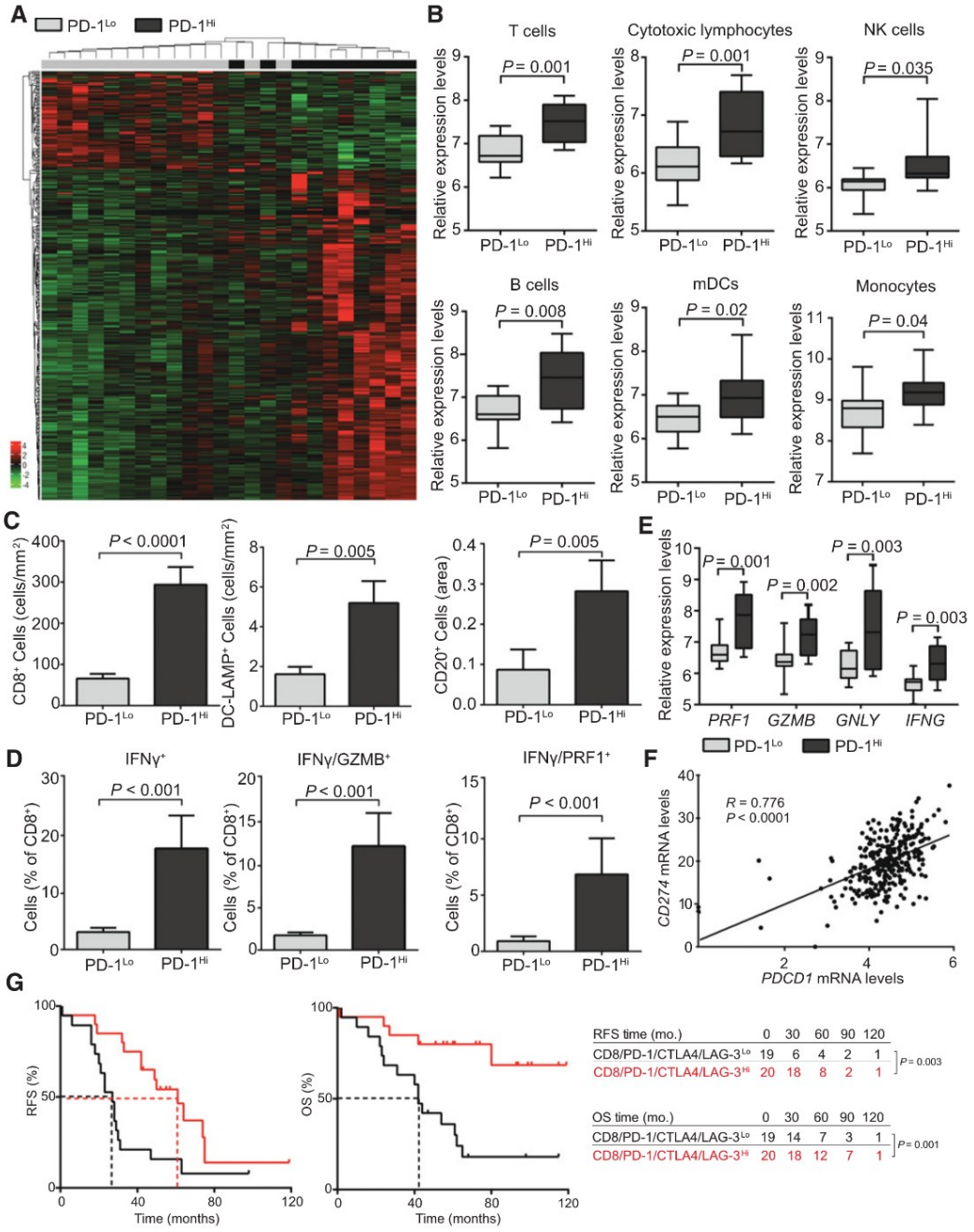

Published OnlineFirst May 10, 2019; DOI: 10.1158/1078-0432.CCR-18-4175

$P < 0.0001$) in HGSC patients from the TCGA public database (Fig. 2E). Conversely, rIFNγ failed to alter the percentage of PD-L1$^+$, PD-1$^+$, and CTLA4$^+$ CD8$^+$ T cells, irrespective of whether the latter were exposed to rIFNγ alone or in the presence of malignant cells that could or could not engage in physical contacts (study group 2; Supplementary Fig. S6). These findings suggest that IFNγ has limited short-term effect on CD8$^+$ T cells isolated from the tumor microenvironment, but favors PD-L1 expression on malignant cells, in line with previous reports (10).

Because both CD8$^+$ T cells and PD-L1 influence disease outcome in patients with HGSC not receiving neoadjuvant chemotherapy, we assessed RFS and OS upon stratifying patients from study group 1 into four subsets (CD8^{Hi}/PD-L1$^+$, CD8^{Hi}/PD-L1$^-$, CD8^{Lo}/PD-L1$^+$, and CD8^{Lo}/PD-L1$^-$). We found that CD8^{Hi}/PD-L1$^+$ patients had improved RFS and OS as compared with their CD8^{Hi}/PD-L1$^-$ counterparts ($P = 0.01$ and $P = 0.0064$, respectively; Fig. 2F). Importantly, the same did not hold true in the CD8^{Lo} patient subset (Fig. 2F). Taken together, these findings indicate that high PD-L1 levels in the TME of HGSC infiltrated by CD8$^+$ CTLs are indicative of an active IFNγ-dependent immune response that positively influences disease outcome.

Tumor infiltration by PD-1$^+$ cells correlates with improved antitumor immunity in HGSC patients

We performed RNA-sequencing to compare gene-expression profiles from 24 HGSCs from study group 1 for which PD-1 status had been evaluated by IHC. We identified a set of 425 transcripts that are significantly overrepresented in samples from PD-1^{Hi} lesions as compared with their PD-1^{Lo} counterparts (Fig. 3A; Supplementary Table S6). Pathway studies revealed a strong association of such DEGs and immune system activation and inflammation. Alongside, we used the MCP-counter R package to estimate the relative expression levels of gene sets linked to specific immune cell populations in the TME of PD-1^{Hi} versus PD-1^{Lo} patients. Compared with their PD-1^{Lo} counterparts, PD-1^{Hi} HGSCs exhibited overrepresentation of gene sets specific for T cells ($P = 0.001$), cytotoxic lymphocytes ($P = 0.001$), NK cells ($P = 0.035$), B cells ($P = 0.008$), DCs ($P = 0.02$), and monocytes ($P = 0.04$; Fig. 3B). Next, we performed IHC to obtain further insights into the links between PD-1$^+$ cell infiltration and the abundance of CD8$^+$ CTLs, DC-LAMP$^+$ DCs, and CD20$^+$ B cells in HGSC samples (study group 1). We observed higher densities of CD8$^+$ T cells ($P < 0.0001$), DC-LAMP$^+$ DCs ($P = 0.005$), and CD20$^+$ B cells ($P = 0.005$) in the TME of PD-1^{Hi} patients as compared with their PD-1^{Lo} counterparts (Fig. 3C; Supplementary Fig. S7), corroborating the notion that PD-1^{Lo} lesions have a scarce immune infiltrate. To investigate the functional profile of CD8$^+$ CTLs from PD-1^{Hi} versus PD-1^{Lo} HGSCs, we harnessed study group 2 (Supplementary Table S1) to perform flow cytometry on freshly resected samples that were also previously scored for PD-1$^+$ cell infiltration by IHC. PD-1^{Hi} lesions contained a significantly higher percentage of CD8$^+$ CTLs staining positively for IFNγ ($P < 0.001$), IFNγ and GZMB ($P < 0.001$), and IFNγ and perforin 1 (PRF1, another T-cell effector molecule; $P < 0.001$) upon nonspecific activation *ex vivo*, as compared with their PD-1^{Lo} counterparts (Fig. 3D). Consistently, the mRNAs coding for multiple CD8$^+$ T-cell effector molecules including *IFNG*, *PRF1*, *GZMB*, and *GNLY* were overrepresented in PD-1^{Hi} versus PD-1^{Lo} HGSCs, as determined by RNA-sequencing in study group 1 (Fig. 3E). Moreover, we found a strong correlation between the transcripts coding for PD-1 (*PDCD1*) and PD-L1 (*CD274*) ($R = 0.776$; $P < 0.0001$) in HGSC patients from the TCGA database (Fig. 3F). However, stratifying patients from Study group 1 into four subsets based on the frequency of tumor-infiltrating CD8$^+$ T cells and PD-1$^+$ cells (CD8^{Hi}/PD-1^{Hi}, CD8^{Hi}/PD-1^{Lo}, CD8^{Lo}/PD-1^{Hi}, and CD8^{Lo}/PD-1^{Lo}) failed to ameliorate the prognostic assessment provided by tumor-infiltrating CD8$^+$ T cells only (Supplementary Fig. S8A). This is in line with (i) the fact that the density of tumor-infiltrating PD-1$^+$ cells had no prognostic value in multivariate analyses (Table 3); (ii) and the robust correlation between the density of tumor-infiltrating PD-1$^+$ and CD8$^+$ cells (Fig. 1D), which is also evident when the sizes of CD8^{Hi}/PD-1^{Hi}, CD8^{Hi}/PD-1^{Lo}, CD8^{Lo}/PD-1^{Hi}, and CD8^{Lo}/PD-1^{Lo} groups are compared (Supplementary Fig. S8A). The same applies to costratification based on CD8 and LAG-3 (study group 1; Supplementary Fig. S8B). Conversely, the density of tumor-infiltrating CTLA4$^+$ cells behaves as PD-L1 levels in that CD8^{Hi}/CTLA4^{Hi} patients had improved RFS and OS compared with their CD8^{Hi}/CTLA4^{Lo} counterparts ($P = 0.06$ and $P = 0.002$, respectively; study group 1; Supplementary Fig. S8C). Notably, PD-L1 levels and infiltration by CTLA4$^+$ cells were the two parameters investigated in this study with lowest degree of correlation with the intratumoral abundance of CD8$^+$ T cells (Fig. 1D), indicating that low CTLA4 expression can be harnessed to identify CD8^{Hi} HGSC patients with relatively poor disease outcome.

Finally, we evaluated the combined prognostic value of tumor infiltration by CD8$^+$, PD-1$^+$, CTLA4$^+$, and LAG-3$^+$ cells by stratifying study group 1 in two groups of patients based on high or low density of all parameters. Not surprisingly, patients with high levels of HGSC-infiltrating CD8$^+$, PD-1$^+$, CTLA4$^+$, and LAG-3$^+$ cells had superior RFS and OS as compared with their low counterparts ($P = 0.003$ and $P = 0.001$, respectively; Fig. 3G).

Figure 3.

Tumor infiltration by PD-1$^+$ cells correlates with improved antitumor immunity in HGSC patients. **A,** Hierarchical clustering of 425 transcripts that were significantly changed in 12 PD-1^{Hi} patients as compared with their 12 PD-1^{Lo} counterparts, as determined by RNA-sequencing (study group 1). **B,** Relative expression levels of gene sets associated with T cells, CD8$^+$ T cells, NK cells, B cells, mDCs, and monocytes across PD-1^{Hi} and PD-1^{Lo} HGSCs, as determined by MCP-counter on RNA-seq data from study group 1. Box plots: lower quartile, median, upper quartile; whiskers, minimum, maximum. **C,** Density of CD8$^+$ T cells, DC-LAMP$^+$ DCs, and CD20$^+$ B cells in the tumor nests in PD-1^{Lo} and PD-1^{Hi} HGSCs from study group 1 ($n = 80$). Box plots: lower quartile, median, upper quartile; whiskers, minimum, maximum. **D,** Percentage of IFNγ$^+$, IFNγ$^+$/GZMB$^+$, and IFNγ$^+$/PRF1$^+$ cells among CD3$^+$CD8$^+$ cells from the 20 HGSCs of PD-1^{Lo} and PD-1^{Hi} patients after nonspecific stimulation (study group 2). Box plots: lower quartile, median, upper quartile; whiskers, minimum, maximum. **E,** Relative expression levels of *PRF1, GZMB, GNLY,* and *IFNG* in 154 PD-1^{Lo} and 154 PD-1^{Hi} HGSCs from the TCGA public database, as determined by RNA-seq. plots: lower quartile, median, upper quartile; whiskers, minimum, maximum. **F,** Correlation between the *PDCD1* mRNA expression levels and *CD274* mRNA expression in 308 HGSC patients from the TCGA public database. R, Pearson correlation coefficient. **G,** RFS and OS of 80 HGSC patients from study group 1 who did not receive neoadjuvant chemotherapy, upon stratification based on median density of CD8$^+$, PD-1$^+$, CTLA4$^+$, and LAG-3$^+$ cells in tumor nests. Survival curves were estimated by the Kaplan–Meier method, and differences between groups were evaluated using the log-rank test. The number of patients at risk are reported.

Published OnlineFirst May 10, 2019; DOI: 10.1158/1078-0432.CCR-18-4175

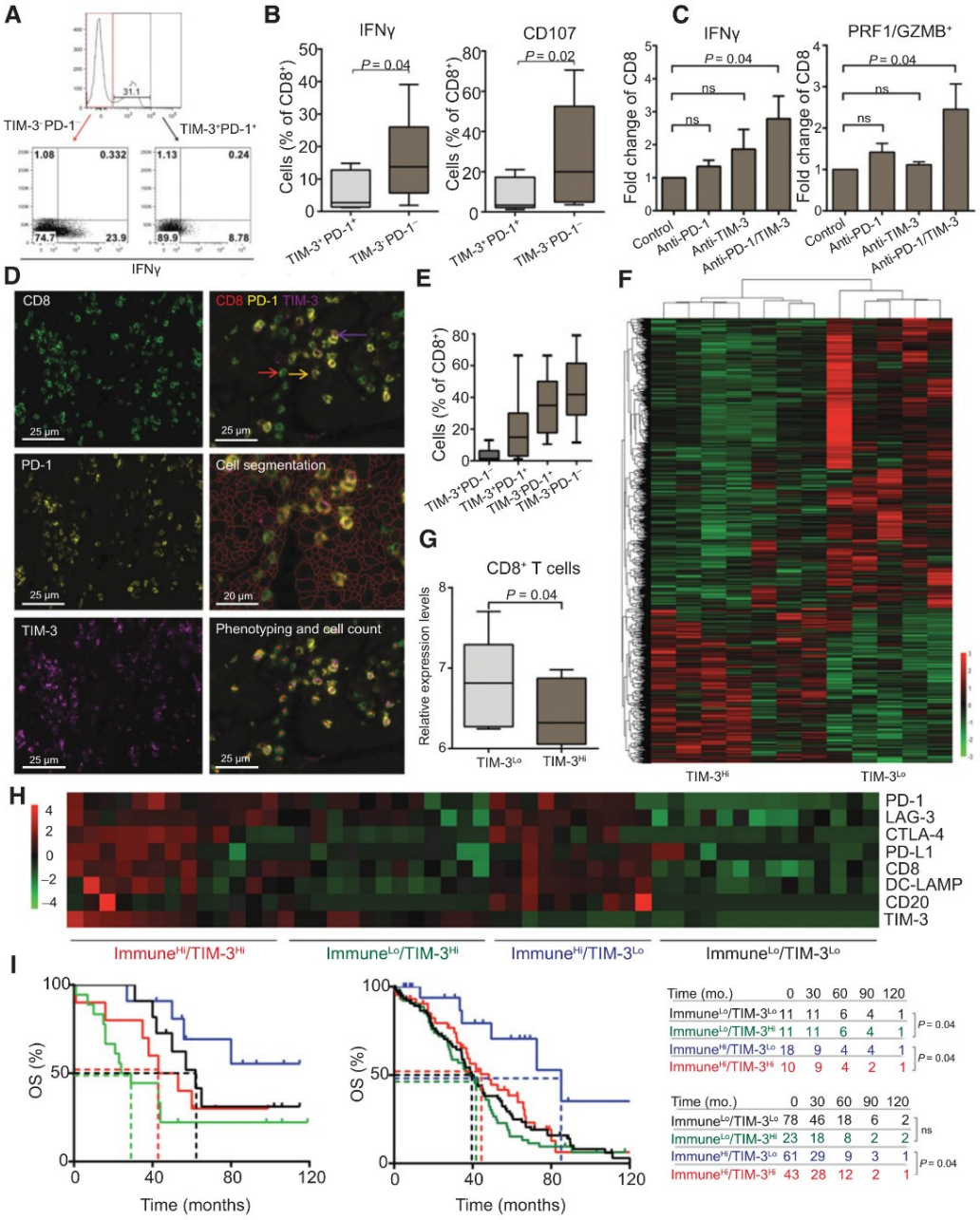

Published OnlineFirst May 10, 2019; DOI: 10.1158/1078-0432.CCR-18-4175

TIM-3 dictates clinically relevant immunosuppression in the TME of HGSCs

We were surprised by the fact that neither the PD-1/PD-L1 axis, neither CTLA4, nor LAG-3 appears to mediate clinically relevant immunosuppressive effects in the TME of chemotherapy-naïve HGSC patients (Figs. 1–3). We therefore investigated whether immunosuppression in this context would rather be under the control of another coinhibitory receptor, namely, TIM-3. To this aim, we first investigated the impact of TIM-3 expression on the functional properties of $CD8^+$ TILs from 20 freshly resected HGSCs (study group 2; Supplementary Table S1) using flow cytometry (Fig. 4A). Remarkably, about one third of tumor-infiltrating $CD8^+$ T cells expressed TIM-3 (mean 31.3%; SEM 32.6%), near to invariably in conjunction with PD-1. Nonspecific stimulation induced IFNγ production and CD107a exposure preferentially in $TIM\text{-}3^-PD\text{-}1^-$ cells as compared with their $TIM\text{-}3^+PD\text{-}1^+$ counterparts ($P = 0.04$ and $P = 0.02$, respectively; Fig. 4B). Moreover, incubation with anti-TIM3 and anti–PD-1 antibodies (but not with either antibody alone) increased the ability of bulk tumor-infiltrating $CD8^+$ T cells to respond to nonspecific stimulation *in vitro* by synthetizing IFNγ and cytolytic molecules (i.e., GZMB, PRF1; study group 2; Fig. 4C). Thus, $TIM\text{-}3^+PD\text{-}1^+$ cells from the HGSC TME stand out as a functionally impaired $CD8^+$ T-cell subpopulation with limited effector functions.

We have previously shown that the intratumoral levels of $PD\text{-}1^+$ cells correlate with improved (rather than poor) disease outcome in chemotherapy-naïve HGSC patients (Fig. 1B and C), largely as they reflect $CD8^+$ CTL infiltration in this setting (Fig. 1D; Supplementary Fig. S8A). Thus, we interrogated the impact of tumor infiltration by $TIM\text{-}3^+$ cells on the immunologic profile of HGSCs and disease outcome. To this aim, we harnessed multispectral immunofluorescence staining combined with automated image analysis on a subset of 50 samples from study group 1 (Fig. 4D). In line with flow cytometry data (Fig. 4A), around 31.3% of the $CD8^+$ T cells infiltrating HGSC expressed TIM-3, most often in combination with PD-1 (Fig. 4E). We then selected 6 $TIM\text{-}3^{Lo}$ patients and compared their transcriptional profile with that of 6 $TIM\text{-}3^{Hi}$ individuals (study group 1). We identified 1,460 genes that were significantly overrepresented in samples from $TIM\text{-}3^{Lo}$ patients relative to their $TIM\text{-}3^{Hi}$ counterparts (Fig. 4F; Supplementary Table S7), and functional studies revealed a strong association between such DEGs and immune system activation and inflammation. Moreover, compared with their $TIM\text{-}3^{Hi}$ counterparts, $TIM\text{-}3^{Lo}$ tumors exhibited overrepresentation (rather than underrepresentation, as expected if TIM-3 behaved as a mere biomarker for T cells) of gene sets specific for $CD8^+$ T cells ($P = 0.04$), as determined by MCP-counter R package (Fig. 4G).

As we observed a negative correlation between infiltration by $TIM\text{-}3^+$ cells and the levels of several transcripts associated with T cells and immune system activation, we next evaluated the immunologic profile of the TME in $TIM\text{-}3^{Lo}$ *versus* $TIM\text{-}3^{Hi}$ tumors (as previously determined by multispectral immunofluorescence staining) by IHC (study group 1; Fig. 4H). This approach identified 4 different clusters of patients, which were characterized by either high levels of PD-L1 and extensive infiltration by $CD8^+$, $PD\text{-}1^+$, $CTLA4^+$, $LAG\text{-}3^+$, $CD20^+$, and $DC\text{-}LAMP^+$ cells ($Immune^{Hi}$) or the opposite situation ($Immune^{Lo}$), combined with abundant or limited infiltration by TIM-3 cells ($Immune^{Hi}/TIM\text{-}3^{Hi}$, $Immune^{Hi}/TIM\text{-}3^{Lo}$, $Immune^{Lo}/TIM\text{-}3^{Hi}$, and $Immune^{Lo}/TIM\text{-}3^{Lo}$; Fig. 4H).

Importantly, $Immune^{Hi}/TIM\text{-}3^{Lo}$ patients had improved OS as compared with their $Immune^{Hi}/TIM\text{-}3^{Hi}$ counterparts ($P = 0.04$), and so did $Immune^{Lo}/TIM\text{-}3^{Lo}$ patients as compared with their $Immune^{Lo}/TIM\text{-}3^{Hi}$ counterparts ($P = 0.04$; Fig. 4I). Such an effect could not be attributed to statistical differences in any parameter other than infiltration by $TIM\text{-}3^+$ cells within the $Immune^{Hi}$ and $Immune^{Lo}$ patient subgroups (Supplementary Table S8). Similarly, $Immune^{Lo}/TIM\text{-}3^{Lo}$ patients had improved OS as compared with their $Immune^{Lo}/TIM\text{-}3^{Hi}$ counterparts ($P = 0.04$; Fig. 4I). Univariate Cox regression confirmed the negative prognostic impact of tumor infiltration by $TIM\text{-}3^+$ cells (HR = 1.03; 95% confidence interval = 1.00–1.06; $P = 0.04$; Table 2), and the significance of this association was validated by multivariate analysis (HR = 1.41; 95% confidence interval = 1.1–1.9; $P = 0.03$) (Table 3). To corroborate our findings in an independent patient cohort, we retrieved normalized *HAVCR2* levels (TIM-3) for 308 patients with HGSC from the TCGA database and stratified these them into 4 groups based on TIM-3 expression and the expression of genes linked to $CD8^+$ T cells (*CD8A*), DCs (*LAMP3*, which codes for DC-LAMP) and B cells (*MS4A1*). Also in this setting, $Immune^{Hi}/TIM\text{-}3^{Lo}$ had improved OS as compared with their $Immune^{Hi}/TIM\text{-}3^{Hi}$ counterparts ($P = 0.04$; Fig. 4I). Altogether, these findings document a critical role for TIM-3 in the establishment of clinically relevant immunosuppression in TME of patients with HGSC.

Discussion

Coinhibitory receptors expressed on T cells play a major role in the establishment of clinically relevant immunosuppression

Figure 4.

TIM-3 dictates clinically relevant immunosuppression in the TME of HGSC. **A,** Gating strategy for $TIM\text{-}3^+PD\text{-}1^+$ $TIM\text{-}3^-PD\text{-}1^-$ cells (study group 2). The percentage of cells in each gate is reported. **B,** Percentage of $IFN\gamma^+$ and $CD107^+$ $CD8^+$ T cells among $TIM\text{-}3^+PD\text{-}1^+$ and $TIM\text{-}3^-PD\text{-}1^-$ $CD8^+$ T cells. **C,** Fold change of $IFN\gamma^+$ and $PRF1/GZMB^+$ $CD8^+$ T cells after incubation with anti–PD-1, anti–TIM-3, and combination of anti–PD-1/anti–TIM-3 antibodies (study group 2). **D,** Representative images of CD8, PD-1, and TIM-3 multispectral immunofluorescence (left). Cells expressing CD8 (red arrow), cells coexpressing CD8 and PD-1 (yellow arrow), and cells coexpressing CD8, PD-1, and TIM-3 (violet arrow). For automated counting, inForm software allows cell segmentation based on DAPI staining of the nucleus and morphometric characteristics (right). **E,** Percentage of $TIM\text{-}3^+PD\text{-}1^-$, $TIM\text{-}3^+PD\text{-}1^+$, $TIM\text{-}3^-PD\text{-}1^+$, and $TIM\text{-}3^-PD\text{-}1^-$ $CD8^+$ T cells as determined by *in situ* immunofluorescence in study group 1. **F,** Hierarchical clustering of 1,460 transcripts that were significantly changed in 6 $TIM\text{-}3^{Hi}$ patients as compared with their 6 $TIM\text{-}3^{Lo}$ counterparts from study group 1, as determined by RNA-sequencing. **G,** Relative expression levels of gene sets associated with $CD8^+$ T cells across $TIM\text{-}3^{Hi}$ and $TIM\text{-}3^{Lo}$ HGSCs, as determined by MCP-counter on RNA-seq data from study group 1. Box plots: lower quartile, median, upper quartile; whiskers, minimum, maximum. **H,** Clustering of 50 HGSC patients from study group 1 based on densities of $PD\text{-}1^+$, $LAG\text{-}3^+$, $CTLA\text{-}4^+$, $PD\text{-}L1^+$, $CD8^+$, $DC\text{-}LAMP^+$, $CD20^+$, and $TIM\text{-}3^+$ cells as determined by IHC and multispectral immunofluorescence. **I,** OS of 50 and 308 HGSC patients from study group 1 and the TCGA public database who did not receive neoadjuvant chemotherapy, upon stratification based on the median density of $TIM\text{-}3^+$ cells and immune infiltrate as indicated by clustering heat map. Survival curves were estimated by the Kaplan–Meier method, and differences between groups were evaluated using the log-rank test. The number of patients at risk is reported.

Published OnlineFirst May 10, 2019; DOI: 10.1158/1078-0432.CCR-18-4175

in the microenvironment of most (if not all) human malignancies (28–30). Consistent with this notion, immune-checkpoint blockers that prevent the binding of coinhibitory receptors with their cognate ligands mediate robust clinical efficacy in subsets of patients affected by melanoma, NSCLC, and urothelial carcinoma (31). This is especially true when coinhibitory ligands such as PD-L1 are highly expressed in the TME (3, 4, 28). Recent data indicate that PD-L1^{+} ovarian cancer patients may also obtain clinical benefits from PD-1-targeting immune-checkpoint blockers (32), reinstating the value of PD-L1 as a predictive biomarker for preselecting patients who are likely to respond to immunotherapies targeting the PD-1/PD-L1 axis.

The predictive value of PD-L1 has largely been attributed to its ability to identify tumors with active PD-1 signaling (33). Here, we demonstrate that high levels of PD-L1 are associated with improved disease outcome among chemotherapy-naïve (and immunotherapy-naïve) HGSC patients (Fig. 1), implying that the prognostic value of PD-L1 in our cohort of patients cannot be attributed to its ability to identify a therapeutic target for PD-1 blockers. Rather, our data suggest that high PD-L1 levels constitute a biomarker for spontaneous IFNγ-mediated antitumor immunity (Fig. 2). Consistent with this interpretation, HGSC patients with robust tumor infiltration by CD8^{+} T cells, but low levels of PD-L1 exhibited remarkably poor disease outcome as compared with patients with high levels of tumor-infiltrating T cells but high PD-L1 expression in the TME (Fig. 2). Moreover, tumor infiltration by T cells expressing coinhibitory receptors such as PD-1, CTLA4, and LAG-3 was associated with superior (rather than inferior) RFS and OS (Fig. 1), and neither of these parameters was able to improve patient stratification based on the intratumoral levels of CD8^{+} T cells only, with the possible exception of CTLA4 (Supplementary Fig. S8A–S8C). Thus, in the TME of chemotherapy-naïve HGSC patients, PD-1 and LAG-3 largely behave as biomarkers of infiltration by CD8^{+} T cells (Fig. 1D; Supplementary Fig. S8A–S8C), while PD-L1 expression identifies a clinically relevant, spontaneous anticancer immune response. To our surprise, a low density of CTLA4^{+} cells appears to identify a subgroup of CD8^{Hi} HGSC patients with relatively poor (rather than good) disease outcome as compared with their CD8^{Hi}CTLA^{Hi} counterparts. Potentially, such an unexpected finding may either reflect the expression of CTLA4 by myeloid cells supporting antitumor immunity (34) or originate from the relatively low number of patients in the CD8^{Hi}CTLA4^{Lo} group.

We were surprised to find that neither of the major coinhibitory receptors we analyzed at first was associated with an independent negative prognostic value in our patient cohort, which led us to refocus our attention on the comparatively less known molecule TIM-3. We found that one third of CD8^{+} T cells that infiltrate chemotherapy-naïve HGSCs express TIM-3, generally in association with PD-1 (Fig. 4A and E). Not only such TIM-3^{+}PD-1^{+} cells exhibit signs of functional exhaustion, both at baseline and upon nonspecific stimulation (Fig. 4B and C), but their abundance conveys a negative independent prognostic value that can be harnessed to obtain improved patient stratification (Fig. 4I). Moreover, only CD8^{+} T cells from TIM-3^{Hi} (but not TIM-3^{Lo}) patients are sensitive to TIM-3 blockade (in combination with PD-1, but not CTLA4, blockade; Supplementary Fig. S8D). These findings are in line with data from other groups identifying the negative impact of TIM-3 expression on tumor-infiltrating CD8^{+} T cells in multiple oncological settings (27, 35–38). Moreover, they suggest that targeting TIM-3 with immune-checkpoint blockers may be a particularly promising approach for the treatment of HGSC. To the best of our knowledge, although multiple clinical trials are currently assessing the therapeutic profile of TIM-3-targeting agents in open-label settings, no study specifically testing TIM-3 inhibitors in ovarian cancer patients is currently recruiting participants (source: www.clinicaltrials.gov).

In conclusion, our findings demonstrate that PD-L1 and TIM-3 are biomarkers of active and suppressed, respectively, spontaneous immunity against HGSC. Besides identifying in TIM-3 a potentially actionable target for the treatment of HGSC patients, these data suggest that the ability of PD-L1 expression levels to identify patients who are likely to respond to PD-1– or PD-L1–targeting agents may reflect (at least to some extent or in some setting) the preexistence of a natural immune response against the tumor.

Disclosure of Potential Conflicts of Interest

L. Galluzzi is a consultant/advisory board member for Astra Zeneca, OmniSEQ, and The Luke Heller Foundation, and reports receiving commercial research grants from Lytix and Phosplatin. No potential conflicts of interest were disclosed by the other authors.

Authors' Contributions

Conception and design: J. Fucikova, J. Laco, L. Galluzzi, R. Spisek
Development of methodology: J. Fucikova, M. Hensler, L. Kasikova, L. Belicova, J. Pineau, A. Gey, E. Tartour
Acquisition of data (provided animals, acquired and managed patients, provided facilities, etc.): J. Fucikova, J. Rakova, M. Hensler, L. Kasikova, L. Belicova, K. Hladikova, P. Skapa, J. Laco, I. Praznovec, M.J. Halaska, T. Brtnicky, R. Kodet, J. Pineau, A. Gey, E. Tartour, A. Ryska
Analysis and interpretation of data (e.g., statistical analysis, biostatistics, computational analysis): J. Fucikova, J. Rakova, M. Hensler, L. Kasikova, L. Belicova, K. Hladikova, L. Pecen, A. Fialova, J. Pineau, A. Gey, E. Tartour, L. Galluzzi
Writing, review, and/or revision of the manuscript: J. Fucikova, L. Kasikova, I. Truxova, P. Skapa, M.J. Halaska, J. Pineau, A. Gey, E. Tartour, A. Ryska, L. Galluzzi, R. Spisek
Administrative, technical, or material support (i.e., reporting or organizing data, constructing databases): J. Fucikova, J. Rakova, L. Kasikova
Study supervision: J. Fucikova, L. Galluzzi, R. Spisek

Acknowledgments

This study was exclusively sponsored by Sotio, Prague, Czech Republic. This study was supported by program PROGRES Q40/11, by the project BBMRI-CZ LM2015089, and by the European Regional Development Fund-Project BBMRI-CZ.: Biobank network—a versatile platform for research on the etiopathogenesis of diseases, No: EF16 013/0001674. L. Galluzzi is supported by a Breakthrough Level 2 grant from the US Department of Defense (DoD), Breast Cancer Research Program (BRCP; #BC180476P1), by a startup grant from the Department of Radiation Oncology at Weill Cornell Medicine (New York), by industrial collaborations with Lytix (Oslo, Norway) and Phosplatin (New York), and by donations from Phosplatin (New York), the Luke Heller TECPR2 Foundation (Boston) and Sotio a.s. (Prague, Czech Republic).

The costs of publication of this article were defrayed in part by the payment of page charges. This article must therefore be hereby marked *advertisement* in accordance with 18 U.S.C. Section 1734 solely to indicate this fact.

Received December 20, 2018; revised March 19, 2019; accepted May 9, 2019; published first May 10, 2019.

Published OnlineFirst May 10, 2019; DOI: 10.1158/1078-0432.CCR-18-4175

References

1. Fridman WH, Zitvogel L, Sautes-Fridman C, Kroemer G. The immune contexture in cancer prognosis and treatment. Nat Rev Clin Oncol 2017;14:717–34.
2. Galon J, Costes A, Sanchez-Cabo F, Kirilovsky A, Mlecnik B, Lagorce-Pages C, et al. Type, density, and location of immune cells within human colorectal tumors predict clinical outcome. Science 2006;313:1960–4.
3. Skov BG, Kiss K, Ramsted J, Linnemann D. A technique to improve diagnostic information from fine-needle aspirations: immunohistochemistry on cytoscrape. Cancer 2009;117:120–7.
4. Passiglia F, Bronte G, Bazan V, Natoli C, Rizzo S, Galvano A, et al. PD-L1 expression as predictive biomarker in patients with NSCLC: a pooled analysis. Oncotarget 2016;7:19738–47.
5. Truxova I, Kasikova L, Hensler M, Skapa P, Laco J, Pecen L, et al. Mature dendritic cells correlate with favorable immune infiltrate and improved prognosis in ovarian carcinoma patients. J Immunother Cancer 2018;6:139.
6. Chen DS, Mellman I. Elements of cancer immunity and the cancer-immune set point. Nature 2017;541:321–30.
7. Savas P, Salgado R, Denkert C, Sotiriou C, Darcy PK, Smyth MJ, et al. Clinical relevance of host immunity in breast cancer: from TILs to the clinic. Nat Rev Clin Oncol 2016;13:228–41.
8. Hamanishi J, Mandai M, Iwasaki M, Okazaki T, Tanaka Y, Yamaguchi K, et al. Programmed cell death 1 ligand 1 and tumor-infiltrating CD8+ T lymphocytes are prognostic factors of human ovarian cancer. Proc Natl Acad Sci U S A 2007;104:3360–5.
9. Webb JR, Milne K, Kroeger DR, Nelson BH. PD-L1 expression is associated with tumor-infiltrating T cells and favorable prognosis in high-grade serous ovarian cancer. Gynecol Oncol 2016;141:293–302.
10. Taube JM, Anders RA, Young GD, Xu H, Sharma R, McMiller TL, et al. Colocalization of inflammatory response with B7-h1 expression in human melanocytic lesions supports an adaptive resistance mechanism of immune escape. Sci Transl Med 2012;4:127ra37.
11. Schalper KA, Velcheti V, Carvajal D, Wimberly H, Brown J, Pusztai L, et al. In situ tumor PD-L1 mRNA expression is associated with increased TILs and better outcome in breast carcinomas. Clin Cancer Res 2014;20:2773–82.
12. Lipson EJ, Vincent JG, Loyo M, Kagohara LT, Luber BS, Wang H, et al. PD-L1 expression in the Merkel cell carcinoma microenvironment: association with inflammation, Merkel cell polyomavirus and overall survival. Cancer Immunol Res 2013;1:54–63.
13. D'Angelo SP, Shoushtari AN, Agaram NP, Kuk D, Qin LX, Carvajal RD, et al. Prevalence of tumor-infiltrating lymphocytes and PD-L1 expression in the soft tissue sarcoma microenvironment. Hum Pathol 2015;46:357–65.
14. Muenst S, Soysal SD, Gao F, Obermann EC, Oertli D, Gillanders WE. The presence of programmed death 1 (PD-1)-positive tumor-infiltrating lymphocytes is associated with poor prognosis in human breast cancer. Breast Cancer Res Treat 2013;139:667–76.
15. Thompson RH, Dong H, Lohse CM, Leibovich BC, Blute ML, Cheville JC, et al. PD-1 is expressed by tumor-infiltrating immune cells and is associated with poor outcome for patients with renal cell carcinoma. Clin Cancer Res 2007;13:1757–61.
16. Giraldo NA, Becht E, Pages F, Skliris G, Verkarre V, Vano Y, et al. Orchestration and prognostic significance of immune checkpoints in the microenvironment of primary and metastatic renal cell cancer. Clin Cancer Res 2015;21:3031–40.
17. Badoual C, Hans S, Merillon N, Van Ryswick C, Ravel P, Benhamouda N, et al. PD-1-expressing tumor-infiltrating T cells are a favorable prognostic biomarker in HPV-associated head and neck cancer. Cancer Res 2013;73:128–38.
18. Takahashi H, Tomita N, Sakata S, Tsuyama N, Hashimoto C, Ohshima R, et al. Prognostic significance of programmed cell death-1-positive cells in follicular lymphoma patients may alter in the rituximab era. Eur J Haematol 2013;90:286–90.
19. Webb JR, Milne K, Nelson BH. PD-1 and CD103 are widely coexpressed on prognostically favorable intraepithelial CD8 T cells in human ovarian cancer. Cancer Immunol Res 2015;3:926–35.
20. O'Sullivan B, Brierley J, Byrd D, Bosman F, Kehoe S, Kossary C, et al. The TNM classification of malignant tumours-towards common understanding and reasonable expectations. Lancet Oncol 2017;18:849–51.
21. Meinhold-Heerlein I, Fotopoulou C, Harter P, Kurzeder C, Mustea A, Wimberger P, et al. The new WHO classification of ovarian, fallopian tube, and primary peritoneal cancer and its clinical implications. Arch Gynecol Obstet 2016;293:695–700.
22. Solomon B, Young RJ, Bressel M, Urban D, Hendry S, Thai A, et al. Prognostic significance of PD-L1(+) and CD8(+) immune cells in HPV(+) oropharyngeal squamous cell carcinoma. Cancer Immunol Res 2018. doi: 10.1158/2326-6066.CIR-17-0299. [Epub ahead of print].
23. Becht E, Giraldo NA, Lacroix L, Buttard B, Elarouci N, Petitprez F, et al. Estimating the population abundance of tissue-infiltrating immune and stromal cell populations using gene expression. Genome Biol 2016;17:218.
24. Ritchie ME, Phipson B, Wu D, Hu Y, Law CW, Shi W, et al. limma powers differential expression analyses for RNA-sequencing and microarray studies. Nucleic Acids Res 2015;43:e47.
25. Gu Z, Eils R, Schlesner M. Complex heatmaps reveal patterns and correlations in multidimensional genomic data. Bioinformatics 2016;32:2847–9.
26. Bindea G, Mlecnik B, Hackl H, Charoentong P, Tosolini M, Kirilovsky A, et al. ClueGO: a Cytoscape plug-in to decipher functionally grouped gene ontology and pathway annotation networks. Bioinformatics 2009;25:1091–3.
27. Granier C, Dariane C, Combe P, Verkarre V, Urien S, Badoual C, et al. Tim-3 expression on tumor-infiltrating PD-1(+)CD8(+) T cells correlates with poor clinical outcome in renal cell carcinoma. Cancer Res 2017;77:1075–82.
28. Topalian SL, Drake CG, Pardoll DM. Immune checkpoint blockade: a common denominator approach to cancer therapy. Cancer Cell 2015;27:450–61.
29. Pardoll DM. The blockade of immune checkpoints in cancer immunotherapy. Nat Rev Cancer 2012;12:252–64.
30. Tumeh PC, Harview CL, Yearley JH, Shintaku IP, Taylor EJ, Robert L, et al. PD-1 blockade induces responses by inhibiting adaptive immune resistance. Nature 2014;515:568–71.
31. Vanpouille-Box C, Lhuillier C, Bezu L, Aranda F, Yamazaki T, Kepp O, et al. Trial watch: Immune checkpoint blockers for cancer therapy. Oncoimmunology 2017;6:e1373237.
32. Varga A, Piha-Paul S, Ott PA, Mehnert JM, Berton-Rigaud D, Morosky A, et al. Pembrolizumab in patients with programmed death ligand 1-positive advanced ovarian cancer: analysis of KEYNOTE-028. Gynecol Oncol 2018;(152:243–50.
33. Sharpe AH, Pauken KE. The diverse functions of the PD1 inhibitory pathway. Nat Rev Immunol 2018;18:153–67.
34. Halpert MM, Konduri V, Liang D, Chen Y, Wing JB, Paust S, et al. Dendritic cell-secreted cytotoxic T-lymphocyte-associated protein-4 regulates the T-cell response by downmodulating bystander surface B7. Stem Cells Dev 2016;25:774–87.
35. Hladikova K, Partlova S, Koucky V, Boucek J, Fonteneau JF, Zabrodsky M, et al. Dysfunction of HPV16-specific CD8+ T cells derived from oropharyngeal tumors is related to the expression of Tim-3 but not PD-1. Oral Oncol 2018;82:75–82.
36. Zhou Q, Munger ME, Veenstra RG, Weigel BJ, Hirashima M, Munn DH, et al. Coexpression of Tim-3 and PD-1 identifies a CD8+ T-cell exhaustion phenotype in mice with disseminated acute myelogenous leukemia. Blood 2011;117:4501–10.
37. Shayan G, Srivastava R, Li J, Schmitt N, Kane LP, Ferris RL. Adaptive resistance to anti-PD1 therapy by Tim-3 upregulation is mediated by the PI3K-Akt pathway in head and neck cancer. Oncoimmunology 2017;6:e1261779.
38. Sakuishi K, Apetoh L, Sullivan JM, Blazar BR, Kuchroo VK, Anderson AC. Targeting Tim-3 and PD-1 pathways to reverse T cell exhaustion and restore anti-tumor immunity. J Exp Med 2010;207:2187–94.

5.5 Aktivní buněčná imunoterapie na bázi dendritických buněk je založena na vhodně zvolené nádorové linii jako zdroji nádorových antigenů

Cílem aktivní buněčné imunoterapie v léčbě nádorových onemocnění je překonat navozenou toleranci vůči nádorovým buňkám, a zesílit tak protinádorovou imunitní odpověď v těle pacientů. Pro účinnou aktivaci imunitní odpovědi musí docházet k prezentaci nádorových antigenů na povrchu buněk prezentujících antigen (antigen presenting cells, APC) naivním T lymfocytům. Zralé dendritické buňky (dendritic cells, DCs) představují nejúčinnější APC, a jsou proto vhodným cílem pro imunoterapeutické protokoly založené na indukci a posílení specifické složky imunitního systému. Pro úspěšnou imunoterapii na bázi DCs je klíčovým krokem volba vhodného zdroje nádorových antigenů, jejichž spektrum bude co nejvíce odrážet repertoár nádorových antigenů v primárním nádoru. Vzhledem k heterogenitě v expresi nádorových antigenů asociovaných s nádorem (tumor associated antigens, TAAs) v primární nádorové tkáni i v nádorových liniích je potřeba detailně charakterizovat expresní profil TAAs a porozumět významu jednotlivých antigenů v indukci efektivní protinádorové imunitní odpovědi. V této studii jsme analyzovali míru exprese 21 TAAs charakteristických pro ovariální karcinom u primárních nádorů serózního epiteliálního ovariálního karcinomu a výsledný expresní profil jsme porovnali se čtyřmi dostupnými ovariálními nádorovými liniemi. Více než 90 % primárních nádorů mělo významně zvýšenou expresi nádorového antigenu 125 (cancer antigen 125, CA125), folátového receptoru 1 (folate receptor 1, FOLR1), molekuly epiteliální buněčné adheze (epithelial cell adhesion molecule, EPCAM) a mucinu 1 (mucin 1, MUC-1). Zvýšená hladina exprese byla dále detekována pro lidský receptor epidermálního růstového faktoru 2 (human epidermal growth factor receptor-2, Her-2/neu). Vzhledem k největšímu překryvu v expresi TAAs mezi primárními nádory a nádorovými liniemi OV-90 a OVCAR-3 byly tyto dvě linie zvoleny jako nejvhodnější zdroj nádorových antigenů pro aktivní buněčnou terapii na bázi DCs.

K této práci jsem přispěla následovně: 70 %; podílení se na přípravě panelu TAAs charakterizujících ovariální karcinom, pěstování ovariálních nádorových linií, izolace RNA z primárních nádorů a nádorových linií, měření expresního profilu 21 vybraných TAAs.

Research Paper

Expression of tumor antigens on primary ovarian cancer cells compared to established ovarian cancer cell lines

Kamila Kloudová[1,3], Hana Hromádková[1], Simona Partlová[1,3], Tomáš Brtnický[2], Lukáš Rob[2], Jiřina Bartůňková[1], Michal Hensler[3], Michael J. Halaška[2], Radek Špíšek[1,3], Anna Fialová[1,3]

[1]Department of Immunology, Charles University, 2nd Faculty of Medicine, University Hospital Motol, Prague, Czech Republic

[2]Department of Obstetrics and Gynaecology, Charles University, 2nd Faculty of Medicine, University Hospital Motol, Prague, Czech Republic

[3]Research Department, Sotio, Prague, Czech Republic

Correspondence to: *Anna Fialová,* ***email:*** *askallova@centrum.cz*

Keywords: *high-grade serous epithelial ovarian cancer, tumor-associated antigens, immunotherapy, cancer cell lines*

Received: *January 13, 2016* ***Accepted:*** *May 26, 2016* ***Published:*** *June 14, 2016*

ABSTRACT

In order to select a suitable combination of cancer cell lines as an appropriate source of antigens for dendritic cell-based immunotherapy of ovarian cancer, we analyzed the expression level of 21 tumor associated antigens (BIRC5, CA125, CEA, DDX43, EPCAM, FOLR1, Her-2/neu, MAGE-A1, MAGE-A2, MAGE-A3, MAGE-A4, MAGE-A6, MAGE-A10, MAGE-A12, MUC-1, NY-ESO-1, PRAME, p53, TPBG, TRT, WT1) in 4 established ovarian cancer cell lines and in primary tumor cells isolated from the high-grade serous epithelial ovarian cancer tissue. More than 90% of tumor samples expressed very high levels of CA125, FOLR1, EPCAM and MUC-1 and elevated levels of Her-2/neu, similarly to OVCAR-3 cell line. The combination of OV-90 and OVCAR-3 cell lines showed the highest overlap with patients' samples in the TAA expression profile.

INTRODUCTION

Ovarian cancer is one of the most frequent malignancies with the highest mortality rate among all gynecological tumors [1, 2]. Rapid expansion of the disease and the lack of highly sensitive and specific biomarkers allowing for early diagnosis account for the fact that about 70% of patients are diagnosed at the stage of advanced and disseminated disease with poor prognosis [3].

Surgery and chemotherapy based on platinum and taxane derivates represent the standard treatment modalities for ovarian cancer [4]. Although over 80% of patients are highly responsive to the frontline treatment, the persistence of a small number of resistant tumor cells (minimal residual disease), leads to relapse in 60-70% of patients within 2-5 years [5, 6]. Induction of anti-tumor immune response might represent an additional treatment modality leading to the stabilization or slowing down of the tumor growth at the stage of minimal residual disease.

In order to design appropriate cancer immunotherapy strategies, it is important to comprehensively characterize antigenic profile of primary ovarian cancer cells and to understand the relevance of individual tumor antigens for the induction of efficient immune response. In this study, we analyzed the expression level of 21 tumor associated antigens on ovarian cancer cells isolated from the tumor tissue resected during the radical surgery for the serous epithelial ovarian cancer, which is the most common histological subtype of the diagnosed cases. We compared the results obtained on primary tumor cells with 4 ovarian cancer cell lines in order to select the most suitable cell line combination for use in dendritic cell (DC)-based cancer immunotherapy protocols described in Podrazil et al., 2015 [7]. We also evaluated the presence of tumor antigen specific antibodies in the peripheral blood of tested patients and the relationship between the TAA expression and progression-free survival.

RESULTS

Expression of tumor associated antigens on primary ovarian cancer cells, selected cell lines and PBMC

We measured the expression of mRNA levels of 21 TAAs, namely BIRC5, CA125, CEA, DDX43, EPCAM, FOLR1, Her-2/neu, MAGE-A1, MAGE-A2, MAGE-A3,

MAGE-A4, MAGE-A6, MAGE-A10, MAGE-A12, MUC-1, NY-ESO-1, PRAME, p53, TPBG, TRT and WT1, on isolated serous epithelial ovarian cancer cells and compared the obtained data to the expression profiles of 4 estabilished ovarian cancer cell lines, OV-90, SKOV-3 OVCAR-3 and CAOV-3. Additionally, we evaluated the expression levels of TAAs on PBMCs obtained from patients and healthy controls. As expected, there was significant variability in the pattern and expression levels of investigated antigens between tested ovarian cancer cell lines and tumor cells obtained from patients (Figure 1).

Most of the tumor samples analyzed (> 90%) expressed very high levels of CA125, FOLR1, EPCAM and MUC-1 and intermediate levels of Her-2/neu, similarly to the OVCAR-3 cell line. All of these antigens showed significantly higher expression levels in tumor tissues in comparison to control ovarian tissue samples ($p < 0.01$). WT1 and p53, which are considered as biomarkers for

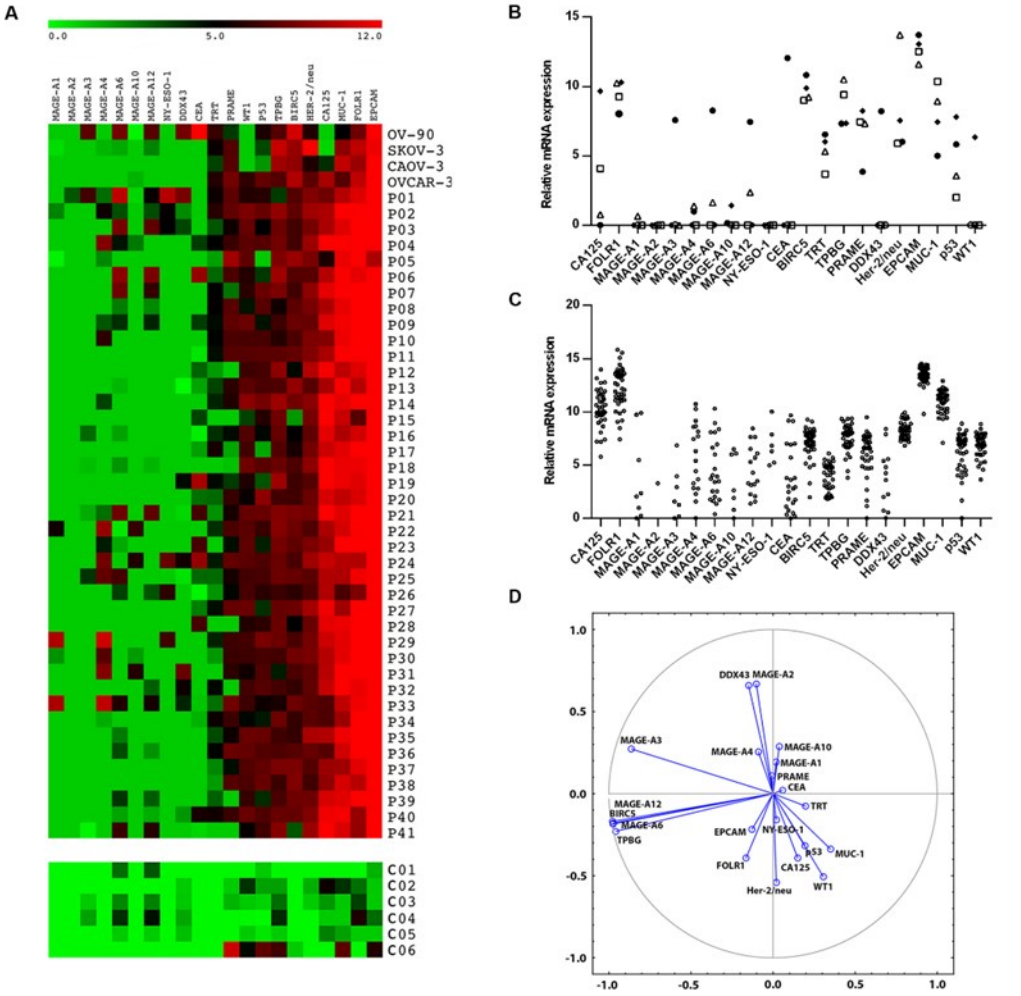

Figure 1: Relative mRNA expression of twenty one TAAs (BIRC-5, CA-125, CEA, DDX-43, EpCAM, FBP, HER-2/neu, MAGE-A1, MAGE-A2, MAGE-A3, MAGE-A4, MAGE-A6, MAGE-A10, MAGE-A12 NY-ESO-1, PRAME, p53, TPBG, TRT, WT-1) in cancer cell lines, primary tumor cells and control ovarian tissue (C01 – C06). Results were normalized to the expression of reference β-actin. Data are expressed as a heat map **A.**, relative mRNA expression of TAAs in cell lines (**B.** ● OV-90, □ CAOV-3, Δ SKOV-3, ♦ OVCAR-3) and patients **C. D.** represents visualization of the TAA clusters extracted using Principal Component Analysis.

high-grade serous ovarian carcinoma, were expressed in 82.9% and 70.7% of samples, respectively. Additionally, intermediate levels of PRAME, TPBG and BIRC5 were detected in > 60% of patients' samples. The expression level of BIRC5 was significantly higher in tumor tissues than in control ovarian samples ($p = 0.015$). From the cell lines analyzed, OV-90 and OVCAR-3 together cover the highest proportion of TAAs expressed on patients' samples (76.2%). The expression profile of TAAs on PBMCs did not differ between the patient group and the controls (Figure S1).

Pattern of tumor associated antigens expression

Statistical analysis showed that MAGE-A3, MAGE-A6, MAGE-A12, BIRC5 and TPBG were co-expressed in a cluster. The correlations among the expression levels of MAGE-A6, MAGE-A12, BIRC5 and TPBG are very strong, with $r > 0.99$ and $p < 0.001$. Correlations between MAGE-A3 and the other 4 TAAs are also highly significant, with $r > 0.70$ and $p < 0.001$. Other cluster was formed by MAGE-A2 with DDX43 ($r = 0.81$; $p < 0.001$) (Figure 1D). Patients who subsequently relapsed showed markedly higher levels of MAGE-A10 and CA125 expression ($p = 0.09$ and $p = 0.08$, respectively) in the primary tumor samples in comparison to patients who remained in remission (Figure 2). Indeed, 100% of patients with high expression levels of MAGE-A10 ($n = 3$), as shown in Figure 1A, underwent a relapse. Additionally, we have observed a significant decrease ($p < 0.01$) in the expression level of the Cluster 1 (MAGE-A3, MAGE-A6, MAGE-A12, BIRC-5 and TPBG) in relapsed patients in comparison with the patients in remission (Figure 2C).

Detection of tumor antigen specific antibodies

Additionally, the presence of IgG antibodies against NY-ESO-1, Her-2/neu, MAGE-A3, MAGE-A4, MAGE-A10 and CA125 was analyzed in patients'sera. We only detected antibodies against NY-ESO-1, namely in 7.5% of patients. The titer of NY-ESO-1 antibodies (expressed as OD) significantly positively correlated with the level of expression of NY-ESO-1 mRNA.

DISCUSSION

The profile of TAAs expressed on primary tumor samples is known to be very heterogenous. To select the suitable cell lines for DC-based ovarian cancer immunotherapy protocols, we analyzed the TAA profile of 41 fresh high-grade serous ovarian tumor samples and 4 established ovarian cancer cell lines. The combination of OV-90 and OVCAR-3 cell lines covered the highest proportion of antigens most frequently expressed on primary tumor samples.

As expected, most of the tumor samples analyzed (> 90%) expressed very high levels of CA125, FOLR1, EPCAM and MUC-1 and elevated levels of Her-2/neu, similarly to OVCAR-3 cell line. All of these antigens showed significantly higher expression levels in tumor tissues in comparison to control ovarian tissue samples. The most frequently tested ovarian cancer-associated antigen, the surface glycoprotein CA125, is usually evaluated in serum samples as a marker of disease progression, although with a limited specificity [8, 9]. In our study, markedly higher levels of CA125 and MAGE-A10 were detected in patients who underwent a relapse in comparison to the patients in remission. However, due to the prospective design of this study, we were not able to confirm these TAAs as independent prognostic factors via Cox proportional hazard model so far. Additionally, as the proportion of samples overexpressing MAGE-A10 was very low ($n = 3$), it is essential to analyze a larger cohort of patients to validate MAGE-A10 as a potential negative prognostic marker.

All of these antigens are promising targets for immunotherapy. EPCAM, which is known to be a stable

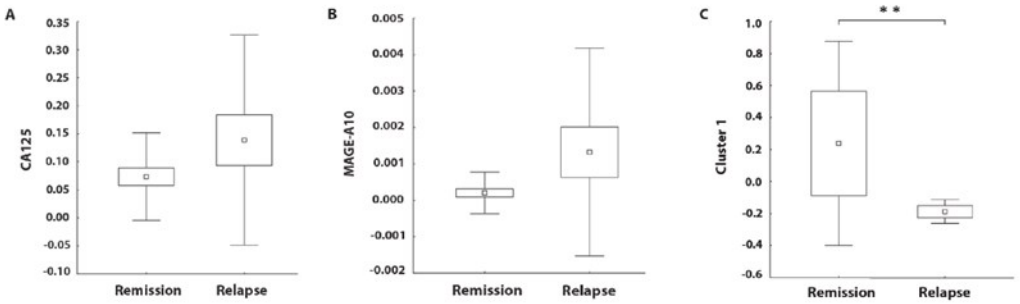

Figure 2: Relative mRNA expressions of CA125, MAGE-A10 and a Cluster 1 (MAGE-A3, MAGE-A6, MAGE-A12, BIRC-5 and TPBG) with regard to the progression-free survival. The boundaries of the box indicate the S.E.M., and the lines in the box represent the mean. Whiskers indicate the SD. ** $p < 0.01$ (Mann-Whitney U test).

antigen expressed in primary, metastatic as well as recurrent disease [10], is an intensively studied target of passive immunotherapy mediated by monoclonal antibodies, such as catumaxomab and catumaxomab/ Removab® [11]. Similarly, anti-CA125 monoclonal antibodies (Abagovomab, Oregovomab) and anti-FRα monoclonal antibody (Farletuzumab) are tested in clinical studies with promising results [11]. Additionally, FRα -specific cytotoxic T lymphocytes (CTL) were detected in malignant ascites [12, 13] as well as peripheral blood [14] of ovarian cancer patients, thus indicating that FRα peptides are immunogenic *in vivo*. Consequently, FRα -loaded DC vaccines were reported to be on trial recently [11]. Similarly, MUC-1 specific tumor infiltrating/ associated CTL were detected in ovarian cancer patients [15]. Therapies targeting MUC-1 consists of monoclonal antibodies, peptide, carbohydrate, DNA, and dendritic cell vaccines, or small molecules (aptamers).

From the group of antigens frequently expressed at intermediate levels, p53, WT1 and Her-2/neu have been currently tested in clinical trials as promising targets of ovarian cancer immunotherapy. Rahma et al (2011) [16] tested in phase II trial two formulations of wt p53:264-272 peptide – subcutaneous administration of the peptide admixed with Montanide and GM-CSF or intravenous administration of peptide-pulsed DCs. Results showed that p53-specific immune responses could be generated with either protocol. Amplification of the Her-2/neu gene and over-expression of the Her-2/neu protein have been reported in a number of different tumor types including breast, colon, gastric, ovarian, esophageal and endometrial. For some of these cancers, anti-Her-2/neu treatment has become an essential part of the therapy A Phase I study showed that vaccination with Her-2/neu peptides could induce a strong and long lived CD4 and CD8 specific response [17]. Similarly to Her-2/neu, WT1 is expressed in a wide spectrum of hematological and solid tumors, including high-grade serous ovarian cancer. Kobayashi et al. (2014) [18] reported that WT1-pulsed DC – based vaccine was able to generate specific T cell responses in patients with recurrent ovarian cancer; however, there was no correlation between the observed immune response and overall survival time. Two from the antigens expressed at intermediate levels, namely BIRC5 and TPBG, were co-expressed in a cluster together with MAGE-A3, MAGE-A6 and MAGE-A12 (Cluster 1). Surprisingly, patients in remission expressed significantly higher levels of Cluster 1 than patients who underwent a relapse. However, the prognostic significance of Cluster 1 remains to be confirmed using Cox proportional hazard model after the follow-up care endpoint.

We have documented a heterogeneous and individual pattern of tumor antigen expression on primary tumor cells. This underlines the importance of the choice of the appropriate spectrum of tumor antigens in cancer immunotherapy trials. Ideal tumor antigen should be unanimously expressed on all tumor cells. However, none of the antigens analyzed in this study fulfills this criterion. This argues for the use of multiple tumor antigen approaches for the cancer immunotherapy of the ovarian cancer. Such strategy, if successful, would lead to the development of a complex immune response targeting different proteins and enhancing the chance of a long term control of tumor progression. Ovarian cancer cell lines selected in our study as the most suitable for DC-based immunotherapy protocols of high-grade ovarian cancer, namely OV-90 and OVCAR-3, cover together 76.2% of measured TAAs, including the most promising immunotherapy targets. Phase I/II clinical trial in metastatic prostate cancer patients treated with docetaxel combined with vaccines of LNCaP prostate cancer cell line – pulsed DCs showed induction and maintenance of PSA specific T cells and longer than expected survival [7]. Phase II clinical trial regarding the efficacy of the vaccine based on the same protocol to treat ovarian cancer is already in progress (NCT02107937).

MATERIALS AND METHODS

Patients

Peripheral blood and primary tumor tissue were obtained from 41 patients in stage III – IV of high-grade serous epithelial ovarian cancer, undergoing initial cytoreductive surgery at the University Hospital Motol in Prague. None of the patients enrolled in the study had received neoadjuvant chemotherapy prior to the surgery. Peripheral blood mononuclear cells (PBMC) and sera obtained from healthy donors were used as controls. Control ovarian tissue was obtained from patients undergoing surgery for ovarian cysts. Control C06 was human adult ovary full-length cDNA template obtained from Biosettia (San Diego, CA). All tissue specimens were collected with patient consent, and the study was approved by the Institutional Review Board of the University Hospital Motol. The clinico-pathological characteristics of the patients are summarized in Table 1.

Isolation of primary tumor cells and PBMC

Fresh tumor tissue was minced with scissors and digested in PBS containing 1 mg/ml of Collagenase D (Roche, Basel, Switzerland) at 37 °C for 30 min, mechanically dissociated using the gentleMACS™ Dissociator (Miltenyi Biotec, Auburn, CA) and passed through a 100 μm nylon cell strainer (BD Biosciences, Franklin Lakes, NJ). Tumor cells were enriched using Ficoll-Paque density gradient solution (GE Healthcare, Waukesha, WI). Equally, PBMC from blood samples were isolated using Ficoll-Paque density gradient solution (GE Healthcare).

Table 1: Clinicopathological characteristics of the EOC patients in the study

Variable	No.	%
Total no. of patients	41	
Age		
Mean	60	
Range	42-82	
FIGO stage		
III	41	100
Histological subtype		
High Grade Serous	41	100
Relapse		
Yes	17	41.5
No	22	53.7
ND	2	4.9

Cell lines

The ovarian cancer cell lines OV-90, SKOV-3 and OVCAR-3 obtained from ATCC were cultured in RPMI 1640, CAOV-3 was cultured in DMEM. Culture media were supplemented with 10% heat inactivated FBS + L-glutamine + penicillin-streptomycin (all from Lonza) at 37°C and 5% CO2.

Flow cytometry analysis

Tumor cell suspensions were stained with specific antibodies against EPCAM and CD45 (BioLegend, San Diego, CA). Proportions of EPCAM+CD45- tumor cells in the final cell suspension were assessed by flow cytometry using BD FACS Aria and FlowJo software.

RNA extraction

Cellular suspensions containing at least 80% of EPCAM positive cells were used for RNA extraction. In the case of lower purity, the tumor cells were enriched by EasySep® Human EpCAM Positive Selection Kit (STEMCELL Technologies, Vancouver, Canada).

Total RNA was prepared from enriched tumor cell suspension using RNeasy mini or micro kit (Qiagen, Hilden, Germany). The DNase I (Qiagen, Hilden, Germany) treatment was performed during isolation. RNA concentrations were determined with a NanodropVC 2000c UV-Vis spectrophotometer (Thermo Scientific),

Reverse transcription and qPCR

RNA was transcribed into cDNA by iScript™ Reverse Transcription Supermix (BIO-RAD) according to manufacturer's instructions.

The identity of qPCR products in each assay was verified by sequencing. Levels of various transcripts were evaluated by quantitative real-time PCR (qPCR) using CFX96 Real-Time System (BIO-RAD) and Kapa Probe Fast qPCR kit in the presence of specific primers and TaqMan probes obtained from TIB- MOLBIOL (Berlin, Germany). PCR conditions were 95°C for 3 min and 50 cycles of 95°C for 15 s and 60°C for 1min. We measured the mRNA expression for twenty one TAAs (BIRC5, CA125, CEA, DDX43, EPCAM, FOLR1, Her-2/neu, MAGE-A1, MAGE-A2, MAGE-A3, MAGE-A4, MAGE-A6, MAGE-A10, MAGE-A12, MUC-1, NY-ESO-1, PRAME, p53, TPBG, TRT, WT1) and for β-actin used as a reference gene. The relative expression of the target genes were normalized to the level of β-actin. All values are presented as means ± SEM. Specificity of the amplified PCR product was assessed by sequencing. The sequences of primers pairs and probes are summarised in Table S1.

Detection of tumor antigen specific antibodies

Recombinant proteins NY-ESO-1, Her-2/neu, MAGE-A4 (Origene, Rockville, US), CA125 (R&D Systems) and MAGE-A3, MAGE-A10 (Abnova, Taipei, Taiwan) were diluted in Carbonate Coating Buffer (Invitrogen, Prague, Czech Republic) to a final concentration of 1 μg/ml and coated to 96-well plates overnight at 4°C. Plates were blocked for 1 hour with Assay Buffer (Invitrogen, Carlsbad, CA). Patients and control sera diluted to 1:50, 1:100 and 1:200 were incubated in the antigen-coated wells for 2 h. Plates were then incubated with secondary antibody (goat polyclonal antibody to human IgG, Abcam, Cambridge, UK) for 1 hour. TMB (Invitrogen) was used as a substrate.

Reaction was stopped after 20 minutes by adding Stop Solution (Invitrogen). Plates were immediately read with absorbance at 450 nm. As a positive control the Cytomegalovirus Glycoprotein B protein was used. The cutoff value designating positive reaction was assessed as the mean OD of 15 sera obtained from healthy controls (NHS) + 3SD.

Statistical analysis

Statistical analyses were performed using Statistica® 10.0 software (StatSoft, Tulsa, OK). TAA clusters were extracted using Principal Components Analysis. Differences between tumor tissues and control samples, as well as differences between patients in remission and patients with a relapsed EOC were tested using Mann-Whitney U Test. The results were considered statistically significant when $p < 0.05$.

CONFLICTS OF INTEREST

The authors declare that they have no competing interests.

GRANT SUPPORT

This project was supported by research grant IGA NT14533 from the Czech Ministry of Health.

REFERENCES

1. Friedlander ML. Prognostic factors in ovarian cancer. Seminars in oncology. 1998; 25:305-314.
2. Gilks CB. Subclassification of ovarian surface epithelial tumors based on correlation of histologic and molecular pathologic data. International journal of gynecological pathology. 2004; 23:200-205.
3. Rosenthal AN, Jacobs IJ. The role of CA 125 in screening for ovarian cancer. The International journal of biological markers. 1998; 13:216-220.
4. Bookman MA. Standard treatment in advanced ovarian cancer in 2005: the state of the art. International journal of gynecological cancer. 2005; 15:212-220.
5. Ozols RF, Bundy BN, Greer BE, Fowler JM, Clarke-Pearson D, Burger RA, Mannel RS, DeGeest K, Hartenbach EM, Baergen R, Gynecologic Oncology G. Phase III trial of carboplatin and paclitaxel compared with cisplatin and paclitaxel in patients with optimally resected stage III ovarian cancer: a Gynecologic Oncology Group study. Journal of clinical oncology. 2003; 21:3194-3200.
6. du Bois A, Luck HJ, Meier W, Adams HP, Mobus V, Costa S, Bauknecht T, Richter B, Warm M, Schroder W, Olbricht S, Nitz U, Jackisch C, Emons G, Wagner U, Kuhn W, et al. A randomized clinical trial of cisplatin/paclitaxel versus carboplatin/paclitaxel as first-line treatment of ovarian cancer. Journal of the National Cancer Institute. 2003; 95:1320-1329.
7. Podrazil M, Horvath R, Becht E, Rozkova D, Bilkova P, Sochorova K, Hromadkova H, Kayserova J, Vavrova K, Lastovicka J, Vrabcova P, Kubackova K, Gasova Z, Jarolim L, Babjuk M, Spisek R, et al. Phase I/II clinical trial of dendritic-cell based immunotherapy (DCVAC/PCa) combined with chemotherapy in patients with metastatic, castration-resistant prostate cancer. Oncotarget. 2015; 6:18192-18205. doi: 10.18632/oncotarget.4145.
8. Canney PA, Moore M, Wilkinson PM, James RD. Ovarian cancer antigen CA125: a prospective clinical assessment of its role as a tumour marker. British journal of cancer. 1984; 50:765-769.
9. Shi JX, Qin JJ, Ye H, Wang P, Wang KJ, Zhang JY. Tumor associated antigens or anti-TAA autoantibodies as biomarkers in the diagnosis of ovarian cancer: a systematic review with meta-analysis. Expert review of molecular diagnostics. 2015; 15:829-852.
10. Bellone S, Siegel ER, Cocco E, Cargnelutti M, Silasi DA, Azodi M, Schwartz PE, Rutherford TJ, Pecorelli S, Santin AD. Overexpression of epithelial cell adhesion molecule in primary, metastatic, and recurrent/chemotherapy-resistant epithelial ovarian cancer: implications for epithelial cell adhesion molecule-specific immunotherapy. International journal of gynecological cancer. 2009; 19:860-866.
11. Schwab CL, English DP, Roque DM, Pasternak M, Santin AD. Past, present and future targets for immunotherapy in ovarian cancer. Immunotherapy. 2014; 6:1279-1293.
12. Kim DK, Lee TV, Castilleja A, Anderson BW, Peoples GE, Kudelka AP, Murray JL, Sittisomwong T, Wharton JT, Kim JW, Ioannides CG. Folate binding protein peptide 191-199 presented on dendritic cells can stimulate CTL from ovarian and breast cancer patients. Anticancer research. 1999; 19:2907-2916.
13. Peoples GE, Anderson BW, Lee TV, Murray JL, Kudelka AP, Wharton JT, Ioannides CG. Vaccine implications of folate binding protein, a novel cytotoxic T lymphocyte-recognized antigen system in epithelial cancers. Clinical cancer research. 1999; 5:4214-4223.
14. Knutson KL, Krco CJ, Erskine CL, Goodman K, Kelemen LE, Wettstein PJ, Low PS, Hartmann LC, Kalli KR. T-cell immunity to the folate receptor alpha is prevalent in women with breast or ovarian cancer. Journal of clinical oncology. 2006; 24:4254-4261.
15. Ioannides CG, Fisk B, Jerome KR, Irimura T, Wharton JT, Finn OJ. Cytotoxic T cells from ovarian malignant tumors can recognize polymorphic epithelial mucin core peptides. Journal of immunology. 1993; 151:3693-3703.
16. Rahma OE, Ashtar E, Czystowska M, Szajnik ME, Wieckowski E, Bernstein S, Herrin VE, Shams MA, Steinberg SM, Merino M, Gooding W, Visus C, Deleo AB, Wolf JK, Bell JG, Berzofsky JA, Whiteside TL, Khleif

SN. A gynecologic oncology group phase II trial of two p53 peptide vaccine approaches: subcutaneous injection and intravenous pulsed dendritic cells in high recurrence risk ovarian cancer patients. Cancer Immunology, Immunotherapy. 2011; 61:373-384.

17. Knutson KL, Disis ML. Expansion of HER2/neu-specific T cells ex vivo following immunization with a HER2/neu peptide-based vaccine. Clinical breast cancer. 2001; 2:73-79.

18. Kobayashi M, Chiba A, Izawa H, Yanagida E, Okamoto M, Shimodaira S, Yonemitsu Y, Shibamoto Y, Suzuki N, Nagaya M; DC-vaccine study group at the Japan Society of Innovative Cell Therapy (J-SICT). The feasibility and clinical effects of dendritic cell-based immunotherapy targeting synthesized peptides for recurrent ovarian cancer. Journal of Ovarian Research. 2014; 7:48.

6 SHRNUJÍCÍ ZÁVĚR

Nádory hlavy a krku jsou heterogenní skupinou nádorových onemocnění, jejichž společnou vlastností je silně imunosupresivní prostředí, vytvářené komplexními únikovými mechanismy nádorových buněk imunitnímu dohledu. Důsledkem imunosuprese je nedostatečná protinádorová imunitní odpověď a progrese nádorového onemocnění. Překonání imunosuprese a posílení T-buněčné imunitní odpovědi pomocí imunoterapie je cílem tisíců klinických studií, ať už ve formě monoterapie nebo v různých kombinacích s dalšími léčebnými modalitami. Pro léčbu HNSCC byla v USA a Evropě doposud schválena imunoterapie založená na blokaci PD-1 – PD-L1 dráhy pomocí monoklonálních protilátek αPD-1, nivolumabu a pembrolizumabu. Navzdory velkému pokroku, který inhibitory kontrolních bodů imunitních reakcí přinesly v léčbě nádorových onemocnění, většina pacientů s HNSCC na tuto léčbu neodpovídá. Nádorové mikroprostředí je příliš komplexní a role některých inhibičních molekul v procesu karcinogeneze není jednoznačná. Detailní pochopení povahy nádorového mikroprostředí a jednotlivých složek imunitního infiltrátu je zcela zásadní k pochopení únikových mechanismů nádorových buněk a k dosažení lepších výsledků v rámci imunoterapie HNSCC. Předkládaná dizertační práce významně rozšiřuje znalosti o kompozici a funkčních vlastnostech imunitního infiltrátu v nádorovém prostředí HNSCC. Jako první poukazuje na významně odlišný imunitní profil nádorového mikroprostředí u HPV-asociovaných vs. toxicky indukovaných nádorů, charakterizovaný vysokou infiltrací CD8+ T lymfocyty, jejichž zastoupení i silnější aktivační potenciál u HPV-pozitivních pacientů je spojován s lepší prognózou. Tato práce dále popisuje funkční kapacitu HPV-specifických CD8+ T lymfocytů u HPV-asociovaných nádorů, vzhledem k expresi inhibičních molekul, a poukazuje na význam komplementární léčby, jejíž implementace by mohla podstatně zvýšit HPV-specifickou imunitní reakci a odpověď na léčbu u pacientů s HPV-asociovanými OPC. Vzhledem k významnosti specifických T-lymfocytů v protinádorové imunologii je naprostá většina výzkumného zájmu i klinických studií soustředěna na posílení specifické T-buněčné odpovědi. Vzhledem k neuspokojivým výsledkům imunoterapie v klinické praxi u pacientů s HNSCC a k vysoké morbiditě doprovázející standardní léčbu, je potřeba zaměřit se v rámci imunoterapie na další potenciální cíle. Tato práce objasňuje silnou asociaci mezi frekvencí HPV-specifických CD8+ T lymfocytů a přítomností a funkční kapacitou B lymfocytů infiltrujících nádory, a poukazuje tak na význam nejen T-lymfocytů v modulaci protinádorové imunity HNSCC, ale také neméně významné složky specifické imunity –

B-lymfocytů, a jejich prognostický význam. Společně s T lymfocyty by se tak B lymfocyty, které se ukázaly být také velmi silným prognostickým markerem, mohly stát jedním z klíčových cílů nových imunoterapeutických protokolů. Z našich výsledků vyplývá, že budoucnost imunoterapie HNSCC je pravděpodobně založena především na vhodné kombinaci více přístupů, jako jsou inhibitory kontrolních bodů imunitních reakcí s terapeutickými vakcínami proti HPV, nebo inhibice PD-1 – PD-L1 dráhy v kombinaci s aktivací B lymfocytů. Vhodně zvolená multispektrální imunoterapie má, na rozdíl od monoterapie, velký potenciál zabránit vzniku adaptivní rezistence, a překonat tak nežádoucí imunosupresi.

7 SEZNAM LITERATURY

Alexandrov, L.B., S. Nik-Zainal, D.C. Wedge, S.A. Aparicio, S. Behjati, A.V. Biankin, G.R. Bignell, N. Bolli, A. Borg, A.L. Borresen-Dale, S. Boyault, B. Burkhardt, A.P. Butler, C. Caldas, H.R. Davies, C. Desmedt, R. Eils, J.E. Eyfjord, J.A. Foekens, M. Greaves, F. Hosoda, B. Hutter, T. Ilicic, S. Imbeaud, M. Imielinski, N. Jager, D.T. Jones, D. Jones, S. Knappskog, M. Kool, S.R. Lakhani, C. Lopez-Otin, S. Martin, N.C. Munshi, H. Nakamura, P.A. Northcott, M. Pajic, E. Papaemmanuil, A. Paradiso, J.V. Pearson, X.S. Puente, K. Raine, M. Ramakrishna, A.L. Richardson, J. Richter, P. Rosenstiel, M. Schlesner, T.N. Schumacher, P.N. Span, J.W. Teague, Y. Totoki, A.N. Tutt, R. Valdes-Mas, M.M. van Buuren, L. van 't Veer, A. Vincent-Salomon, N. Waddell, L.R. Yates, I. Australian Pancreatic Cancer Genome, I.B.C. Consortium, I.M.-S. Consortium, I. PedBrain, J. Zucman-Rossi, P.A. Futreal, U. McDermott, P. Lichter, M. Meyerson, S.M. Grimmond, R. Siebert, E. Campo, T. Shibata, S.M. Pfister, P.J. Campbell, and M.R. Stratton. 2013. Signatures of mutational processes in human cancer. *Nature* 500:415-421.

Andersen, A.S., A.S. Koldjaer Solling, T. Ovesen, and M. Rusan. 2014. The interplay between HPV and host immunity in head and neck squamous cell carcinoma. *International journal of cancer* 134:2755-2763.

Andre, K., S. Schraub, M. Mercier, and P. Bontemps. 1995. Role of alcohol and tobacco in the aetiology of head and neck cancer: a case-control study in the Doubs region of France. *European journal of cancer. Part B, Oral oncology* 31B:301-309.

Ang, K.K., J. Harris, R. Wheeler, R. Weber, D.I. Rosenthal, P.F. Nguyen-Tan, W.H. Westra, C.H. Chung, R.C. Jordan, C. Lu, H. Kim, R. Axelrod, C.C. Silverman, K.P. Redmond, and M.L. Gillison. 2010. Human papillomavirus and survival of patients with oropharyngeal cancer. *The New England journal of medicine* 363:24-35.

Ansell, S.M., A.M. Lesokhin, I. Borrello, A. Halwani, E.C. Scott, M. Gutierrez, S.J. Schuster, M.M. Millenson, D. Cattry, G.J. Freeman, S.J. Rodig, B. Chapuy, A.H. Ligon, L. Zhu, J.F. Grosso, S.Y. Kim, J.M. Timmerman, M.A. Shipp, and P. Armand. 2015. PD-1 blockade with nivolumab in relapsed or refractory Hodgkin's lymphoma. *The New England journal of medicine* 372:311-319.

Argiris, A., K.J. Harrington, M. Tahara, J. Schulten, P. Chomette, A. Ferreira Castro, and L. Licitra. 2017. Evidence-Based Treatment Options in Recurrent and/or Metastatic Squamous Cell Carcinoma of the Head and Neck. *Frontiers in oncology* 7:72.

Ault, K.A., and I.I.S.G. Future. 2007. Effect of prophylactic human papillomavirus L1 virus-like-particle vaccine on risk of cervical intraepithelial neoplasia grade 2, grade 3, and adenocarcinoma in situ: a combined analysis of four randomised clinical trials. *Lancet* 369:1861-1868.

Badoual, C., S. Hans, N. Merillon, C. Van Ryswick, P. Ravel, N. Benhamouda, E. Levionnois, M. Nizard, A. Si-Mohamed, N. Besnier, A. Gey, R. Rotem-Yehudar, H. Pere, T. Tran, C.L. Guerin, A. Chauvat, E. Dransart, C. Alanio, S. Albert, B. Barry, F. Sandoval, F. Quintin-Colonna, P. Bruneval, W.H. Fridman, F.M. Lemoine, S. Oudard, L. Johannes, D. Olive, D. Brasnu, and E. Tartour. 2013. PD-1-expressing tumor-infiltrating T cells are a favorable prognostic biomarker in HPV-associated head and neck cancer. *Cancer research* 73:128-138.

Balkwill, F.R., M. Capasso, and T. Hagemann. 2012. The tumor microenvironment at a glance. *Journal of cell science* 125:5591-5596.

Bekeredjian-Ding, I., M. Schafer, E. Hartmann, R. Pries, M. Parcina, P. Schneider, T. Giese, S. Endres, B. Wollenberg, and G. Hartmann. 2009. Tumour-derived prostaglandin E and transforming growth factor-beta synergize to inhibit plasmacytoid dendritic cell-derived interferon-alpha. *Immunology* 128:439-450.

Best, S.R., K.J. Niparko, and S.I. Pai. 2012. Biology of human papillomavirus infection and immune therapy for HPV-related head and neck cancers. *Otolaryngologic clinics of North America* 45:807-822.

Blackburn, S.D., H. Shin, W.N. Haining, T. Zou, C.J. Workman, A. Polley, M.R. Betts, G.J. Freeman, D.A. Vignali, and E.J. Wherry. 2009. Coregulation of CD8+ T cell exhaustion by multiple inhibitory receptors during chronic viral infection. *Nature immunology* 10:29-37.

Brandsma, J.L., and A.L. Abramson. 1989. Association of papillomavirus with cancers of the head and neck. *Archives of otolaryngology--head & neck surgery* 115:621-625.

Burtness, B., K.J. Harrington, R. Greil, D. Soulieres, M. Tahara, G. de Castro, Jr., A. Psyrri, N. Baste, P. Neupane, A. Bratland, T. Fuereder, B.G.M. Hughes, R. Mesia, N. Ngamphaiboon, T. Rordorf, W.Z. Wan Ishak, R.L. Hong, R. Gonzalez Mendoza, A. Roy, Y. Zhang, B. Gumuscu, J.D. Cheng, F. Jin, D. Rischin, and K.-. Investigators. 2019. Pembrolizumab alone or with chemotherapy versus cetuximab with chemotherapy for recurrent or metastatic squamous cell carcinoma of the head and neck (KEYNOTE-048): a randomised, open-label, phase 3 study. *Lancet* 394:1915-1928.

Cancer Genome Atlas, N. 2015. Comprehensive genomic characterization of head and neck squamous cell carcinomas. *Nature* 517:576-582.

Canning, M., G. Guo, M. Yu, C. Myint, M.W. Groves, J.K. Byrd, and Y. Cui. 2019. Heterogeneity of the Head and Neck Squamous Cell Carcinoma Immune Landscape and Its Impact on Immunotherapy. *Frontiers in cell and developmental biology* 7:52.

Catakovic, K., E. Klieser, D. Neureiter, and R. Geisberger. 2017. T cell exhaustion: from pathophysiological basics to tumor immunotherapy. *Cell communication and signaling : CCS* 15:1.

Chaturvedi, A.K., E.A. Engels, R.M. Pfeiffer, B.Y. Hernandez, W. Xiao, E. Kim, B. Jiang, M.T. Goodman, M. Sibug-Saber, W. Cozen, L. Liu, C.F. Lynch, N. Wentzensen, R.C. Jordan, S. Altekruse, W.F. Anderson, P.S. Rosenberg, and M.L. Gillison. 2011. Human papillomavirus and rising oropharyngeal cancer incidence in the United States. *Journal of clinical oncology : official journal of the American Society of Clinical Oncology* 29:4294-4301.

Chellappan, S., V.B. Kraus, B. Kroger, K. Munger, P.M. Howley, W.C. Phelps, and J.R. Nevins. 1992. Adenovirus E1A, simian virus 40 tumor antigen, and human papillomavirus E7 protein share the capacity to disrupt the interaction between transcription factor E2F and the retinoblastoma gene product. *Proceedings of the National Academy of Sciences of the United States of America* 89:4549-4553.

Chiba, S., M. Baghdadi, H. Akiba, H. Yoshiyama, I. Kinoshita, H. Dosaka-Akita, Y. Fujioka, Y. Ohba, J.V. Gorman, J.D. Colgan, M. Hirashima, T. Uede, A. Takaoka, H. Yagita, and M. Jinushi. 2012. Tumor-infiltrating DCs suppress nucleic acid-mediated innate immune responses through interactions between the receptor TIM-3 and the alarmin HMGB1. *Nature immunology* 13:832-842.

Coens, C., S. Suciu, V. Chiarion-Sileni, J.J. Grob, R. Dummer, J.D. Wolchok, H. Schmidt, O. Hamid, C. Robert, P.A. Ascierto, J.M. Richards, C. Lebbe, V. Ferraresi, M. Smylie, J.S. Weber, M. Maio, A. Bottomley, S. Kotapati, V. de Pril, A. Testori, and A.M. Eggermont. 2017. Health-related quality of life with adjuvant ipilimumab versus placebo after complete resection of high-risk stage III melanoma (EORTC 18071): secondary outcomes of a multinational, randomised, double-blind, phase 3 trial. *The Lancet. Oncology* 18:393-403.

Dahlstrand, H.M., and T. Dalianis. 2005. Presence and influence of human papillomaviruses (HPV) in Tonsillar cancer. *Advances in cancer research* 93:59-89.

Day, C.L., D.E. Kaufmann, P. Kiepiela, J.A. Brown, E.S. Moodley, S. Reddy, E.W. Mackey, J.D. Miller, A.J. Leslie, C. DePierres, Z. Mncube, J. Duraiswamy, B. Zhu, Q. Eichbaum, M. Altfeld, E.J. Wherry, H.M. Coovadia, P.J. Goulder, P. Klenerman, R. Ahmed, G.J. Freeman, and B.D. Walker. 2006. PD-1 expression on HIV-specific T cells is associated with T-cell exhaustion and disease progression. *Nature* 443:350-354.

de Mello, R.A., A.F. Veloso, P. Esrom Catarina, S. Nadine, and G. Antoniou. 2017. Potential role of immunotherapy in advanced non-small-cell lung cancer. *OncoTargets and therapy* 10:21-30.

Du, W., M. Yang, A. Turner, C. Xu, R.L. Ferris, J. Huang, L.P. Kane, and B. Lu. 2017. TIM-3 as a Target for Cancer Immunotherapy and Mechanisms of Action. *International journal of molecular sciences* 18:

Duffey, D.C., Z. Chen, G. Dong, F.G. Ondrey, J.S. Wolf, K. Brown, U. Siebenlist, and C. Van Waes. 1999. Expression of a dominant-negative mutant inhibitor-kappaBalpha of nuclear factor-kappaB in human head and neck squamous cell carcinoma inhibits survival, proinflammatory cytokine expression, and tumor growth in vivo. *Cancer research* 59:3468-3474.

Duray, A., S. Demoulin, P. Hubert, P. Delvenne, and S. Saussez. 2010. Immune suppression in head and neck cancers: a review. *Clinical & developmental immunology* 2010:701657.

Faraji, F., M. Zaidi, C. Fakhry, and D.A. Gaykalova. 2017. Molecular mechanisms of human papillomavirus-related carcinogenesis in head and neck cancer. *Microbes and infection* 19:464-475.

Fecher, L.A., S.S. Agarwala, F.S. Hodi, and J.S. Weber. 2013. Ipilimumab and its toxicities: a multidisciplinary approach. *The oncologist* 18:733-743.

Ferris, R.L., G. Blumenschein, Jr., J. Fayette, J. Guigay, A.D. Colevas, L. Licitra, K. Harrington, S. Kasper, E.E. Vokes, C. Even, F. Worden, N.F. Saba, L.C. Iglesias Docampo, R. Haddad, T. Rordorf, N. Kiyota, M. Tahara, M. Monga, M. Lynch, W.J. Geese, J. Kopit, J.W. Shaw, and M.L. Gillison. 2016. Nivolumab for Recurrent Squamous-Cell Carcinoma of the Head and Neck. *The New England journal of medicine* 375:1856-1867.

Fourcade, J., Z. Sun, M. Benallaoua, P. Guillaume, I.F. Luescher, C. Sander, J.M. Kirkwood, V. Kuchroo, and H.M. Zarour. 2010. Upregulation of Tim-3 and PD-1 expression is associated with tumor antigen-specific CD8+ T cell dysfunction in melanoma patients. *The Journal of experimental medicine* 207:2175-2186.

Franco, E.L., L.L. Villa, J.P. Sobrinho, J.M. Prado, M.C. Rousseau, M. Desy, and T.E. Rohan. 1999. Epidemiology of acquisition and clearance of cervical human papillomavirus infection in women from a high-risk area for cervical cancer. *The Journal of infectious diseases* 180:1415-1423.

Fucikova, J., J. Rakova, M. Hensler, L. Kasikova, L. Belicova, K. Hladikova, I. Truxova, P. Skapa, J. Laco, L. Pecen, I. Praznovec, M.J. Halaska, T. Brtnicky, R. Kodet, A. Fialova, J. Pineau, A. Gey, E. Tartour, A. Ryska, L. Galluzzi, and R. Spisek. 2019. TIM-3 dictates functional orientation of the immune infiltrate in ovarian cancer. *Clinical cancer research : an official journal of the American Association for Cancer Research*

Fury, M.G., E. Sherman, D. Lisa, N. Agarwal, K. Algazy, B. Brockstein, C. Langer, D. Lim, R. Mehra, S.K. Rajan, S. Korte, B. Lipson, F. Yunus, T. Tanvetyanon, S. Smith-Marrone, K. Ng, H. Xiao, S. Haque, and D.G. Pfister. 2012. A randomized phase II study of cetuximab every 2 weeks at either 500 or 750 mg/m2 for patients with recurrent or metastatic head and neck squamous cell cancer. *Journal of the National Comprehensive Cancer Network : JNCCN* 10:1391-1398.

Garon, E.B., N.A. Rizvi, R. Hui, N. Leighl, A.S. Balmanoukian, J.P. Eder, A. Patnaik, C. Aggarwal, M. Gubens, L. Horn, E. Carcereny, M.J. Ahn, E. Felip, J.S. Lee, M.D. Hellmann, O. Hamid, J.W. Goldman, J.C. Soria, M. Dolled-Filhart, R.Z. Rutledge, J. Zhang, J.K. Lunceford, R. Rangwala, G.M. Lubiniecki, C. Roach, K. Emancipator, L. Gandhi, and K.-. Investigators. 2015. Pembrolizumab for the treatment of non-small-cell lung cancer. *The New England journal of medicine* 372:2018-2028.

Giarre, M., S. Caldeira, I. Malanchi, F. Ciccolini, M.J. Leao, and M. Tommasino. 2001. Induction of pRb degradation by the human papillomavirus type 16 E7 protein is essential to efficiently overcome p16INK4a-imposed G1 cell cycle Arrest. *Journal of virology* 75:4705-4712.

Gillison, M.L., W.M. Koch, R.B. Capone, M. Spafford, W.H. Westra, L. Wu, M.L. Zahurak, R.W. Daniel, M. Viglione, D.E. Symer, K.V. Shah, and D. Sidransky. 2000. Evidence for a causal association between human papillomavirus and a subset of head and neck cancers. *Journal of the National Cancer Institute* 92:709-720.

Goldberg, M.V., and C.G. Drake. 2011. LAG-3 in Cancer Immunotherapy. *Current topics in microbiology and immunology* 344:269-278.

Golden-Mason, L., B.E. Palmer, N. Kassam, L. Townshend-Bulson, S. Livingston, B.J. McMahon, N. Castelblanco, V. Kuchroo, D.R. Gretch, and H.R. Rosen. 2009. Negative immune regulator Tim-3 is overexpressed on T cells in hepatitis C virus infection and its blockade rescues dysfunctional CD4+ and CD8+ T cells. *Journal of virology* 83:9122-9130.

Hamanishi, J., M. Mandai, M. Iwasaki, T. Okazaki, Y. Tanaka, K. Yamaguchi, T. Higuchi, H. Yagi, K. Takakura, N. Minato, T. Honjo, and S. Fujii. 2007. Programmed cell death 1 ligand 1 and tumor-infiltrating CD8+ T lymphocytes are prognostic factors of human ovarian cancer. *Proceedings of the National Academy of Sciences of the United States of America* 104:3360-3365.

Hartmann, E., B. Wollenberg, S. Rothenfusser, M. Wagner, D. Wellisch, B. Mack, T. Giese, O. Gires, S. Endres, and G. Hartmann. 2003. Identification and functional analysis of tumor-infiltrating plasmacytoid dendritic cells in head and neck cancer. *Cancer research* 63:6478-6487.

Higuchi, T., D.B. Flies, N.A. Marjon, G. Mantia-Smaldone, L. Ronner, P.A. Gimotty, and S.F. Adams. 2015. CTLA-4 Blockade Synergizes Therapeutically with PARP Inhibition in BRCA1-Deficient Ovarian Cancer. *Cancer immunology research* 3:1257-1268.

Hladikova, K., S. Partlova, V. Koucky, J. Boucek, J.F. Fonteneau, M. Zabrodsky, R. Tachezy, M. Grega, R. Spisek, and A. Fialova. 2018. Dysfunction of HPV16-specific CD8+ T cells derived from oropharyngeal tumors is related to the expression of Tim-3 but not PD-1. *Oral oncology* 82:75-82.

Hodi, F.S., S.J. O'Day, D.F. McDermott, R.W. Weber, J.A. Sosman, J.B. Haanen, R. Gonzalez, C. Robert, D. Schadendorf, J.C. Hassel, W. Akerley, A.J. van den Eertwegh, J. Lutzky, P. Lorigan, J.M. Vaubel, G.P. Linette, D. Hogg, C.H. Ottensmeier, C. Lebbe, C. Peschel, I. Quirt, J.I. Clark, J.D. Wolchok, J.S. Weber, J. Tian, M.J. Yellin, G.M. Nichol, A. Hoos, and W.J. Urba. 2010. Improved survival with ipilimumab in patients with metastatic melanoma. *The New England journal of medicine* 363:711-723.

Hoffmann, M., A.S. Ihloff, T. Gorogh, J.B. Weise, A. Fazel, M. Krams, W. Rittgen, E. Schwarz, and T. Kahn. 2010. p16(INK4a) overexpression predicts translational active human papillomavirus infection in tonsillar cancer. *International journal of cancer* 127:1595-1602.

Huang, Y.H., C. Zhu, Y. Kondo, A.C. Anderson, A. Gandhi, A. Russell, S.K. Dougan, B.S. Petersen, E. Melum, T. Pertel, K.L. Clayton, M. Raab, Q. Chen, N. Beauchemin, P.J. Yazaki, M. Pyzik, M.A. Ostrowski, J.N. Glickman, C.E. Rudd, H.L. Ploegh, A. Franke, G.A. Petsko, V.K. Kuchroo, and R.S. Blumberg. 2015. CEACAM1 regulates TIM-3-mediated tolerance and exhaustion. *Nature* 517:386-390.

Husain, N., and A. Neyaz. 2017. Human papillomavirus associated head and neck squamous cell carcinoma: Controversies and new concepts. *Journal of oral biology and craniofacial research* 7:198-205.

Jemal, A., F. Bray, M.M. Center, J. Ferlay, E. Ward, and D. Forman. 2011. Global cancer statistics. *CA: a cancer journal for clinicians* 61:69-90.

Kenter, G.G., M.J. Welters, A.R. Valentijn, M.J. Lowik, D.M. Berends-van der Meer, A.P. Vloon, F. Essahsah, L.M. Fathers, R. Offringa, J.W. Drijfhout, A.R. Wafelman, J. Oostendorp, G.J. Fleuren, S.H. van der Burg, and C.J. Melief. 2009. Vaccination against HPV-16 oncoproteins for vulvar intraepithelial neoplasia. *The New England journal of medicine* 361:1838-1847.

Kogashiwa, Y., M. Yasuda, H. Sakurai, M. Nakahira, Y. Sano, K. Gonda, T. Ikeda, H. Inoue, K. Kuba, S. Oba, J. Ishikawa, Y. Enoki, S. Matsumura, K. Minami, Y. Ebihara, and M. Sugasawa. 2017.

PD-L1 Expression Confers Better Prognosis in Locally Advanced Oral Squamous Cell Carcinoma. *Anticancer research* 37:1417-1424.

Kong, Y., J. Zhang, D.F. Claxton, W.C. Ehmann, W.B. Rybka, L. Zhu, H. Zeng, T.D. Schell, and H. Zheng. 2015. PD-1(hi)TIM-3(+) T cells associate with and predict leukemia relapse in AML patients post allogeneic stem cell transplantation. *Blood cancer journal* 5:e330.

Koyama, S., E.A. Akbay, Y.Y. Li, G.S. Herter-Sprie, K.A. Buczkowski, W.G. Richards, L. Gandhi, A.J. Redig, S.J. Rodig, H. Asahina, R.E. Jones, M.M. Kulkarni, M. Kuraguchi, S. Palakurthi, P.E. Fecci, B.E. Johnson, P.A. Janne, J.A. Engelman, S.P. Gangadharan, D.B. Costa, G.J. Freeman, R. Bueno, F.S. Hodi, G. Dranoff, K.K. Wong, and P.S. Hammerman. 2016. Adaptive resistance to therapeutic PD-1 blockade is associated with upregulation of alternative immune checkpoints. *Nature communications* 7:10501.

Larkins, E., G.M. Blumenthal, W. Yuan, K. He, R. Sridhara, S. Subramaniam, H. Zhao, C. Liu, J. Yu, K.B. Goldberg, A.E. McKee, P. Keegan, and R. Pazdur. 2017. FDA Approval Summary: Pembrolizumab for the Treatment of Recurrent or Metastatic Head and Neck Squamous Cell Carcinoma with Disease Progression on or After Platinum-Containing Chemotherapy. *The oncologist* 22:873-878.

Legat, A., D.E. Speiser, H. Pircher, D. Zehn, and S.A. Fuertes Marraco. 2013. Inhibitory Receptor Expression Depends More Dominantly on Differentiation and Activation than "Exhaustion" of Human CD8 T Cells. *Frontiers in immunology* 4:455.

Leon, X., R. Hitt, M. Constenla, A. Rocca, R. Stupp, A.F. Kovacs, N. Amellal, E.H. Bessa, and J. Bourhis. 2005. A retrospective analysis of the outcome of patients with recurrent and/or metastatic squamous cell carcinoma of the head and neck refractory to a platinum-based chemotherapy. *Clinical oncology* 17:418-424.

Li, X., Y. Takahashi, K. Sakamoto, and T. Nakashima. 2009. Expression of dendritic cell phenotypic antigens in cervical lymph nodes of patients with hypopharyngeal and laryngeal carcinoma. *The Journal of laryngology and otology. Supplement* 5-10.

Li, Y., L. Liang, W. Dai, G. Cai, Y. Xu, X. Li, Q. Li, and S. Cai. 2016. Prognostic impact of programed cell death-1 (PD-1) and PD-ligand 1 (PD-L1) expression in cancer cells and tumor infiltrating lymphocytes in colorectal cancer. *Molecular cancer* 15:55.

Lichtenegger, F.S., M. Rothe, F.M. Schnorfeil, K. Deiser, C. Krupka, C. Augsberger, M. Schluter, J. Neitz, and M. Subklewe. 2018. Targeting LAG-3 and PD-1 to Enhance T Cell Activation by Antigen-Presenting Cells. *Frontiers in immunology* 9:385.

Licitra, L., F. Perrone, P. Bossi, S. Suardi, L. Mariani, R. Artusi, M. Oggionni, C. Rossini, G. Cantu, M. Squadrelli, P. Quattrone, L.D. Locati, C. Bergamini, P. Olmi, M.A. Pierotti, and S. Pilotti. 2006. High-risk human papillomavirus affects prognosis in patients with surgically treated oropharyngeal squamous cell carcinoma. *Journal of clinical oncology : official journal of the American Society of Clinical Oncology* 24:5630-5636.

Lin, J., A.E. Albers, J. Qin, and A.M. Kaufmann. 2014. Prognostic significance of overexpressed p16INK4a in patients with cervical cancer: a meta-analysis. *PloS one* 9:e106384.

Liu, S., H. Zhang, M. Li, D. Hu, C. Li, B. Ge, B. Jin, and Z. Fan. 2013. Recruitment of Grb2 and SHIP1 by the ITT-like motif of TIGIT suppresses granule polarization and cytotoxicity of NK cells. *Cell death and differentiation* 20:456-464.

Long, G.V., V. Atkinson, S. Lo, S. Sandhu, A.D. Guminski, M.P. Brown, J.S. Wilmott, J. Edwards, M. Gonzalez, R.A. Scolyer, A.M. Menzies, and G.A. McArthur. 2018. Combination nivolumab and ipilimumab or nivolumab alone in melanoma brain metastases: a multicentre randomised phase 2 study. *The Lancet. Oncology* 19:672-681.

Lopez-Albaitero, A., J.V. Nayak, T. Ogino, A. Machandia, W. Gooding, A.B. DeLeo, S. Ferrone, and R.L. Ferris. 2006. Role of antigen-processing machinery in the in vitro resistance of squamous cell carcinoma of the head and neck cells to recognition by CTL. *Journal of immunology* 176:3402-3409.

Lundgren, S., J. Berntsson, B. Nodin, P. Micke, and K. Jirstrom. 2016. Prognostic impact of tumour-associated B cells and plasma cells in epithelial ovarian cancer. *Journal of ovarian research* 9:21.

Lydiatt, W.M., S.G. Patel, B. O'Sullivan, M.S. Brandwein, J.A. Ridge, J.C. Migliacci, A.M. Loomis, and J.P. Shah. 2017. Head and Neck cancers-major changes in the American Joint Committee on cancer eighth edition cancer staging manual. *CA: a cancer journal for clinicians* 67:122-137.

Mahmoud, S.M., A.H. Lee, E.C. Paish, R.D. Macmillan, I.O. Ellis, and A.R. Green. 2012. The prognostic significance of B lymphocytes in invasive carcinoma of the breast. *Breast cancer research and treatment* 132:545-553.

Martinez-Zapien, D., F.X. Ruiz, J. Poirson, A. Mitschler, J. Ramirez, A. Forster, A. Cousido-Siah, M. Masson, S. Vande Pol, A. Podjarny, G. Trave, and K. Zanier. 2016. Structure of the E6/E6AP/p53 complex required for HPV-mediated degradation of p53. *Nature* 529:541-545.

Migden, M.R., D. Rischin, C.D. Schmults, A. Guminski, A. Hauschild, K.D. Lewis, C.H. Chung, L. Hernandez-Aya, A.M. Lim, A.L.S. Chang, G. Rabinowits, A.A. Thai, L.A. Dunn, B.G.M. Hughes, N.I. Khushalani, B. Modi, D. Schadendorf, B. Gao, F. Seebach, S. Li, J. Li, M. Mathias, J. Booth, K. Mohan, E. Stankevich, H.M. Babiker, I. Brana, M. Gil-Martin, J. Homsi, M.L. Johnson, V. Moreno, J. Niu, T.K. Owonikoko, K.P. Papadopoulos, G.D. Yancopoulos, I. Lowy, and M.G. Fury. 2018. PD-1 Blockade with Cemiplimab in Advanced Cutaneous Squamous-Cell Carcinoma. *The New England journal of medicine* 379:341-351.

Mimura, K., J.L. Teh, H. Okayama, K. Shiraishi, L.F. Kua, V. Koh, D.T. Smoot, H. Ashktorab, T. Oike, Y. Suzuki, Z. Fazreen, B.R. Asuncion, A. Shabbir, W.P. Yong, J. So, R. Soong, and K. Kono. 2018. PD-L1 expression is mainly regulated by interferon gamma associated with JAK-STAT pathway in gastric cancer. *Cancer science* 109:43-53.

Mori, K., M. Hiroi, J. Shimada, and Y. Ohmori. 2011. Infiltration of m2 tumor-associated macrophages in oral squamous cell carcinoma correlates with tumor malignancy. *Cancers* 3:3726-3739.

Motzer, R.J., B. Escudier, D.F. McDermott, S. George, H.J. Hammers, S. Srinivas, S.S. Tykodi, J.A. Sosman, G. Procopio, E.R. Plimack, D. Castellano, T.K. Choueiri, H. Gurney, F. Donskov, P. Bono, J. Wagstaff, T.C. Gauler, T. Ueda, Y. Tomita, F.A. Schutz, C. Kollmannsberger, J. Larkin, A. Ravaud, J.S. Simon, L.A. Xu, I.M. Waxman, P. Sharma, and I. CheckMate. 2015. Nivolumab versus Everolimus in Advanced Renal-Cell Carcinoma. *The New England journal of medicine* 373:1803-1813.

Nakayama, M., H. Akiba, K. Takeda, Y. Kojima, M. Hashiguchi, M. Azuma, H. Yagita, and K. Okumura. 2009. Tim-3 mediates phagocytosis of apoptotic cells and cross-presentation. *Blood* 113:3821-3830.

Odorizzi, P.M., K.E. Pauken, M.A. Paley, A. Sharpe, and E.J. Wherry. 2015. Genetic absence of PD-1 promotes accumulation of terminally differentiated exhausted CD8+ T cells. *The Journal of experimental medicine* 212:1125-1137.

Ogino, T., H. Shigyo, H. Ishii, A. Katayama, N. Miyokawa, Y. Harabuchi, and S. Ferrone. 2006. HLA class I antigen down-regulation in primary laryngeal squamous cell carcinoma lesions as a poor prognostic marker. *Cancer research* 66:9281-9289.

Pacheco, J.M., D.R. Camidge, R.C. Doebele, and E. Schenk. 2019. A Changing of the Guard: Immune Checkpoint Inhibitors With and Without Chemotherapy as First Line Treatment for Metastatic Non-small Cell Lung Cancer. *Frontiers in oncology* 9:195.

Parry, R.V., J.M. Chemnitz, K.A. Frauwirth, A.R. Lanfranco, I. Braunstein, S.V. Kobayashi, P.S. Linsley, C.B. Thompson, and J.L. Riley. 2005. CTLA-4 and PD-1 receptors inhibit T-cell activation by distinct mechanisms. *Molecular and cellular biology* 25:9543-9553.

Partlova, S., J. Boucek, K. Kloudova, E. Lukesova, M. Zabrodsky, M. Grega, J. Fucikova, I. Truxova, R. Tachezy, R. Spisek, and A. Fialova. 2015. Distinct patterns of intratumoral immune cell

infiltrates in patients with HPV-associated compared to non-virally induced head and neck squamous cell carcinoma. *Oncoimmunology* 4:e965570.

Perry, M.E. 1994. The specialised structure of crypt epithelium in the human palatine tonsil and its functional significance. *Journal of anatomy* 185 (Pt 1):111-127.

Qureshi, O.S., Y. Zheng, K. Nakamura, K. Attridge, C. Manzotti, E.M. Schmidt, J. Baker, L.E. Jeffery, S. Kaur, Z. Briggs, T.Z. Hou, C.E. Futter, G. Anderson, L.S. Walker, and D.M. Sansom. 2011. Trans-endocytosis of CD80 and CD86: a molecular basis for the cell-extrinsic function of CTLA-4. *Science* 332:600-603.

Riaz, N., L. Morris, J.J. Havel, V. Makarov, A. Desrichard, and T.A. Chan. 2016. The role of neoantigens in response to immune checkpoint blockade. *International immunology* 28:411-419.

Ribas, A., R. Dummer, I. Puzanov, A. VanderWalde, R.H.I. Andtbacka, O. Michielin, A.J. Olszanski, J. Malvehy, J. Cebon, E. Fernandez, J.M. Kirkwood, T.F. Gajewski, L. Chen, K.S. Gorski, A.A. Anderson, S.J. Diede, M.E. Lassman, J. Gansert, F.S. Hodi, and G.V. Long. 2017. Oncolytic Virotherapy Promotes Intratumoral T Cell Infiltration and Improves Anti-PD-1 Immunotherapy. *Cell* 170:1109-1119 e1110.

Robert, C., A. Ribas, J.D. Wolchok, F.S. Hodi, O. Hamid, R. Kefford, J.S. Weber, A.M. Joshua, W.J. Hwu, T.C. Gangadhar, A. Patnaik, R. Dronca, H. Zarour, R.W. Joseph, P. Boasberg, B. Chmielowski, C. Mateus, M.A. Postow, K. Gergich, J. Elassaiss-Schaap, X.N. Li, R. Iannone, S.W. Ebbinghaus, S.P. Kang, and A. Daud. 2014. Anti-programmed-death-receptor-1 treatment with pembrolizumab in ipilimumab-refractory advanced melanoma: a randomised dose-comparison cohort of a phase 1 trial. *Lancet* 384:1109-1117.

Robert, C., L. Thomas, I. Bondarenko, S. O'Day, J. Weber, C. Garbe, C. Lebbe, J.F. Baurain, A. Testori, J.J. Grob, N. Davidson, J. Richards, M. Maio, A. Hauschild, W.H. Miller, Jr., P. Gascon, M. Lotem, K. Harmankaya, R. Ibrahim, S. Francis, T.T. Chen, R. Humphrey, A. Hoos, and J.D. Wolchok. 2011. Ipilimumab plus dacarbazine for previously untreated metastatic melanoma. *The New England journal of medicine* 364:2517-2526.

Sabatos, C.A., S. Chakravarti, E. Cha, A. Schubart, A. Sanchez-Fueyo, X.X. Zheng, A.J. Coyle, T.B. Strom, G.J. Freeman, and V.K. Kuchroo. 2003. Interaction of Tim-3 and Tim-3 ligand regulates T helper type 1 responses and induction of peripheral tolerance. *Nature immunology* 4:1102-1110.

Sato-Kaneko, F., S. Yao, A. Ahmadi, S.S. Zhang, T. Hosoya, M.M. Kaneda, J.A. Varner, M. Pu, K.S. Messer, C. Guiducci, R.L. Coffman, K. Kitaura, T. Matsutani, R. Suzuki, D.A. Carson, T. Hayashi, and E.E. Cohen. 2017. Combination immunotherapy with TLR agonists and checkpoint inhibitors suppresses head and neck cancer. *JCI insight* 2:

Schadendorf, D., F.S. Hodi, C. Robert, J.S. Weber, K. Margolin, O. Hamid, D. Patt, T.T. Chen, D.M. Berman, and J.D. Wolchok. 2015. Pooled Analysis of Long-Term Survival Data From Phase II and Phase III Trials of Ipilimumab in Unresectable or Metastatic Melanoma. *Journal of clinical oncology : official journal of the American Society of Clinical Oncology* 33:1889-1894.

Schelhaas, M., B. Shah, M. Holzer, P. Blattmann, L. Kuhling, P.M. Day, J.T. Schiller, and A. Helenius. 2012. Entry of human papillomavirus type 16 by actin-dependent, clathrin- and lipid raft-independent endocytosis. *PLoS pathogens* 8:e1002657.

Schildberg, F.A., S.R. Klein, G.J. Freeman, and A.H. Sharpe. 2016. Coinhibitory Pathways in the B7-CD28 Ligand-Receptor Family. *Immunity* 44:955-972.

Seiwert, T.Y., B. Burtness, R. Mehra, J. Weiss, R. Berger, J.P. Eder, K. Heath, T. McClanahan, J. Lunceford, C. Gause, J.D. Cheng, and L.Q. Chow. 2016. Safety and clinical activity of pembrolizumab for treatment of recurrent or metastatic squamous cell carcinoma of the head and neck (KEYNOTE-012): an open-label, multicentre, phase 1b trial. *The Lancet. Oncology* 17:956-965.

Seiwert, T.Y., Z. Zuo, M.K. Keck, A. Khattri, C.S. Pedamallu, T. Stricker, C. Brown, T.J. Pugh, P. Stojanov, J. Cho, M.S. Lawrence, G. Getz, J. Bragelmann, R. DeBoer, R.R. Weichselbaum, A. Langerman, L. Portugal, E. Blair, K. Stenson, M.W. Lingen, E.E. Cohen, E.E. Vokes, K.P. White, and P.S. Hammerman. 2015. Integrative and comparative genomic analysis of HPV-positive and HPV-negative head and neck squamous cell carcinomas. *Clinical cancer research : an official journal of the American Association for Cancer Research* 21:632-641.

Shayan, G., R. Srivastava, J. Li, N. Schmitt, L.P. Kane, and R.L. Ferris. 2017. Adaptive resistance to anti-PD1 therapy by Tim-3 upregulation is mediated by the PI3K-Akt pathway in head and neck cancer. *Oncoimmunology* 6:e1261779.

Snijders, P.J., F.V. Cromme, A.J. van den Brule, H.F. Schrijnemakers, G.B. Snow, C.J. Meijer, and J.M. Walboomers. 1992. Prevalence and expression of human papillomavirus in tonsillar carcinomas, indicating a possible viral etiology. *International journal of cancer* 51:845-850.

Solomon, B., R.J. Young, M. Bressel, D. Urban, S. Hendry, A. Thai, C. Angel, A. Haddad, M. Kowanetz, T. Fua, J. Corry, S. Fox, and D. Rischin. 2018. Prognostic Significance of PD-L1(+) and CD8(+) Immune Cells in HPV(+) Oropharyngeal Squamous Cell Carcinoma. *Cancer immunology research*

Thurlow, J.K., C.L. Pena Murillo, K.D. Hunter, F.M. Buffa, S. Patiar, G. Betts, C.M. West, A.L. Harris, E.K. Parkinson, P.R. Harrison, B.W. Ozanne, M. Partridge, and G. Kalna. 2010. Spectral clustering of microarray data elucidates the roles of microenvironment remodeling and immune responses in survival of head and neck squamous cell carcinoma. *Journal of clinical oncology : official journal of the American Society of Clinical Oncology* 28:2881-2888.

Triebel, F., K. Hacene, and M.F. Pichon. 2006. A soluble lymphocyte activation gene-3 (sLAG-3) protein as a prognostic factor in human breast cancer expressing estrogen or progesterone receptors. *Cancer letters* 235:147-153.

Turksma, A.W., H.J. Bontkes, H. van den Heuvel, T.D. de Gruijl, B.M. von Blomberg, B.J. Braakhuis, C.R. Leemans, E. Bloemena, C.J. Meijer, and E. Hooijberg. 2013. Effector memory T-cell frequencies in relation to tumour stage, location and HPV status in HNSCC patients. *Oral diseases* 19:577-584.

Vigneswaran, N., and M.D. Williams. 2014. Epidemiologic trends in head and neck cancer and aids in diagnosis. *Oral and maxillofacial surgery clinics of North America* 26:123-141.

Wang, J., T. Yoshida, F. Nakaki, H. Hiai, T. Okazaki, and T. Honjo. 2005. Establishment of NOD-Pdcd1-/- mice as an efficient animal model of type I diabetes. *Proceedings of the National Academy of Sciences of the United States of America* 102:11823-11828.

Wansom, D., E. Light, F. Worden, M. Prince, S. Urba, D.B. Chepeha, K. Cordell, A. Eisbruch, J. Taylor, N. D'Silva, J. Moyer, C.R. Bradford, D. Kurnit, B. Kumar, T.E. Carey, and G.T. Wolf. 2010. Correlation of cellular immunity with human papillomavirus 16 status and outcome in patients with advanced oropharyngeal cancer. *Archives of otolaryngology--head & neck surgery* 136:1267-1273.

Ward, M.J., S.M. Thirdborough, T. Mellows, C. Riley, S. Harris, K. Suchak, A. Webb, C. Hampton, N.N. Patel, C.J. Randall, H.J. Cox, S. Jogai, J. Primrose, K. Piper, C.H. Ottensmeier, E.V. King, and G.J. Thomas. 2014. Tumour-infiltrating lymphocytes predict for outcome in HPV-positive oropharyngeal cancer. *British journal of cancer* 110:489-500.

Webb, J.R., K. Milne, D.R. Kroeger, and B.H. Nelson. 2016. PD-L1 expression is associated with tumor-infiltrating T cells and favorable prognosis in high-grade serous ovarian cancer. *Gynecologic oncology* 141:293-302.

Webb, J.R., K. Milne, and B.H. Nelson. 2015. PD-1 and CD103 Are Widely Coexpressed on Prognostically Favorable Intraepithelial CD8 T Cells in Human Ovarian Cancer. *Cancer immunology research* 3:926-935.

Weber, J.S., S.P. D'Angelo, D. Minor, F.S. Hodi, R. Gutzmer, B. Neyns, C. Hoeller, N.I. Khushalani, W.H. Miller, Jr., C.D. Lao, G.P. Linette, L. Thomas, P. Lorigan, K.F. Grossmann, J.C. Hassel, M. Maio, M. Sznol, P.A. Ascierto, P. Mohr, B. Chmielowski, A. Bryce, I.M. Svane, J.J. Grob,

A.M. Krackhardt, C. Horak, A. Lambert, A.S. Yang, and J. Larkin. 2015. Nivolumab versus chemotherapy in patients with advanced melanoma who progressed after anti-CTLA-4 treatment (CheckMate 037): a randomised, controlled, open-label, phase 3 trial. *The Lancet. Oncology* 16:375-384.

Weinberger, P.M., Z. Yu, B.G. Haffty, D. Kowalski, M. Harigopal, J. Brandsma, C. Sasaki, J. Joe, R.L. Camp, D.L. Rimm, and A. Psyrri. 2006. Molecular classification identifies a subset of human papillomavirus--associated oropharyngeal cancers with favorable prognosis. *Journal of clinical oncology : official journal of the American Society of Clinical Oncology* 24:736-747.

Wherry, E.J. 2011. T cell exhaustion. *Nature immunology* 12:492-499.

Wherry, E.J., J.N. Blattman, K. Murali-Krishna, R. van der Most, and R. Ahmed. 2003. Viral persistence alters CD8 T-cell immunodominance and tissue distribution and results in distinct stages of functional impairment. *Journal of virology* 77:4911-4927.

Woo, S.R., M.E. Turnis, M.V. Goldberg, J. Bankoti, M. Selby, C.J. Nirschl, M.L. Bettini, D.M. Gravano, P. Vogel, C.L. Liu, S. Tangsombatvisit, J.F. Grosso, G. Netto, M.P. Smeltzer, A. Chaux, P.J. Utz, C.J. Workman, D.M. Pardoll, A.J. Korman, C.G. Drake, and D.A. Vignali. 2012. Immune inhibitory molecules LAG-3 and PD-1 synergistically regulate T-cell function to promote tumoral immune escape. *Cancer research* 72:917-927.

Workman, C.J., L.S. Cauley, I.J. Kim, M.A. Blackman, D.L. Woodland, and D.A. Vignali. 2004. Lymphocyte activation gene-3 (CD223) regulates the size of the expanding T cell population following antigen activation in vivo. *Journal of immunology* 172:5450-5455.

Wu, Y., D. Cao, L. Qu, X. Cao, Z. Jia, T. Zhao, Q. Wang, and J. Jiang. 2017. PD-1 and PD-L1 co-expression predicts favorable prognosis in gastric cancer. *Oncotarget* 8:64066-64082.

Yu, X., K. Harden, L.C. Gonzalez, M. Francesco, E. Chiang, B. Irving, I. Tom, S. Ivelja, C.J. Refino, H. Clark, D. Eaton, and J.L. Grogan. 2009. The surface protein TIGIT suppresses T cell activation by promoting the generation of mature immunoregulatory dendritic cells. *Nature immunology* 10:48-57.

Zerfass, K., A. Schulze, D. Spitkovsky, V. Friedman, B. Henglein, and P. Jansen-Durr. 1995. Sequential activation of cyclin E and cyclin A gene expression by human papillomavirus type 16 E7 through sequences necessary for transformation. *Journal of virology* 69:6389-6399.

Zhang, X., J.C. Schwartz, X. Guo, S. Bhatia, E. Cao, M. Lorenz, M. Cammer, L. Chen, Z.Y. Zhang, M.A. Edidin, S.G. Nathenson, and S.C. Almo. 2004. Structural and functional analysis of the costimulatory receptor programmed death-1. *Immunity* 20:337-347.

Zhu, C., A.C. Anderson, A. Schubart, H. Xiong, J. Imitola, S.J. Khoury, X.X. Zheng, T.B. Strom, and V.K. Kuchroo. 2005. The Tim-3 ligand galectin-9 negatively regulates T helper type 1 immunity. *Nature immunology* 6:1245-1252.

Zolkind, P., and R. Uppaluri. 2017. Checkpoint immunotherapy in head and neck cancers. *Cancer metastasis reviews* 36:475-489.

Zou, W., and L. Chen. 2008. Inhibitory B7-family molecules in the tumour microenvironment. *Nature reviews. Immunology* 8:467-477.